
University of Glasgow

# Investigation of JAK2 targets in haematological malignancy

by

Susan Rhodes

Thesis submitted to fulfil the requirements for the degree of Doctor of Philosophy

School of Medical, Veterinary and Life Sciences

September 2017

# Contents

# List of figures

# List of Tables

# Acknowledgements

I would like to express my extreme gratitude to everyone who has helped me reach the end of a true roller coaster. The person who deserves the most appreciation is my fiancé Richard Boal who has had to look after my physical and emotional wellbeing throughout the period of my research, which he has managed so well he now believes me incapable.

I also have to thank my supervisors Helen Wheadon and Mhairi Copland, both who have had to deal with all my anxiety about the research process and when experiments didn't work again and again. They tell me these ups and downs are entirely normal and they see it with all their students. I'm extremely grateful for them trying to make this all feel normal, which always made me feel better. Thank you also for the guiding me through the research grant process and helping to develop the project.

To everyone working in the lab who took the time to teach me how not to kill my samples: Heather Morrison, Ross Kinstrie, Sheila Abrahams, Caitriona O'Connor Alan Hair, Ana Tarafdar; without you all this would have been a much shorter thesis.

Finally, to my family who tried their best to pretend they understood anything I was talking about when I started getting technical about my research. Thank you for being available when I needed you.

# Abstract

Janus kinase 2 (JAK2) is a critical activator of signalling associated with many different receptors, particularly those associated with haematopoiesis and the inflammatory response. Classically JAK2 has been thought of as a cytoplasmic protein, but more recently there is evidence that JAK2 is able to enter the nucleus leading to alteration of epigenetic modifiers and enhancement of JAK2 transcriptional targets. This role in haematopoiesis means that alteration of JAK2 signalling, such as in malignant haematopoiesis, can be a critical factor in the development and maintenance of disease.

The myeloproliferative neoplasms (MPN) are a group of conditions characterised by over-production of myeloid cells as a result of acquired mutations in haematopoietic stem cells. Two well-known MPNs are chronic myeloid leukaemia (CML), driven by the novel oncoprotein BCR-ABL, and polycythaemia vera (PV), driven by the JAK2 V617F activating mutation. JAK2 is critical for normal haematopoiesis through its role in initiating signalling following activation of a receptor by its ligand. In this study we looked several aspects of JAK2 activity, including its effect on gene expression, its activity within the nucleus, and the effect of overactivity on aspects of inflammation.

Here we show that gene expression in both CML and PV patient samples is deregulated compared to normal controls with both previously confirmed alterations such as *BCL2* and *MCL1* in CML and *STAT1* and *MPL* in PV, and novel alterations such as *Rex1* and *SUMO2* in CML and *EGR1* in PV. These alterations at the level of mRNA transcription are validated by significant alterations in cell cycle and apoptosis in cell lines following treatment with JAK2 inhibitors.

As part of the investigation of the activity of JAK2 in the nucleus we hypothesised that JAK2 may interact directly with PML nuclear bodies, a subnuclear structure with numerous regulatory roles in apoptosis, cell cycle, DNA repair and response to infection. Using immunofluorescence based techniques in cell lines and patient samples we showed that JAK2 does interact directly with PML nuclear bodies. This interaction was affected by JAK2 inhibitors in cell lines and increased in PV patient monocytes compared to normal controls. Treatment of cell lines with the

JAK2 inhibitor ruxolitinib and arsenic trioxide, which degrades PML, led to an increase in apoptosis compared to either compound alone, suggesting a meaningful functional interaction in both normal and malignant haematopoiesis.

The role of the JAK2 V617F in cellular function has been extensively investigated particularly in neutrophils and platelets. However the effect of the JAK2 V617F mutation on monocytes and monocyte derived macrophages has not previously been investigated. Here we show that patients with PV have an alteration in monocyte subsets with an increase in the inflammatory intermediate monocytes at the expense of classical monocytes. We also showed that macrophages derived from peripheral blood monocytes obtained from patients with JAK2 V617F positive PV behaved differently from those derived from normal controls. There were alterations both at rest and in response to stimulation in terms of the morphology, with a more inflammatory phenotype seen, and in cytokine release with blunting of some responses and heightening of other. These alterations were seen both in M1 and M2 macrophages.

Overall the work presented in this thesis shows wide ranging alterations in many aspects of cellular behaviour as a result of overactivity of JAK2. Some of these findings have been previously identified and discussed, but there are several key novel findings which progress out understanding of JAK2 function both in normal and malignant haematopoiesis, and the effects of malignant JAK2 activation on cellular behaviour.

# Research output

1. Identification of JAK2 dependent transcriptional regulators in CML. S. Rhodes, M. Copland, L. Hopcroft, P.p. Sayeski, H Wheadon. Presented at the International Society for Experimental Haematology, Vienna 2012[1].

2. JAK2/STAT5 inhibition by nilotinib with ruxolitinib contributes to the elimination of CML CD24+ cells in vitro and in vivo. P. Gallipoli, A. Cook, S. Rhodes, L. Hopcroft, H. Wheadon, A. D. Whetton, H.G. Jorgensen, R. Bhatia, T.L. Holyoake. Blood, 2014: 124(9); 1492-1501[2].

3. Perturbation of JAK2-dependent transcriptional and inflammatory gene expression in polycythaemia vera. S. Rhodes, L, Hopcroft, P.P. Sayeski, M. Copland, H. Wheadon. Presented at the British Society for Haematology Annual Scientific Meeting, Edinburgh 2015 (Abstract 212)[3].

4. Characterising the inflammasome in polycythaemia vera. S. Rhodes, R. Gavrillidou, M. Drummond, M. Copland, H. Wheadon. Presented at the American Society for Haematology Annual Scientific Meeting, Orlando 2015. Awarded an abstract achievement award[4].

# 1 Introduction

## 1.1 Normal haematopoiesis

Haematopoiesis is the process that leads to production of all mature blood cells and is sustained by the multipotent haematopoietic stem cell (HSC). This cell resides in the bone marrow (BM) and has the ability to differentiate into all different blood cell types[5]. The presence of a multipotent cell capable of supporting haematopoiesis was first suggested in 1963 following experiments in mice where BM transplanted into lethally irradiated mice was capable of generating myeloid and erythroid colonies in the spleen[6,7]. It was proposed that these cells contained the HSC after it was shown they were capable of regenerating all peripheral blood cell types confirming both the self-renewal and differentiation potential[6,7].

The classical model of haematopoiesis places long term HSCs, short term HSCs and multipotent progenitors (MPP) at the top of a hierarchy which differentiate through progressively more mature cells under the control of a wide range of cytokines. Underlying this hierarchy is the ability of HSCs to undergo asymmetrical replication leading to the main properties of HSCs, multipotency and self-renewal capability. This asymmetric division results in the production of one daughter cell which is identical to the original stem cell and one daughter cell which is more differentiated than the stem cell (Figure 1.1). This process allows the maintenance of the stem cell pool, while still providing differentiating cells and differs from symmetrical division where 2 identical daughter cells are produced[8]. As the cells differentiate and mature they lose these properties, becoming lineage committed and losing their self-renewal capability, ultimately leading to the generation of a wide range of functionally distinct, terminally differentiated cells which are unable to undergo any further cell divisions. During this differentiation cells will develop towards either a lymphoid or myeloid potential, with the common myeloid progenitor able to produce all myeloid cells[9], and the common lymphoid progenitor producing B cells, T cells and NK cells[10]. More recently other models have been proposed where the cells are more able to switch between lineages to support the production of myeloid cells in response to infection, with the myeloid-based model proposing that all progenitors retain the ability to convert to myelopoiesis allowing a rapid increase in mature myeloid cells in response to infection[11] and a two-tier model where the adult bone marrow produces differentiated cells directly from multipotent cells with no intervening committed oligopotent cells[12]. These varying

models highlight the complexity of the haematopoietic system and the difficulty faced in trying to tease out the mechanisms of blood production in laboratory based models.

**Figure 1.1 Classical model of the haematopoietic system**

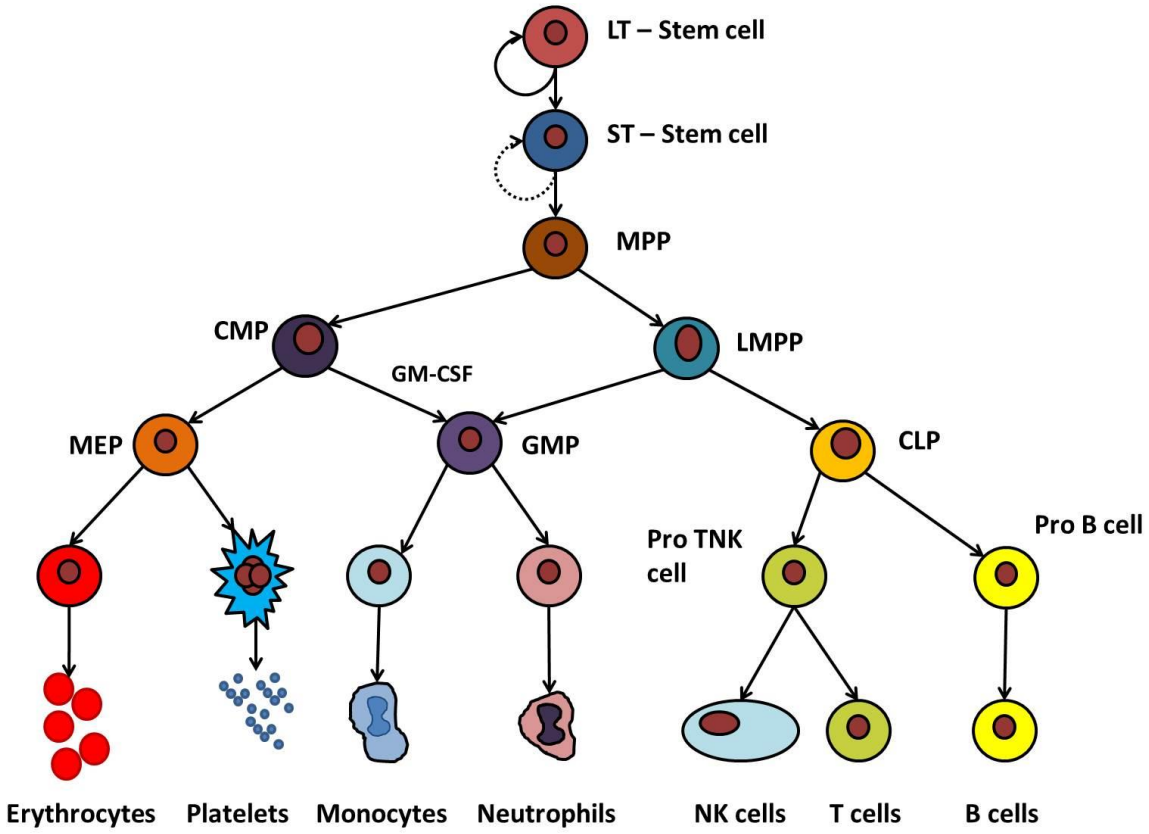


**Mature blood cells are produced in a hierarchical manner starting with haematopoietic stem cells which have the ability to differentiate into any mature cell. Under the influence of cytokines these cells replicate and mature as required to produce the mature cells seen in the blood. LT – long term, ST – short term, MPP – multipotent progenitor, CMP – common myeloid progenitor, LMPP – lymphoid primed multipotent progenitor, MEP – megakaryocytic-erythroid progenitor, GMP – granulocyte-monocyte progenitor, CLP – common lymphoid progenitor.**

An important regulator of haematopoiesis is the stroma in which the cells develop, where cytokines and chemokines that support cell maintenance and development are produced. Haematopoietic stem cells reside in the relatively hypoxic osteoblastic niche, which supports self-renewal and quiescence through interactions of the HSCs with the ligands N-cadherin expressed on the HCSs and Jagged 1 expressed on the osteoblasts[13]. N-cadherin helps to anchor these quiescent stem cells in the osteoblastic niche which keeps them in the

environment to maintain their stem cell properties, while Jagged 1 interferes with the Notch signalling pathway and regulates HSC quiescence and self-renewal capacity. Deletion of Jagged 1 from endothelial cells leads to expansion of HSCs confirming its role in maintaining the HSC pool. Using *in vivo* imaging it is possible to identify a population of HSCs in a more vascular area away from the osteoblastic niche. In this peri-sinusoidal niche the cells are exposed to growth factors which stimulate proliferation and differentiation.

## 1.2 Myelopoiesis

Myelopoiesis refers to production of cells of the myeloid lineage including neutrophils, monocytes, red cells and platelets. Once HSCs have entered a proliferation phase they will lose their self-renewal capacity as they differentiate into mature blood cells, with terminally differentiated myeloid cells having no renewal capacity. The mechanisms underlying normal myelopoiesis have been investigated thoroughly for many years and yet there are still new insights being made in the populations of cells capable of driving myelopoiesis, with the discovery in recent years of a lymphoid primed multipotent progenitor (LMPP) capable of producing lymphocytes and granulocytes, but not erythroid or megakaryocytic cells[14]. This progenitor appears to be separate from the common myeloid progenitor, capable of differentiating into all myeloid cells, and the common lymphoid progenitor, which appears to be the next step for cells differentiating down the lymphoid path (Figure 1.1).

Cytokines control all of haematopoiesis with different cytokines at different stages exerting specific effects. To initiate myelopoiesis primitive cells are exposed to IL-3 and stem cell factor which drives them towards the myeloid lineage. Interleukin (IL)-3 and granulocyte macrophage-colony stimulating factor (GM-CSF) have overlapping activities explained by the shared signalling receptor subunit, the β chain, which is required for high affinity binding of these cytokines to the receptor. The α chain creates the specificity of the receptor by only allowing binding of either IL-3 or GM-CSF. The common β chain leads to a significant degree of functional overlap for IL-3 and GM-CSF in myelopoiesis. Following ligand binding downstream signal transduction events are initiated (Section 1.3), which lead to transcription of genes involved in cell proliferation, differentiation and survival.

### 1.2.1 Granulopoiesis

Granulopoiesis refers to the production of granulocytes which can develop either from the CMP or the LMPP. Both of these can differentiate into granulocyte macrophage progenitors (GMPs) which then develop into granulocyte specific precursors. This ability of two separate precursors involved in granulocyte production increases the number of cells which can respond to severe infection, thus maximising the first line of defence against disseminated pathogens[15].

Production of granulocytes is regulated by the interaction of growth factors, signalling pathways and transcription factors. Part of the regulation involves the effects of different factors on cells at different stages of maturation. Once cells have developed into the myeloid lineage the action of granulocyte colony stimulating factor (G-CSF) is the key to driving granulocytic development. G-CSF exists as a 20kDa protein which is produced mainly by cells of the monocyte/macrophage lineage. In addition to this fibrobalsts, T-lymphocytes and endothelial cells will produce G-CSF in response to stimulation by inflammatory cytokines, such as TNF-αm IFN-γ and IL-1[16]. G-CSF interacts with its receptor, which leads to activation of the JAK2/STAT5 pathway leading to transcription of factors which drive granulocytic maturation[17].

Interestingly it appears that expression of transcription factors associated with granulocytic development have a profound effect on lineage commitment. CCAAT-enhancer binding protein α (C/EBPα) and Purine box factor 1 (PU.1) regulate the expression of both G-CSFR and GM-CSFR; with mice lacking these two transcription factors have a more profound reduction in granulocyte production than those with G-CSF and G-CSFR deleted[18,19].

### 1.2.2 Erythropoiesis

Erythropoiesis specifically refers to the production of mature red cells the site of which changes from fetal development, with liver and spleen being the main sites, through to adult life, where the bone marrow produced mature cells. The earliest stage of erythropoiesis is the burst-forming unit-erythroid (BFU-E) followed by colony-forming unit-erythroid (CFU-E)[20]. BFU-E and CFU-E are identifiable following colony formation assay of BM cells, but are morphologically indistinct from early precursors of other lineages. Morphologically the earliest identifiable stage is the proerythroblast which progresses through early and late normoblasts,

reticulocytes and finally mature erythrocytes (Figure 1.2). Prior to release from the bone marrow the cells extrude their nucleus with the final stage of maturation being the loss of RNA from the cytoplasm and development of the classic biconcave disc of the mature erythrocyte. Red cells circulate for 100-120 days before being destroyed by splenic macrophages[20].

**Figure 1.2 Erythropoiesis**

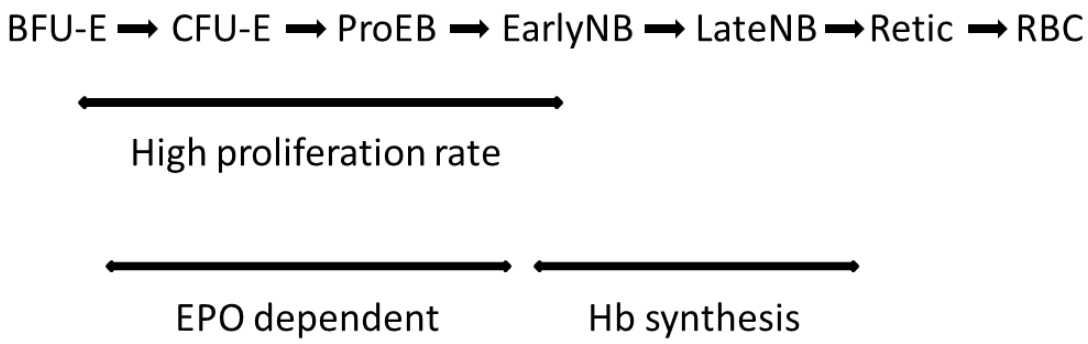


**Progression of erythropoiesis from highly proliferative EPO-dependent erythroid precursors with progressive maturation to enucleated and haemoglobinised mature red cells which are released into the peripheral circulation. BFU-E – burst forming unit – erythroid, CFU-E – colony forming unit – erythroid, proEB – proerythroblast, NB – normoblast, Retic – reticulocyte, RBC – red blood cell.**

The main cytokine controlling the production of red cells is erythropoietin (EPO) which is produced by interstitial cells in the peritubular capillary bed of the kidneys in response to hypoxic conditions. EPO receptors are initially expressed on BFU-E cells and maximally expressed on CFU-E cells. CFU-E cells require the presence of EPO to prevent apoptosis and to stimulate maturation. Although EPO is the main driver of erythropoiesis there are multiple other cytokines involved which help to maintain early precursors and stimulate differentiation. Some of these are similar to those needed for early myelopoiesis including IL-3[16].

EPO was the first cytokine to be purified, following a long process using large volumes of urine from anaemic patients[21]. Sequencing of the protein and cloning of the EPO gene[22,23] followed, allowing production of recombinant EPO for laboratory investigation of its actions and subsequently treatment of EPO deficient anaemias[24]. EPO is a 34kDa protein produced in response to hypoxia by interstitial fibroblasts in the kidney. EPO has a short half-life of around 5 hours and

has a low plasma concentration in the absence of anaemia, but can increase by a factor of 1000 in response to hypoxic stress. The best known action of EPO is on erythroid precursors in the bone marrow, however, since the identification of the EPO receptor on the surface of non-erythroid cells the activity of this cytokine has been shown to be much more diverse. As a result it is clear that EPO has direct effects on immune cells, endothelial cells and BM stroma cells in the haematopoetic system, as well as cells of the nervous system[25] and heart[26] among others.

### 1.2.3 Thrombopoiesis

Platelets in the peripheral blood are derived from megakaryocytes in the BM. Megakaryocytes are large multinucleate cells that tend to exist individually beside blood vessels in the marrow where they release platelets directly into the blood stream by extending cytoplasmic processes between the endothelial cells of the blood vessels and shedding this projection[27]. The primary regulator of the maturation of megakaryocytes is thrombopoietin (TPO)[28], which is released by stromal cells in the marrow. In addition to this the stromal cells also release chemokine (C-X-C motif) ligand 12 (CXCL12), which attracts megakaryocytes to the marrow microenvironment, and express SCF which acts in synergy with TPO to stimulate growth of megakaryocytes[29]. TPO is also produced from the liver and released into the blood stream, where platelets absorb and destroy it[30]. Traditionally it has been thought that this leads to an alteration in the amount of TPO reaching the bone marrow dependent on the number of platelets in the peripheral blood. Recent evidence has shown that aging platelets become desialylated and bind to the Ashwell-Morell receptor (AMR) in the liver[31], which signals through JAK2/STAT3. This study showed that mice lacking AMR had reduced platelet production, while those that lacked sialyltransferase activity had increased platelet production. This mechanism is thought to partly explain the thrombocytopenia seen with JAK2 inhibitors[31].

### 1.2.4 Monocyte and macrophage development

Monocytes and macrophages are part of the mononuclear phagocyte system, which develop from the myeloid lineage. Monocyte precursors derive from the GMP, which differentiate into macrophage and dendritic cell precursors (MDP). MDPs are able to produce monocytes, classical dendritic cells and plasmacytoid dendritic cells[32]. Once they have reached their differentiated state, monocytes circulate in the peripheral blood and BM for 1 to 3 days before entering the tissues and differentiating into macrophages. There is a large pool of monocytes in the spleen which can rapidly mobilise during infection or inflammation to provide macrophages to the affected tissues[33]. Monocytes can be categorised according to the cell surface expression of CD14 and CD16 as classical, non-classical and intermediate monocytes[34]. Classical monocytes make up the majority found in the peripheral blood and are involved in phagocytosis and production of inflammatory cytokines. Non-classical monocytes comprise approximately 5-10% of monocytes and tend to have a more anti-inflammatory and immunoregulatory role through the production of IL-1 receptor antagonist (IL-1 RA). The intermediate population makes up less than 5% of the total monocyte pool and are actively pro-inflammatory, producing IL-6, IL-1β and in response to LPS, TNF-α[35]. There is evidence to show that monocytes play a key role in autoimmune disorders[36], atherosclerosis[37] and cancer biology[38] both directly and through differentiation into macrophages.

Once monocytes leave the circulation and enter the tissues they begin to undergo further differentiation to macrophages[39]. Tissue macrophages associate closely with T helper cells, that act as regulators of the type of response and therefore the type of macrophages that develop. In the context of inflammation and direct damage to organisms the $T_H1$ mediated response predominates, while tissue remodelling and immune regulation generates a $T_H2$ mediated response[40] (Figure 1.3). Macrophages have been a source of interest in solid malignancy as macrophages are known to associate with tumours and promote angiogenesis, support metastasis and decrease the local pro-inflammatory anti-tumour response[41,42].

**Figure 1.3 Macrophage interactions with T cells**

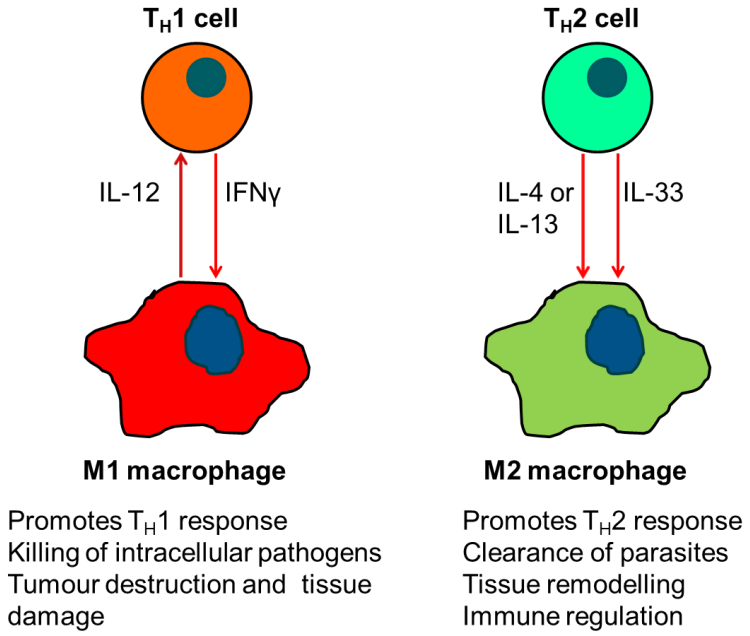


## 1.3 Cytokine signalling in haematopoiesis

Cytokines are soluble regulators required to maintain the fine balance required for normal haematopoiesis and can stimulate the whole system to respond to a physiological stress such as infection or bleeding. Cytokines bind to receptors expressed on target cells and trigger signalling pathways which result in a receptor-specific gene transcriptional programme being triggered[43]. Numerous pathways are involved in cytokine signalling and control of the associated transcriptional programme triggered by activation of receptors. Key cytokines in haematopoiesis include EPO which drives red cell development[20], TPO which is critical in the production of platelets[30], and GM-CSF and G-CSF which are involved in granulopoiesis[44,45]. All of these cytokines signal through receptors which are associated only with JAK2 in a homodimeric configuration[46]. Many other receptors, including IFNγ, are associated with two different JAK proteins in a heterodimeric fashion and this is particularly common in inflammatory cytokine receptors[47,48]. The binding of ligand to their receptor leads to activation of the JAK proteins (Table 1.1) which in turn activates other cellular pathways either directly or indirectly, which have complementary activity to the canonical JAK-STAT pathway (Figure 1.6). These include the PI3K-Akt-mTOR pathway, the Ras-Raf-MEK-ERK pathway, and indirectly the NFκB pathway.

### 1.3.1 PI3K-Akt signalling

Phosphoinositide-3-kinase (PI3K) plays a critical role in the differentiation of haematopoietic cells. PI3K consists of a family of proteins which exist in three subclasses (class I, II, III) with class I being of most importance in the haematopoietic system. Following activation of a cytokine receptor PI3K is activated by tyrosine kinases, including JAK2[49], with the active PI3K going on to transform phosphatidylinositol 4,5 bisphosphate to phosphatidylinositol 3,4,5 triphosphate ($PIP_3$). $PIP_3$ then goes on to activate Akt, a protein kinase, which acts as the main effector of the pathway by activating mTOR signalling and inhibiting FoxO activity. This leads to a reduction in transcriptional targets of FoxO, which results in a reduction in cell cycle inhibition and apoptosis. In addition to this mTOR signalling is activated which drives cell cycle progression and proliferation[50] (Figure 1.4). This pathway has been found to be significantly upregulated in a number of haematological malignancies, including acute and chronic leukaemias[51,52], lymphoma[49] and myeloproliferative neoplasms (MPN)[53]. Most of these abnormalities are as a result of increased signalling through a normal pathway[52]. It is also overactive in solid tumours, such as breast cancer[54], colorectal cancers[55] and prostate cancers[56], where there are often activating mutations present[57].

**Figure 1.4 PI3K-Akt signalling**

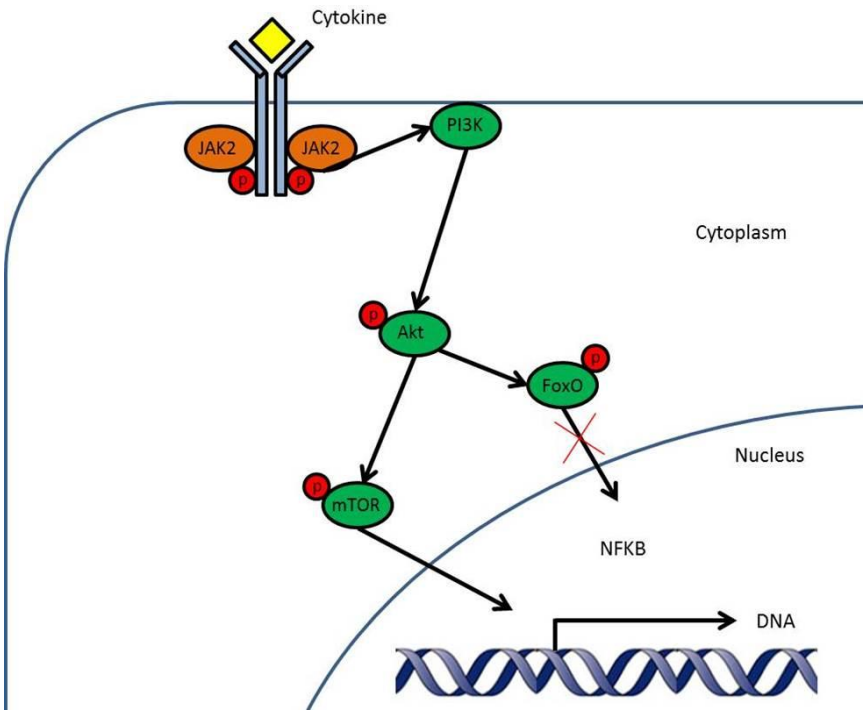


**Activation of PI3K leads to the activation of Akt which in turns co-ordinates signals to reduce apoptosis and drive cell cycle progression. This is achieved primarily through inhibiting FoxO activity and promoting mTOR signalling.**

### 1.3.2 RAS-RAF-MEK-ERK pathway

This pathway plays a key role in proliferation and preventing the apoptosis of cells and is commonly over-active in malignant cells of several types[52,58]. The initiation of signalling in this pathway is by activation of cytokine receptor, with common ligands including IL-3, GM-CSF, EPO and G-CSF. The active receptor leads to the formation of an activating complex consisting of SHC (Scr homology 2 domain containing) transforming protein 1 (SHC1), growth factor receptor bound protein 2 (GRB2) and son of sevenless (SOS) which in turn leads to farnesylation of Ras and its attachment to the cell membrane[59]. Ras exists in several isoforms which vary according to tissue and developmental stage. Once Ras has translocated to the cell membrane its GTPase activity is triggered, and in combination with Src kinases activates Raf, which in turn activates MAPK/ERK kinase (MEK). MEK exists in seven forms and activates four effector proteins; MEK1/2 activating ERK1/2, MEK3/6 activating p38, MEK4/7 activating Jun N-terminal kinase (JNK) and MEK5 activating ERK5. The effector proteins ERK1/2 interacts with and regulates over 100 proteins including transcription factors involved in cell proliferation and differentiation. The JNK and p38 pathways are activated by cellular stress and mediate a wider range of responses from inflammation, cell survival and cell migration[60,61] As with other signalling pathways the Ras-Raf-MEK-ERK pathway has been found to play a role in solid tumours, with activating mutations of Ras isoforms in lung[62] and colon cancer[63], and mutations of B Raf in malignant melanoma[64]. In haematological malignancy there can be other mutations which can directly stimulate the pathway to drive increased signalling, such as that seen in CML as a result of BCR-ABL directly activating the pathway[52].

**Figure 1.5 RAS-RAF-MEK-ERK signalling pathway**

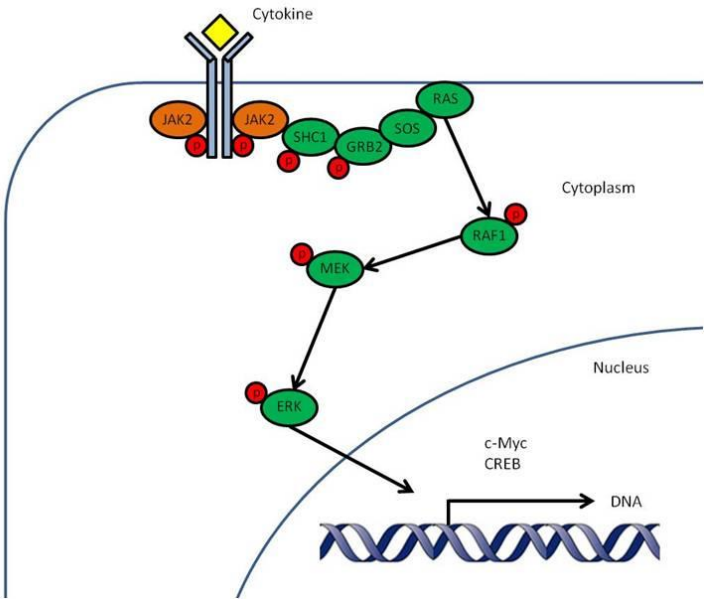


**RAS-RAF-MEK-ERK signalling starts with the formation of an activating complex consisting of SHC1, GRB2 and SOS. This activated the pathway through farnesylation of RAS. This then goes on to phosphorylate RAF, which in turn activates MEK, then ERK, which enters the nucleus activating cell survival and proliferation genes.**

### 1.3.3 NFκB signalling

Nuclear factor kappa-light-chain-enhancer of activated B cells (NFκB) is a transcriptionally active complex which exists in the cytoplasm bound to an inhibitory protein (IκB) which keeps it inactive[65]. The canonical NFκB pathway is activated as part of the innate immune system in response to physical, physiological or oxidative stress leading to degradation of the inhibitory protein, which allows the complex to enter the nucleus and effect transcriptional alterations. There are five proteins in the NFκB family which contain a Rel domain in the N-terminus (p50, p52, RelA (p65), RelB, c-Rel). The proteins exist in a dimerised state and will have different transcriptional effects depending on the combination of subunits. Both p50 and p52, when bound homodimerically, will act as transcriptional repressors, but will become activators when bound with any of RelA, RelB or c-Rel[66]. These latter three proteins will always act as transcriptional activators. The canonical pathway is activated directly by several receptors, including Toll-like receptors (TLRs), TNF-α and IL-1. In addition to receptor mediated activation, the NFκB pathway can be activated by other cell signalling pathways and transcriptional regulators, including Akt and STAT3[67]. The role of JAK2 in NFκB signalling is less direct than in the previously discussed pathways. Both the NFκB pathway and JAK2 are activated by TLR4[68], and JAK2 activates STAT3 directly and Akt through PI3K. The biggest role JAK2 plays however is in the potentiation of inflammatory signalling that leads to the release, by immune cells, of further inflammatory ligands which then go on to activate NFκB[69,70].

### 1.3.4 JAK/STAT pathway

The Janus kinase/signal transducers and activators of transcription (JAK/STAT) pathway is probably the most investigated pathway in cellular biology. The JAKs and STATs were initially identified separately in association with interferon (IFN) signalling in the late 1980's and early 1990's[71–73] with all JAKs and STATs identified by 1995[73]. The connection between JAKs and STATs in IFN signalling was clarified in 1993[74], and by 1994 it was clear the pathway was utilised by many other cytokine receptors. Four JAK proteins have been identified (JAK1, JAK2, JAK3 and TYK2) which attach in different combinations to transmembrane cytokine receptors[75]. Activation of the receptor leads to a conformational change which allows the JAK proteins to cross-phosphorylate and activate each other at multiple sites, with phosphorylation of tyrosines 1007 and 1008 being a mark of JAK2 activation[76]. The canonical JAK/STAT pathway results following the JAK activation and the formation of a binding site for STATs by phosphorylation of the cytoplasmic portion of the receptor. There are 7 STAT proteins (STAT1, STAT2, STAT3, STAT4, STAT5a, STAT5b and STAT6) which are phosphorylated by JAKs and dimerise before entering the nucleus and initiating a transcriptional programme (Figure 1.6).

**Figure 1.6 Canonical JAK/STAT signalling**

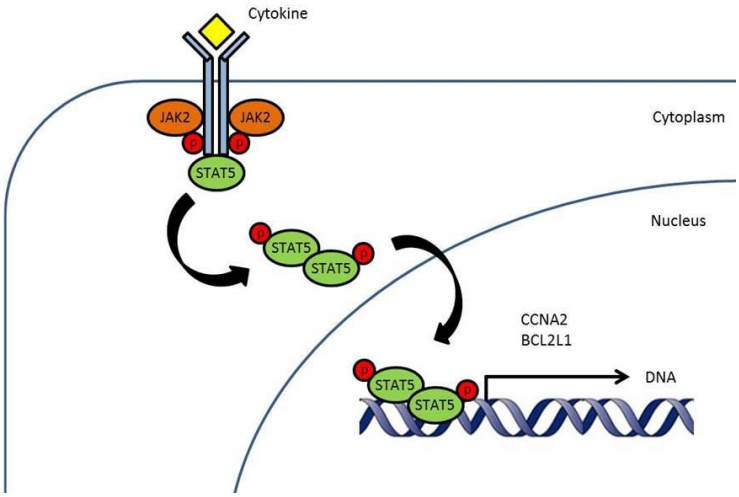


**Canonical JAK/STAT signalling relates to the activation of JAK following conformational change of the receptor after binding with its ligand. This then leads to phosphorylation of the receptor and the relevant STAT proteins, which dimerise and enter the nucleus to trigger the relevant transcriptional program.**

In haematopoiesis JAK2 is particularly important and associates with a number of key receptors including EPO receptor, TPO receptor, G-CSF receptor, GM-CSF receptor, IL-3 receptor and IL-6 receptor. It also combines with other JAK proteins in a number of important inflammatory cytokine receptors including IFN-γ receptor, IL-5 receptor and IL-12 receptor (Table 1.1). The importance of JAK2 in haematopoiesis, particularly erythropoiesis, was shown in *Jak2* knockout mouse experiments where heterozygous mice were interbred. The *Jak2*$^{-/+}$ offspring developed normally while the *Jak2*$^{-/-}$ phenotype resulted in embryonic lethality at 12 days after conception with features of severe anaemia and little evidence of normal erythropoiesis in the foetal liver[77].

**Table 1.1 Receptors associated with JAK/STAT signalling in myelopoiesis and inflammation**

| Receptors | JAK proteins | STATs | Cells expressing receptor |
|---|---|---|---|
| EPO, TPO, G-CSF, GM-CSF | JAK2/JAK2 | STAT5 | Myeloid progenitors |
| IFN-γ | JAK1/JAK2 | STAT1 | B + T cells and macrophages |
| IFN-α | JAK1/TYK | STAT1 | |
| IL-4 | JAK1/JAK3 | STAT6 | B + T cells, NK and mast cells |
| IL-7 | JAK1/JAK3 | STAT1,3,5 | Pre-B cells, T cells and DCs |

### 1.3.4.1 JAK2 signalling in the nucleus

There is recent evidence showing that JAK2 enters the nucleus[78] and mediates epigenetic alterations which lead to profound alterations in the transcriptional landscape[79,80]. JAK2 is unable to enter the nucleus alone as it lacks a nuclear translocation signal, a protein sequence allowing transfer of a protein from the cytoplasm to the nucleus. There are several different nuclear localisation signals used by different proteins to enter the nucleus[81,82,83], but no sequence that would allow transport to the nucleus has been identified on JAK proteins. On activation and phosphorylation, particularly of the tyrosine residues at position 1007 and 1008 (Y1007/1008), a chain of small ubiquitin-like molecule (SUMO) proteins is able to attach to JAK2 and allow it to enter the nucleus (Figure 1.7). This was shown by expressing truncated JAK2 or the constitutively active JAK2 V617F mutant in HEK-293 and there was a reduction of SUMOylation in the truncated JAK2 mutants, but an increase in SUMOylation of the JAK2 V617F mutant[78].

**Figure 1.7 Nuclear translocation of JAK2**

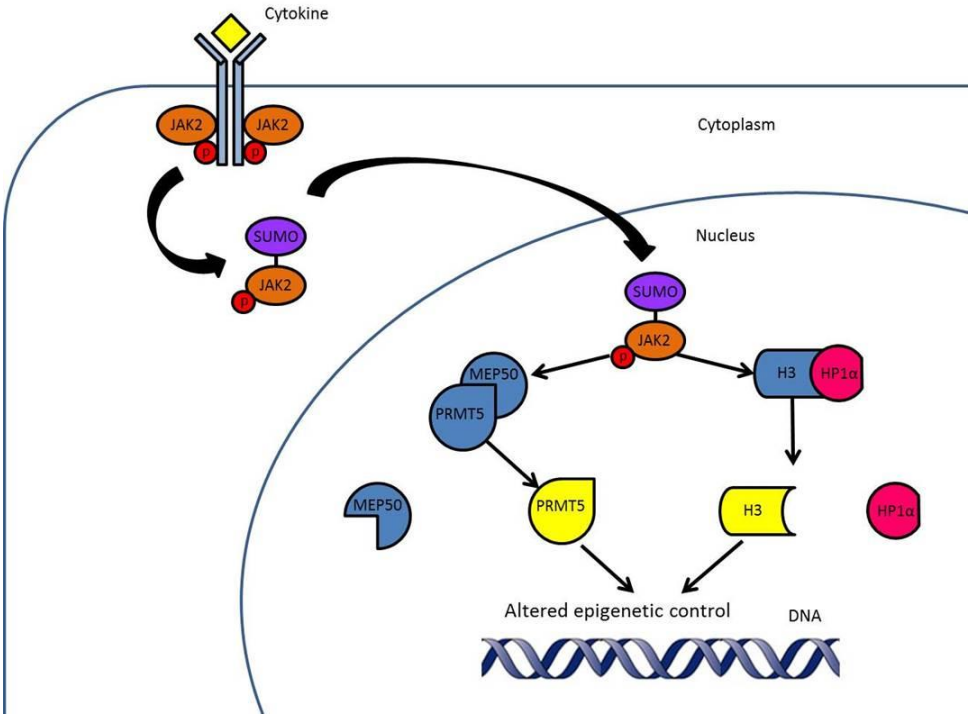


**Following activation JAK2 can be SUMOylated allowing it to enter the nucleus. JAK2 can then act on modifiers of histone activity and on histone H3 directly to alter global gene expression.**

Histones are proteins that are important in the folding and unfolding of DNA to allow transcription of the genes necessary for each individual cells function. Histones undergo a range of post-translational modifications that “switch on” or “switch off” genes within the cell[84]. On entering the nucleus it has been show that JAK2 phosphorylates a tyrosine residue on histone H3 at position 41 which leads to dissociation of the inhibiting regulatory protein heterochromatin protein 1 α (HP1α)[79] and also separates methylosome protein 50 (MEP50) and protein arginine methyltransferase 5 (PRMT5) which together act as a repressor of transcription by modifying histones, transcriptional elongation factors and the tumour suppressor p53[85]. To better characterise the effect of JAK2 in the nucleus chromatin immunoprecipitation of the phosphorylated H3Y41 (H3Y41ph) mark and parallel DNA sequencing (ChIP-Seq) was carried out. This showed distinct patterns of localisation that overlapped other recognised epigenetic and transcription factor binding patterns. In particular JAK2 localised with the H3K4me3 histone mark, an indicator of active promoter sites, and with sites that were also known STAT5 binding sites[80]. This confirmed the role JAK2 plays in gene transcription through a multi-level interaction with the STAT transcription factors and directly through alteration of histone biology.

## 1.4 Myeloproliferative neoplasms

The myeloproliferative neoplasms are a group of disorders that are characterised by the overproduction of the myeloid lineage with different genetic somatic mutations driving each of these conditions. Some of these occur only in the specific conditions, such as JAK2 Exon 12 mutations in polycythaemia vera (PV) and TEL-PDGFR in chronic myelomonocytic leukaemia (CMML), while others are associated with multiple conditions, such as t(9;22) in chronic myeloid leukaemia (CML) and acute lymphoblastic leukaemia (ALL), and JAK2 V617F in MPN, myelodysplasia (MDS) and acute myeloid leukaemia (AML). These mutations result in constitutively overactive proteins which drive an expansion of different parts of myelopoiesis resulting in disease specific phenotypes.

**Table 1.2 Myeloproliferative neoplasms and common mutations**[86]

| Subclassification | Condition | Mutations |
|---|---|---|
| BCR-ABL positive MPN | Chronic myeloid leukaemia | t(9;22) |
| BCR-ABL negative MPN | Polycythaemia vera | JAK2 V617F, JAK2 Exon 12 |
| | Essential thrombocythaemia | JAK2 V617F, CALR, MPL W515 |
| | Myelofibrosis | JAK2 V617F, CALR, MPL W515 |
| MPN/MDS overlap | Chronic myelomonocytic leukaemia | TEL-PDGFR |

### 1.4.1 Chronic myeloid leukaemia

CML is a condition characterised by expansion of the myeloid lineage and the presence of a balanced translocation between chromosomes 9 and 22 resulting in the production of the novel oncoprotein, BCR-ABL. The first clinical description of CML was attributed to John Hughes Bennett in 1845 in the Edinburgh Medical and Surgical Journal[87] who also drew the first microscope images of leukaemia. An abnormally small chromosome was identified in several patients with CML in Philadelphia in 1960[88] and was named after the city of its discovery. In 1973 it was recognised this abnormal chromosome arose from the t(9;22)[89] and in 1982 it was found that the Ableson murine leukaemia viral oncogene homolog 1 gene (*ABL*) on chromosome 9 was translocated to the breakpoint cluster region gene (*BCR*) on 22[90] resulting in the BCR-ABL fusion protein. This novel oncoprotein is a constitutively active tyrosine kinase that has effects on a large number of cellular

processes including apoptosis, proliferation, differentiation and cell adhesion. These are as a result of the effect of BCR-ABL on key signalling pathways including the JAK/STAT pathway, PI3K/Akt pathway, and Ras/Raf/MEK/Erk, which are all important in the regulation of proliferation and differentiation of myeloid cells[52]. BCR-ABL can exist in several different forms and is associated with different disease phenotypes; BCR-ABL p210 is commonly associated with CML, but can also occur in ALL. BCR-ABL p185 is typically associated with ALL[91], while BCR-ABL p230 is associated with the extremely rare chronic neutrophilic leukaemia[92]. These different versions are a result of different breakpoints in the *BCR* and *ABL* genes resulting in different molecular weight proteins. The mechanism by which these different isoforms result in different disease phenotypes is unknown.

Patients with CML may present with an asymptomatic leucocytosis identified on routine peripheral blood testing. When CML patients do present with symptoms these can be general, in the form of night sweats, fever and weight loss, or related to specific complications of disease such as abdominal discomfort from enlarged liver or spleen. CML progresses through three stages, chronic phase, accelerated phase and blast crisis. Patients can present at any stage, with about 85% presenting in chronic phase which carries a better prognosis and the remaining 15% presenting in either accelerated phase or blast crisis[93]. Patients presenting in chronic phase can be stratified as low, intermediate or high risk based on clinical parameters at presentation using several prognostication tools. These tools can be used to predict the overall survival of these patients following treatment. There are three commonly used prognostication tools used in CML; the Sokal[94], Hasford[95] and European treatment and outcomes study (EUTOS)[96] scores. All three use clinical characteristics at diagnosis, prior to any treatment. The Sokal score is based on age spleen size palpable on examination, platelet count and peripheral blood blast count, with blast count and spleen size being the strongest predictors of survival. Most patients in this cohort were treated with single agent chemotherapy, mostly busulphan[94]. The Hasford score added peripheral blood eosinophil and basophil count, with most patients here being treated with interferon α alone or in combination[95]. The EUTOS score was developed more recently with most patients in this cohort being treated within 6 months of diagnosis with a tyrosine kinase inhibitor and is based only on the peripheral blood basophil count and spleen size[96]. This final score is used to predict the likelihood

of achieving a complete cytogenetic response, which had only been achieved in a small proportion of patients prior to the introduction of TKI therapy.

Treatment of CML changed dramatically following the introduction of the tyrosine kinase inhibitor (TKI), imatinib. This is a small molecule inhibitor of BCR-ABL, with additional activity against platelet derived growth factor receptor alpha (PDGFRA)[97] and c-kit[98], that acts though competitive inhibition by blocking the ATP binding site[99]. It was developed by Novartis and entered into clinical trial use in the late 1990s and was approved for use in the treatment of CML in early 2000s. Prior to this time patients were treated with IFN-α and hydroxycarbamide, which could control the disease for a time, but did not prevent progression for the majority of patients[100]. For the majority of patients the only long term solution was allogeneic bone marrow transplantation and this was only available to patients who were both fit and had a donor option available. A proportion of patients did achieve prolonged remissions with IFN-α, but the side effects of sweats and lethargy frequently made it difficult to tolerate[100].

The introduction of imatinib changed this after it was shown it could induce deep molecular remissions and maintain them over time in patients with blast crisis CML[101] and subsequently in newly diagnosed chronic phase patients[102]. This led to the development of several other TKIs, with a total of five currently available to clinicians in the treatment of CML; imatinib, nilotinib, dasatinib, bosutinib and ponatinib. This has led to drastic alterations in the expectations of patient outcomes in CML with the majority expected to have a normal life span[103]. Unfortunately most patients need to remain on therapy lifelong as they continue to have a detectable level of BCR-ABL in the peripheral blood. Even those who manage to achieve a sustained complete molecular response will relapse following discontinuation of their imatinib in approximately 50% of cases[104].

Signalling of the JAK2 pathway in CML is enhanced by several mechanisms. BCR-ABL has a direct effect on phosphorylation of JAK2 and STAT5 as well as driving autocrine production of cytokines which signal through JAK2 associated receptors. Recently an additional mechanism has been identified in the formation of a complex between JAK2 and BCR-ABL through a third protein, Ableson helper integration site 1 (AHI-1). This complex may be important for the maintenance of

leukaemic stem cells in CML and may offer a therapeutic target for eradication of the disease[105].

### 1.4.2 BCR-ABL negative myeloproliferative neoplasms

The myeloproliferative neoplasms have been recognised as clinical entities for over a century with the first description of myelofibrosis (MF) occurring in 1879 by Heuck[106], while PV was first described in 1892 by Vaquez[107] and essential thrombocythaemia (ET) in 1934 by Epstein and Goedel[108]. Additionally a report in 1903 classified polycythaemia into primary polycythaemia, polycythaemia secondary to other causes and relative polycythaemia as a result of reduced plasma volume, which is still in use today[109].

The MPNs are conditions where there is excess proliferation of cells of the myeloid lineage. ET is characterised by thrombocytosis with or without leukocytosis, while PV has an increase in red cell mass with or without thrombocytosis and leukocytosis. MF is often associated with cytopenias, but can also have thrombocytosis or leukocytosis and is diagnosed by the presence of reticulin fibrosis on bone marrow trephine. All three conditions can be associated with splenomegaly, cytokine driven symptoms, such as sweats, fevers and lethargy, chronic inflammation and thrombotic complications. The diagnosis of these conditions was purely based on clinicopathological appearances which included peripheral blood and bone marrow appearances in combination with the clinical history leading to the generation of clinical guidelines to improve diagnostic accuracy[86]. In 2005 a point mutation in exon 14 of the JAK2 gene was identified and reported by 4 groups[110,111,112,113]. This mutation causes a substitution of phenylalanine for valine at position 617 (JAK2 V617F), resulting in loss of the inhibitory effect of the pseudokinase domain and constitutive activation of the JAK2 tyrosine kinase, leading to chronic uncontrolled activation of the JAK2/STAT pathway without the need for receptor activation by ligand.

**Figure 1.8 Structure of JAK2 protein**

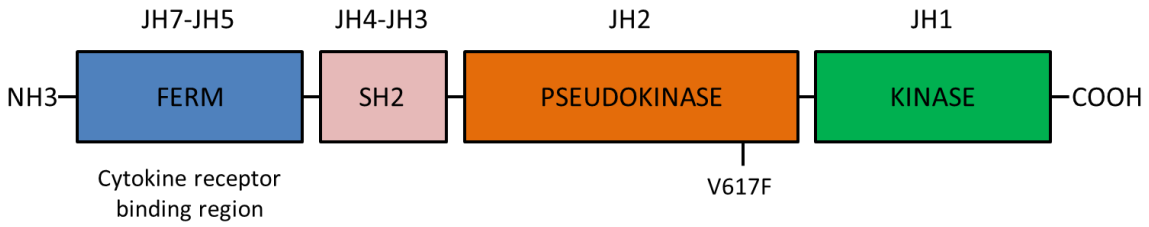


**JAK2 is a tyrosine kinase with a typical structure. The FERM domain allows localisation with the cytokine receptor while the SH2 domain allows docking of proteins phosphorylated by JAK2. The pseudokinase domain negatively regulates the kinase activity of JAK2 and the kinase domain contains the active site of JAK2. FERM 4.1 – ezrin – radixin – moesin, SH2 Src Homology 2.**

The JAK2 V617F mutation is the most common, occurring in 97% of PV patients, 60% of ET patients and 60% of MF patients and led to a search for additional mutations associated with MPN. This has led to an additional three groups of driver mutation being identified; the JAK2 exon 12 mutations occur in 2% of JAK2 V617F negative PV patients and have a distinct clinical phenotype compared to the V617F positive patients[114], activating mutations of the gene for the TPO receptor, *MPL*, which signals through JAK2, and is mutated in 5-10% of ET and MF patients[115,116], and calreticulin mutations occurring in 25-30% of ET and MF[117]. Calreticulin is involved in calcium homeostasis in the endoplasmic reticulum[118], however the mutated form of the protein found in MPN is able to activate the MPL receptor directly leading to activation of JAK2 and STAT[119]. As a result these patients retain a gene expression profile associated with JAK/STAT signalling confirming that this pathway remains the key driver of disease[120]. One of these four mutations is required to initiate and maintain disease and they rarely occur simultaneously. Additional mutations are seen in MPN (ASXL, IDH1/2, SRSF2) which affect prognosis when present, but are not required to initiate disease[121,122]. Interestingly there is evidence that suggests the clinical course of disease is altered by the order in which mutations are acquired[123]. The discovery of these mutations has led to incorporation of them into diagnostic algorithms and as prognostic markers, particularly in MF where patients with the CALR mutation have a better prognosis than those with JAK2 or MPL mutations and those with no identifiable driver mutation doing worse than either group. The additional

mutations attenuate these risks and worsen the prognosis if found with any of the driver mutations[124,125].

Many of these patients are asymptomatic or have low grade chronic symptoms which they attribute to minor complaints. As a result patients are often diagnosed when bloods are done for another reason or when they present with a complication directly attributable to the underlying MPN, particularly arterial or venous thrombosis although the latter is becoming less common with increasing use of routine blood testing in the community.

The seriousness of arterial or venous thrombosis as a complication underlies the current treatment recommendations for PV where patients are started on cytoreductive therapy due to the high risk for thrombotic complications, with age and previous vascular events being the best predictors for further thrombosis[126]. The efficacy of low-dose aspirin to reduce thrombosis was shown in the ECLAP study[127], where 100mg aspirin daily was shown to reduce the risk of non-fatal myocardial infarction and stroke or death from cardiovascular causes by 41%. At present there is no definite predictive model for risk of transformation to MF or to AML although higher leucocyte count has been associated with an increased risk of fibrotic transformation[128]. Therefore the aim of therapy is to minimise further arterial and venous thrombotic events through antiplatelet therapy and aggressive management of cardiac risk factors for all patients in combination with cytoreduction.

The mechanism underlying thrombosis is complex. Peripheral counts have a part to play as a result of altering the viscosity of blood. There is also evidence showing that controlling counts, particularly platelets and leucocytes, in the normal range reduces the risk of thrombosis[127], however the fact that this risk does not return to baseline for age suggests there is more contributing to the risk. The JAK2 V617F mutation has been shown to play a role in thrombosis with ET patients who are JAK2 V617F positive being more likely to have a thrombotic event than those who are negative. In patients with PV a higher JAK2 V617F allele burden is associated with an increased risk of thrombosis particularly in those with an allele burden over 75%. Additionally there is evidence that a higher leukocyte count is associated with an increase in the risk of thrombosis, although there is no evidence that

reduction to the normal range of the leucocytes results in a reduction in thrombosis risk.

In the last decade there has been increasing interest in the inflammatory state associated with MPN. Patients have elevated inflammatory cytokine (IL-6, IL-18, TNF-α) and elevated markers of inflammation (CRP, pentraxin 3). Interestingly there is evidence suggesting a link with higher levels of inflammatory cytokines and increased risk of thrombosis which is unrelated to peripheral blood cell counts. There is clear evidence that increased peripheral counts increases the risk of thrombosis which is thought to relate to rheological abnormalities induced by increased blood viscosity related to elevated counts. However there is clear evidence that platelets and white cells are more active than normal with ET and PV patients excreting increased thromboxane A2 metabolites, and neutrophils expressing higher levels of CD11b, a marker of activation.

**Figure 1.9 Model of MPN associated thrombophilia**

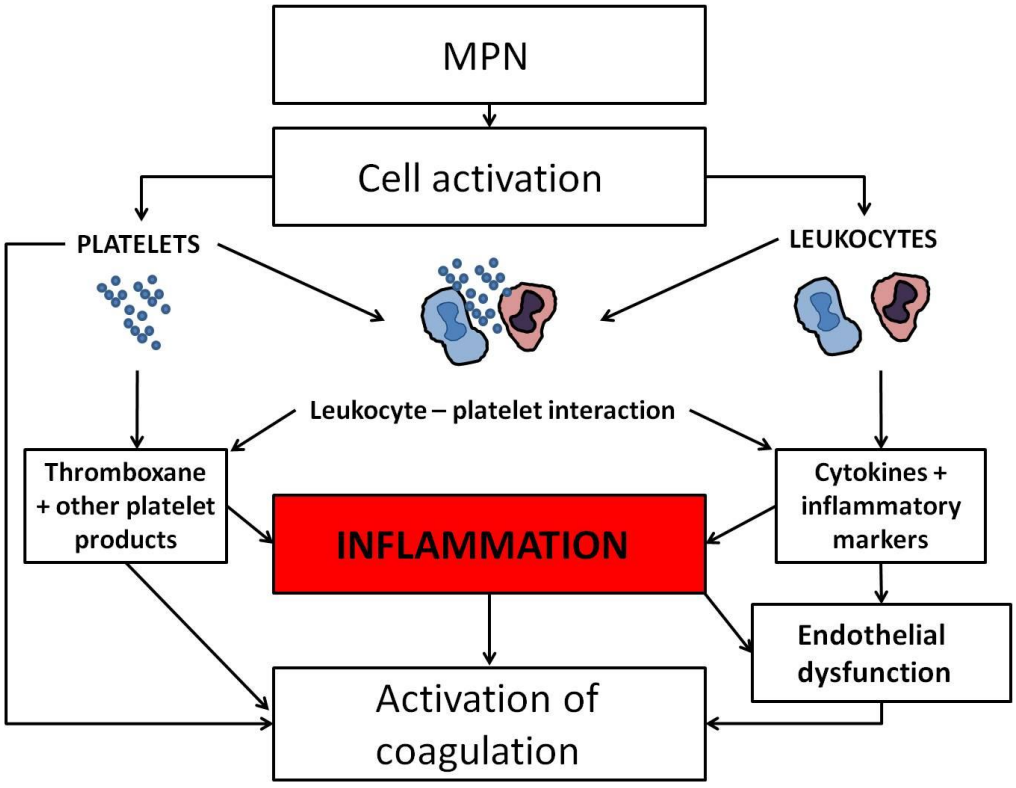


**A model of the thrombophilia associated with MPN showing the central role of inflammation in combination with platelet and leukocyte activation as drivers of endothelial dysfunction and risk of thrombosis.**

The MPNs occur in between 0.5-1.5 per 100,000 per year in Western populations. Population studies prior to the introduction of the JAK2 inhibitor ruxolitinib show an overall median survival of about 6 years from diagnosis for MF[35] compared to 14 years for PV[34] and almost 20 years for ET[36]. All three conditions have a median survival less than age matched controls[36]. The commonest causes of death for these patients are thrombosis, haematological malignancy and second non-haematological malignancy[34].

All patients have an increased risk of thrombosis with arterial and venous events being a common presenting complaint of patients, with the MPN diagnosis being suspected on admission bloods. The underlying cause of thrombosis is thought to be partly related to the elevated counts and certainly it is recognised that controlling peripheral counts with cytoreductive therapy or therapeutic venesection can reduce the risk of thrombotic events, however patients with MPN continue to have a higher than expected risk of thrombotic events. It is thought this is a major contributor to the documented poorer life expectancy seen in these patients compared to age matched controls in ET and PV[129].

The current treatment options for ET and PV remain largely unchanged over the last few decades with cytoreduction using venesection (PV only), hydroxycarbamide or anagrelide as appropriate. Venesection controls the production of red cells by inducing a therapeutic iron deficiency, but can also cause cognitive impairment and restless legs. Hydroxycarbamide inhibits ribonuclease reductase resulting in a decrease in the production of deoxyribonucleotides, which in turn leads to a reduction in DNA synthesis and control of the peripheral counts, with potential side effects of cytopenias, gastrointestinal upset and skin ulceration. Anagrelide is only used to control the platelet count as it inhibits the maturation of platelets from megakaryocytes, although the precise mechanism underlying this is unclear. None of these therapies alter the natural history of the disease or affect disease burden[130,131].

The identification of the JAK2 V617F mutation as the driver of myeloproliferative neoplasms and the success of imatinib in CML led to the development of JAK2 specific inhibitors to use in the treatment of these disorders. The first to successfully enter routine clinical use for the treatment of symptomatic MF was ruxolitinib[132], a specific inhibitor for JAK1 and JAK2, which has been shown to

have a significant improvement in symptoms burden in patients with MF. It has also shown some survival benefit for these patients, thought to be as a result of improved nutritional status[132]. Unfortunately about 50% of patients who start ruxolitinib have to stop it either as a result of cytopenias, through other side effects or through lack of efficacy[132].

Trials have been done looking at ruxolitinib in patients with PV who were intolerant of or had an inadequate response to hydroxycarbamide therapy with the RESPONSE trial looking at 222 patients randomised to ruxolitinib or best available therapy (BAT) and assessing symptom improvement, spleen size reduction and haematocrit control. The patients treated with ruxolitinib had a higher rate of complete haematological response, improvement in symptoms and reduction in allele burden compared to those treated with BAT. This indicates that in PV there are patients who will benefit from therapy with ruxolitinib[133], which has recently been licenced for PV patients who are intolerant or unresponsive to hydroxycarbamide. Other JAK2 inhibitors have entered clinical trial, but have had to be withdrawn due to unacceptable side effects. Fedratinib was withdrawn after patients on the JAKARTA trials developed significant neurological toxicity[134]. Pacritinib was also recently put on clinical hold by the FDA following deaths from cardiac complications[135].

It has long been recognised that over the course of the disease the MPNs can transform. Most commonly this is ET to PV or MF, or PV into MF, but all three can transform directly to AML (Figure 1.10), which tends to be poorly responsive to current chemotherapies and therefore has a poor outcome[136]. This is particularly the case for older or less physically fit patients as the option of allogeneic bone marrow transplantation is not available, which remains the only real curative option for these patients.

**Figure 1.10 Progression of MPN**

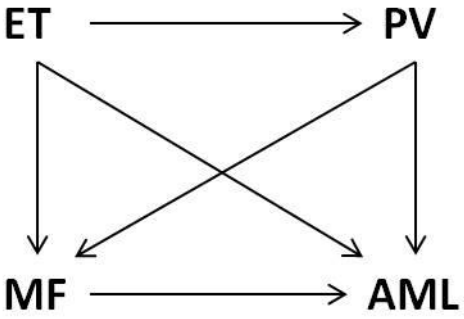


**The myeloproliferative neoplasms can transform as shown above. This occurs in approximately 10% of patients, with the majority of patients continuing with the condition they were first diagnosed with.**

The mechanism behind transformation is complex. There appears to be an increased JAK2 V617F mutation allele burden with progression from ET, through PV into MF, and patients presenting with *de novo* ET tend to have a lower allele burden than those with either de novo PV or MF, suggesting that the increase in aberrant JAK2 signalling leads to an alteration of phenotype and worsening severity of disease[137]. In addition to this there is often acquisition of additional mutations as the disease progress[136]. It is felt these are as a result of genomic instability consequent on the increased proliferation and reduced apoptosis associated with these conditions.

### 1.4.3 Malignant JAK/STAT signalling

Abnormal signalling through the JAK/STAT pathway has been found to be important in many malignancies, both haematological[138] and solid tumours[139,140]. In myeloid malignancies aberrant JAK2 signalling is associated with poor prognosis in AML[141], and has been shown to be important in the maintenance of CML[105,2]. Activating mutations of JAK2 have been found in ALL[142] as well as MPN[111], and various translocations involving JAK2 have been described in atypical CML[143], AML and ALL[144]. Amplification at 9p24, the gene locus containing JAK2, has been shown to confer a worse outcome for breast cancer patients[139] and inhibition of JAK2 and STAT3 increases apoptosis in colon cancer cells *in vitro*[145,146].

## 1.5 Inflammation

Immunity is a complex process that developed to combat infective micro-organisms and is tightly controlled in normal circumstances to prevent damage to self. There are two major components to the immune response, an innate response designed to immediately mobilise to remove any infection[147], and adaptive immunity, which results in production of antibodies, therefore taking longer to initiate but is specific for each pathogen[148]. Innate immunity involves predominantly neutrophils, monocytes and macrophages, although macrophages are also important in triggering the adaptive immune system[147]. The adaptive immune system is mediated by T and B lymphocytes and results in antibody production which is specific for an individual pathogen. Inflammation results from the influx of immune cells of the innate response to the affected area and is characterised by localised swelling, erythema, pain and heat. Inflammation is part of the innate immune system and is mediated by granulocytes and the inflammatory cytokines released by these cells which help to control local tissue damage or infection. In most cases inflammation is localised to the area of damage, but in certain circumstances such as disseminated infection or in many rheumatological conditions inflammation occurs throughout the body. In the context of widespread infection treatment of this with antimicrobials will remove the trigger for inflammation and allow symptoms to settle. However in many incurable medical conditions there is chronic inflammation associated with an abnormal response within the body.

### 1.5.1 Inflammation in MPN

In MPN the presence of the JAK2 V617F mutation leads to an alteration in the signalling of haematopoietic cells important in inflammation with evidence of alteration of neutrophil reactive oxygen species generation[149], alteration in serum inflammatory cytokine levels[150] and an altered reactivity to these cytokines[48]. Of interest is the fact that the malignant clone is not the sole source of inflammatory cytokine production. MPN cells alter the surrounding stromal cells in the bone marrow to produce more inflammatory cytokines which give a survival advantage to the MPN clone compared to normal cells. This includes the production of TNF-α which reduces the proliferative activity of normal haematopoietic cells, but MPN cells are resistant to this and may actually proliferate more in the presence of TNF-α[151]. This chronic inflammation is implicated in the thrombotic complications and

progression of MPN to acute leukaemia[152]. The incidence of cardiovascular event has been found to be increased in the presence of chronic inflammation in other conditions such as rheumatoid arthritis[153] and cardiovascular disease itself is now viewed as an inflammatory disease of the endothelium[154]. In MPN the chronic inflammation, in addition to excessively reactive platelets, hyperviscosity from elevated red cell and white cell counts and altered vessel rheology combine to make thrombosis a particular issue for patients[155]. In addition to this the chronic inflammatory milieu results in damage to HSCs leading to attrition of the HSC numbers and may be the driver for the development of AML, which in MPN rarely retains the driver mutation responsible[156].

## 1.6 Promyelocytic leukaemia protein and SUMOylation

Within eukaryotic cells there are a number of sub-nuclear structures which exist to carry out specific functions within the nucleus. These nuclear bodies include nucleoli, Cajal bodies, splicing speckles and PML nuclear bodies (NB)[157] and are involved in regulating and coordinating many aspects of normal nuclear functioning. PML NBs comprise multiple PML units in combination with Sp100 and SUMO 1, 2 and 3 chains[158]. These SUMO chains are important in maintaining the structure of the NBs but also interact with other proteins that localise there[158]. At least 50 other proteins have been shown to interact with NBs, involved in numerous cellular processes, including apoptosis, by potentiating signalling via FAS ligand[159] and TNF-α[160], DNA repair[161], transcriptional control by sequestering or marking for degradation transcriptional regulators, p53 function through inhibition of mouse double minute 2 (MDM2) and post-translational modification of p53[162], and response to viral infections through the type I and II IFNs[163]. As a result dysfunction of these nuclear bodies has been related to numerous pathological processes. Generally PML is viewed as a tumour suppressor as a result of these functions. This is confirmed by the finding that solid tumours have abnormally low or absent levels of PML[164]. The exception to this is leukaemia stem cells in CML, where there is an unexpectedly high level of PML mRNA transcripts[165].

An important disease that led to the identification of PML, is acute promyelocytic leukaemia (APML)[166,167], a rare acute myeloid leukaemia characterised by a translocation between chromosomes 15 and 17. The product of this translocation

was found to be a fusion protein combining PML with the retinoic acid receptor α (PML-RARA). This fusion protein led to disruption of the normal PML nuclear body structure and dispersal of the fusion protein throughout the nucleus[168]. This abnormality seemed to be sufficient to produce the entire clinical phenotype of maturation arrest and uncontrolled proliferation of abnormal promyelocytes indicating an important role for PML NBs in myeloid proliferation and differentiation[169].

Other that the pathogenic role in APML and unexpectedly high levels in CML stem cells, little is known about PML in myeloid malignancies. In MPN the chronic inflammation seen would be expected to increase the levels of PML. In addition to this the requirement for SUMOylation to allow JAK2 to enter the nucleus would allow JAK2 to interact with PML NBs, raising the possibility that JAK2 and PML interact directly to facilitate the nuclear effects of JAK2.

## 1.7 Aims

The overall aim of this study is to investigate novel effects of JAK2 overactivity in two haematological malignancies with increased JAK2 signalling; CML, where there is increased stimulation of normal JAK2, and PV, where there is constitutive activity as a result of the JAK2 V617F.

1. To identify and characterise a direct JAK2 gene expression profile, and investigate if this is deregulated in myeloid malignancies with increased JAK2 activity.

2. To examine the functional effects of JAK2 inhibition in myeloid malignancies.

3. To explore the hypothesis that JAK2 may interact with PML and elicit its direct effects within the nuclear bodies.

4. To investigate the inflammatory phenotype seen in JAK2 V617F positive PV.

5. To examine the function of innate immune cells in JAK2 V617F positive PV.

# 2. Materials and Methods

## 2.1 Materials

### 2.1.1 Small molecule inhibitors

Ruxolitinib, TG101209 and AT9283 were obtained from Stratech Scientific Ltd in powder form. Nilotinib was provided under MTA from Novartis Pharma. All inhibitors were dissolved in DMSO and stored at -20$^0$C as a stock solution of 10mM. $As_2O_3$ was dissolved in 1M NaOH at a concentration of 100mM. This was made fresh for each use of the inhibitor. All inhibitors were diluted to final concentration in complete media for the cell type being treated.

### 2.1.2 Tissue culture supplies

| Company | Reagent | Catalogue no |
|---|---|---|
| Life Technologies, UK | Roswell Park Memorial Institute (RPMI) 1640 media | 21875-034 |
| | Iscove's Modified Dulbecco's Medium (IMDM) | 21980-032 |
| | L-Glutamine | 25030-081 |
| | Sterile water | A12873-04 |
| | Foetal bovine serum (FBS) | 10270-106 |
| | Phosphate buffered saline (PBS) | 10010015 |
| Promocell, Germany | Monocyte Attachment Medium | C-28051 |
| | Macrophage Base Medium DXF | C-28057 |
| | Macrophage Detachment Solution DXF | C-41330 |
| Stem Cell Technologies, UK | Stemspan SFEM II | 09655 |
| Labtech, UK | Biosera foetal calf serum (FCS) | FB-1001S |
| Sigma Aldrich, UK | Horse serum | H1138 |
| | Histopaque®-1077 | 10771 |
| | XTT salt (2,3-Bis-(2-Methoxy-4-Nitro-5-Sulfophenyl)-2H-Tetrazolium-5-Carboxanilide) | X4626 |
| | Phenazine methosulphate | P9625 |
| | Arsenic trioxide | A1010 |
| | Lipopolysaccharides from *E. Coli* | L5293 |

| | | |
|---|---|---|
| | 0111:B4 | |
| Peprotech, UK | Human IL-3 | 200-03 |
| | Human IL-4 | 200-04 |
| | Human IL-6 | 200-06 |
| | Human G-CSF | 300-23 |
| | Human GM-CSF | 300-03 |
| | Human M-CSF | 300-25 |
| | Human stem cell factor (SCF) | 300-25 |
| | Human FLT-3 ligand (FLT-3L) | 300-19 |
| | Human IFN γ | 300-02 |
| Greiner Bio One, UK | 25mm$^3$ tissue culture flasks | 690175 |
| | 75mm$^3$ tissue culture flasks | 658175 |
| | 75mm$^3$ suspension cell culture flasks | 658195 |
| | 6 well plates | 657160 |
| | 12 well plates | 665180 |
| | 24 well plates | 662102 |
| | 96 well plates | 655180 |
| Thermo Fisher Scientific, UK | Nunc 25mm$^3$ flasks | 136196 |
| | Nunc 75mm$^3$ flasks | 178905 |
| | Delta-coated 6 well plates | 140685 |
| | Delta-coated 24 well plates | 142485 |
| | 8-well Nunc™ Lab-Tek™ II Chamber Slide™ | 154534 |
| | Sodium hydroxide | 10396240 |
| | Portex Kwill filling tube | 1317493 |
| Stratech | Ruxolitinib | S1378-SEL |
| | TG101209 | S2692-SEL |
| | AT9283 | S1134-SEL |
| Miltenyi | LS columns | 130-042-401 |
| | CliniMACS® CD34 reagent | 171-01 |
| Acros Organics | Dextran, high fraction | AC40626 |
| Octapharma | Human serum albumin 20% (Albunorm) | PL10673/0031 |
| Bio-Rad | Bio-Plex Pro™ Human Cytokine 27-plex Assay | M500KCAF0Y |
| | Bio-Plex Pro™ Human IFNα2 | |

| | | |
|---|---|---|
| | Bio-Plex Pro™ Human Gro-α | |
| Molecular Devices | SpectraMax M5 Microplate Reader<br>SoftMax Pro | |

### 2.1.3 Flow cytometry reagents

| Company | Reagent | Catalogue no |
|---|---|---|
| BD Bioscience, UK | Annexin V FITC | 556420 |
| | 7-AAD | 559925 |
| | Propidium iodide (PI)/RNase staining buffer | 550825 |
| | Mouse anti-human CD14 FITC | 555397 |
| | Mouse anti-human CD16 APC | 561304 |
| | Mouse anti-human CD68 FITC | 562117 |
| | Mouse anti-human CD80 PE-Cy7 | 561135 |
| | Mouse anti-human CD86 BV421TM | 562432 |
| | Mouse anti-human CD163 PerCP-CyTM 5.5 | 563887 |
| | Mouse anti-human CD206 PE | 555954 |
| | Mouse anti-human CD34 APC | 555624 |
| | Mouse anti-human CD45-FITC | 555482 |
| | FACSCanto | |
| eBioscience | Affymetrix Ultracomp beads | 01-2222-41 |
| PAA | Hanks buffered saline solution (HBSS) | H15-008 |
| | | |

### 2.1.4 Polymerase chain reaction reagents

| Company | Reagent | Catalogue no |
|---|---|---|
| Qiagen | RNEasy Plus mini kit | 74134 |
| | RNEasy Plus micro kit | 74034 |
| | Multiplex PCR kit | 206143 |
| Life Technologies | Superscript® III reverse transcriptase | 18080-044 |
| | RNaseOUT™ recombinant ribonuclease inhibitor | 10777-019 |
| | GeneAmp® dNTP blend | N8080260 |

| | | |
|---|---|---|
| | PicoPure® RNA isolation kit | KIT0204 |
| Fluidigm | 2x Assay loading reagent<br>20x DNA binding dye | 85000736<br>100-3783 |
| Bio-Rad | SsoFast™ EvaGreen Supermix with low ROX | 1725210 |
| New England BioLabs | Exonuclease I (E. coli)<br>Exonuclease I reaction buffer | M0293<br>B0293 |
| Integrated DNA Technologies | Custom Oligo-dT | |

### 2.1.5 Immunoblotting

| Company | Reagent | Catalogue no |
|---|---|---|
| Sigma Aldrich | Ammonium persulphate (APS) | A9164 |
| | Sodium azide | S8032 |
| | N,N,N′,N′-Tetramethylethylenediamine (TEMED) | T9281 |
| | Glycerol | G6279 |
| | Ponceau S | P7170 |
| | Sigma 7-9® | T1378 |
| | Sodium dodecyl sulfate (SDS) | L3771 |
| | Glycine | G8898 |
| | Sodium Chloride | S7653 |
| | Bromophenol blue | 114391 |
| | 2-Mercaptoethanol | M7522 |
| | Ethylenediaminetetraacetic acid disodium salt dehydrate (EDTA) | E5134 |
| | Methanol | 24229 |
| | Phenylmethanesulfonyl fluoride (PMSF) | P7626<br>590088 |
| | Sodium metavanadate | S7920 |
| | Sodium Fluoride | 243655 |
| | Sodium Molybdate | P4265 |
| | Pepstatin A | A1153 |
| | Aprotinin | L2884 |

| | | |
|---|---|---|
| | Leupeptin<br>Soyabean trypsin inhibitor<br>NP-40 | T9777<br>T6522<br>NP40 SIGMA |
| Roche | Bovine Serum Albumin Fraction V | 10735094001 |
| Marvel | Skimmed milk powder | |
| Santa Cruz | Rabbit anti-human JAK2 antibody<br>Mouse anti-human PML antibody<br>Rabbit anti-human STAT1 antibody<br>Rabbit anti-human STAT5 antibody<br>Mouse anti-human B-Actin antibody<br>Rabbit anti-human SHPTP2 antibody | sc-294<br>sc-966<br>sc-343<br>sc-835<br>sc-47778<br>sc-280 |
| Cell signalling | Rabbit anti-human phospho-STAT1 antibody<br>Rabbit anti-human phospho-STAT5 antibody<br>PathScan® BCR-ABL activity assay | 7649<br>9351<br>5300 |
| Abcam | Mouse anti-human SUMO 2/3 antibody | ab81371 |
| Millipore | Rabbit anti-human phospho-JAK2 antibody<br>Rabbit anti-human JAK2 antibody<br>Immobilon™ Western Chemiluminescent HRP substrate | 04-1098<br>06-1310<br>WBKLS0500 |
| Thermo Fisher Scientific | Mouse anti-human JAK2 antibody<br>CL-XPosure™ Film | MA5-15632<br>34089 |
| Dako | Goat anti-rabbit HRP conjugated antibody<br>Goat anti-mouse HRP conjugated antibody | P0448<br>P0447 |
| GE Healthcare Life Sciences | Amersham Protran 0.45Nitrocellulose membrane<br>Whatman™ 3mm CHR blotting paper | 10600002<br>3030-917 |
| Bio-Rad | Quick Start Bradford Protein Assay Kit | 500-0201 |
| Kodak | Autoradiography Cassette | |
| Konica Minolta | Xomat SRX-101A Developer | |

### 2.1.6 Immunofluorescence and Duolink

| Company | Reagent | Catalogue no |
|---|---|---|
| Sigma Aldrich | Poly-L-Lysine | P9155 |
| | Sodium tetraborate | 221732 |
| | Ovalbumin | A5378 |
| | Triton X-100 | T9284 |
| | Sodium azide | S8032 |
| | Duolink® in-situ PLA® probe anti-mouse MINUS | DUO92004 |
| | Duolink® in-situ PLA® probe anti-rabbit PLUS | DUO92002 |
| | Duolink® in-situ detection reagents RED | DUO92008 |
| | Duolink® in-situ mounting medium with DAPI | DUO82040 |
| C. A. Hendley | 10 well multispot slides | PH088 |
| Roche | Bovine Serum Albumin Fraction V | 10735094001 |
| GPR | Paraformaldehyde | 294474L |
| Thermo Fisher Scientific | Acetone | 10162180 |
| Vector Laboratories | Vectashield® mounting media with DAPI | H-1200 |
| Santa Cruz | Rabbit anti-human JAK2 antibody | sc-294 |
| | Mouse anti-human PML antibody | sc-966 |
| | Normal mouse IgG | sc-2025 |
| | Normal rabbit IgG | sc-2027 |
| Abcam | Mouse anti-human SUMO 2/3 antibody | ab81371 |

# 2.2 Preparation of media and solutions

## 2.2.1 Tissue culture cells and media

### 2.2.1.1 Cell lines

| Cell line | Origin | Karyotype |
|---|---|---|
| K562 | Established from pleural effusion of patient with blast crisis CML | 61-68<3n>XX, -X, -3, +7, -13, -18, +3mar, del(9)(p11/13), der(14)t(14;?)(p11;?), der(17)t(17;?)(p11/13;?), der(?18)t(15;?18)(q21;?q12), del(X)(p22) |
| UKE1 | Established from peripheral blood of patient with ET at leukaemic transformation and retaining JAK2 V617F mutation | 48 XX, +8, +19 [14]<br>45 XX, -7, del(11)(p14) [8] |
| SET2 | Established from peripheral blood of patient with ET at leukaemic transformation and retaining JAK2 V617F mutation | 46-47<2n>XX, +13, -14, +21, +mar, add(4)(p15), der(5)t(5;19)(q11;q13), der(7)t(7;14)(q31;q11), del(9)(p11p24)ins(9;?21)(p11;p11p12), add(9)(q11)t(9;22)(p24;q12), der(13)del(13)(q11-q13)t(13;21)(q34;q11-12), der(13)t(13;21)(q34;q11-12), ins(16;9)(q22;?p23p24), der(19)t(9;19)(p24;q13), ider(?21;9)(p10p13;p24), der(21)r(21;9)(p1?1q1?1;p24p2?3); carries multiple rearrangements affecting 9p24 amplification; resembles published karyotype |

#### 2.2.1.2 Media for cell lines

| Cell line | Complete media | Volume |
|---|---|---|
| K562 | RPMI 1640 | 500ml |
| | FBS | 50ml |
| | L-Glutamine | 5ml |
| UKE1 | IMDM | 500ml |
| | FCS | 50ml |
| | Horse serum | 50ml |
| | L-Glutamine | 5ml |
| SET2 | RPMI 1640 | 500ml |
| | FCS | 100ml |
| | L-Glutamine | 5ml |

#### 2.2.1.3 Resuspension solution

| | |
|---|---|
| Human serum albumin 20% | 50ml |
| PBS | 950ml |
| EDTA | 1mM |

#### 2.2.1.4 Freezing solution for CML CD34 cells

| | |
|---|---|
| Human serum albumin 5% | 40ml |
| DMSO | 10ml |

#### 2.2.1.5 Media for CML primary samples

| **High growth factor media** | |
|---|---|
| Stemspan II | 20ml |
| SCF 100ng/ml | 200µl |
| FLT-3L 100ng/ml | 200µl |
| IL-3 20ng/ml | 40µl |
| IL-6 20ng/ml | 40µl |
| G-CSF 20ng/ml | 40µl |
| **Low growth factor media** | |
| Stemspan II | 30ml |
| SCF | 3µl |
| FLT-3L | 3µl |
| IL-3 | 0.6µl |
| IL-6 | 0.6µl |
| G-CSF | 0.6µl |

#### 2.2.1.6 Macrophage generation

| **M1 polarisation** | |
|---|---|
| Macrophage Base Medium DXF | |
| GM-CSF | 5ng/ml |
| **M1 stimulation** | |
| Macrophage Base Medium DXF | |
| LPS | 100ng/ml |
| IFN-γ | 20ng/ml |
| **M2 polarisation** | |
| Macrophage Base Medium DXF | |
| M-CSF | 50ng/ml |
| **M2 stimulation** | |
| Macrophage Base Medium DXF | |
| M-CSF | 10ng/ml |
| IL-4 | 20ng/ml |

## 2.2.2 Tissue culture solutions

### 2.2.2.1 DAMP solution for thawing cryopreserved CD34+ cells

| | |
|---|---|
| DNase II solution | 2ml |
| $MgCl_2$ 1M | 1.25ml |
| Trisodium citrate 0.155M | 53ml |
| Human serum albumin 20% | 25ml |
| PBS without $Ca^{2+}$ or $Mg^{2+}$ | 418.75ml |

## 2.2.3 Flow cytometry solutions

### 2.2.3.1 PBS + 2% FBS

| | |
|---|---|
| PBS | 49ml |
| FBS | 1ml |

## 2.2.4 PCR solutions

### 2.2.4.1 Reverse transcription mix 1

| | |
|---|---|
| Oligo dT | 1µl |
| dNTPs | 1µl |
| RNA | 500ng |
| RNase free water | 12µl – RNA volume |

### 2.2.4.2 Reverse transcription mix 2

| | |
|---|---|
| 5x buffer | 4µl |
| DTT | 1µl |
| RNase | 0.5µl |
| Superscript III | 0.5µl |

### 2.2.4.3 Pre-amplification mix

| | |
|---|---|
| Qiagen Multiplex PCR master mix | 2.5µl |
| 500nM pooled primers | 0.5µl |
| RNase free water | 0.75µl |
| cDNA | 1.25µl |

#### 2.2.4.4 Exonuclease treatment

| | |
|---|---|
| RNase free water | 1.4µl |
| Exonuclease I reaction buffer | 0.2µl |
| Exonuclease I (E. coli) | 0.4µl |

#### 2.2.4.5 Assay mix for Fluidigm qRT PCR

| | |
|---|---|
| 2x Assay loading reagent | 3µl |
| TE buffer | 0.3µl |
| Mixed forward and reverse primer | 2.7µl |

#### 2.2.4.6 Sample mix for Fluidigm qRT PCR

| | |
|---|---|
| 20x DNA binding dye | 0.3µl |
| SsoFast™ EvaGreen Supermix with low ROX | 3µl |
| Pre-amplified sample | 2.7µl |

#### 2.2.4.7 Primer list

| Gene | Primer pair (5'-3') |
|---|---|
| *AURA* | ggcaaacacataccaagagacc<br>gctcagagaagtacttgaacac |
| *AURB* | ggaagacaatgtgtggcacc<br>gcatcacacaacgagacctatc |
| *B2M* | ttgtctttcagcaaggactgg<br>atgcggcatcttcaaacctcc |
| *BACH* 1 | gagacagtgaatcctgttcagc<br>gcacaagcttactccagaacag |
| *BCL2* | gagaaatcaaacagaggccg<br>ctgagtacctgaaccggca |
| *BCL2L1* | ggtgagtcggatcgcagc<br>cagcggttgaagcgttcc |
| *BID* | ggaaccgttgttgacctcac<br>gaggagcacagtgcggat |
| *BNIP3L* | gtatcagactggtccagtagacc<br>ccgcagaatttctgaaggtgttc |
| *CCNA2* | ctaccatgaggatattcacacatacc<br>gttctcctacttcaactaaccagtcc |
| *CCND1* | tgcatctacaccgacaactcc<br>ggagaacaaacagatcatccgc |
| *CCND2* | tacaccgacaactccatcaagc<br>cctcatgacttcattgagcacat |
| *CCNF* | cacaaagcatccatattgcactgc<br>gtaggagctggtcagacatcc |

| | |
|---|---|
| *CDC25B* | gaatcctccgaatcttctgatgc<br>atagactggaagcgtctgatgg |
| *CDK1* | aactacaggtcaagtggtagcc<br>ggatgtgcttatgcaggattcc |
| *CDKN1B* | ggctaactctgaggacacgc<br>gcaaccgacgattcttctactca |
| *CDYL* | tgtgcttgaggaatccaaagcc<br>ggatggactccatgttaaagtacttg |
| *CENPF* | gccaagaatatgcacaacgtcc<br>cattctccttgatctgactcgc |
| *CISH* | catagccaagaccttctcctacc<br>tgacagcgtgaacaggtagc |
| *CRLF2* | gtgcaggtgacatggaatgc<br>agagaatgtcgtctcgctgc |
| *DHX9-DEAH* | caactggaatccttggactagtagc<br>gcaagcaatcttgcaggagag |
| *DUSP1* | catcaagaatgctggaggaagg<br>aggcgaagcatcatctctcc |
| *EGR1* | atccacacaggccagaagc<br>gatcttggtatgcctcttgc |
| *EGR2* | ttgaccagatgaacggagtg<br>tggtttctaggtgcagagacg |
| *ENOX2* | gagctggagggaacctgattt<br>cactggcactaccaaactgca |
| *EZH2* | ctgaggatgtggatactcctcc<br>gctcctctaaccatgtttacaactatc |
| *FOXM1* | ggatgtgaatcttcctagaccacc<br>ccaacatccagtggcttcga |
| *FOXO3A* | cggaccttcatctctgaactcc<br>ggacctgctcacttcggact |
| *GAPDH* | acggatttggtcgtattggg<br>attttggagggatctgctc |
| *GBP1* | aggccacatcctagttctgc<br>tccaggagtcattctggttgt |
| *GBP2* | ccaggaggttaccgtctcttt<br>gccacatcctccttggact |
| *GCSF* | actctggacagtgcaggaagc<br>tggcacagcttgtaggtggc |
| *GCSFR* | aagcatgtccccacaactgtgtc<br>tgattatgtgcaggcctgg |
| *GMCSF* | gtcatctcagaaatgtttgacctcc<br>ttgtagtggctggccatcatgg |
| *GDF3* | ctctctcaacagctccaattatgc<br>gctctaccaggacaataatgacaat |
| *GN2BL* | tccacaccttgaccagcttg<br>gcagattgtctctggatctc |
| *HDAC3* | ctgtgtaacgcgagcagaac<br>gcaaggcttcaccaagagtc |
| *HOXA9* | ctgttcaacatgtacctcaccag<br>gaccgagcaaaagacgagtga |
| *HOXB4* | ctggatgcgcaaagttcac<br>agcggttgtagtgaaattcctt |

| | |
|---|---|
| *HSP90* | cataacgatgatgagcagtacgc<br>caatctcctttattcttcgttcctcc |
| *ID1* | cggaatccgaagttggaacc<br>gacacaagatgcgatcgtcc |
| *IFIT1* | agaacggctgcctaatttacag<br>gctccagactatccttgacctg |
| *IFIT3* | acttgaggcagacaggaagact<br>cagggaattcttggtgacctc |
| *IFNAR1* | agcacacaccatggatgaaa<br>tcaagaagactttcgcagca |
| *IFNAR2V1* | agtcttgaggcaaggtctcg<br>cttaatcactggggcacagg |
| *IFNAR2V2* | tagcctccccaaagtcttga<br>cttaatcactggggcacagg |
| *IFNGR1* | tgcataccgaagacaatcca<br>gatgctgccaggttcagact |
| *IFNGR2* | ttctccaaacgctttgaacc<br>tctcatgtctgcagggacag |
| *IKZF1* | gtggccgaagctataaacagc<br>cctatcttgcacaggtcttctgc |
| *IRF1* | tgggacatcaacaaggatgc<br>tggccttgctcttagcatct |
| *IRF2* | gccagacatttgccaagttg<br>gttgctgaggtactgtttgc |
| *IRF3* | gaactcaggagttggggactt<br>cccagtaactcatccagaatgtc |
| *IRF4* | tgtcccatgacgtttgga<br>tcctgtcacctggcaacc |
| *IRF5* | tctacgaggtctgctccaatg<br>aggcttggcaacatcctct |
| *IRF6* | cgatcattaacccaggatcc<br>ctgatccacagttctggaga |
| *IRF7* | gagaagagcctggtcctggt<br>aaggaagcactcgatgtcgt |
| *IRF8* | ccaggactgatttgggagaa<br>agtggctggttcagctttgt |
| *IRF9* | catccccatctcctggaa<br>gccctgaaagtacctgacca |
| *IRGM* | gcctgatgagcttactccagtg<br>acccaatgcttatggtgtgg |
| *JAK2* | ggatcctacacagtttgaagagag<br>ccttctttcagagccatcatacg |
| *LMO2* | cgtgcctatgagatgacaatgc<br>ggacatctacgagtggactaaga |
| *MAPK1* | taaggtgccatggaacaggc<br>ggattgaagtagaacaggctctgg |
| *MCL1* | cattcctgatgccaccttct<br>tcgtaaggacaaaacgggac |
| *MGST3* | cagaacacgttggaagtgtatcc<br>gctcctcgactacgcttgc |
| *MPL* | gctagctcccaaggcttctt<br>cttcctcttcgcagttctcc |

| | |
|---|---|
| *mTOR* | gagagaagtttccagagaagattcc<br>gcacaaggacagtgtcatgg |
| *NFKB1* | gggatctactagaagtcacatctgg<br>ggaagatgtggtggaggatttg |
| *NFKB2* | acctggtaacacacagtgacc<br>gcatgtgactaagaagaacatgatgg |
| *NME1* | gagacttctgcatacaagttggc<br>ggtagattacacgagctgtgctc |
| *NOLA1* | taaggtgccttatttcaatgctcc<br>cagtggcagcagcttatatgg |
| *OAS1* | gaaggcagctcacgaaacc<br>agctgcctccaacccttt |
| *OAS2* | cctgcctttaatgcactgg<br>atgagccctgcataaacctc |
| *OAS3* | ctggcactgggatttgcta<br>caaacctgagcatccagca |
| *OBR* | tgggcacaaggacttaattttc<br>tgaaattgtttcaggctcca |
| *PI3K* | gcatgccaattggtctgtatcc<br>cgagatcctctctctgaaatcac |
| *PML* | tacgccttctccatcaaagg<br>tctgggctgtcgttgtattg |
| *RanBP1* | tgacgtcaagctcctgaagc<br>ccactacatcacgccgatgat |
| *Rex1* | atcatccctaagcgaatcgc<br>caggtagatgttcttgctgg |
| *RNF20* | ggtgtctcttcaacggaggaa<br>tagtgaggcatcatcagtggc |
| *SENP1* | atgttccacaagaagtgcagc<br>gtttcgaggtaaagacttcggc |
| *SOCS1* | gacccttctcacctcttga<br>taggaggtgcgagttcaggt |
| *SOCS2* | gatcgactactatgttcagatgtgc<br>ggtgagcctacagagatgctg |
| *SOCS3* | gacttcgattcgggaccag<br>aacttgctgtgggtgaccat |
| *SPRY2* | agatccataagcacggtcagc<br>aagctcacctggcttgagc |
| *STAT1* | acctaacgtgctgtgcgtag<br>cctgctccaggaattttgag |
| *STAT2* | ttgggtgctactaccaggaga<br>tgttgcagttcatccacctg |
| *STAT3* | cctagatcggctagaaaactgg<br>gggtccccttgtaggaaac |
| *STAT4* | cgttggtcgtggtcttaactc<br>cccaggtgaggtgaccat |
| *STAT5* | acagatcaagcaagtggtcc<br>ccaggtcgaattctccatcc |
| *STAT6* | ggtcgcagttcaacaagga<br>gtccaggacaccatcaaacc |
| *SUMO2* | gaaagcctattgtgaacgacagg<br>catcctccatttccaactgtgc |

| | |
|---|---|
| *SUMO3* | ttcaagatcaagaggcacacg<br>ggagtgtcagtttcattgattggc |
| *SURVIVIN* | tccgcagtttcctcaaattc<br>gttgcgctttcctttctgtc |
| *TAF1* | ggaccaatgaagaaggataaggacc<br>tgtgttgcttcctgaggtcc |
| *TFDP1* | taacggcacaaggttctctgc<br>cgatgacttcaacgagaatgacg |
| *TNFSF10* | gaaagaggtcctcagagagtagc<br>cattcattcctgagcaacttgc |
| *TYW1* | attgtcatcaagacgcagggc<br>gttgcgaatcccttcgctgtt |
| *UBA2* | aagatcaaaggcacaggttgc<br>gcattcataaccagtataaactgtcgg |
| *UBASH3B/STS1* | ccatgagacattacaggtcatctacc<br>ggacgtgccatagatccaacc |
| *UBC9* | cacgatgaacctcatgaactgg<br>cgggtgaaataatggtggttcg |

### 2.2.4.8 Taqman probes

| Gene | Probe ID |
|---|---|
| ***ABCA1*** | Hs00194045_m1 |
| ***ATP5B*** | Hs00969569_m1 |
| ***AXL*** | Hs01064444_m1 |
| ***B2M*** | Hs00984230_m1 |
| ***Cathepsin B*** | Hs00947433_m1 |
| ***Cathepsin D 70*** | Hs00157205_m1 |
| ***Cathepsin L*** | Hs00964650_m1 |
| ***Cathepsin S*** | Hs00175407_m1 |
| ***CCL13*** | Hs00234646_m1 |
| ***CCL17*** | Hs00171074_m1 |
| ***CCL18*** | Hs00268113_m1 |
| ***CCL2*** | Hs00234140_m1 |
| ***CCL2*** | Hs00234140_m1 |
| ***CCL20*** | Hs01011368_m1 |
| ***CCL22*** | Hs00171080_m1 |
| ***CCL24*** | Hs00171082_m1 |
| ***CD13*** | Hs00174265_m1 |
| ***CD14*** | Hs00169122_g1 |
| ***CD16*** | Hs00275547_m1 |
| ***CD163*** | Hs00174705_m1 |
| ***CD204 (MSR1)*** | Hs00234007_m1 |
| ***CD206 (MRC1)*** | Hs00267207_m1 |
| ***CD280 (Mrc2)*** | Hs00195862_m1 |
| ***CD36*** | Hs01567185_m1 |
| ***CD68*** | Hs02836816_g1 |
| ***CD91*** | Hs00233856_m1 |
| ***CD93*** | Hs00362607_m1 |
| ***COX1*** | Hs00924803_m1 |
| ***COX2*** | Hs00153133_m1 |

| | |
|---|---|
| ***CSF1*** | Hs00174164_m1 |
| ***CSF-1R 30*** | Hs00911250_m1 |
| ***CXCL10*** | Hs00171042_m1 |
| ***CXCL4*** | Hs00427220_g1 |
| ***CXCL8*** | Hs00174103_m1 |
| ***CXCL9*** | Hs00171065_m1 |
| ***CYC1*** | Hs04187151-g1 |
| ***E-Cadherin 60*** | Hs01013958_m1 |
| ***EGF*** | Hs01099999_m1 |
| ***EMP1*** | Hs00608055_m1 |
| ***ENOX2*** | Hs00197268_m1 |
| ***Fibronectin 1*** | Hs00900058_m1 |
| ***FOXP3 89*** | Hs01085834_m1 |
| ***GAPDH*** | Hs99999905_m1 |
| ***Gas6*** | Hs01090305_m1 |
| ***GATA3*** | Hs00231122_m1 |
| ***GPNMB*** | Hs01095679_m1 |
| ***GUSB*** | Hs99999908_m1 |
| ***HMOX*** | Hs01110250_m1 |
| ***IFNγ*** | Hs00989291_m1 |
| ***IGF1*** | Hs01547656_m1 |
| ***IGF1 50*** | Hs01547656_m1 |
| ***IL10*** | Hs00174086_m1 |
| ***IL12a*** | Hs01073447_m1 |
| ***IL13*** | Hs00174379_m1 |
| ***IL-1b*** | Hs00174097_m1 |
| ***IL21*** | Hs00222327_m1 |
| ***IL23α*** | Hs00372324_m1 |
| ***IL4*** | Hs00174122_m1 |
| ***IL6*** | Hs00174131_m1 |
| ***IL8*** | Hs00174103_m1 |
| ***iNOS*** | Hs00167248_m1 |
| ***Lamp2*** | Hs00174474_m1 |
| ***LGALS3 (galectin 3)*** | Hs00173587_m1 |
| ***LYVE-1*** | Hs01119300_g1 |
| ***Mer TK*** | Hs01031973_m1 |
| ***MMP1*** | Hs00899658_m1 |
| ***MMP12 40*** | Hs00899662_m1 |
| ***MMP2*** | Hs01548727_m1 |
| ***MMP3*** | Hs00968305_m1 |
| ***MMP9*** | Hs00234579_m1 |
| ***MPO*** | Hs00924296_m1 |
| ***NOS3*** | Hs01574659_m1 |
| ***PARG*** | Hs00608256_m1 |
| ***PDGFC*** | Hs01044219_m1 |
| ***PGE2R*** | Hs00168754_m1 |
| ***PLAU*** | Hs01547054_m1 |
| ***PPARg*** | Hs01115513_m1 |
| ***Psap*** | Hs01551096_m1 |
| ***RORγ*** | Hs00536545_m1 |

| | |
|---|---|
| ***SEPP1*** | Hs01032845_m1 |
| ***SOCS3*** | Hs01000485_g1 |
| ***STAT1*** | Hs00234829_m1 |
| ***STAT3*** | Hs00374280_m1 |
| ***STAT4*** | Hs00231372_m1 |
| ***STAT5A*** | Hs00234181_m1 |
| ***STAT5B*** | Hs00273500_m1 |
| ***STAT6*** | Hs00598625_m1 |
| ***t-BET*** | Hs00894391_g1 |
| ***TBP*** | Hs99999910_m1 |
| ***TGFb1*** | Hs00171257_m1 |
| ***Tie 1*** | Hs00892696_m1 |
| ***TIMP2*** | Hs00234278_m1 |
| ***TNFa*** | Hs00174128_m1 |
| ***TREM2*** | Hs00219132_m1 |
| ***TYW1*** | Hs00936870_m1 |
| ***UBE2D2*** | Hs00366152_m1 |
| ***VEGFA*** | Hs00173626_m1 |
| ***VEGFC*** | Hs00153458_m1 |

## 2.2.5 Immunoblotting solutions

### 2.2.5.1 Tris HCl

| | |
|---|---|
| Sigma 7-9® | 1M |
| Hydrochloric acid | Added dropwise to pH 8.8, 7.5 or 6.8 |

### 2.2.5.2 Protein solubilisation buffer

| | |
|---|---|
| Sigma 7-9® pH 7.5 | 50mM |
| Sodium Chloride | 150mM |
| Nonidet P40 (NP-40) | 1% |
| Glycerol | 10% |
| Ethylenediamine Tetraacetic acid (EDTA) | 5mM |

#### 2.2.5.3 Phosphatase and Protease Inhibitor concentrations

| | |
|---|---|
| Sodium Orthovanadate | 1mM |
| Sodium Molybdate | 1mM |
| Sodium Fluoride | 1mM |
| Phenylmethylsulphonyl Fluoride | 4µg/mL |
| Pepstatin A | 0.7µg/mL |
| Aprotinin | 10µg/mL |
| Leupeptin | 10µg/mL |
| Soybean trypsin inhibitor | 10µg/mL |

#### 2.2.5.4 Polyacrylamide gels

| | **7.5%** | **8%** | **10%** | **5% stacking gel** |
|---|---|---|---|---|
| ddH2O | 5.6ml | 5.35ml | 4.35ml | 6ml |
| 1M Tris HCl pH8.8 | 5.6ml | 5.6ml | 5.6ml | - |
| 1M Tris HCl pH6.8 | - | - | - | 1.25ml |
| 10% SDS | 250µl | 250µl | 250µl | 150µl |
| 30% Acrylamide | 3.75ml | 4ml | 5ml | 1.67ml |
| 10% APS | 100µl | 100µl | 100µl | 50µl |
| TEMED | 20µl | 20µl | 20µl | 20µl |

#### 2.2.5.5 Tris-buffered saline (TBS) pH7.5

| | |
|---|---|
| Sigma 7-9® | 20 mM |
| Sodium Chloride | 150 mM |
| Hydrochloric acid | Added dropwise to pH 7.5 |

#### 2.2.5.6 TBS NP-40 (TBS-N)

| | |
|---|---|
| Sigma 7-9® pH 7.5 | 20 mM |
| Sodium Chloride | 150 mM |
| Hydrochloric acid | Added dropwise to pH 7.5 |
| NP-40 | 0.05% |

#### 2.2.5.7 Running buffer

| | |
|---|---|
| Glycine | 192mM |
| Sigma 7-9® | 25mM |
| Sodium dodecyl sulfate | 3.5mM |

#### 2.2.5.8 Semi dry transfer buffer

| | |
|---|---|
| Glycine | 40mM |
| Sigma 7-9® | 48mM |
| Sodium dodecyl sulfate | 1.3mM |

#### 2.2.5.9 5x BSA blocking solution (dissolved in TBS)

| | |
|---|---|
| Bovine Serum Albumin Fraction V | 5% |
| Ovalbumin | 1% |
| Sodium azide | 0.01% |

#### 2.2.5.10 5x milk blocking solution (dissolved in TBS)

| | |
|---|---|
| Skimmed milk powder | 5% |
| Sodium azide | 0.01% |

### 2.2.6 Immunofluorescence and Duolink solutions

#### 2.2.6.1 Poly-L-lysine

| | |
|---|---|
| Poly-L-lysine | 0.5mg/ml |
| Sodium tetraborate | 100mM |

#### 2.2.6.2 5x Block in PBS

| | |
|---|---|
| Bovine Serum Albumin Fraction V | 5% |
| Ovalbumin | 1% |
| Triton X100 | 0.2% |

#### 2.2.6.3 PLA probe mix

| | |
|---|---|
| Duolink® in-situ PLA® probe anti-mouse MINUS | 3µl |
| Duolink® in-situ PLA® probe anti-rabbit PLUS | 3µl |
| 5x block in PBS | 9µl |

#### 2.2.6.4 Ligation mix

| | |
|---|---|
| Duolink® 5x Ligation master mix | 3.2µl |
| Duolink® Ligase | 0.4µl |
| $ddH_2O$ | 12.4µl |

#### 2.2.6.5 Amplification mix

| | |
|---|---|
| Duolink® 5x Amplification master mix | 3.2µl |
| Duolink® Polymerase | 0.2µl |
| $ddH_2O$ | 12.6µl |

#### 2.2.6.6 Wash buffer A (pH 7.4)

| | |
|---|---|
| Tris hydrochloride | 10mM |
| Sodium Chloride | 150mM |
| Tween 20 | 0.05% |

#### 2.2.6.7 Wash buffer B (pH 7.5)

| | |
|---|---|
| Tris hydrochloride | 200mM |
| Sodium Chloride | 100mM |

# 2.3 Methods

## 2.3.1 Cell culture and cellular techniques

### 2.3.1.1 Culture of cell lines

K562 cells were cultured in RPMI 1640 medium supplemented with 10% FBS and 1% L-glutamine. UKE-1 cells were cultured in IMDM supplemented with 10% horse serum, 10% FCS and 1% L-glutamine. SET-2 cells were cultured in RPMI 1640 supplemented with 20% heat inactivated FCS and 1% L-glutamine.

### 2.3.1.2 XTT bioreduction assay

XTT (2,3-Bis-(2-Methoxy-4-Nitro-5-Sulfophenyl)-2H-Tetrazolium-5-Carboxanilide) bioreduction assays were used to assess the growth of K562, UKE1 and SET2 cells, when cultured in the presence or absence of the JAK2 inhibitors or $As_2O_3$. The cells were cultured for 72 hours in 96 well plates in the presence of a serially diluted concentration of each inhibitor allowing for 11 different concentrations for each drug. $1x10^4$ cells were seeded in each well in 100µl of media. Following culture, 25µl of solution containing 1 mg/ml XTT salt and 25µM phenazine methosulfate (PMF) was added to each well and incubated at 37˚C for 2-4 hours. During this incubation, live cells metabolise the reagents to soluble formazan. This leads to a colour change in the media which can be measured by visual absorbance at 495nm on a SpectraMax M5 plate reader. Results were analysed using SoftMax Pro software.

### 2.3.1.3 Cell viability by trypan blue exclusion

$1x10^5$/ml K562, UKE1 or SET2 cells were cultured and treated with increasing concentrations of the JAK2 inhibitors for 72 hours. The cell suspension and 1% trypan blue were mixed 1:1 and 10µl was placed on a counting chamber. Trypan blue exclusion cell counts were carried out at 24, 48 and 72 hours to assess cell viability.

#### 2.3.1.4 Peripheral blood mononuclear cell isolation

Peripheral blood was obtained from consented patients and healthy controls then diluted with an equal volume of 1x PBS before being carefully layered on the surface of room temperature Histopaque 1077. The samples were then centrifuged at 400xg for 30 minutes. The interface containing the mononuclear cells was removed, washed in PBS then either frozen in human albumin and DMSO (2.2.1.4) and stored at -80˚C or had RNA and protein extracted by the protocols described below (Sections 2.3.3.1 and 2.3.4.1).

#### 2.3.1.5 Culture of CML CD34+ cells

CML CD34+ cells were separated using positive selection through LS columns and CliniMACS® CD34 reagent. The quality of enrichment was assessed by flow cytometry using CD45 and CD34, before samples were placed in resuspension solution and mixed 1:1 with freezing solution. Cells were frozen in a controlled manner overnight to -80˚C and stored in liquid nitrogen. CML CD34+ cells were subsequently defrosted at 37˚C before slowly adding DAMP solution drop-wise over 20 minutes while gently agitating the sample. Following centrifugation at 192xg for 10 minutes, the pellet was loosened and washed in DAMP solution twice before counting and resuspending in 20 ml Stemspan II with high growth factors (Table 2.2.1.5) and culturing overnight in suspension cell culture flasks at 37˚C with 5% $CO_2$. Cells were then counted again the next morning to ensure adequate cell viability before separating for treatment with ruxolitinib 1μM and nilotinib 5μM alone or in combination. Cells were cultured for 8 hours in Stemspan II with low growth factors (Table 2.2.1.5) and appropriate treatment in 6 well plates at 37˚C with 5% $CO_2$, before being processed for RNA and protein.

#### 2.3.1.6 Neutrophil separation

Whole peripheral blood was mixed with 10% dextran solution and incubated at room temperature for 20 minutes in a 50ml syringe. The top layer was then removed by carefully ejecting through a Kwill filling tube until the red cell layer reached the tip. This was then mixed with 1x PBS before passing through a Ficoll gradient as described above (2.3.1.4). Neutrophils were taken from the densest layer before washing in PBS 3 times with centrifugation between washes for 10 minutes at 350xg. $1x10^6$ neutrophils were then cultured in 2ml Promocell DXF base media on Nunc Delta coated 12 well plates for 24 hours alone, with 20% normal or PV serum with or without LPS stimulation. The media was then harvested and centrifuged at 350xg to remove cells, then 3000xg to remove debris. The media was then snap frozen and stored at -80˚C before analysis by Luminex cytokine profiling.

#### 2.3.1.7 Culture of PV PB MNCs

Polycythaemia vera and normal control PB MNCs were separated as above, washed 3 times in 1x PBS with centrifugation for 10 minutes at 350xg between washes. $1x10^6$ cells were immediately resuspended in 2ml Stemspan II media with ruxolitinib 500nM or $As_2O_3$ 1μM alone or in combination and cultured for 24, 48 and 72 hours in 12 well plates at 37˚C with 5% $CO_2$. At those time points cells were prepared for apoptosis (Section 2.3.2.1) and cell cycle analysis (Section 2.3.2.2) as described below.

#### 2.3.1.8 Macrophage generation

Peripheral blood MNCs were isolated as described above and resuspended in Promocell monocyte adhesion media (MAM) on Nunc Delta coated plates for cytokine analysis and in Labtech chambered slides for immunofluorescence. After incubating at 37˚C for 1.5 hours, non-adherent cells were washed off using MAM. Macrophages were generated according to the Promocell® macrophage generation protocol. Briefly, the remaining adherent cells were cultured in M1 or M2 polarisation media for 5 days (2.2.1.4) before supplementing with an additional 50% by volume of fresh polarisation media and culturing for another 3 days. Following this, the media was removed and non-adherent cells centrifuged at 350xg for 10 minutes and resuspended in appropriate media for the following culture conditions (Figure 2.1) with serum making up 20% of the final volume.

**Figure 2.1 Experimental conditions for macrophage and neutrophils culture**

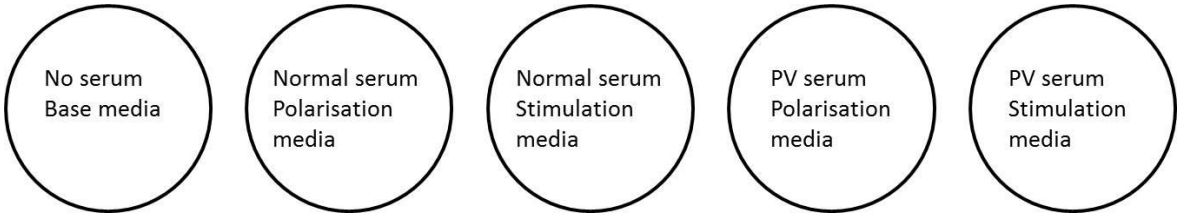


**Culture conditions for generation of macrophages from peripheral blood monocytes. M1 polarisation media was the Promocell® macrophage differentiation base media supplemented with GM-CSF 5ng/ml, with stimulation media using the same base media supplemented with LPS 100ng/ml and IFNγ 20ng/ml. M2 polarisation media was the Promocell® macrophage differentiation base media supplemented with M-CSF 50ng/ml, with stimulation media using the same base media supplemented with M-CSF 10ng/ml and IL-4 20ng/ml.**

After 24 hours, media was collected, snap frozen in liquid nitrogen, stored at -80˚C and subsequently analysed using Luminex cytokine analysis. Immunofluorescence samples were processed as described below (Section 2.3.5).

#### 2.3.1.9 Processing of patient serum samples

Patient samples were collected following informed consent into serum separator tubes. These were then allowed to sit at room temperature for 1 hour to allow coagulation to occur. Samples were then centrifuged at 3000xg for 10 minutes and serum snap frozen in liquid nitrogen before storing at -80˚C. Samples were then analysed using Luminex cytokine analysis.

#### 2.3.1.10 Luminex cytokine analysis

Using the Bio-Rad Bio-Plex Pro™ Human Cytokine 27-plex Assay and adding Bio-Plex Pro™ Human IFNα2 and Bio-Plex Pro™ Human Gro-α following recommended dilutions from the manufacturer, media samples and serum samples were analysed as per the manufacturers' protocol. This assay is based on uniquely colour-coded magnetic beads which are able to detect one specific protein and are identified by one laser in a specific flow cytometry machine. The beads are incubated with the sample and bind the protein of interest. This is then detected by a biotinylated antibody which is detected with streptavidin-PE. The beads are then drawn up in single file and the second laser is able to identify the level of protein bound to each bead based on the fluorescence intensity. This is then compared to a standard curve run at the same time to calculate the concentration.

### 2.3.2 Flow cytometry

Fluorescence activated cell sorting (FACS) or flow cytometry is a technique that allows identification of cellular characteristics through the application of fluorescent labelled antibodies or proteins. Coloured lasers excite the fluorochrome when the antibody is attached to a cell and the emitted light is detected. This allows the number of cells expressing a particular protein to be quantified as a percentage of the total number of cells. Multiple antibodies can be added at a time providing they are labelled with fluorochromes that emit different colours. Cells are then passed through a BD Bioscience FACS Canto which is capable of detecting up to 8 colours simultaneously based on 3 lasers.

### 2.3.2.1 Apoptosis analysis

$1x10^5$/ml K562, UKE1, SET2 cells, PV and normal PB MNCs were cultured in the presence of the JAK2 inhibitors or $As_2O_3$ for 24, 48 and 72 hours, as indicated. The cells were counted and $2x10^5$ cells were taken for each condition then washed twice with PBS supplemented with 2% FBS with centrifugation at 400xg or 5 minutes between washes. The cells were then suspended in HBSS with 5µl/$1x10^6$ cells of FITC-conjugated Annexin V and 5µl/$1x10^6$ cells of 7AAD for 15 minutes prior to analysis by flow cytometry using the BD FACSCanto. Annexin V will attach to phosphatidylserine when it appears on the cell surface during apoptosis, while 7AAD is a DNA binding dye which is unable to pass through intact cell membranes. Therefore live cells will not bind either of these while cells in late apoptosis will bind both. The data was then analysed using Flowjo software (Figure 2.2)

**Figure 2.2 Apoptosis assay**

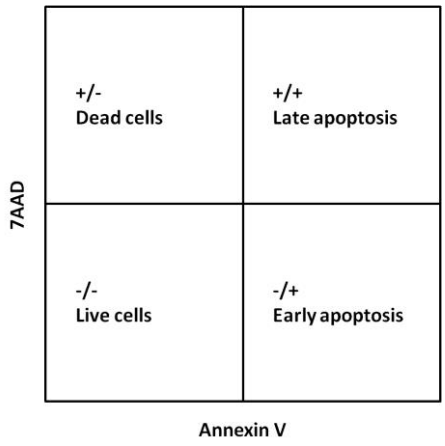


**Apoptosis assay using Annexin V and 7AAD separates cells by apoptotic state based on differential uptake of Annexin V and 7AAD. Quadrant markers are by 7AAD/Annexin V.**

### 2.3.2.2 Propidium iodide staining and cell cycle analysis

$1x10^5$/ml K562, UKE1, SET2 cells, PV and normal PB MNCs cells were cultured in the presence of the JAK2 inhibitors for 24, 48 and 72 hours, as indicated. The cells were counted and $2x10^5$ cells were taken and washed twice with PBS supplemented with 2% FBS. The cells were fixed in 1ml of ice cold 70% ethanol while agitating cells on a vortex machine at 1200rpm and stored at -20˚C for between 1 and 7 days. The cells were then washed again in PBS and suspended in 200µl of PI/RNase staining buffer for 15 minutes before analysis by flow cytometry. The data was then analysed using Flowjo software using a histogram to separate cells into G0-G1 and S-G2-M based on the peaks and troughs seen in the control sample (Figure 2.3).

**Figure 2.3 Propidium iodine assessment of cell cycle**

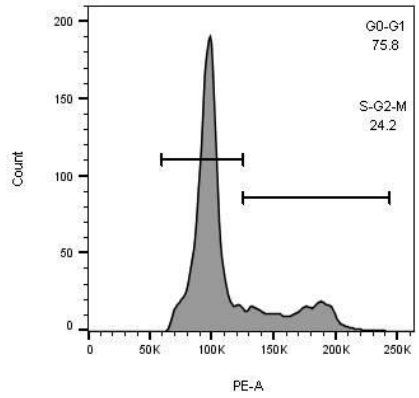


**Propidium iodide binds to DNA and will indicate a change in cell cycle as the amount of DNA increases in the cell through mitosis until the cell divides. Prior to adding the PI the cell needs to be fixed in ethanol for at least 24 hours to permeabilise the cell membrane to allow PI to enter the cell.**

### 2.3.2.3 Monocyte subset assessment

Following separation of MNCs from PB, $5x10^5$ cells were washed with PBS + 2% FBS twice. Cells were then incubated for 15 minutes with mouse anti-human CD14 FITC and mouse anti-human CD16 APC. Monocytes were identified using forward and side scatter before being separated into classical, non-classical and intermediate subsets according to CD14 and CD16 expression (Figure 2.4).

**Figure 2.4. Monocyte subset analysis**

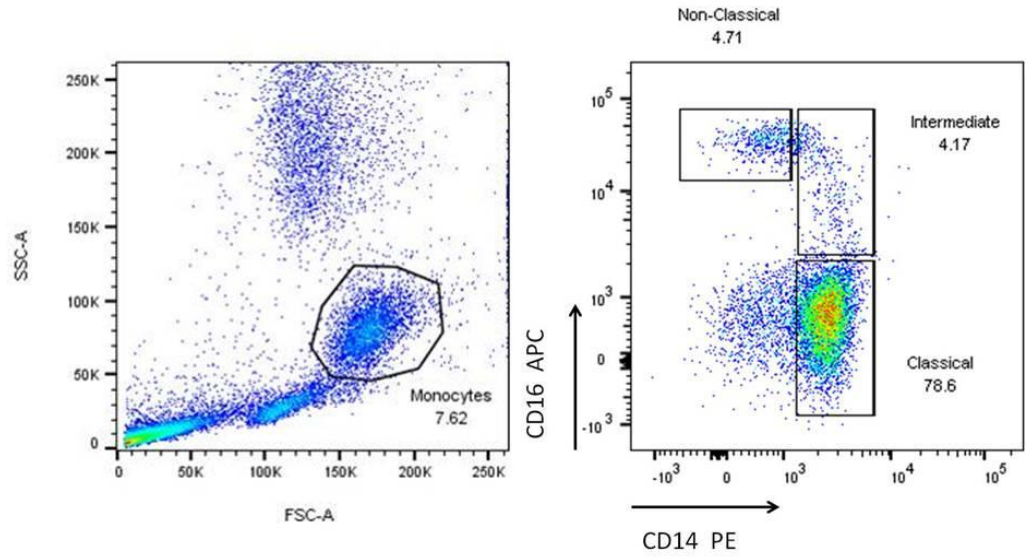


**Using flow cytometry the monocytes were identified using forward and side scatter to identify the size and granularity of the peripheral blood cells. The monocytes were than assessed for CD14 and CD16 to identify classical, non-classical and intermediate subsets.**

## 2.3.3 PCR techniques

K562, UKE1 and SET2 cells were cultured in complete media with JAK2 inhibitors for 24 hours before harvesting for RNA extraction and gene expression analysis. Patient samples and normal controls were harvested and processed immediately following Histopaque 1077 separation as described above (2.3.1.4).

### 2.3.3.1 RNA extraction

Cells were harvested, lysed and total RNA was prepared using the RNA extraction kits as per manufacturer's instructions. Briefly, for the Qiagen RNEasy Mini and Micro Plus kits, cells were suspended in the suggested volume for cell number of guanidine-thiocyanate-containing lysis buffer and homogenised using a 1ml syringe and 26G needle.

**Table 2.1. RNA extraction kits used for cell number**

| Extraction kit | Cell line cell number | Primary sample cell number | Volume of RNase-free water |
|---|---|---|---|
| Qiagen RNEasy Mini Plus | 0.5-5x$10^6$ cells | 1-10x$10^6$ cells | 30µl |
| Qiagen RNEasy Micro Plus | 0.2-0.5x$10^6$ cells | 0.5-1x$10^6$ cells | 14µl |
| PicoPure® RNA isolation kit | - | <0.5x$10^6$ cells | 11µl |

The homogenised lysate was then passed through a genomic DNA removal column by centrifuging the column at 10,000xg for 30 seconds. 70% ethanol is then mixed with the flow through and transferred to a spin column which binds the RNA in the sample. The sample is then cetrifuged at 10,000xg for 15 seconds and washed three times with the provided buffers with centrifugation at 10,000xg for 15 seconds between each wash. Finally the column is dried with a one minute centrifugation at 14,000xg for the RNEasy Mini kit or 5 minutes with an open lid for the RNEasy Micro kit.RNase free water is added to the spin column membrane to elute the RNA during a final centrifugation step. RNA concentration and quality was determined on the Nanodrop Spectrophotometer using 2µl of the sample, at 260nm and stored at -20˚C before use or at -80˚C for long term storage.

#### 2.3.3.2 Quantitative real time PCR by Fluidigm®

Quantitative real-time PCR (qRT PCR) is a technique used to determine the level of gene transcription to messenger RNA (mRNA). After RNA is extracted from cells it is turned into cDNA. By using oligo dT to attach to the poly-A tail of mRNA as the basis for the reverse transcription there is selection for mRNA over other types of RNA. cDNA for different genes is therefore produced in the same proportions as the mRNA it was derived from. This can then be used in quantitative PCR reactions where a fluorescent label (e.g. Evagreen) that binds to double stranded DNA is used as a measure of the abundancy of the gene of interest. This is achieved by amplifying the DNA with specific primers and setting a threshold level of fluorescence to indicate when the signal becomes positive. Therefore high abundance genes will cross this threshold in the early PCR cycles, while low abundance genes will have a higher cycle threshold (CT) value. This CT value represents the point at which a real signal is detected over a background level. This CT value can then be compared to a normal or no drug control using calculations which use the average of a number of control, or housekeeping, genes, the difference between the gene of interests CT and the housekeeping CT (the ΔCT), and the difference between the delta CT of the sample of interest and its control (the ΔΔCT). The $2^{-\Delta\Delta CT}$ method[170] can then be used to show the relative expression of the gene of interest compared to normal, where normal is expressed as 1.

#### 2.3.3.3 Reverse transcription

Up to 500ng of RNA was reverse transcribed to cDNA using the high fidelity reverse transcriptase Superscript III. The first step is to attach the oligo dTs to the mRNA using reverse transcription mix 1 (2.2.4.1) and the cycling conditions for step 1 (Table 2.2). 6µl of reverse transcription mix 2 (2.2.4.2) is then added to each sample and put through step 2 of the cycling conditions below (Table 2.2).

**Table 2.2 Reverse transcription cycling conditions**

| Reverse transcription | Step 1 | Step 2 | |
|---|---|---|---|
| Temperature | 65˚C | 55˚C | 70˚C |
| Time | 5 minutes | 60 minutes | 15 minutes |

Samples were pre-amplified for the genes to be studied and housekeeping genes using the pre-amplification mix (2.2.4.3) for 16 cycles (Table 2.3). Remaining primers were removed following pre-amplification using the exonuclease mix (2.2.4.4) and the cycling conditions below (Table 2.4).

**Table 2.3. Pre-amplification cycling conditions**

| Pre-amplification | Denature step | Cycling | | | Final extension |
|---|---|---|---|---|---|
| Temperature | 94˚C | 94˚C | 60˚C | 72˚C | 72˚C |
| Time | 15 minutes | 30 seconds | 90 seconds | 90 seconds | 10 minutes |

**Table 2.4. Exonuclease treatment cycling conditions**

| Exonuclease treatment | Step 1 | Step 2 |
|---|---|---|
| Temperature | 37˚C | 80˚C |
| Time | 30 minutes | 15 minutes |

Real-time PCR was then carried out in triplicate for each sample with a no sample control in each run, using Fluidigm Biomark technology using the 48:48 or 96:96 Fluidigm chips according to the manufacturer's instructions. The chips were initially primed with line control fluid before loading the primer and samples, where the primers were loaded as part of the assay mix (2.2.4.5) and the samples as part of the sample mix (2.2.4.6). The design of the chip allows each sample to be tested with each primer set from loading into a single well generating 2304 data points for the 48:48 chip and 9216 data points for the 96:96 chip. Data was analysed using the $2^{-\Delta\Delta CT}$ compared to control to show a fold change in expression. Internal sample control was provided by averaging 5 housekeeping genes (*GN2BL, B2M, RNF20, TYW1 and ENOX2*) within each sample.

**Table 2.5. Quantitative RT-PCR by Fluidigm**

| Fluidigm qRT PCR | Hot start | Cycling | | Melting curve |
|---|---|---|---|---|
| Temperature | 95˚C | 95˚C | 60˚C | 60˚C to 95˚C |
| Time | 60 seconds | 5 seconds | 20 seconds | 1˚C increase every 3 seconds |

## 2.3.4 Immunoblotting techniques

### 2.3.4.1 Protein extraction

1-5x$10^6$ cells were harvested following culture in JAK2 inhibitors or $As_2O_3$ and washed three times with 1xPBS without $Ca^{2+}$ or $Mg^{2+}$ and centrifuged at 400xg for 5 minutes. The pellet was resuspended in ice-cold solubilisation buffer supplemented with phosphatase and protease inhibitors and resuspended at 30µl/1x$10^6$ cells for K562 and SET2 or 20µl/1x$10^6$ for UKE1 and left to solubilise for 30 minutes on ice. The cell debris was pelleted by centrifugation at 21,000xg for 10 minutes at 4˚C and the supernatant stored at -20˚C for short-term storage or -80˚C for long-term storage. The cell lysate concentration was quantified using the Quick Start Bradford Protein Assay Kit with BSA used for the standards to generate a standard curve. This is a colorimetric protein assay based on a shift of absorbance of Coomassie Brilliant Blue dye when bound to protein under acidic conditions. This results in a change of colour from brown to blue and can be measured by visual absorbance at 595nm on the SpectraMax M5 plate reader using SoftMax Pro software.

### 2.3.4.2 SDS-PAGE Western blotting

Gel solutions were prepared as per Table 2.6. 7.5% gels were used to separate proteins larger than 50 kDa and 10% gels were for proteins smaller than 50 kDa. 20µg of cell lysates were fractionated by SDS-PAGE in 1x Running Buffer (Table 4.) at 80 Volts for 30 minutes and 180 Volts for 45 minutes. The separated proteins were then transferred to nitrocellulose membranes (Amersham Protran) using a semi-dry transfer method. The membranes and nitrocellulose were saturated in 1x semi-dry transfer buffer. The gel was placed on top of the membrane and was sandwiched between eight 9cm x 6cm Whatman paper strips (4 on bottom and 4 on top), and were compressed to remove any air bubbles. The proteins were transferred at 40mA/gel for 60 minutes and the transfer was

confirmed using Ponceau S Solution staining. The membranes were then washed in 1xTBS to remove Ponceau S. The nitrocellulose was blocked in 5% BSA or 5% milk (Table 2.6) to prevent non-specific binding for 1-2 hours. Following blocking, the nitrocellulose was incubated in primary antibody and 1x blocking solution overnight with gentle agitation on a rocker. Unbound antibody was washed with 1x TBS-N pH 7.5 4 times each for 10 minutes. Secondary antibodies which were conjugated to horseradish peroxidase (HRP) were used at a dilution of 1:10,000 and incubated for 1-2 hours. Secondary antibody was then washed with 1x TBS-N as before, and was followed by three 1x TBS washes. The membranes were placed in chemiluminescent HRP substrate for 2 minutes, and then placed in a cassette before they were exposed to X-ray film. The film was developed using a Konica Minolta SRX-101A developer in a dark room.

**Table 2.6. Antibodies for SDS-PAGE Western blotting**

| Antibody | Dilution | Block |
|---|---|---|
| JAK2 | 1:1000 | 5% BSA |
| Phospho-JAK2 | 1:1000 | 5% BSA |
| PML | 1:500 | 5% BSA |
| SUMO 2/3 | 1:2000 | 5% milk |
| Daxx | 1:2000 | 5% milk |
| Sp100 | 1:1000 | 5% milk |
| BCR-ABL Pathscan | 1:1000 | 5% BSA |
| pSTAT1 | 1:1000 | 5% BSA |
| STAT1 | 1:1000 | 5% BSA |
| pSTAT5 | 1:1000 | 5% BSA |
| STAT5 | 1:1000 | 5% BSA |

## 2.3.5 Immunofluorescence techniques

### 2.3.5.1 Immunofluorescence for K562, monocytes and macrophages

PTFE glass slides were prepared by adding 30 µl/well of 5 µg/ml Poly-L-Lysine in Borate buffer and allowed to air dry. Wells were washed twice with PBS immediately before use. Cells were harvested, counted, resuspended in an appropriate volume of the culture media used in each experiment and seeded at $6x10^4$/well and the slides incubated at 37˚C for 45 minutes. The wells were washed once with PBS and 4% formaldehyde was added to fix cells for 10

minutes at room temperature. The cells were then washed x3 with PBS and 0.5% Triton-X in PBS was added to permeabilise the cells at room temperature, for 15 minutes. Following PBS wash, cells were then blocked at room temperature with 5x block for 1-2 hours. The blocking solution was removed and the wells washed once with PBS. Appropriate concentrations of primary antibody were added to each well and the slides were incubated at 4˚C overnight. The primary antibody was removed and the wells were washed x5 with PBS. 1:200 dilutions of appropriate secondary antibody were prepared (Alexa Fluor 488 or 594; mouse or rabbit) and 25-30 µl was added to appropriate wells and left for 1 hour. Secondary antibody was removed and the wells washed x5 with PBS. DAPI mounting solution was used to fix and seal the slides with cover slips. The slides were visualised on a Zeiss TS 100 inverted microscope and pictures were taken using Axio-vision software.

#### 2.3.5.2 Immunofluorescence for UKE1 and SET2 cells

PTFE glass slides were prepared as above (2.1.1.1). Cells were harvested, counted, resuspended in ice cold acetone at a concentration of $6x10^6$/ml to fix and permeabilise the cells. 10µl of the cell suspension was immediately added to each well and incubated on ice for 20 minutes. The slides were then allowed to air dry prior to washing 3 times with PBS. Cells were then blocked in 5x blocking solution without Triton X100 and processing thereafter was as above.

#### 2.3.5.3 Duolink®

PTFE glass slides were prepared as outlined above up to and including the blocking stage. Following blocking, appropriate concentrations of two primary antibodies (Table 2.7), one raised in rabbit and one in mouse, were added to each well and the slides were incubated at 4˚C overnight. The primary antibody was removed and the wells were washed x5 with PBS. The PLA probe mix was prepared and incubated at room temperature for 20 minutes prior to adding 15µl to each well and incubating in a humidified chamber at 37˚C for 1 hour. The cells were washed x5 with 1x wash buffer A, then ligation mix was prepared and 16µl added to each well before incubating in a humidified chamber at 37˚C for 30 minutes. Following a further five washes with 1x wash buffer A, 16µl of amplification mix was added and incubated in the dark in a humidified chamber at 37˚C for 100 minutes. This was then removed and the slides washed x5 with 1x wash buffer B and twice with 0.01x wash buffer B. DAPI mounting solution was

used to fix and seal the slides with cover slips. The slides were visualised on a Zeiss TS 100 inverted microscope and images recorded using Axio-vision software. Comparative fluorescence was measured using Image J software (National Institute for Health) for corrected total cell fluorescence using the equation overall cell fluorescence-(area of cell measured x mean background fluorescence) where overall cell fluorescence is measured using integrated density and the mean background fluorescence is measured using the mean grey value for at least 10 areas in the image with no cells present[171].

**Table 2.7. Primary antibodies for immunofluorescence and Duolink**

| Antibody | Dilution |
|---|---|
| JAK2 | 1:200 |
| Phospho-JAK2 | 1:100 |
| PML | 1:50 |
| SUMO 2/3 | 1:100 |
| JAK2 | 1:100 |
| Daxx | 1:100 |
| Sp100 (sc-25568) | 1:100 |

### 2.3.6 Statistics

Statistical analysis was carried out using GraphPad Prism 6. The statistical method used is described in each figure and include one way ANOVA, two way ANOVA, and Students *t* test. Statistical significance is defined as $p \leq 0.05$.

# 3 Activity of JAK2 in CML

## 3.1 Introduction

As previously discussed CML is characterised by the presence of the BCR-ABL oncogene which results from the Philadelphia chromosome, t(9;22)[88,89,90]. This protein has tyrosine kinase activity which drives aberrant signalling in a number of pathways, leading to its characteristic phenotype of myeloid expansion and reduced adhesion of precursors in the bone marrow[172]. In addition to the abnormalities seen in the peripheral blood patients often present with inflammatory symptoms of fevers, night sweats and weight loss. This inflammatory phenotype is driven by a cocktail of cytokines produced by the CML clone, which helps to support the expansion of the disease[173]. Many of these cytokines are produced in an autocrine fashion and so do not result in an increase in serum levels. In fact with G-CSF there is a decrease in serum concentrations in chronic phase disease compared to normal individuals, which starts to increase again as the disease progresses through accelerated phase and blast crisis[174,175]. CML cells do produce G-CSF and it is thought that production of soluble G-CSF receptor is responsible for reducing the level in the serum. Interestingly another cytokine important in myeloid differentiation, IL-3, does not change its levels at all in the serum of patients with CML compared to normal individuals[175].

BCR-ABL is known to interact with the JAK2/STAT5 pathways through several mechanisms[105]. BCR-ABL positive cells produce cytokines which have a paracrine effect on the cells, often signalling through JAK2-associated receptors[173]. In addition to this BCR-ABL directly phosphorylates both JAK2 and STAT5 resulting in ongoing activation of the pathway without the need for ligand binding to receptors[176,2]. Finally BCR-ABL and JAK2 form a complex with Ableson helper integration site 1 (AHI-1), where AHI-1 acts as a bridging complex between BCR-ABL and JAK2. BCR-ABL attaches to the WD40-repeat domain of AHI-1, while JAK2 interacts with the N-terminal[105]. Disruption of this complex using imatinib and TG101209 led to an increase in apoptosis in CML cells which was particularly marked in the CD34+ve stem/progenitor cell compartment[105]. These studies all indicate the importance of JAK2 signalling in CML and suggest that combining therapies targeting both ABL and JAK2 kinase activity may be able to overcome the resistance to single agent BCR-ABL targeted therapy especially in the leukaemia stem cell compartment.

## 3.2 Results

### 3.2.1 Microarray data of JAK2 targets

JAK2 as a target has generated a lot of interest as a result of its role in cell signalling in both normal tissues and in disease[177]. JAK2 is known to be essential for haematopoiesis especially in response to cytokines which drive myelopoiesis. It is known to be associated with many cytokine receptors and is best known for its role in inflammation and haematopoiesis[17]. JAK2 signalling is abnormal in many haematological malignancies[2,112,141,178] and so identifying gene targets of JAK2 signalling has been of particular interest over the last decade. In this project two microarrays were identified and used as a basis for the gene expression experiments[79,179]. The first used the JAK2 null cell line γ2A and compared the gene expression in a microarray with the same cells transduced with wild type JAK2 (GEO accession number GSM16418). This identified 621 genes with at least a two-fold alteration in expression, many requiring only the presence of JAK2 in the cell to result in alteration with no need for ligand activation of JAK2[179]. The second paper looked at the entry of JAK2 into the nucleus and its ability to phosphorylate histone 3, analysis revealed that one of the key alterations occurred in LMO2 expression, which does not have a STAT5 binding site, and was downregulated by inhibition of JAK2 in the JAK2 V617F containing HEL cell line[79]. Using the information available in these two microarrays, and with permission from the authors, we approached Dr Lisa Hopcroft, a bioinformatician, who analysed the data and produced transcriptional regulation maps using Metacore software (Figure 3.1). Using this map, genes were selected at hubs of interaction and at downstream points from these interactions to study pathways in detail. Some genes were subsequently not pursued due to lack of expression in the cells being studied, such as androgen receptor. In addition to this, to validate these targets, known genes affected by JAK2 were identified from the literature and included in the gene expression studies. The pathways identified included;

- Cell cycle- *CDC25B*, *CDKN1B*, *TFDP1*, *CCND2*
- Apoptosis- *TNFSF10* (*TRAIL2*), *BNIP3L* (*NIX*), *BCL2L1*, *FOXO3A*
- Differentiation and proliferation- *HOXA9*, *LMO2*, *FOXM1*, *UBASH3B* (*STS1*), *EGR1*

- Transcription factors- *DHX9-DEAH* (*DDX9*), *BACH1*, *RXRB*, *TFDP1*, *TAF1*, *HSP90*, *IKZF1*

- JAK2 associated receptors- *CRLF2*, *GM-CSF*, *G-CSF*

- JAK2 pathway- *JAK2*, *STAT5*, *SOCS2*

- IFN response- *IRF 1-9*, *IFN-α* and *-γ* receptors

**Figure 3.1 Metacore interaction map of JAK2 dependent transcriptional regulators**

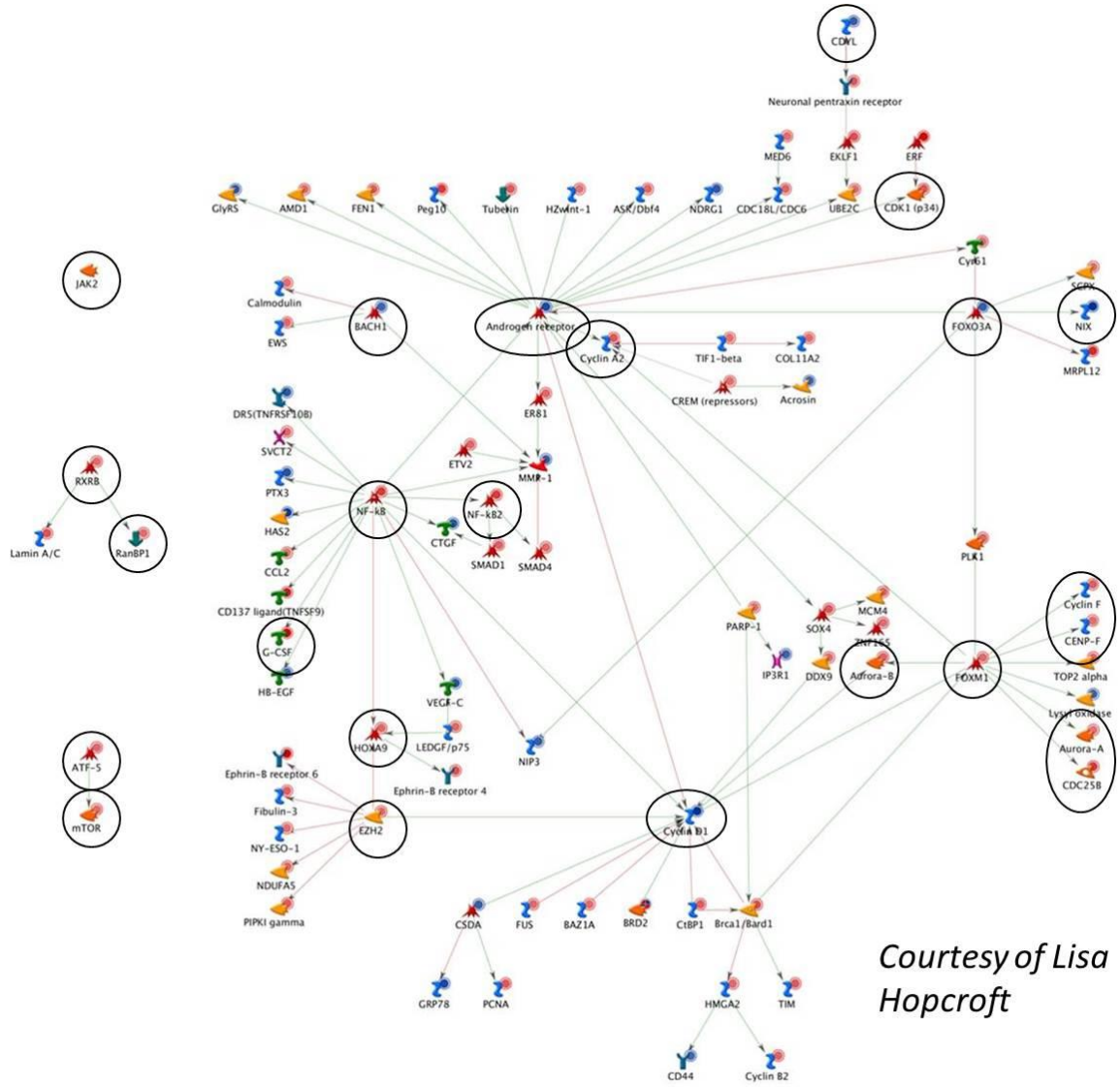


**Data from the microarrays were entered into Metacore and genes associated with transcription were mapped to identify JAK2 dependent targets. The genes used in gene expression experiments are circled.**

### 3.2.2 Gene expression of K562 cells treated with JAK2 inhibitors

The abnormal signalling pathway activity induced by JAK2 leads to deregulation of a number of important genes in CML samples, these abnormalities are sometimes the same in CML CD34+ cells and CML mononuclear cells (MNC), while others have very different expression patterns depending on the maturity of the cells. This may indicate a true difference in the CML cells as they differentiate, or reflect an alteration in the expression of these genes in normal cells. The abnormalities cover a wide range of cellular processes including apoptosis, cellular differentiation, transcriptional regulation, and inflammation showing a global dysregulation of the gene expression in this condition. The expression patterns confirm some previously described abnormalities, including increased expression of G-CSF, which is important in myeloid cell development, and decreased expression of IRF8, which is thought to play a key role in the switch between granulocytic and monocytic differentiation (Figures 3.2 and 3.3).

**Figure 3.2 Heatmap of the gene expression of CML CD34+ cells**

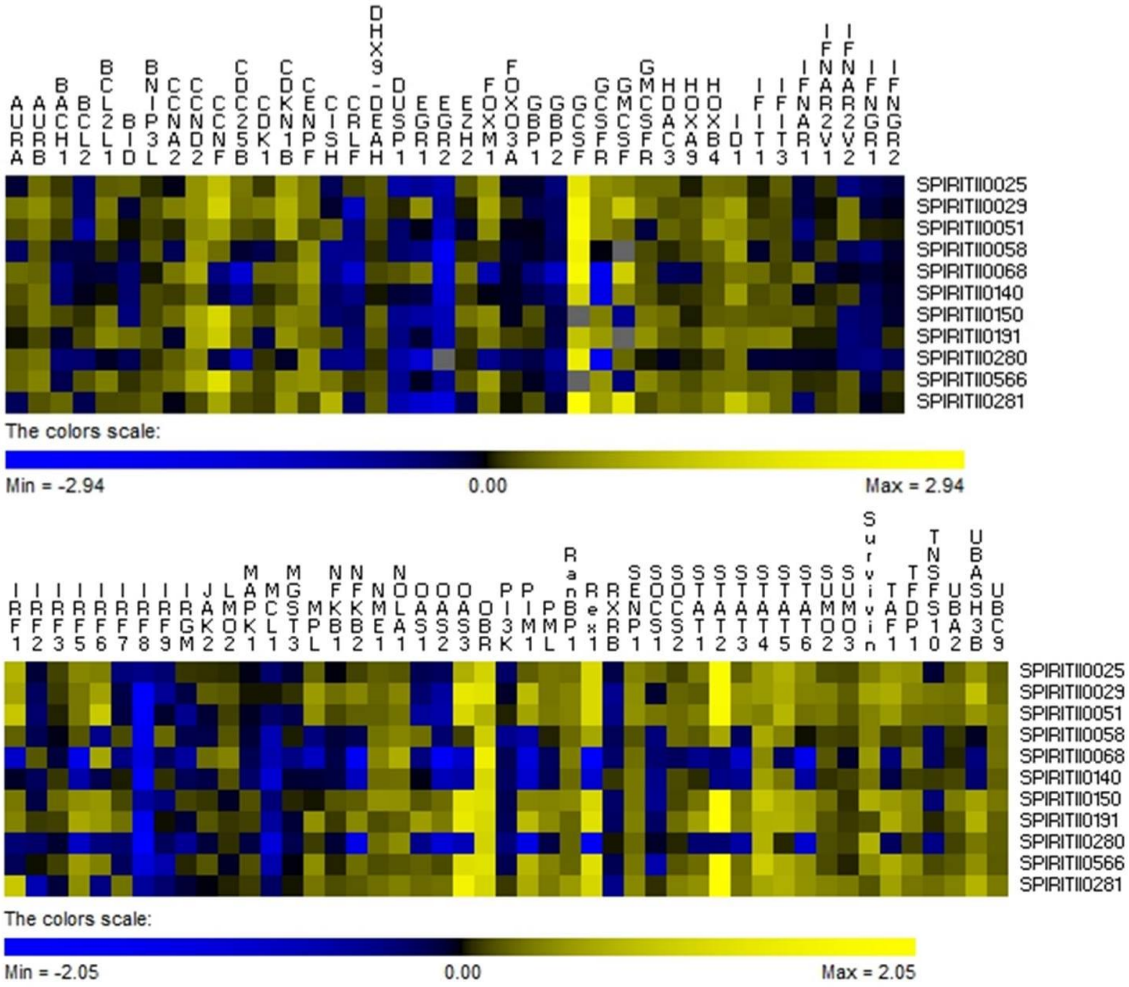


**Using the data from the microarrays, genes were selected and primers designed to look at JAK2 dependent genes and the interferon response (Table 2.2.4.8). Fluidigm quantitative real time PCR was performed and the relative expression of the genes compared to normal controls was calculated using the $2^{-\Delta\Delta CT}$ method. A base 10 logarithmic transformation was then performed and this data was entered in to PermutMatrix to generate a heatmap representation of the gene expression. PB MNC samples were run on multiple chips with different primer sets.**

**Figure 3.3 Heatmaps of the gene expression of CML PB MNCs**

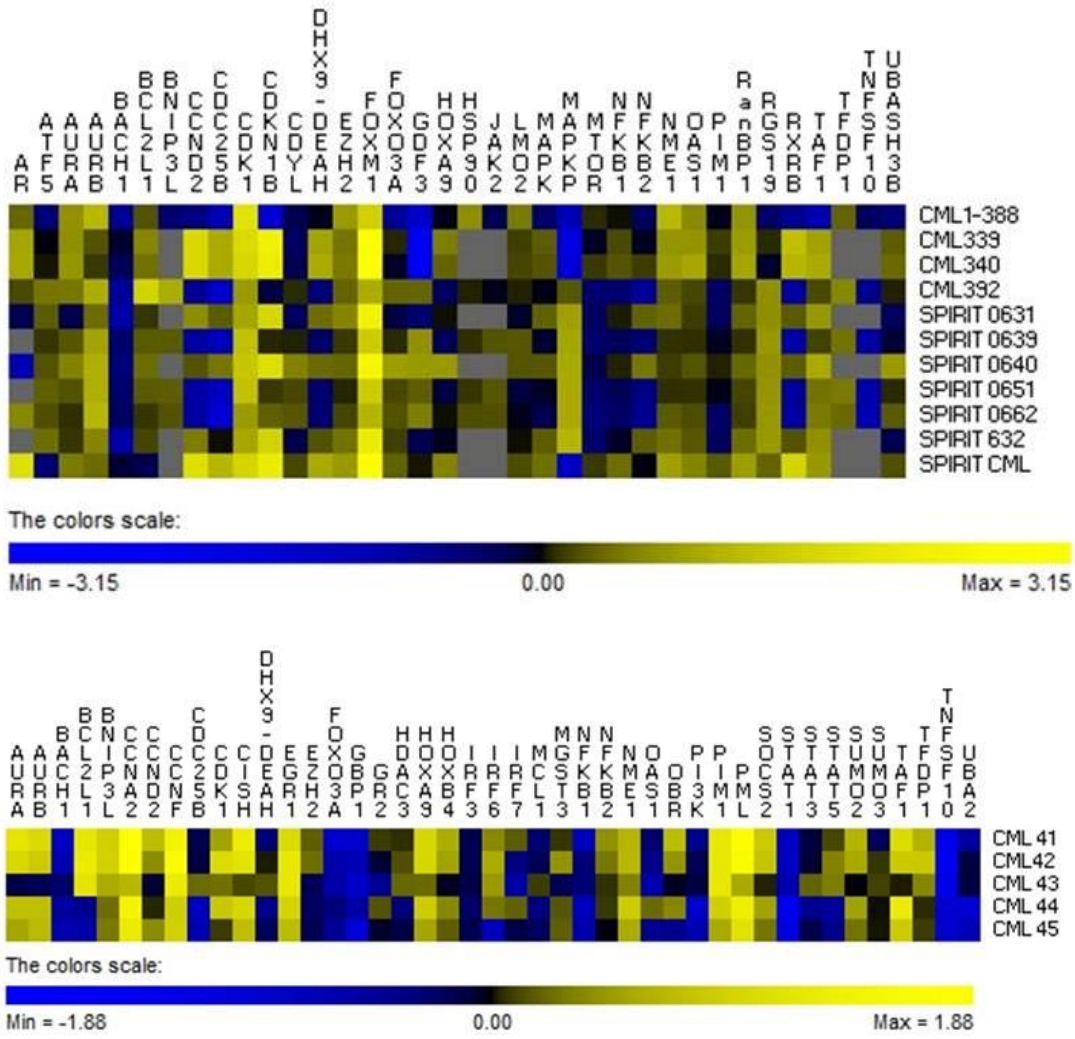


**Using the data from the microarrays, genes were selected and primers designed to look at JAK2 dependent genes and the interferon response (Table 2.2.4.8). Fluidigm quantitative real time PCR was performed and the relative expression of the genes compared to normal controls was calculated using the $2^{-\Delta\Delta CT}$ method. A base 10 logarithmic transformation was then performed and this data was entered in to PermutMatrix to generate a heatmap representation of the gene expression. PB MNC samples were run on multiple chips with different primer sets.**

The heatmaps give useful information about the overall abnormal expression in these cells. However it is interesting to separate these by cellular process to get a better idea of how these are altered by the presence of the BCR-ABL oncogene in more primitive stem and progenitor populations compared to the more mature peripheral blood MNC.

### 3.2.2.1 Changes in expression profiles of apoptosis genes in CML

Apoptosis is the process of programmed cell death which is important in preventing abnormal cells from expanding. These abnormalities can be due to abnormal DNA replication, and therefore pose a threat of neoplastic disease, or can be a defence mechanism against infection, particularly intracellular organisms, such as viral disease[180]. In CML apoptosis of the abnormal clone is reduced as a direct result of the *BCR-ABL* oncogene altering the apoptotic pathways through constitutive pro-survival signalling. BCR-ABL increases protein expression of the anti-apoptotic BCL2 and BCL2L1 as well as preventing release of cytochrome C from the mitochondria leading to inhibition of the apoptotic pathway and a survival advantage to the malignant clone[181]. Figure 3.4 demonstrates a significant increase in the gene expression of *BCL2L1* in CML CD34+ cells when compared to normal donor CD34+ cells, this in keeping with the reported literature. In addition to this there is a reduction in *MCL1* in CD34+ cells which does not persist as the cells mature. *MCL1* exists in several isoforms with the longer product acting as an inhibitor of apoptosis, while the shorter form promotes it[182]. The increase in *BCL2L1* persists as the cells differentiate while the pro-apoptotic protein, *BNIP3L*, becomes significantly increased. Aberrant expression of *BNIP3L* has recently been identified as part of a high risk panel of genes predicting failure to achieve an early molecular response in chronic phase CML treated with imatinib[183], while a reduced expression in solid tumours is also associated with a poor prognosis[184].

**Figure 3.4 Apoptosis in CML**

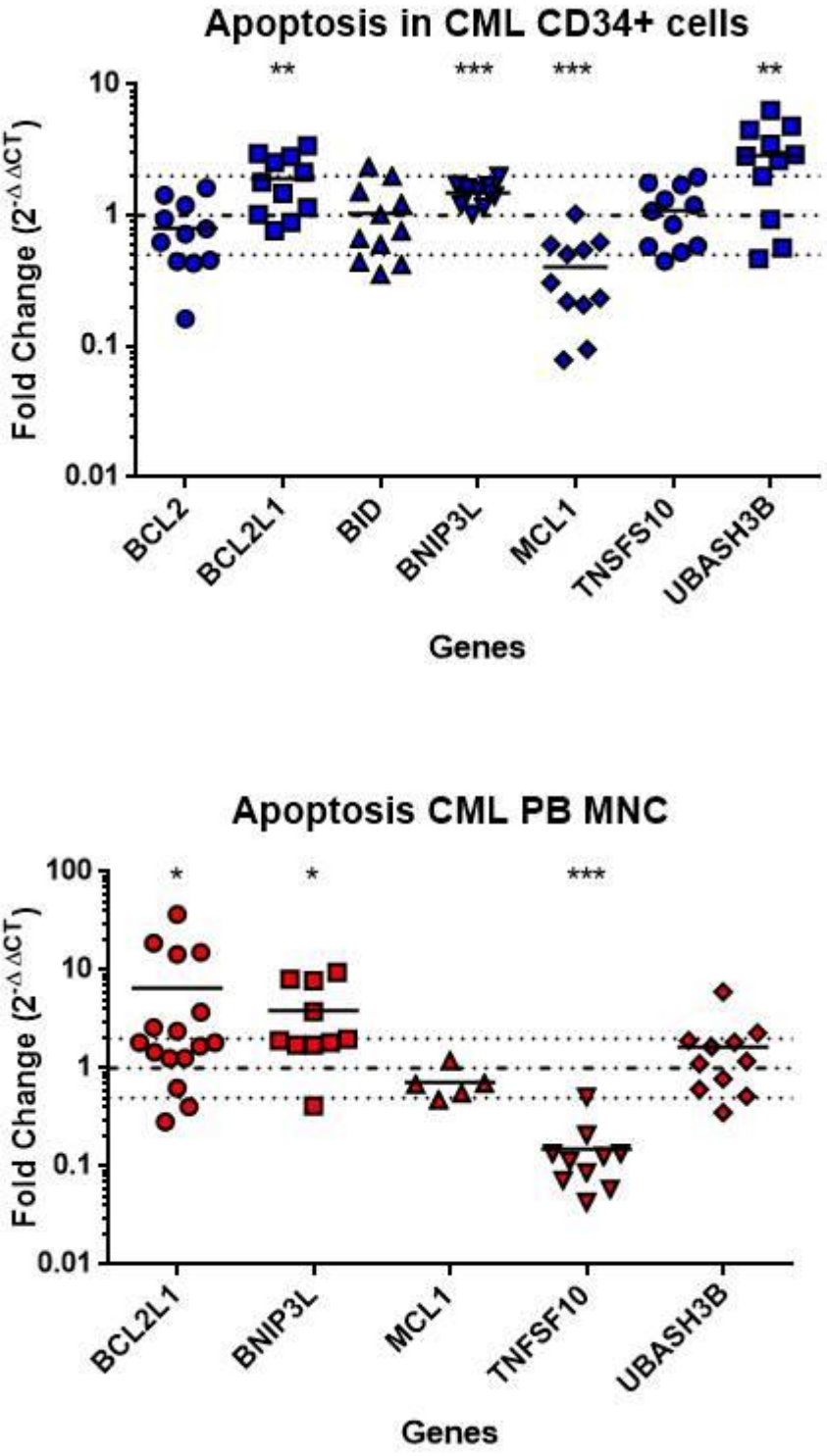


**Fluidigm® quantitative real time PCR was carried out on RNA extracted from chronic phase CML patient samples. The fold change compared to normal was calculated using the $2^{-\Delta\Delta CT}$ method. The data points were then graphed using GraphPad Prism 6 and a two tailed Students *t*-test was used to calculate significance (* $p \leq 0.05$, ** $p \leq 0.01$, *** $p \leq 0.001$). The two dotted lines indicate a 2-fold change from the control, indicated by the dashed line.**

#### 3.2.2.2 Changes in expression profiles of cytokine signalling genes in CML

Cytokine signalling plays a key role in the maintenance of CML cells, with JAK2/STAT5 and PI3K signalling previously identified as being important in the signalling profile of CML. These data show that in CD34+ve cells mRNA production of *STAT2, STAT4* and *STAT5* are increased when compared to normal, along with an increase in the transcription of *G-CSF*, *GM-CSF* and *G-CSF* receptor, while *STAT1* is unexpectedly decreased in PB MNCs. Interestingly mRNA transcription of the important deregulated signalling pathways involved in CML, *JAK2* and *PI3K* were not altered in CD34+ve cells, but PI3K appears to be decreased in PB MNCs. Lastly the JAK2 regulatory proteins are also differentially expressed in CD34+ve cells when compared to PB MNCs with no significant changes in the negative regulators *CISH* or *SOCS2* in CD34+ve cells, while in PB MNCs there is a significant increase in the expression of both *CISH* and *SOCS2*. (Figure 3.5).

**Figure 3.5 Cytokine signalling in CML**

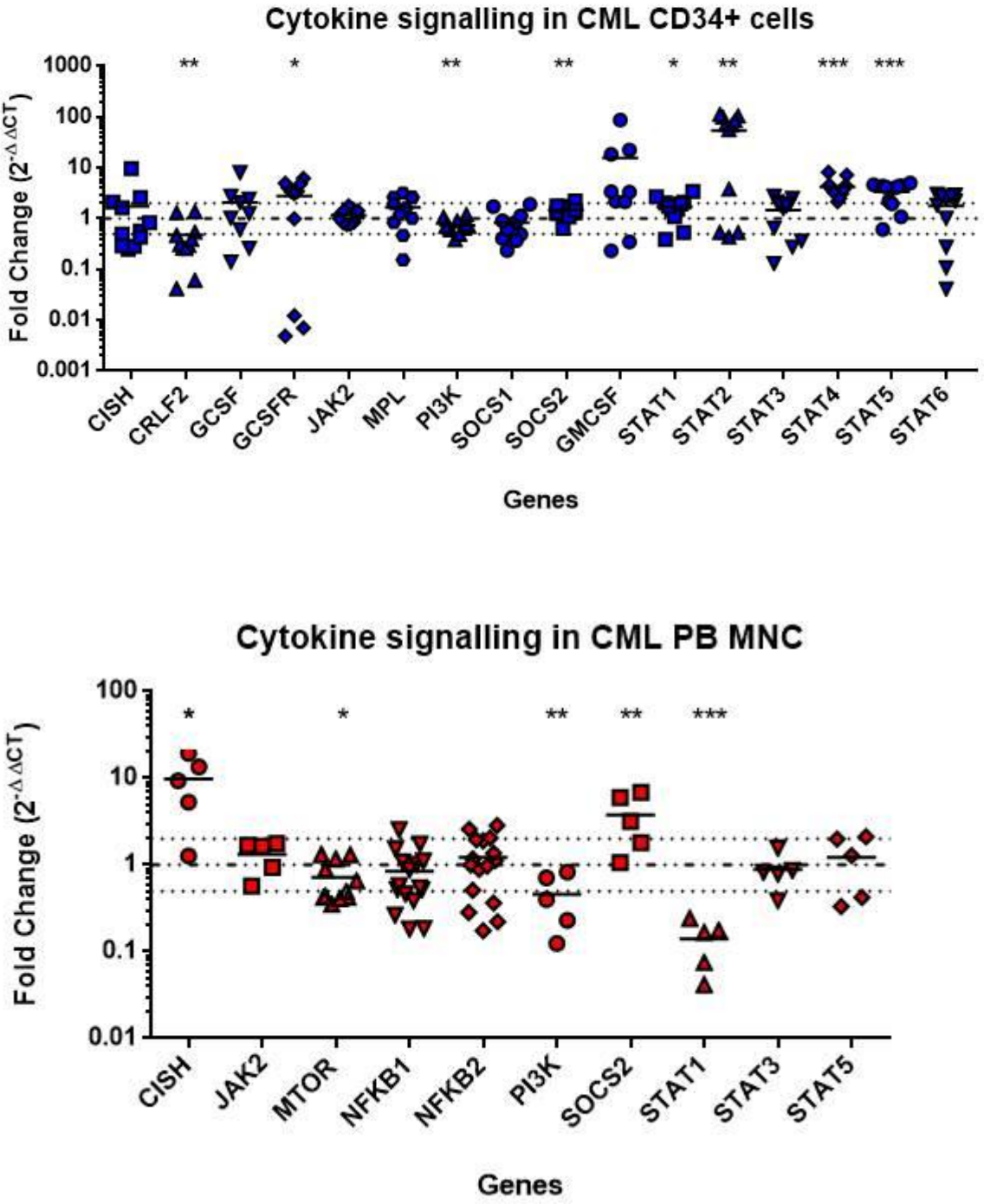


**Fluidigm® quantitative real time PCR was carried out on RNA extracted from chronic phase CML patient samples. The fold change compared to normal was calculated using the $2^{-\Delta\Delta CT}$ method. The data points were then graphed using GraphPad Prism 6 and a two tailed Students *t*-test was used to calculate significance (* $p \leq 0.05$, ** $p \leq 0.01$, *** $p \leq 0.001$). The two dotted lines indicate a 2-fold change from the control, indicated by the dashed line.**

#### 3.2.2.3 Changes in expression profiles of transcriptional regulation genes in CML

Regulation of gene transcription lies at the heart of all cellular processes, with signalling and responses designed to alter transcriptional machinery activity and thereby enhance or inhibit target gene expression. This then leads to targeted increases or decreases in protein levels, which in turn affect cellular activity. Transcriptional regulation in CML is complex with numerous signalling pathways and nuclear processes having been reported to be altered. In Figure 3.6 there is clear alteration in the transcriptional activator *PIM1* in both CD34+ve cells and PB MNCs. PIM1 has been shown to be elevated in CML as a result of BCR-ABL induced STAT5 activation and leads to a reduction in expression of pro-apoptotic $Bcl_{xS}$ altering the function of BAD[185,186], which ultimately leads to a reduction in apoptosis in these cells (Figure 3.4).

FOXM1 controls the expression of several cell cycle genes including *CCNA2* and *CCND1*. It also regulates the degradation of CDK2 inhibitors CDKN1A and CDKN1B[187]. It is therefore not surprising that *FOXM1* is expressed in proliferating cells, but not in terminally differentiated or quiescent cells. In both the CD34+ve cells and PB MNCs there is an increase in the expression of *FOXM1*. This is likely to represent a genuine increase in the CD34+ve cells, however in the PB MNCs this probably relates to the low levels of expression seen in normal PB cells as these are terminally differentiated, whereas in CML a large number of immature cells occur in the peripheral blood (Figure 3.6).

Other interesting alteration include the increase in Rex1, a marker of pluripotency found in undifferentiated embryonic stem cells, which is markedly downregulated as the cells begin to differentiate[188]. This increase in Rex1 has not been previously reported in CML CD34+ and may play an important role in sustaining the self-renewal of the early stem/progenitor cells. Interestingly reports of Rex1 in solid tumours relates to a reduction in levels compared to normal tissue (Figure 3.6)[189].

**Figure 3.6 Transcriptional regulation in CML**

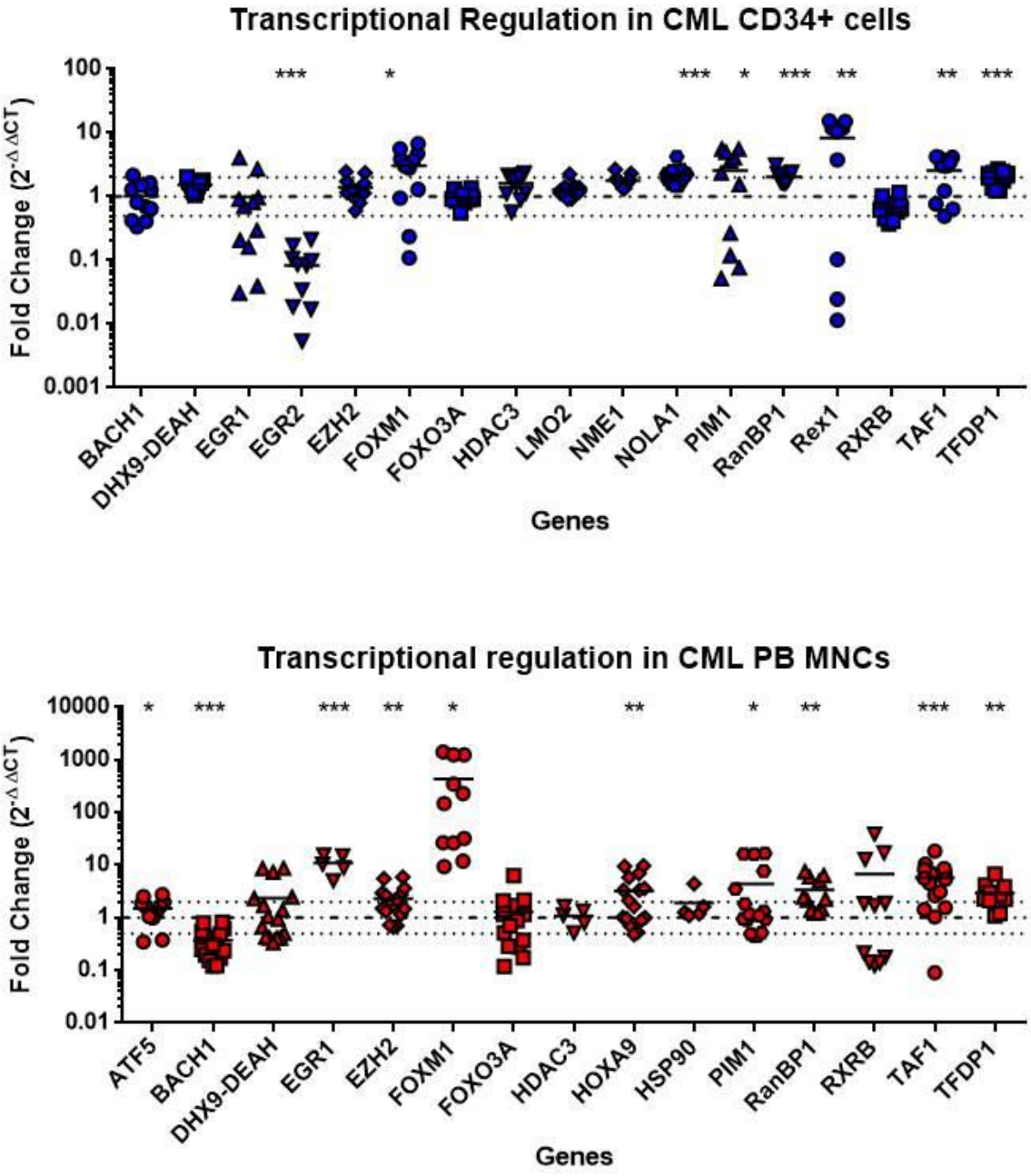


**Fluidigm® quantitative real time PCR was carried out on RNA extracted from chronic phase CML patient samples. The fold change compared to normal was calculated using the $2^{-\Delta\Delta CT}$ method. The data points were then graphed using GraphPad Prism 6 and a two tailed Students *t*-test was used to calculate significance (* $p \leq 0.05$, ** $p \leq 0.01$, *** $p \leq 0.001$). The two dotted lines indicate a 2-fold change from the control, indicated by the dashed line.**

#### 3.2.2.4 Changes in expression profiles of cell cycle genes in CML

Regulation of cell cycle is critical to the maintenance of normal cell numbers within a tissue. Over activity of the cell cycle leads to proliferation of cells and expansion of a tissue. In CML BCR-ABL upregulates a number of cell cycle proteins and downregulates inhibitors of the cell cycle in the myeloid lineage leading to marked expansion of all stages of granulopoiesis[172]. The gene analysis data confirms the upregulation of several key regulators of cell cycle progression including *CCND2* in CD34+ve cells and *CCNA2* in PB MNCs. In addition to this there is upregulation of *CCNF* in both CD34+ve cells and in PB MNCs. Interestingly there is also an increase in the expression of the cyclin-dependent kinase inhibitor *CDKN1B* in both PB MNCs and CD34+ve cells. It is likely this is driven by a negative feedback loop attempting to regulate the over active cell cycle (Figure 3.7).

**Figure 3.7 Cell cycle regulation in CML**

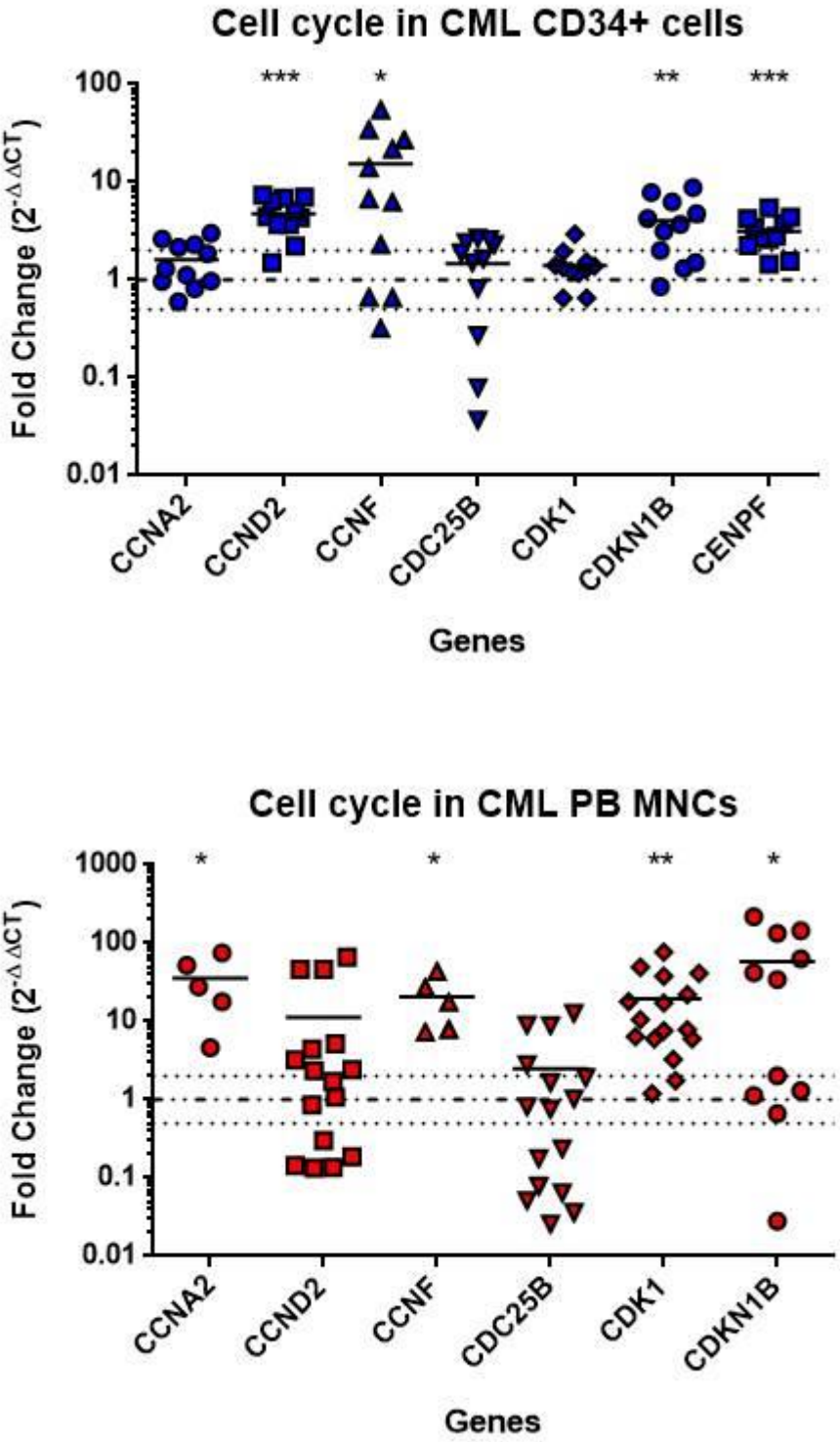


**Fluidigm® quantitative real time PCR was carried out on RNA extracted from chronic phase CML patient samples. The fold change compared to normal was calculated using the $2^{-\Delta\Delta CT}$ method. The data points were then graphed using GraphPad Prism 6 and a two tailed Students *t*-test was used to calculate significance (* $p \leq 0.05$, ** $p \leq 0.01$, *** $p \leq 0.001$). The two dotted lines indicate a 2-fold change from the control, indicated by the dashed line.**

### 3.2.2.5 Changes in expression profiles of inflammation genes in CML

At presentation many patients complain of symptoms common to a number of haematological malignancies, namely sweats, fevers, weight loss and fatigue. Weight loss and fatigue can be explained by the tumours use of nutrients; however fevers and sweats are more likely to relate to a degree of inflammation associated with the condition. The cells affected by CML are intrinsic to the innate immune system and are intimately involved in the production of cytokines involved in regulating the immune system. It is therefore not surprising that the expression profile of genes associated with inflammation, specifically the interferon response, are abnormal. In the gene expression profiles below this is borne out with several of the interferon response genes being either up- or down-regulated. Previous work has shown that *IRF8* is down regulated in CML[190] and is confirmed here. There is also evidence that reintroducing *IRF8* into BCR-ABL positive cells will rescue the abnormal gene expression profile seen in CML[190]. The reduced expression of *IRF4* has also been previously reported[191], this appears to relate to a deficiency in the T cell compartment expressing this response factor, with an increase following initiation of interferon α therapy correlating to a good response. Interestingly mouse models with *IRF8*-/- developed a CML-like disease, which was more severe when *IRF4* was also knocked out. *IRF1* and *IRF6* were also up regulated, however there is little information about IRF6 in CML, with most data relating to abnormal keratinocyte differentiation in the context of inactivating mutations[192]. The altered profile of *IRF* expression reflects the imbalance/altered sensitivity of cytokine/chemokine signalling occurring in CML, which is probably driven by the combination of autocrine secretion of cytokines and BCR-ABL mediated JAK2 activation, observed in these patients (Figure 3.8).

Small-ubiquitin modifiers (SUMO) are involved in post-translational modifications of numerous proteins in a wide range of cellular processes. The addition of a SUMO chain can alter protein activity, cellular localisation, or mark it for degradation. It is interesting to note that in CML samples there is an increase in *SUMO* cycle gene expression. This may reflect this increased cellular activity seen in the disease, but it is not something that has previously been studied and warrants further investigation (Figure 3.8).

**Figure 3.8 Inflammation in CML**

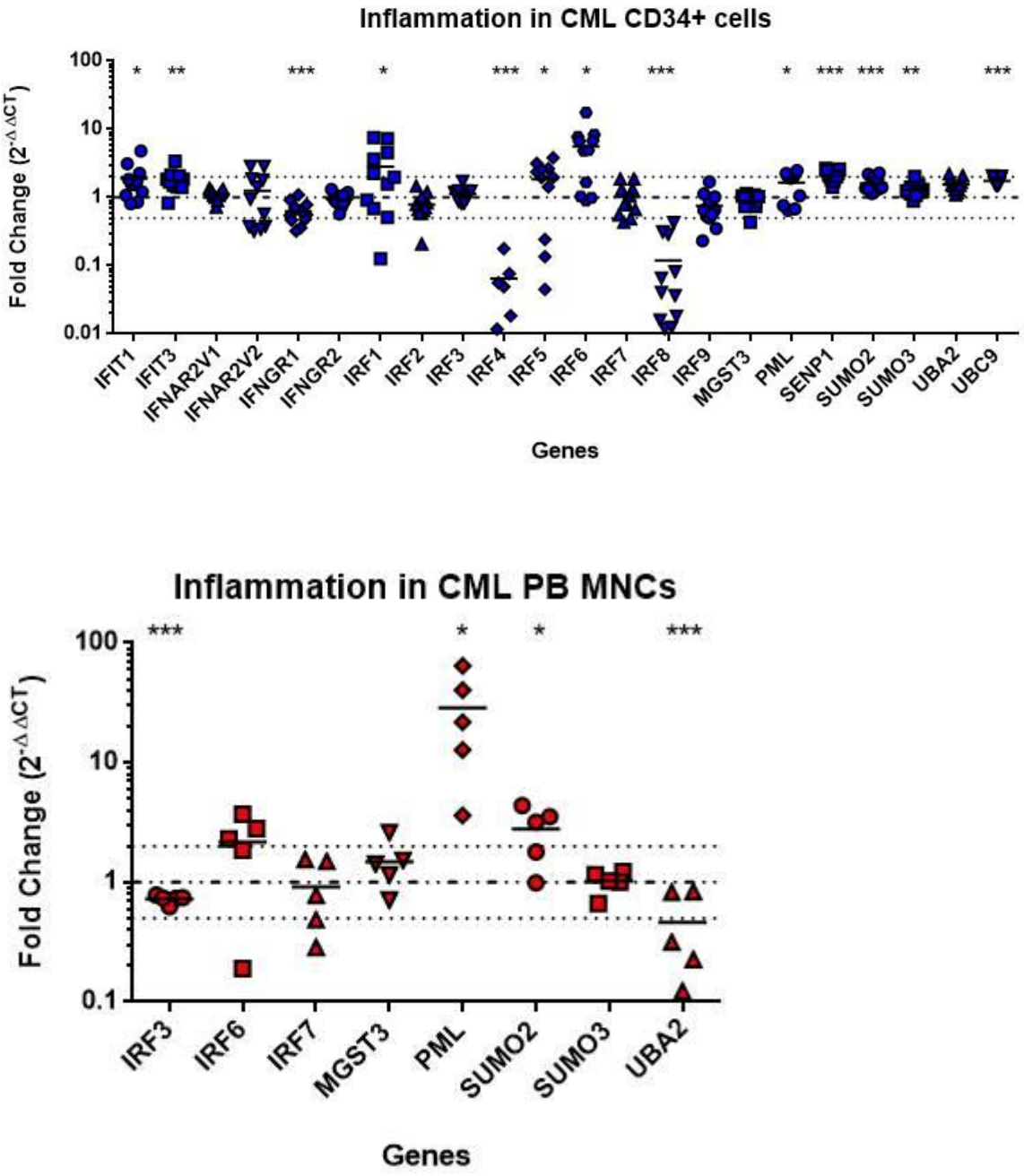


**Fluidigm® quantitative real time PCR was carried out on RNA extracted from chronic phase CML patient samples. The fold change compared to normal was calculated using the $2^{-\Delta\Delta CT}$ method. The data points were then graphed using GraphPad Prism 6 and a two tailed Students *t*-test was used to calculate significance (* $p \leq 0.05$, ** $p \leq 0.01$, *** $p \leq 0.001$) The two dotted lines indicate a 2-fold change from the control, indicated by the dashed line.**

Taken together these data confirm that JAK related/mediated downstream gene expression in CML is markedly deregulated with a wide range of cellular processes affected.

### 3.2.3 Establishing the dose of JAK2 inhibitors for K562 cells

We decided to look at the effect of JAK2 inhibition on CML cells, as JAK2 plays an important role in the pathogenesis of the disease. In order to do this we used the K562 cell line, an CML blast crisis cell line that retained the Philadelphia chromosome on transformation. Initially we determined a range of concentrations of three JAK2 inhibitors (Figure 3.9), two of which are relatively specific for JAK2 with only a few additional targets at higher concentrations (TG101209[193] and ruxolitinib[194]), with the third having a wider range of additional targets (AT9283[195]) including aurora kinase activity at approximately the same concentrations as the effect of JAK2. Aurora kinase regulation was identified as a downstream mediator of JAK2 from the microarray analysis in Figure 3.1, making dual inhibition by AT9283 an interesting avenue to investigate in CML. The additional kinase targets of TG101209 include FLT3, which has been shown to be of significance in progression of CML[196], and RET which has not been shown to have a role in CML, but has been shown to be mutated in other malignancies such as papillary thryroid cancer[197]. The main additional target of ruxolitinib is JAK1. While there is data about the role of JAK2 in CML, the role of JAK1 is not clear. It may be that in the CML clone itself JAK1 has little importance, however the effect of the CML cells on other haematopoietic and inflammatory cells may mean JAK1 has a peripheral role in the disease.

**Figure 3.9 XTT assay results for JAK2 inhibitors**

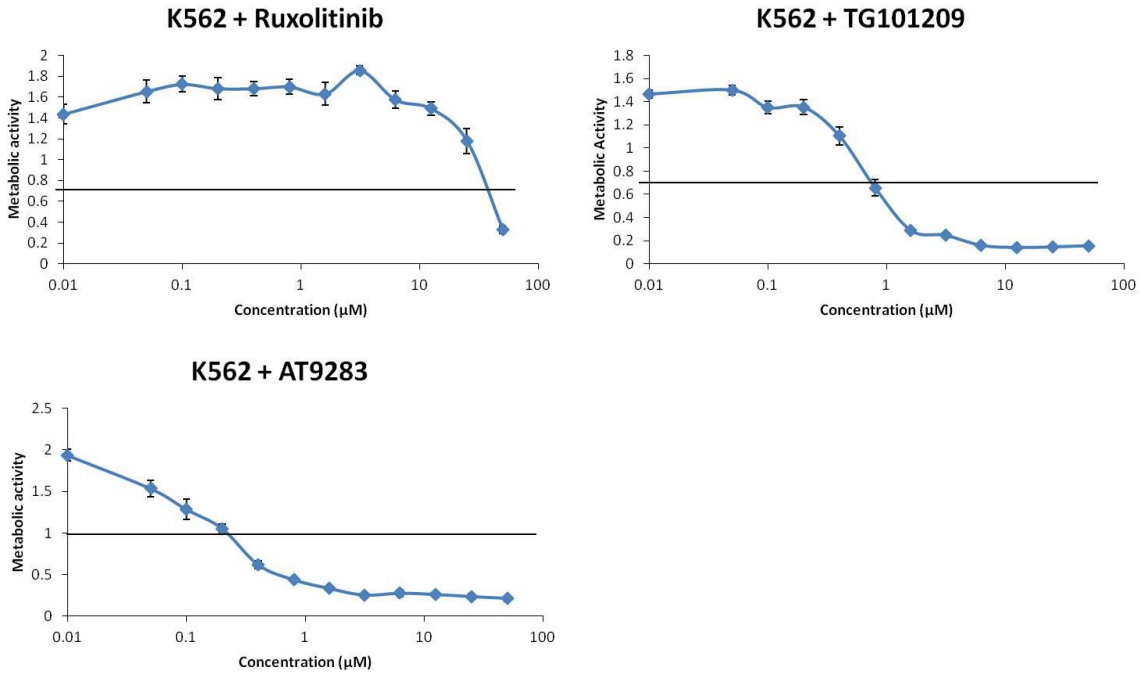


**XTT assays were carried out in 8 simultaneous wells with the mean plotted in the above graphs +/-standard deviation. Solid line indicates the dose of inhibitor necessary to reduce the metabolic activity by 50%. The no drug control is indicated by the plot point furthest to the left on the X axis.**

K562 cells were cultured in the presence of serially diluted JAK2 inhibitors for 72 hours before adding the XTT/PMF solution. After 4 hours the visual absorbance was measured as a surrogate for metabolic activity. For each JAK2 inhibitor this gave an indication of the drug effects which could be used to narrow the range for trypan blue exclusion counts. Trypan blue exclusion was carried out at 24, 48 and 72 hours and the $IC_{50}$ dose calculated based on these results (Table 3.1). Following identification of the $IC_{50}$ a lower and higher dose were also included that were shown to result in an alteration in cell counts at 72 hours, but had live cells present at 24 hours. These doses were then used to analyse changes in gene expression and protein expression using Western blotting and immunofluorescence techniques. The $IC_{50}$ doses identified here are comparable to those previously reported for these inhibitors in K562 cells[176,198].

**Table 3.1 Doses chosen for K562 cells following trypan blue exclusion**

| Cell line | Ruxolitinib | TG101209 | AT9283 |
|---|---|---|---|
| K562 | 10μM<br>20μM<br>50μM | 0.1μM<br>1μM<br>5μM | 0.01μM<br>0.1μM<br>1μM |

**Concentrations of each JAK2 inhibitor used in subsequent experiments, based on the results of trypan blue exclusion testing.**

### 3.2.4 Effect of JAK2 inhibitors on downstream targets of JAK2 in K562 cells

K562 cells were cultured in each of the three concentrations of ruxolitinib TG101209 and AT9283 for 24 hours as outlined above, before having protein extracted and prepared for Western blotting (Section 2.3.4). The activity of JAK2 inhibitors in K562 cells was assessed by probing protein samples for phosphorylation of downstream targets of JAK2. AT9283 was able to affect phosphorylation of BCR-ABL directly as previously reported, with the reduction in activity of BCR-ABL seen by the reduction of phosphorylation of CRKL at the higher doses of AT9283. Phosphorylation of JAK2 was affected by AT9283 in a dose dependent manner, while with TG101209 it appeared to increase with the lower doses before decreasing with 5μM TG101209. A similar effect on phosphorylation of STAT3 was seen with TG101209 where there was an initial increase with the lower doses and a decrease with the 5μM dose. Ruxolitinib increased the phosphorylation of CRKL without any alteration of phosphorylation of BCR-ABL, and although there have been reports of activity of ruxolitinib on BCR-ABL activity at doses above 20μM this was not seen in this study. Despite an initial increase in phospho-STAT3 with 10μM ruxolitinib there was a subsequent reduction with 50μM ruxolitinib. The sample treated with DMSO alone did not alter protein expression compared to untreated samples and probing with SHP2 as a loading control indicates protein loading was equal (Figure 3.10).

**Figure 3.10 Western blotting of protein lysates from K562 cells treated with JAK2 inhibitors for 24 hours**

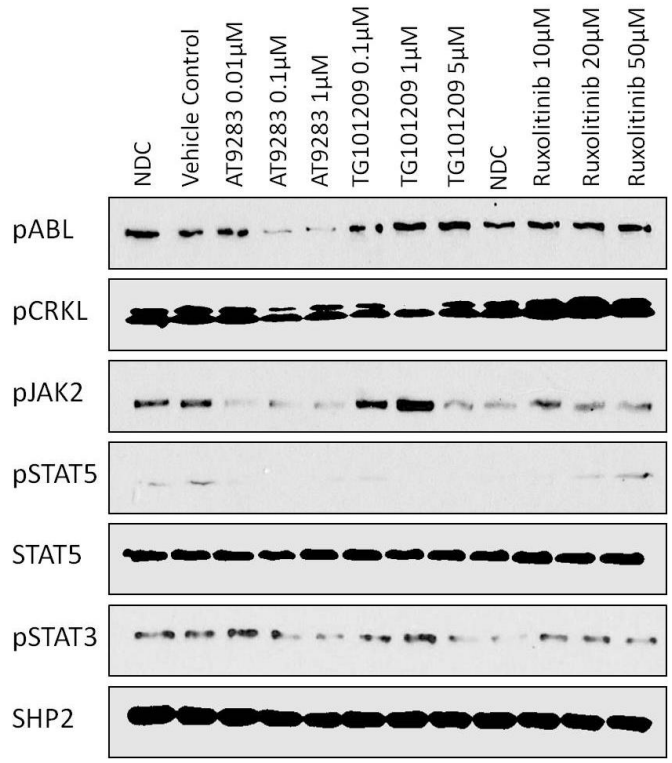


**Protein samples were obtained from K562 cells following 24 hours of culture in media alone or supplemented with increasing doses of ruxolitinib, TG101209 or AT9283. The lysates were then run according to the protocol described previously (2.4.4.2). The nitrocellulose membranes were then probed using antibodies to the proteins indicated above and detected using HRP-conjugated antibodies. Equal protein loading of the samples was ensured by probing for SHP2. Three independent experiments were carried out with this image being representative of these.**

### 3.2.5 Effect of JAK2 inhibition on gene expression of JAK2 targets in K562 cells

K562 cells were treated for 24 hours with the doses of each inhibitor indicated above, as at this time point in the trypan blue counts there was little cell death, and therefore cells were still viable for RNA extraction. RNA was then processed to prepare for Fluidigm® real time PCR as described previously (Section 2.4.3). With K562 cells 39 genes (Table 2.2.4.7) were analysed for each of the 3 JAK2 inhibitors. The heat map demonstrates that treatment with JAK2 inhibitors results in an alteration of the gene expression in K562 cells. The expression pattern is most similar when cells are treated with ruxolitinib and TG10209, with more marked changes observed with the higher drug doses, while AT9283 produces a different pattern of alteration. This likely reflects the wider range of cellular targets affected by AT9283 (Figure 3.11).

**Figure 3.11 Gene expression heat map of K562 cells treated with JAK2 inhibitors**

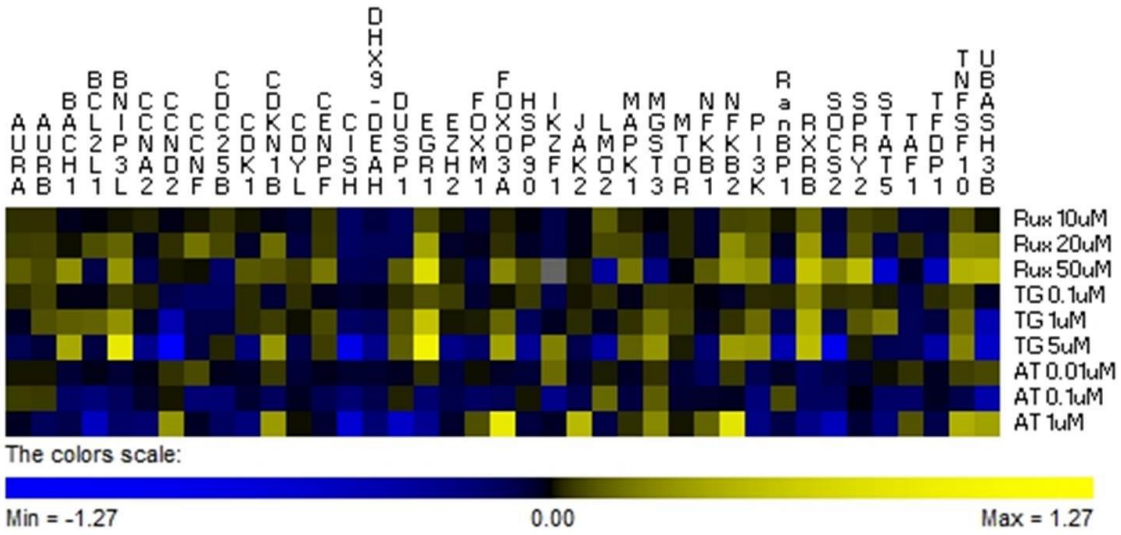


**Fluidigm® quantitative real time PCR was performed on RNA extracted from K562 cells treated with increasing doses of JAK2 inhibitors and the relative expression of the genes compared to untreated cells was calculated using the $2^{-\Delta\Delta CT}$ method, values represent the mean of 3 independent experiments. A base 10 logarithmic transformation was then performed and this data was entered in to PermutMatrix to generate a heat map representation of the gene expression of K562 cells treated with JAK2 inhibitors.**

Examining the analysed data of K562 cells treated with each of the JAK2 inhibitors separately, the significant alterations in gene expression achieved by the highest dose of each inhibitor were graphed below. Ruxolitinib achieved the least number of significant alterations in gene expression and these were predominantly related to transcriptional regulators of haematopoiesis (*LMO2*) and cell cycle progression (*RanBP1* and *TFDP1*). There is a significant reduction in the expression of *STAT5* which acts as a downstream target of both JAK2 and BCR-ABL, and is a key transcriptional regulator of many gene targets of both of these kinases (Figure 3.12).

**Figure 3.12 Gene expression of K562 cells following treatment with ruxolitinib**

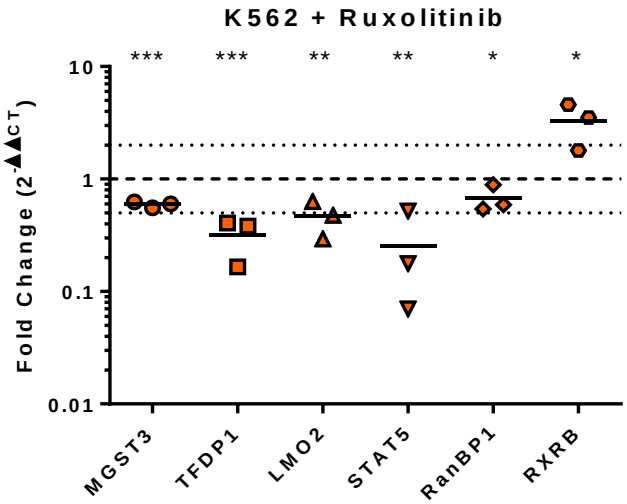


**Fluidigm® quantitative real time PCR was carried out on RNA extracted from K562 cells treated with ruxolitinib 50μM for 24 hours. The fold change compared to untreated samples was calculated using the $2^{-\Delta\Delta CT}$ method. The data points were then graphed using GraphPad Prism 6 and a two tailed Students *t*-test was used to calculate significance (* p ≤ 0.05, ** p ≤ 0.01, *** p ≤ 0.001). The two dotted lines indicate a 2- fold change from the control, indicated by the dashed line.**

When K562 cells were treated with TG101209 there was a wider range of significant alterations in gene expression. CCND2 is important in the transition of G1 to S phase in the cell cycle, it is increased in primary CML samples and a known target of JAK2 signalling. Treatment with TG101209 lead to a marked reduction in the expression of *CCND2* compared to untreated cells. This alteration was accompanied by an increase in the expression of *CDKN1B*, an inhibitor of several CDK proteins. Cytokine signalling genes are also affected with reduction in the expression of two negative regulators of JAK2 signalling *CISH* and *SOCS2*. Again both of these are altered in CML primary samples with an increase in the level of both in CML PB MNCs. Both *CISH* and *SOCS2* are targets of JAK2/STAT5 signalling acting as negative regulators and the decrease in expression following treatment is likely to reflect the reduction in signalling through this pathway. Alterations in *RanBP1*, *RXRB* and *TFDP1* are similar to those seen in ruxolitinib treated cells (Figure 3.13).

**Figure 3.13 Gene expression of K562 cells following treatment with TG101209**

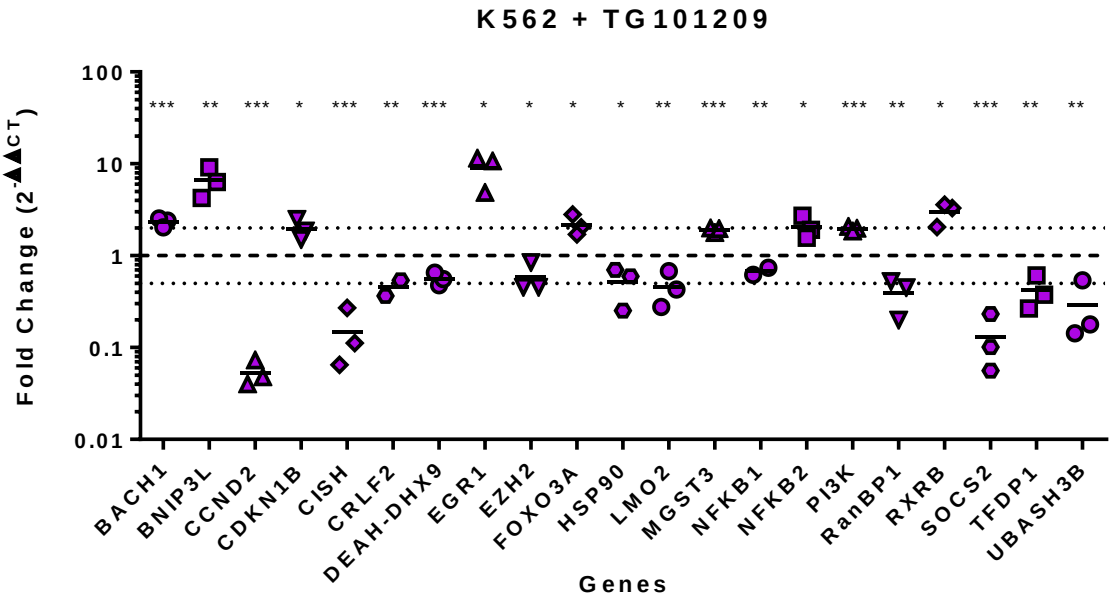


**Fluidigm® quantitative real time PCR was carried out on RNA extracted from K562 cells treated with TG101209 5μM for 24 hours. The fold change compared to untreated samples was calculated using the $2^{-\Delta\Delta CT}$ method. The data points were then graphed using GraphPad Prism 6 and a two tailed Students *t*-test was used to calculate significance (* p ≤ 0.05, ** p ≤ 0.01, *** p ≤ 0.001). The two dotted lines indicate a 2- fold change from the control, indicated by the dashed line.**

AT9283 is an inhibitor with a wide range of cellular targets predominantly the aurora kinases, JAK2 and JAK3. This leads to a different pattern of altered gene expression, although the reduction in negative regulators of JAK2 signalling is still seen in these cells with a reduction in *CISH* and *SOCS2*. Previous reports have suggested that JAK2 inhibition leads to a reduction in *LMO2* expression, however here there is an increase. There is also an unexpected increase in *CCND2*, which may relate to the effect of AT9283 on other targets such as the aurora kinases, however the reduction in *CDK1* and increase in *CDKN1B* is more in keeping with the expected effect of JAK2 inhibition (Figure 3.14).

**Figure 3.14 Gene expression of K562 cells following treatment with AT9283**

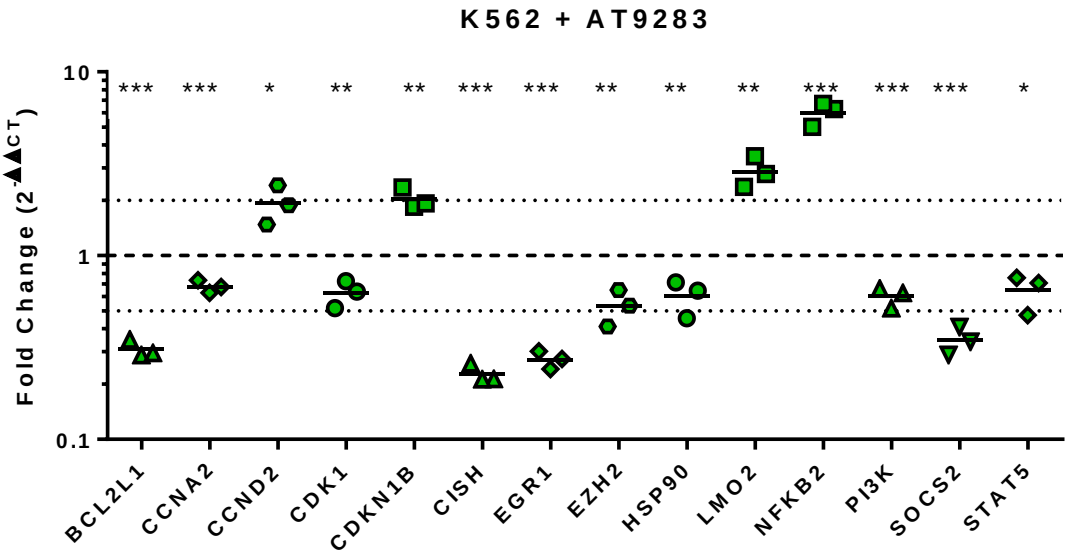


**Fluidigm® quantitative real time PCR was carried out on RNA extracted from K562 cells treated with AT9283 1μM for 24 hours. The fold change compared to untreated samples was calculated using the $2^{-\Delta\Delta CT}$ method. The data points were then graphed using GraphPad Prism 6 and a two tailed Students *t*-test was used to calculate significance (* p ≤ 0.05, ** p ≤ 0.01, *** p ≤ 0.001). The two dotted lines indicate a 2-fold change from the control, indicated by the dashed line.**

### 3.2.6 Apoptosis is increased in K562 cells following treatment with JAK2 inhibitors

In order to confirm the functional significance of the changes in gene expression induced by the inhibitors, apoptosis was assessed by culturing K562 cells in JAK2 inhibitors for 24, 48 and 72 hours. At each of these time points cells were washed and incubated with Annexin V and 7AAD to identify cells undergoing apoptosis. At 24 hours the only significant alteration was in the cells treated with TG101209 5μM with a reduction in live cells and an increase in those entering early apoptosis. By 48 hours all treatment groups were showing evidence of undergoing significant apoptosis (Tables 3.2).

Cells treated with ruxolitinib for 72 hours showed no significant changes in the number of apoptotic or dead cells at 10μM and 20μM concentrations. However when this was increased to 50μM there was a significant decrease in the percentage of live cells and increase in dead cells and those in late apoptosis compared to the other concentrations of ruxolitinib and to untreated cells (Figure 3.15). A similar outcome was seen in cells treated with TG101209 alone, with the highest concentration of 5μM producing more marked effects on live cells, late apoptosis and dead cells compared to the other concentrations of TG101209 and to untreated cells (Figure 3.16). However with AT9283 there was a significant alteration seen in the cells treated at both 0.1μM and 1μM compared to untreated cells and those treated with 0.01μM (Figure 3.17). The cells treated with ruxolitinib produced the smallest change in apoptosis. This is consistent with the gene expression changes where there were no significant alterations in apoptotic genes following treatment with ruxolitinib, while treatment with TG101209 and AT9283 resulted in a wider range of alteration in gene expression including a reduction in anti-apoptotic BCL2L1 following treatment with AT9283 and an increase in pro-apoptotic BNIP3L.

**Table 3.2 Apoptosis at 24 and 48 hours in K562 cells treated with JAK2 inhibitors**

| 24 hours | Live | +/- | Early | +/- | Late | +/- | Dead | +/- |
|---|---|---|---|---|---|---|---|---|
| NDC | 84% | 6.0 | 9.3% | 5.0 | 5.6% | 1.4 | 1.1% | 0.8 |
| Ruxolitinib 10μM | 84.1% | 4.9 | 11.7% | 2.5 | 3.5% | 4.3 | 0.7% | 3.3 |
| Ruxolitinib 20μM | 85% | 8.7 | 10.3% | 2.8 | 4% | 6.3 | 0.7% | 6.8 |
| Ruxolitinib 50μM | 79.8% | 29.8 | 12.9% | 13.9 | 5.8% | 2.7 | 1.5% | 1.1 |
| TG101209 0.1μM | 91.6% | 11.7 | 3.2% | 6.5 | 3.6% | 0.6 | 1.6% | 0.3 |
| TG101209 1μM | 86.2% | 10.3 | 7.5% | 4.4 | 5.4% | 0.4 | 0.9% | 0.3 |
| TG101209 5μM | 60.6% | 12.9 | 29% | 4.5 | 9.2% | 0.7 | 1.2% | 0.8 |
| AT9283 0.01μM | 83.7% | 3.2 | 4.9% | 1.8 | 7.5% | 1.4 | 3.8% | 0.9 |
| AT9283 0.1μM | 69.1% | 7.5 | 8.7% | 2.7 | 14.2% | 1.9 | 7.9% | 0.5 |
| AT9283 1μM | 59.9% | 29.0 | 29.8% | 7.6 | 8.7% | 1.7 | 1.6% | 0.6 |

| 48 hours | Live | +/- | Early | +/- | Late | +/- | Dead | +/- |
|---|---|---|---|---|---|---|---|---|
| NDC | 94.8% | 0.3 | 1.3% | 0.5 | 2.3% | 0.3 | 1.6% | 0.1 |
| Ruxolitinib 10μM | 96% | 0.2 | 0.8% | 0.2 | 1.3% | 0.4 | 1.9% | 0.7 |
| Ruxolitinib 20μM | 91.8% | 1.3 | 1.3% | 0.6 | 2.8% | 0.4 | 4.1% | 1.7 |
| Ruxolitinib 50μM | 79.5% | 9.2 | 6.3% | 3.2 | 9.8% | 4.8 | 4.5% | 1.5 |
| TG101209 0.1μM | 96.1% | 0.8 | 1.2% | 0.6 | 1.2% | 0.4 | 1.5% | 0.2 |
| TG101209 1μM | 92.4% | 2.4 | 2.8% | 1.2 | 1.9% | 0.4 | 2.9% | 1.1 |
| TG101209 5μM | 62.1% | 3.3 | 8.4% | 1.9 | 19.6% | 2.3 | 9.9% | 1.4 |
| AT9283 0.01μM | 90.6% | 3.0 | 1.1% | 0.2 | 3.6% | 1.5 | 4.6% | 1.8 |
| AT9283 0.1μM | 62.3% | 3.3 | 7.9% | 1.2 | 17.8% | 0.9 | 12.1% | 2.8 |
| AT9283 1μM | 38.8% | 2.6 | 4.1% | 0.5 | 12.8% | 3.2 | 44.3% | 3.6 |

**The tables show the percentage of events analysed by FACS for Annexin V and 7AAD in each of the four quadrants on the equating to the live cell population, those cells undergoing the early and late stages of apoptosis and dead cells. The SEM is in the column to the right of each condition (n=3). Statistical analysis was by two-way ANOVA with Tukeys post-test correction. Significant changes compared to NDC are highlighted in red ($p \leq 0.05$).**

**Figure 3.15 Apoptosis in K562 cells treated with Ruxolitinib**

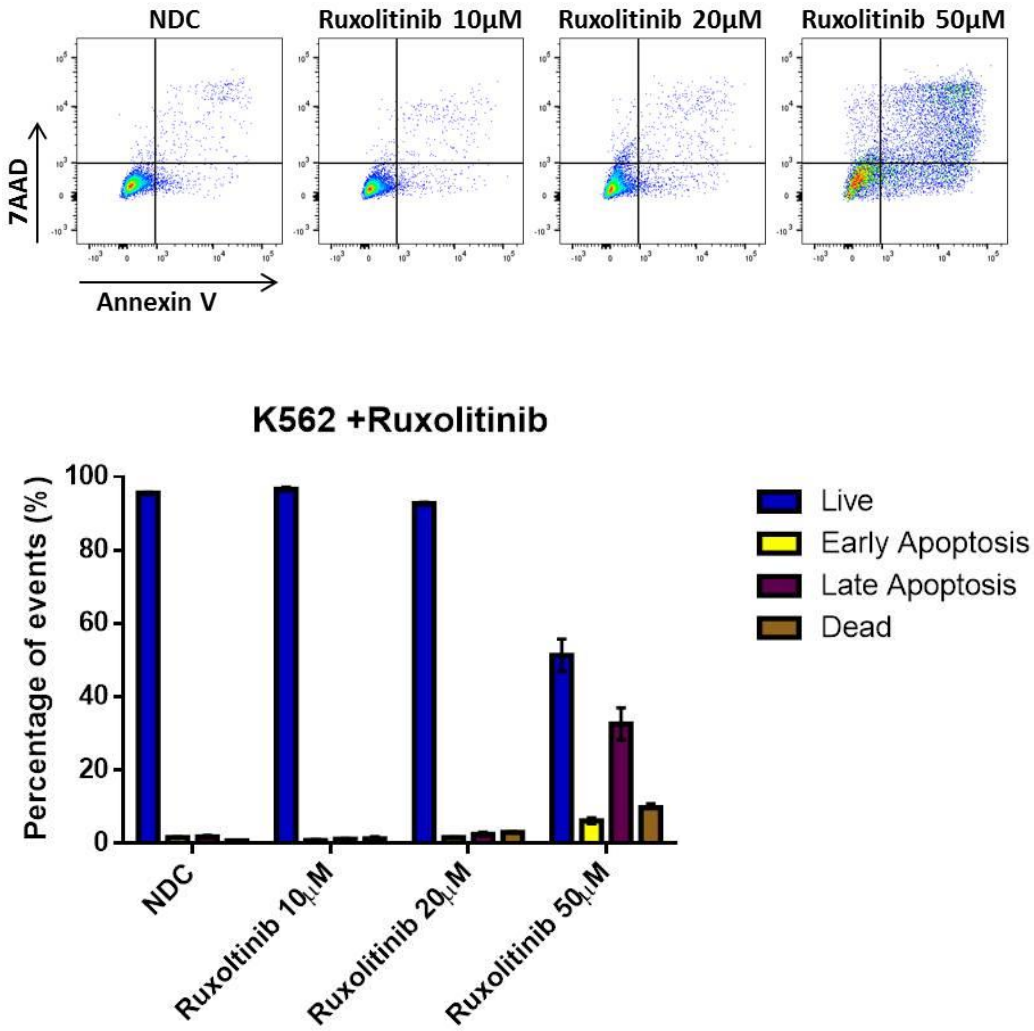


| Live | | | |
|---|---|---|---|
| Rux 10 | NS | | |
| Rux 20 | NS | NS | |
| Rux 50 | **** | **** | **** |
| | NDC | Rux 10 | Rux 20 |

| Early | | | |
|---|---|---|---|
| Rux 10 | NS | | |
| Rux 20 | NS | NS | |
| Rux 50 | NS | NS | NS |
| | NDC | Rux 10 | Rux 20 |

| Late | | | |
|---|---|---|---|
| Rux 10 | NS | | |
| Rux 20 | NS | NS | |
| Rux 50 | **** | **** | **** |
| | NDC | Rux 10 | Rux 20 |

| Dead | | | |
|---|---|---|---|
| Rux 10 | NS | | |
| Rux 20 | NS | NS | |
| Rux 50 | ** | ** | * |
| | NDC | Rux 10 | Rux 20 |

**The dot plots show representative results from the apoptosis assay by FACS. The bar graphs show the changes in live cells, early and late apoptosis, and dead cells treated with ruxolitinib at 72 hours presented as the mean +/- SEM (n=3). Statistical significance was determined by two-way ANOVA with Tukey's post-test correction for multiple comparisons (* p≤0.05, ** p≤0.01, ***p p≤0.001, **** p≤0.0001). The tables show the significance of each comparison for each stage of apoptosis.**

**Figure 3.16 Apoptosis in K562 cells treated with TG101209**

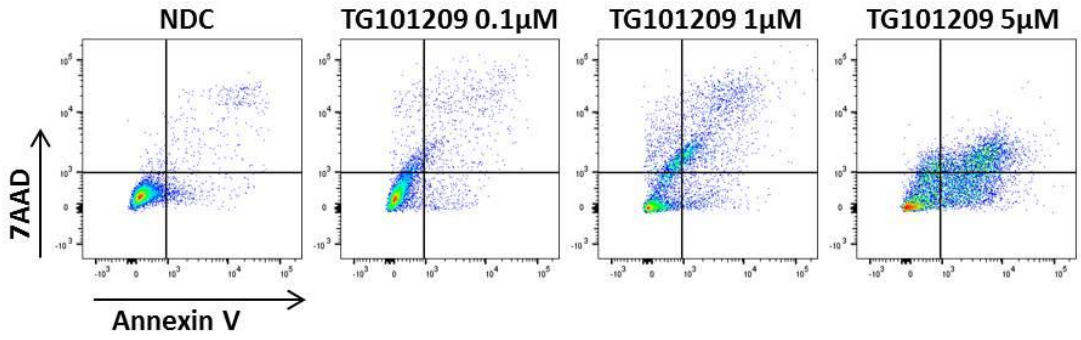


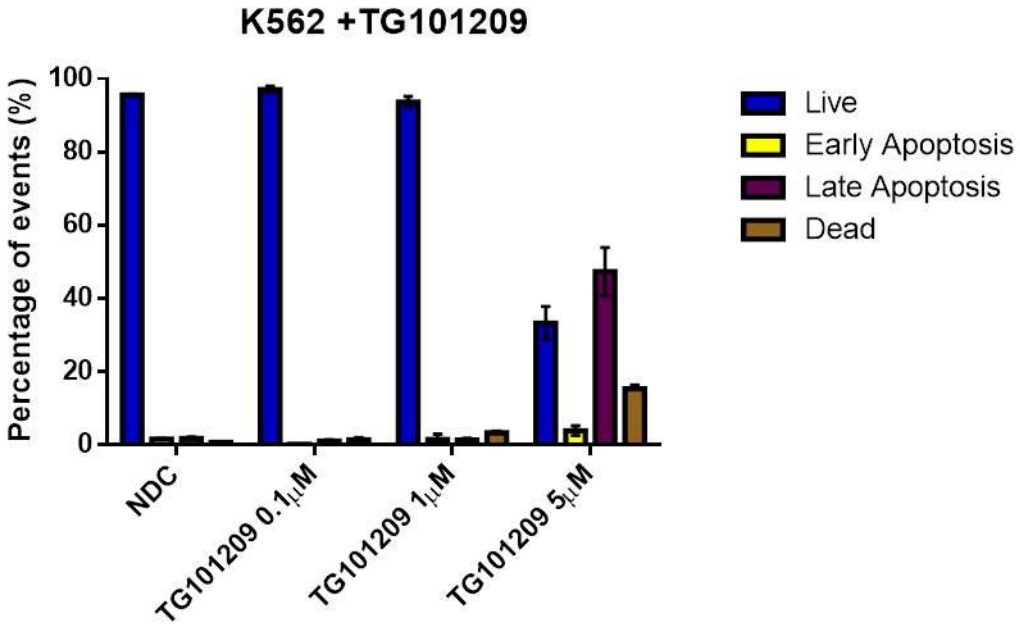


| Live | | | |
|---|---|---|---|
| TG 0.1 | NS | | |
| TG 1 | NS | NS | |
| TG 5 | **** | **** | **** |
| | NDC | TG0.1 | TG1 |

| Early | | | |
|---|---|---|---|
| TG 0.1 | NS | | |
| TG 1 | NS | NS | |
| TG 5 | NS | NS | NS |
| | NDC | TG0.1 | TG1 |

| Late | | | |
|---|---|---|---|
| TG 0.1 | NS | | |
| TG 1 | NS | NS | |
| TG 5 | **** | **** | **** |
| | NDC | TG0.1 | TG1 |

| Dead | | | |
|---|---|---|---|
| TG 0.1 | NS | | |
| TG 1 | NS | NS | |
| TG 5 | *** | *** | ** |
| | NDC | TG0.1 | TG1 |

**The dot plots show representative results from the apoptosis assay by FACS. The bar graphs show the changes in live cells, early and late apoptosis, and dead cells treated with TG101209 at 72 hours presented as the mean +/- SEM (n=3). Statistical significance was determined by two-way ANOVA with Tukey's post-test correction for multiple comparisons (* p≤0.05, ** p≤0.01, ***p p≤0.001, **** p≤0.0001). The tables show the significance of each comparison for each stage of apoptosis.**

**Figure 3.17 Apoptosis in K562 cells treated with AT9283**

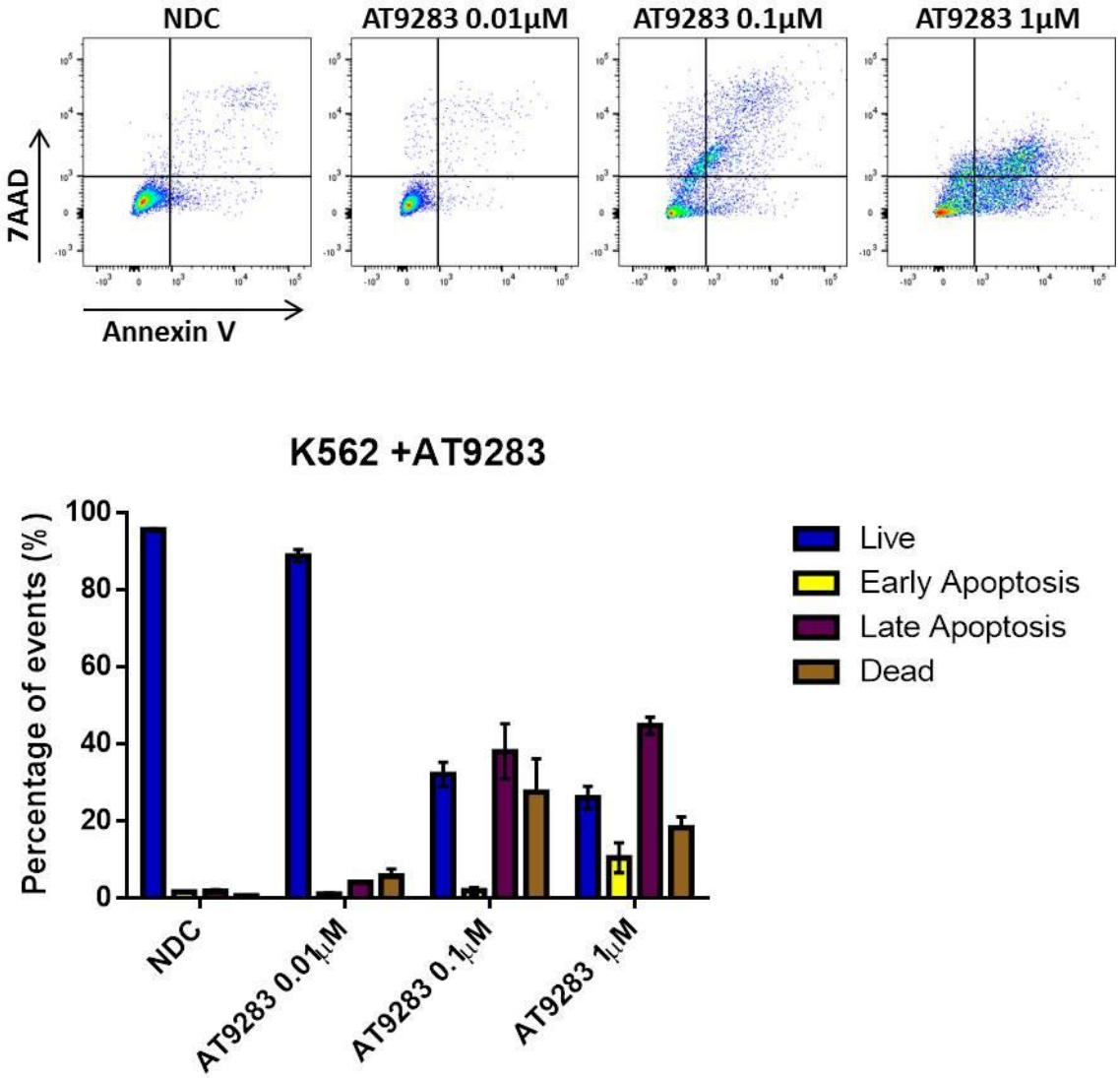


| Live | | | |
|---|---|---|---|
| AT0.01 | NS | | |
| AT0.1 | **** | **** | |
| AT1 | ***** | **** | NS |
| | NDC | AT0.01 | AT0.1 |

| Early | | | |
|---|---|---|---|
| AT0.01 | NS | | |
| AT0.1 | NS | NS | |
| AT1 | NS | NS | NS |
| | NDC | AT0.01 | AT0.1 |

| Late | | | |
|---|---|---|---|
| AT0.01 | NS | | |
| AT0.1 | **** | **** | |
| AT1 | ***** | **** | NS |
| | NDC | AT0.01 | AT0.1 |

| Dead | | | |
|---|---|---|---|
| AT0.01 | NS | | |
| AT0.1 | **** | *** | |
| AT1 | ** | NS | NS |
| | NDC | AT0.01 | AT0.1 |

**The dot plots show representative results from the apoptosis assay by FACS. The bar graphs show the changes in live cells, early and late apoptosis, and dead cells treated with AT9283 at 72 hours presented as the mean +/- SEM (n=3). Statistical significance was determined by two-way ANOVA with Tukey's post-test correction for multiple comparisons (* p≤0.05, ** p≤0.01, ***p p≤0.001, **** p≤0.0001). The tables show the significance of each comparison for each stage of apoptosis.**

As shown there is a progressive increase in apoptosis at 72 hours of treatment. This ability to induce a greater degree of apoptosis by AT9283 treatment likely reflects its wider range of targets, enabling inhibition of multiple pathways within the cells, in particular cellular proliferation and division through its ability to inhibit JAK2 and Aurora kinases respectively. There is also some evidence that AT9283 has activity against BCR-ABL[198], which we also confirmed by western blotting with reduced pABL and pCRKL levels following treatment of K562 cells with AT9283.

### 3.2.7 Cell cycle is altered in K562 cells following treatment with JAK2 inhibitors

Cell cycle alterations play an important role in the expansion of the malignant CML clone. As shown above there is alteration in the gene expression of key regulators of the cell cycle which results in the malignant cells dividing more frequently. This, in combination with a reduction in apoptosis, leads to a proliferative advantage over the normal cells. Following on from the alterations in cell cycle genes observed, next we looked at the effect of the JAK2 inhibitors on the cell cycle in K562 cells.

Following treatment with ruxolitinib for 72 hours there is an increase in the percentage of cells in S, G2 and M phase which suggests that cells have entered the cell cycle, but become blocked at this stage (Figure 3.18). This is not seen in cells treated with TG101209 (Figure 3.19), which would suggest that JAK2 inhibition alone is insufficient to achieve this alteration in cell cycle. Cells treated with AT9283 were more difficult to assess due to the effect of Aurora kinase B inhibition which is known to cause a failure of mitosis and accumulation in the cells of multiple nuclei (Figure 3.20). The cell cycle assay relies on the staining properties of propidium iodide, which binds to DNA with a fluorescence intensity proportional to the amount of DNA present. As a result of the increased number of nuclei present in the cells treated with AT9283 it was not possible to extract useful information about the cell cycle.

**Figure 3.18 Cell cycle analysis of K562 cells following treatment with ruxolitinib**

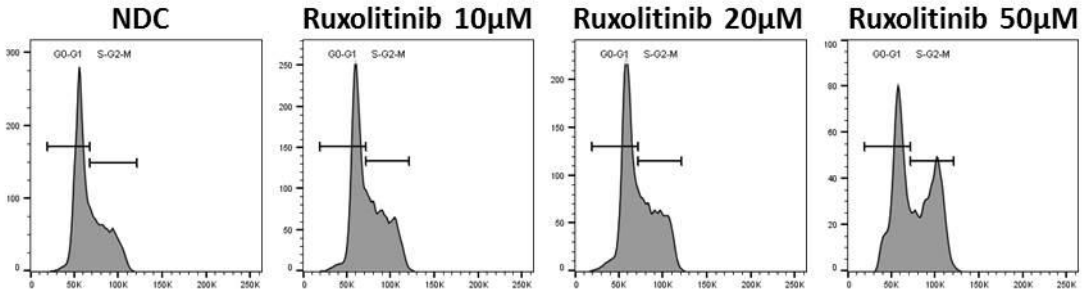


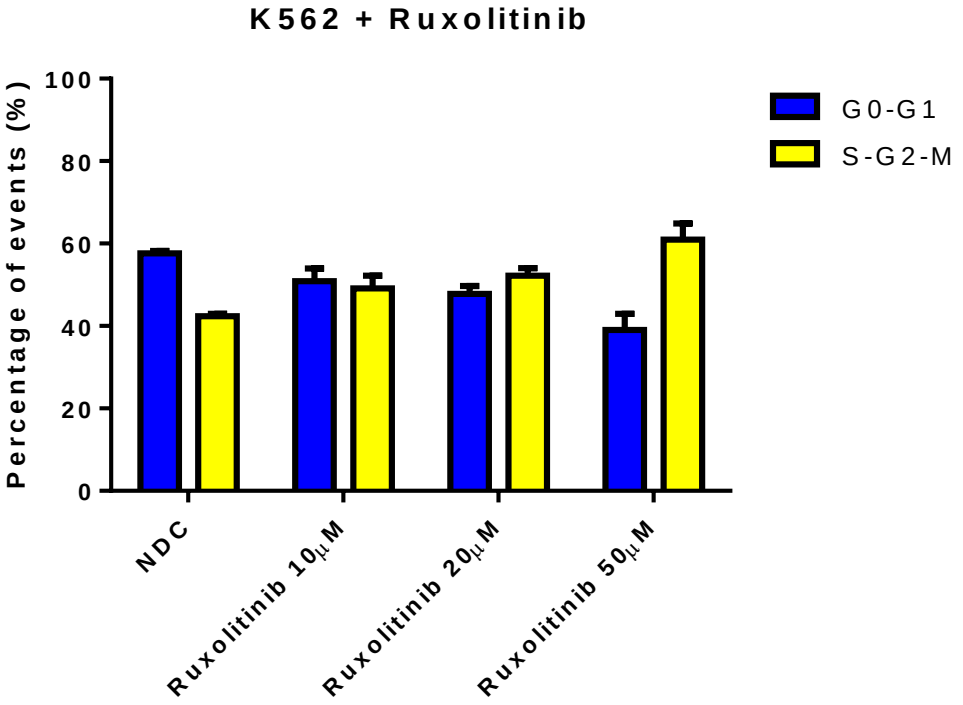


| G0-G1 | | | |
|---|---|---|---|
| **Rux10** | NS | | |
| **Rux20** | NS | NS | |
| **Rux50** | *** | * | NS |
| | **NDC** | **Rux10** | **Rux20** |

| S-G2-M | | | |
|---|---|---|---|
| **Rux10** | NS | | |
| **Rux20** | NS | NS | |
| **Rux50** | *** | * | NS |
| | **NDC** | **Rux10** | **Rux20** |

**The histogram plots show representative results from FACS and show the gating strategy used. The bar graphs show the changes in cell cycle following treatment with ruxolitinib for 72 hours, highlighting those actively undergoing cell cycle (S-G2-M) and those that are quiescent (G0-G1). They are presented as the mean +/- SEM (n=3). Statistical significance was determined by two-way ANOVA with Tukey's post-test correction for multiple comparisons (* p≤0.05, ** p≤0.01, ***p p≤0.001, **** p≤0.0001).**

**Figure 3.19 Cell cycle analysis of K562 cells following treatment with TG101209**

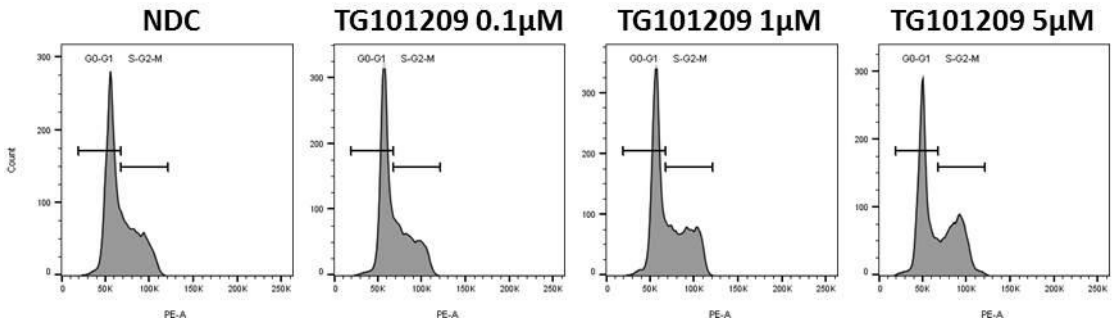


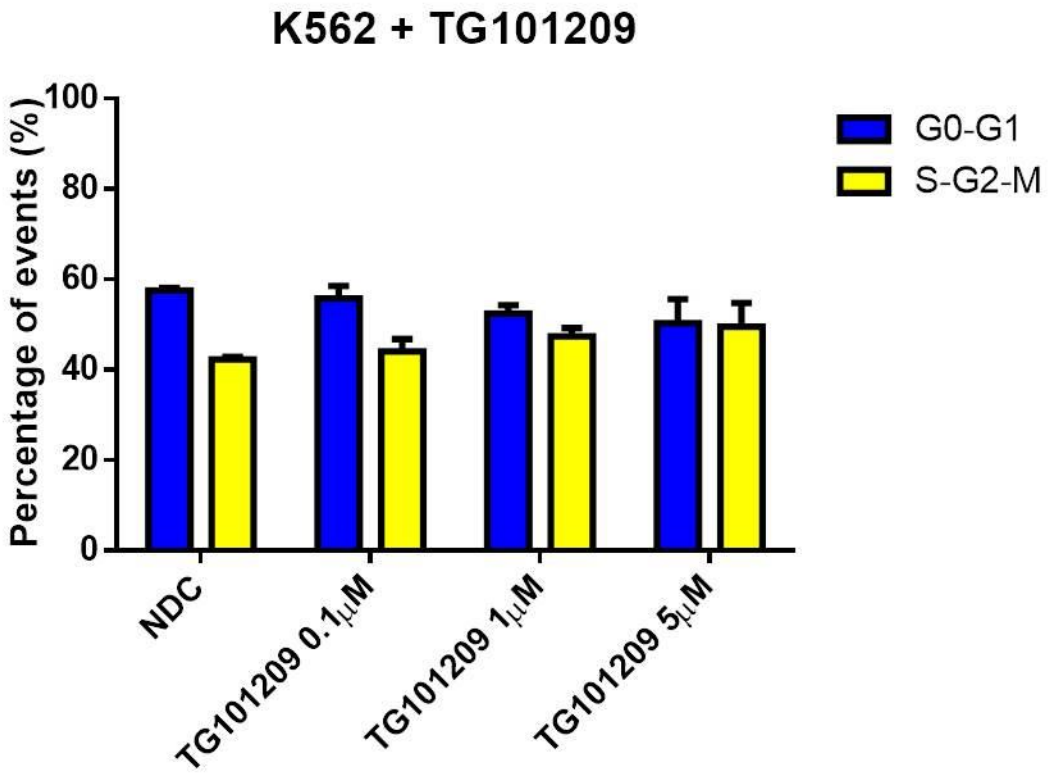


| G0-G1 | | | |
|---|---|---|---|
| **TG0.1** | NS | | |
| **TG1** | NS | NS | |
| **TG5** | NS | NS | NS |
| | **NDC** | **TG0.1** | **TG1** |

| S-G2-M | | | |
|---|---|---|---|
| **TG0.1** | NS | | |
| **TG1** | NS | NS | |
| **TG5** | NS | NS | NS |
| | **NDC** | **TG0.1** | **TG1** |

**The histogram plots show representative results from FACS and show the gating strategy used. The bar graphs show the changes in cell cycle following treatment with TG101209 for 72 hours, highlighting those actively undergoing cell cycle (S-G2-M) and those that are quiescent (G0-G1). They are presented as the mean +/- SEM (n=3). Statistical significance was determined by two-way ANOVA with Tukey's post-test correction for multiple comparisons (* p≤0.05, ** p≤0.01, ***p p≤0.001, **** p≤0.0001).**

**Figure 3.20 Cell cycle analysis of K562 cells following treatment with AT9283**

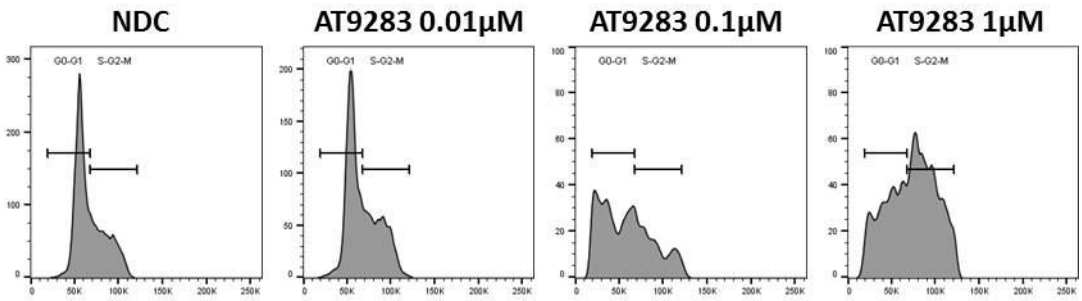


**The histogram plots show representative results from the PI staining and FACS analysis. When the normal gating strategy was applied it was difficult to extract any meaningful data from cells treated with AT9283.**

### 3.2.8 Immunofluorescence of K562 cells following treatment with JAK2 inhibitors or IFN-γ

To further assess the effect of JAK2 inhibition on protein expression and interaction we looked at the interaction of JAK2 with two important proteins in the inflammatory response SUMO2/3 and PML. Phosphorylated JAK2 has previously been shown to acquire the ability to enter the nucleus following the addition of a SUMO2/3 chain[78]. Additionally it has been shown that JAK2 interacts with histone 3 to increase transcription at important sites for haematopoiesis[79,80]. However it is still unclear as to how JAK2 interacts with H3 within the nucleus, one possibility is the role of PML nuclear bodies (NBs) in transcriptional and epigenetic changes. NB's are known to assemble SUMOylated proteins within precise sites and to be regulated by inflammation. We therefore postulated that JAK2 may interact directly with PML NBs, a sub-nuclear structure with an important regulatory role in many cellular processes, which interacts with proteins in the nucleus based on the presence of SUMO chains. As a result we decided to look at the interaction of JAK2 with SUMO2/3 following stimulation with IFNγ, which is known to increase SUMO protein expression. In addition we then investigated what effects JAK2 inhibitors would have on this process. K562 cells were treated for 24 hours with each treatment arm before being processed for immunofluorescence to determine cellular location by the Duolink immunofluorescent co-localisation assay.

Immunofluorescence was used to identify the localisation of proteins in the cytoplasm and nucleus. As expected, PML is seen in discrete structures within the nucleus and increases in abundance when cells are treated with IFNγ. JAK2 is seen in both the cytoplasm and in the nucleus which is consistent with previous reports and SUMO2/3 is located throughout the cell with higher fluorescence seen in a similar distribution as PML, which is likely to reflect the high concentrations of SUMOylated proteins seen within the PML NBs (Figure 3.21).

**Figure 3.21 Immunofluorescence of K562 cells following treatment with JAK2 inhibitors or IFN-γ**

**a) K562 cells probed for JAK2 and PML**

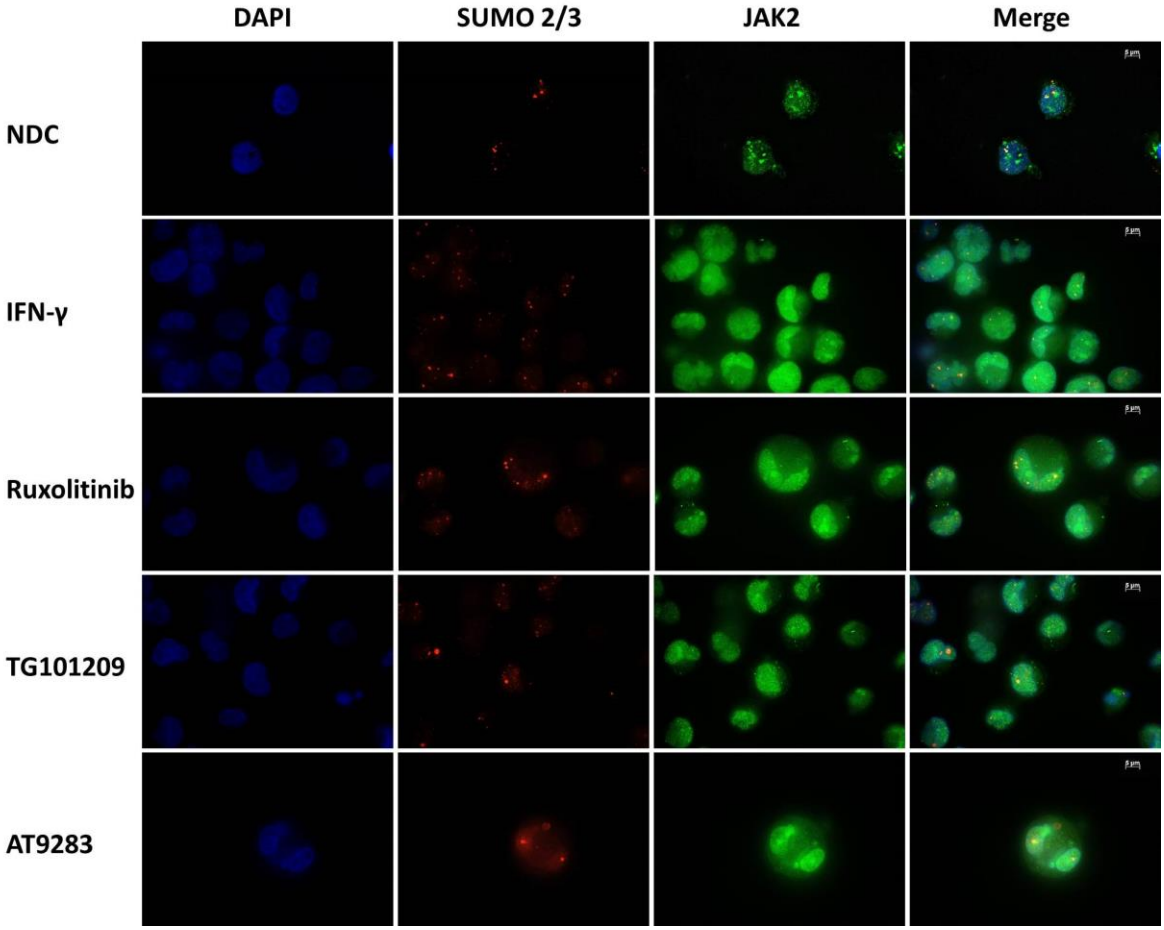

**b) K562 cells probed for JAK2 and SUMO2/3**

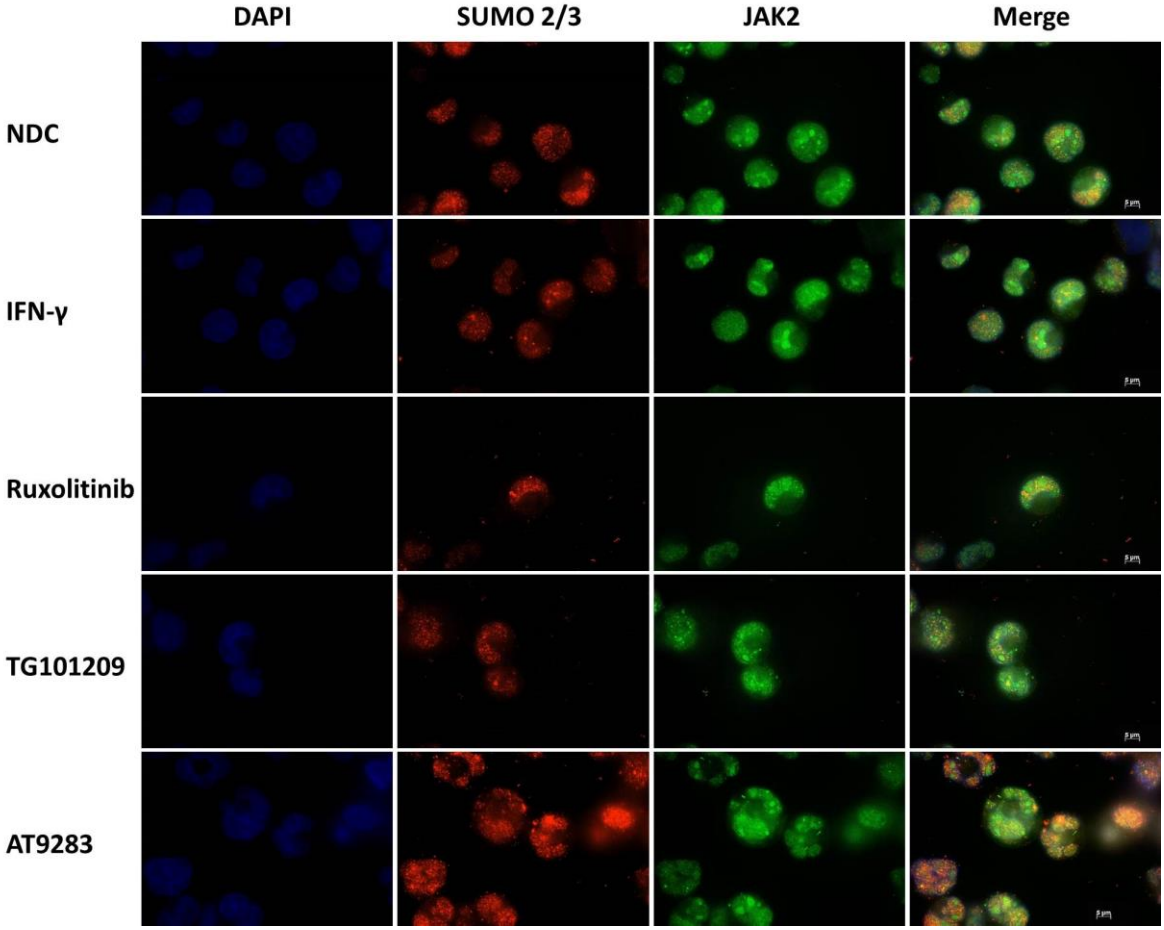


**K562 cells were treated for 24 hours then prepared for immunofluorescence as described previously. 3 separate experiments were carried out and representative images are shown above with cells being assessed for JAK2 and PML in a) and for JAK2 and SUMO in b).**

Duolink indicated that following 24 hours of stimulation with IFNγ there was little change in the association of JAK2 and SUMO2/3, while there was a marked increase in the association of JAK2 with PML. Conversely ruxolitinib treatment resulted in an increase in the association of JAK2 with SUMO2/3 and a reduction in JAK2 and PML. TG101209 treatment led to a slight, but non-significant increase in the association of JAK2 with PML and a significant increase in the association of JAK2 with SUMO2/3 (Figure 3.22 b). The reasons for the increase in association with JAK2 and SUMO2/3 following JAK2 inhibition may relate to the mechanism of action of the inhibitors, as they do not alter the phosphorylation status of JAK2 at the Y1007/1008 site, essential for the binding of SUMO. What is interesting is that this increase in the association does not lead to an increase in the association of

JAK2 with PML, but instead either led to a small change or a significant decrease in the association depending on the inhibitor used (Figure 3.22b). This suggests the interaction of JAK2 with PML requires more than just the presence of a SUMO chain.

**Figure 3.22 Duolink co-localisation assay in K562 cells treated with JAK2 inhibitors**

**a)**

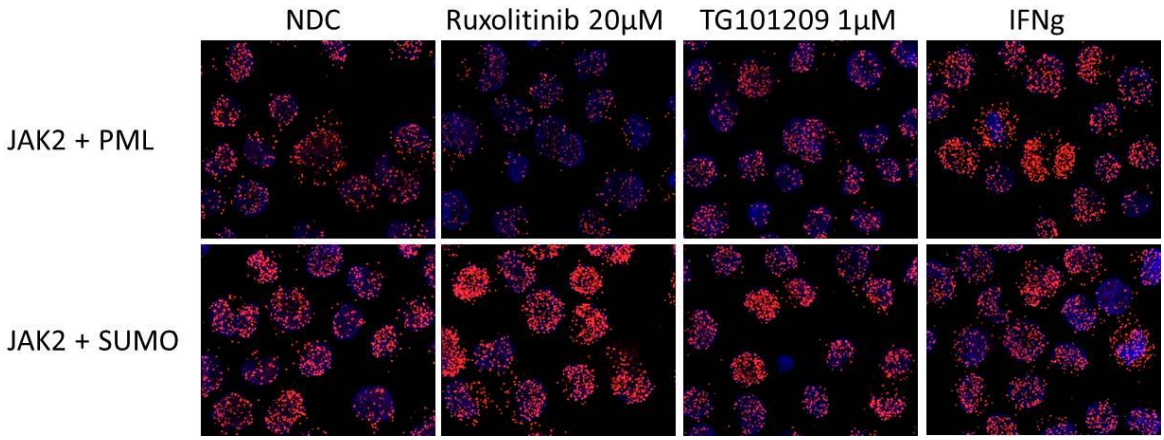


**b)**

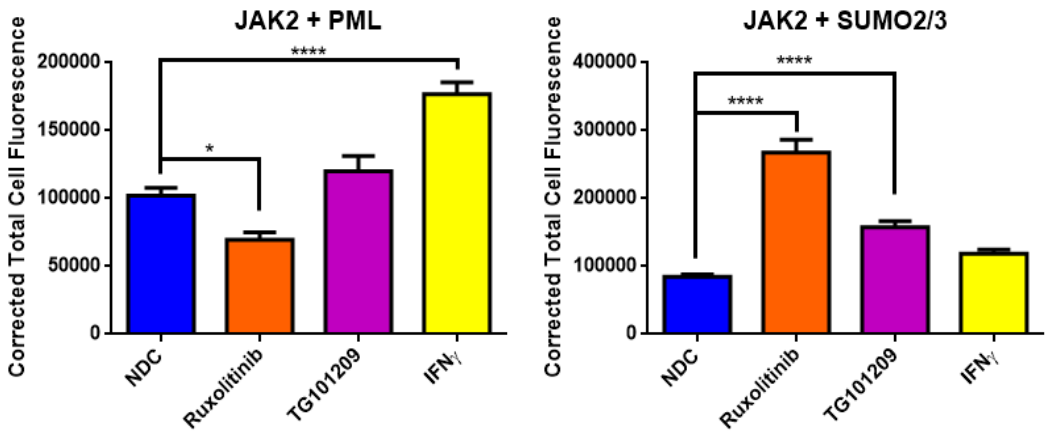


**K562 cells were treated for 24 hours then prepared for Duolink immunofluorescent co-localisation assay as described previously. 80 cells were counted for each treatment in 3 separate experiments with the corrected total cell fluorescence calculated. The images (3a) are representative of the experiments while the graphs (3b) show the average of the corrected total cell fluorescence for all 3 experiments +/- SEM. AT9283 was not included due to a lack of adherence of sufficient cells for analysis. Statistical significance was determined by one way ANOVA with Dunnett's correction for multiple comparisons (* p≤0.05, ** p≤0.01, *** p≤0.001, **** p≤0.0001).**

### 3.2.9 Effect of JAK2 inhibition on JAK2 downstream targets in CML CD34 +ve cells

In order to determine the efficacy of ruxolitinib on JAK2 downstream targets in primary samples, CML CD34+ve cell were treated with nilotinib and ruxolitinib either alone or in combination. The inhibitors chosen were within the clinical dose, with concentrations of; nilotinib 5μM and ruxolitinib 1μM chosen as physiologically achievable doses. Three CD34+ve chronic phase CML samples were treated with these two inhibitors alone and in combination. Following the defrosting process two samples had sufficient cells for both RNA and protein to be made, with the remaining sample only having a sufficient number of cells for RNA. As a result three samples were used for Fluidigm® real time PCR to assess gene expression, while only two were assessable in Western blots. The protein extracted from these experimental arms was probed for downstream targets to confirm specificity of the inhibitors. The results showed that nilotinib effectively inhibited the phosphorylation of CRKL, JAK2 and STAT5, while ruxolitinib reduced the phosphorylation of STAT5 compared to untreated samples, but was unable to completely inhibit the phosphorylation alone as a single agent as BCR-ABL is known to directly phosphorylate STAT5. It is interesting that there is still a reduction in STAT5 phosphorylation, suggesting that JAK2 still has a role to play in the overall activation of STAT5 despite the activity of BCR-ABL directly on STAT5 (Figure 3.23).

**Figure 3.23 Western blotting of CML CD34+ve samples treated with nilotinib and ruxolitinib**

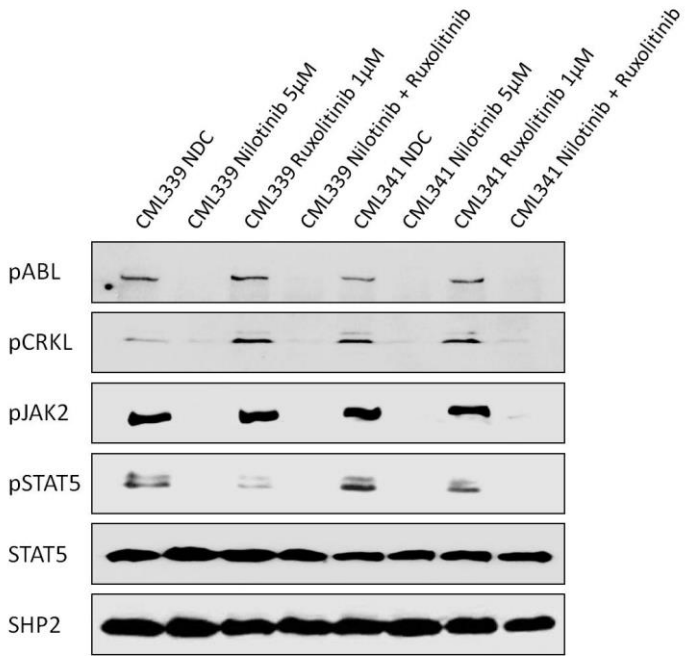


**Protein samples were obtained from CML CD34+ve selected samples following eight hours of culture in media alone or supplemented with nilotinib 5μM, ruxolitinib 1μM, or both in inhibitors together. The lysates were then run according to the protocol described previously (2.4.4.2). The nitrocellulose membranes were then probed using antibodies to the proteins indicated above and detected using HRP-conjugated antibodies. Equal protein loading of the samples was ensured by probing for SHP2.**

### 3.2.10 Alteration in gene expression of JAK2 targets in CML CD34 +ve cells treated with nilotinib and ruxolitinib

Next we examined the effects of nilotinib and ruxolitinib alone and in combination on the JAK2 target genes previously investigated from the microarray analysis (Figure 3.1). The graphs below show genes known to be deregulated in untreated patient samples (Figure 3.2). They also show the effects on gene expression in the samples following treatment with nilotinib and ruxolitinib alone and in combination (Figure 3.24). As shown in the heatmap the three samples did not always result in the same response to treatment, however there is a clear effect from each of the inhibitors, which is often compounded when added together. The individual graphs highlight genes shown to be deregulated in untreated samples which displayed interesting responses following treatment.

**Figure 3.24 Heatmap of CML CD34+ve samples treated with nilotinib and ruxolitinib**

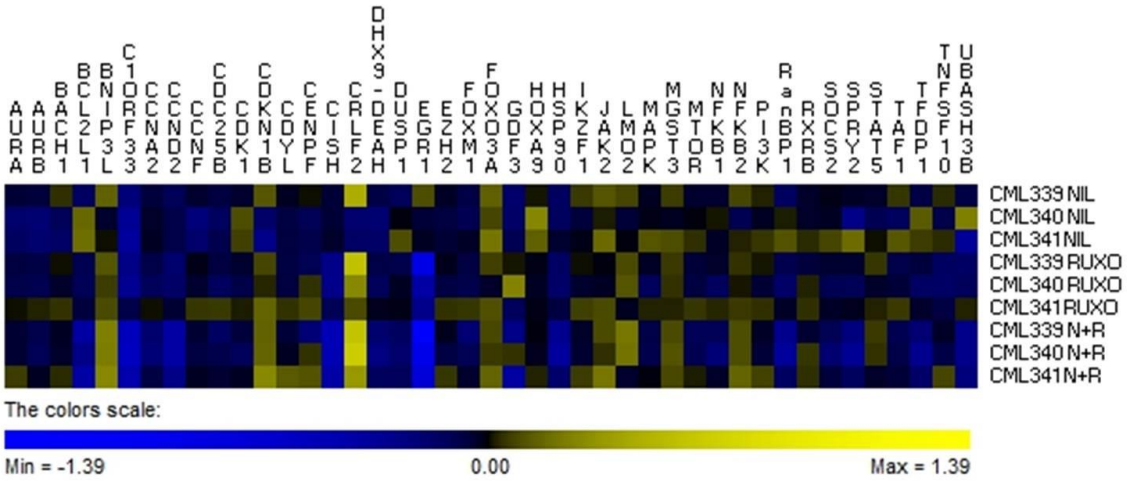


**Fluidigm quantitative real time PCR was performed on 3 CML CD34+ve samples following treatment with nilotinib and ruxolitinib alone and in combination. Each sample was run in triplicate. The relative expression of the genes compared to the no drug control for each sample was calculated using the $2^{-\Delta\Delta CT}$ method. A base 10 logarithmic transformation was then performed and this data was entered in to PermutMatrix to generate a heatmap representation of the gene expression with the three samples grouped together according to treatment arms.**

CISH is a negative regulator of JAK2 signalling, and is increased in CML PB MNCs. When CML CD34+ve samples were treated with nilotinib, there was little change in expression compared with no treatment with a fold change similar to baseline, while ruxolitinib achieved a two-fold reduction in the expression, compared to normal. However, when combined nilotinib and ruxolitinib produced a significant alteration compared to the other treatment conditions. This is likely to represent a reduction of the requirement for negative regulation of cytokine signalling as a result of the combined inhibition of BCR-ABL and JAK2 activity (Figure 3.25).

**Figure 3.25 CISH expression in CML CD34+ve samples following treatment with nilotinib and ruxolitinib**

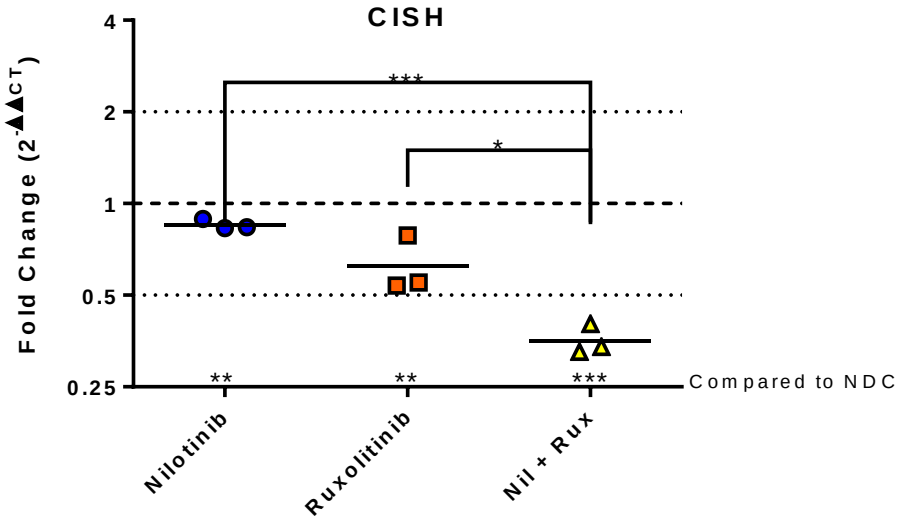


**Fluidigm® quantitative real time PCR was carried out on RNA extracted from chronic phase CML CD34+ve samples following treatment with nilotinib 5μM and ruxolitinib 1μM alone and in combination. The fold change compared to normal was calculated using the $2^{-\Delta\Delta CT}$ method. The data points were then graphed using GraphPad Prism 6 and a two tailed Students *t*-test was used to calculate significance (* p ≤ 0.05, ** p ≤ 0.01, *** p ≤ 0.001), with comparisons made between untreated samples and between each treatment arm. The two dotted lines indicate a 2- fold change from the control, indicated by the dashed line.**

BCL2L1 is an anti-apoptotic gene altered in both the CD34+ve cells and PB MNCs of CML samples, while BNIP3L is involved in apoptosis of cells following exposure to cellular stresses and is convincingly increased in the peripheral blood cells, but was more borderline in the CML CD34+ve cells when compared to normal CD34+ve cells. When treated with nilotinib or ruxolitinib alone there was little effect seen in *BCL2L1* expression in CD34+ve cells although the alteration seen in ruxolitinib treated cells is significant due to the compactness of the results. When combined the dual inhibition resulted in a significant reduction in the expression of *BCL2L1* compared to each treatment arm and untreated cells. However with *BNIP3L* there was an increase in the expression, which suggests the combination of BCR-ABL and JAK2 inhibition produces a sufficient stress on the cells to drive apoptotic cell death (Figure 3.26)

**Figure 3.26 BCL2L1 and BNIP3L expression in CML CD34+ve samples following treatment with nilotinib and ruxolitinib**

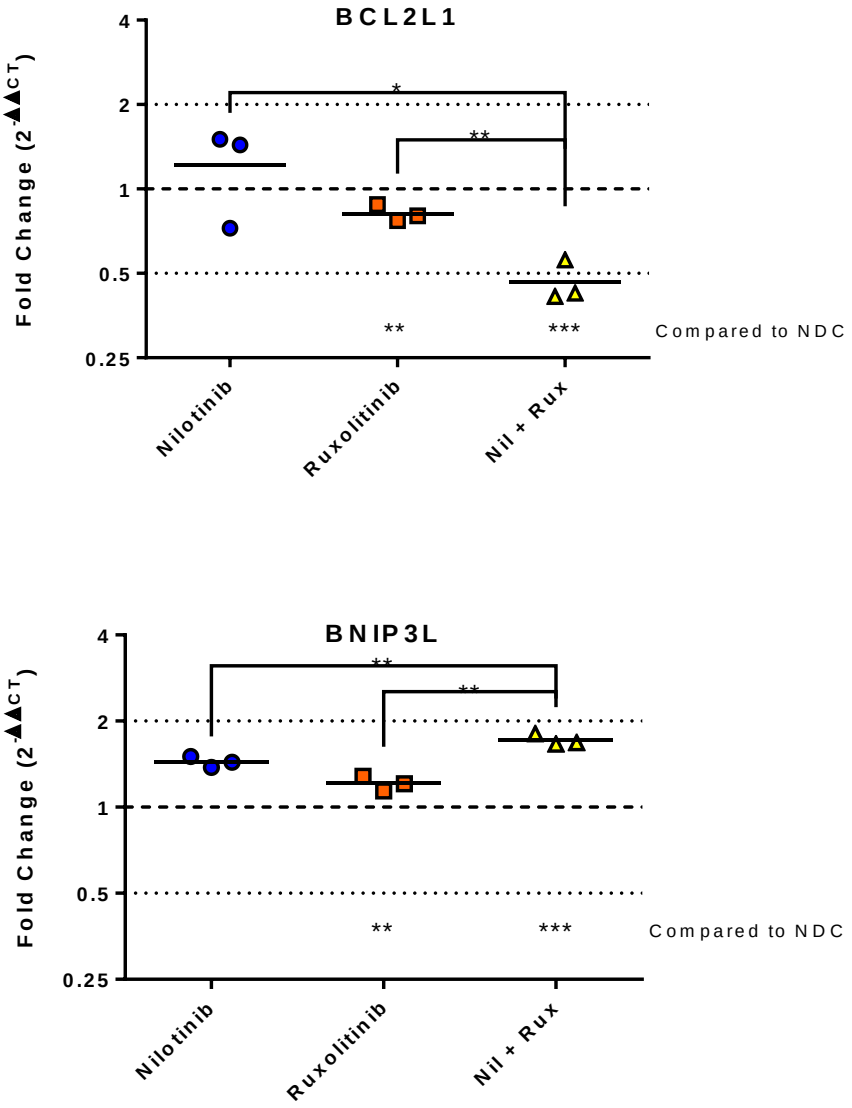


**Fluidigm® quantitative real time PCR was carried out on RNA extracted from chronic phase CML CD34+ve samples following treatment with nilotinib 5μM and ruxolitinib 1μM alone and in combination. The fold change compared to normal was calculated using the $2^{-\Delta\Delta CT}$ method. The data points were then graphed using GraphPad Prism 6 and a two tailed Students *t*-test was used to calculate significance (* p ≤ 0.05, ** p ≤ 0.01, *** p ≤ 0.001), with comparisons made between untreated samples and between each treatment arm. The two dotted lines indicate a 2- fold change from the control, indicated by the dashed line.**

EGR1 is an early response transcription factor which induces the expression of many proteins involved in cell growth and differentiation, apoptosis and stress responses. In CML CD34+ve cells there was a wide range of expression with some patients displaying up- and others down-regulation whereas others were unchanged when compared to normal CD34+ cells. However in PB MNCs there was a consistent and significant increase in *EGR1* expression compared to normal MNCs, although this analysis was performed in a smaller cohort of samples. When treated with nilotinib CML CD34+ve cells express *EGR1* at the same levels as untreated cells, while there was a significant decrease in expression when cells were treated with ruxolitinib alone. In cells treated with dual inhibition there was a marked decrease in expression which is significant when compared with untreated cells and those treated with nilotinib alone. This suggests that although BCR-ABL has an effect on *EGR1* expression this can be bypassed in the event of BCR-ABL inhibition, while JAK2 has a direct effect on *EGR1* expression and may be the mechanism of ongoing activity in the presence of BCR-ABL inhibition as dual inhibition has a greater affect than either inhibitor alone (Figure 3.27).

**Figure 3.27 EGR1 expression in CML CD34+ve samples following treatment with nilotinib and ruxolitinib**

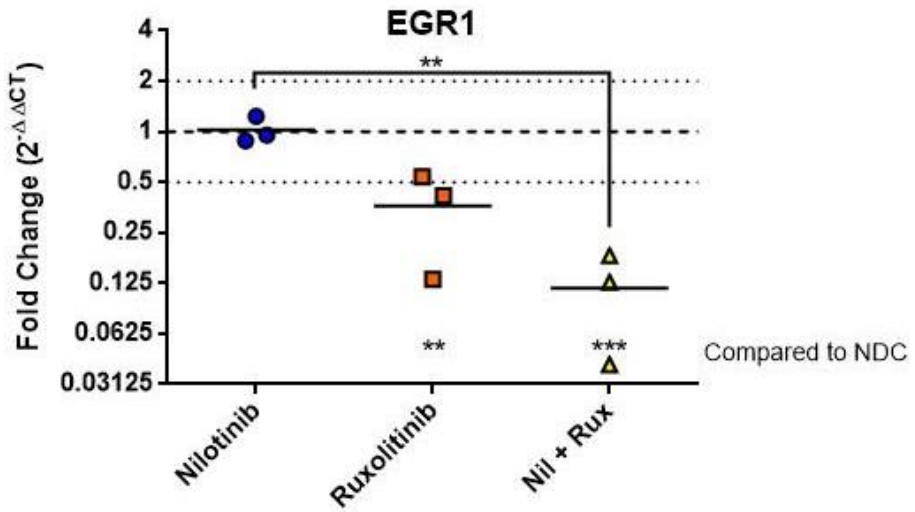


**Fluidigm® quantitative real time PCR was carried out on RNA extracted from chronic phase CML CD34+ve samples following treatment with nilotinib 5μM and ruxolitinib 1μM alone and in combination. The fold change compared to normal was calculated using the $2^{-\Delta\Delta CT}$ method. The data points were then graphed using GraphPad Prism 6 and a two tailed Students *t*-test was used to calculate significance (* p ≤ 0.05, ** p ≤ 0.01, *** p ≤ 0.001), with comparisons made between untreated samples and between each treatment arm. The two dotted lines indicate a 2- fold change from the control, indicated by the dashed line.**

CCND2 is a key regulator in cell cycle progression which forms a complex with the cyclin dependent kinases 4 and 6 to initiate cell cycle transition from G1 to S phase. *CCND2* is consistently elevated in CML CD34+ve cells and when these cells were treated with single inhibitors there was very little change in the expression levels, although these changes are significant by two tailed Students *t*-test. However when the inhibitors were combined there was a significant reduction in the expression of this gene, both compared to untreated cells and to each inhibitor individually, which suggests that neither JAK2 or BCR-ABL is responsible for the control of *CCND2* expression alone, and both kinases activate pathways involved in its regulation (Figure 3.28)

**Figure 3.28 CCND2 expression in CML CD34+ve samples following treatment with nilotinib and ruxolitinib**

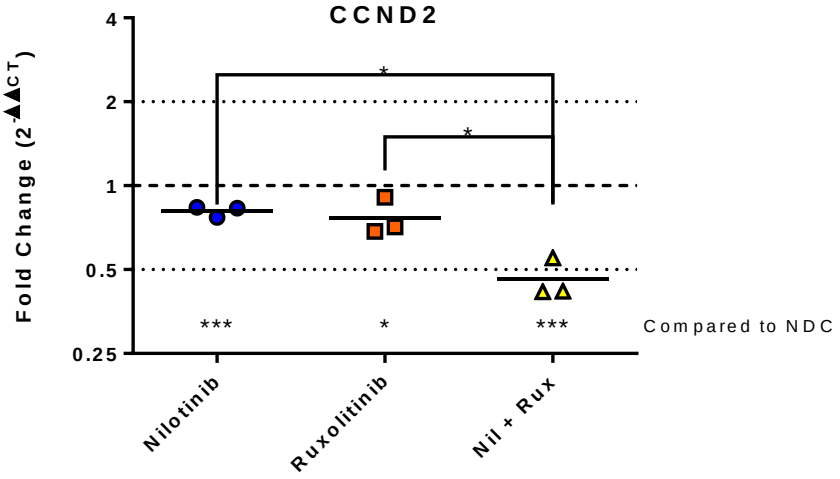


**Fluidigm® quantitative real time PCR was carried out on RNA extracted from chronic phase CML CD34+ve samples following treatment with nilotinib 5μM and ruxolitinib 1μM alone and in combination. The fold change compared to normal was calculated using the $2^{-\Delta\Delta CT}$ method. The data points were then graphed using GraphPad Prism 6 and a two tailed Students *t*-test was used to calculate significance (* p ≤ 0.05, ** p ≤ 0.01, *** p ≤ 0.001), with comparisons made between untreated samples and between each treatment arm. The two dotted lines indicate a 2- fold change from the control, indicated by the dashed line.**

## 3.3 Discussion

### 3.3.1 Proliferation and cell cycle in CML

One of the defining characteristics of CML is the marked proliferation and expansion of myeloid cells at all stages, detected in the bone marrow and the peripheral blood. The cause of this is the effect of BCR-ABL activity on a number of cellular signalling pathways that regulate the proliferation of myeloid cells. JAK2 signalling has been shown repeatedly to be upregulated, but there are differing opinions on whether JAK2 itself has any role to play[2,176,199]. There are some who feel that the activation of STATs directly by BCR-ABL makes the activity of JAK2 less important. However there have been a number of papers in the last few years suggesting that the interaction of JAK2 and BCR-ABL in CML is important and the pathway is activated not just by the direct effect on STAT signalling. A paper by Gallipoli *et al* in 2014 showed that combining BCR-ABL inhibition using nilotinib with JAK2 inhibition with ruxolitinib lead to an increased toxic effect on CML CD34+ve cells when compared with the effects observed by each drug alone. Interestingly this combination did not affect normal CD34+ve cells to the same degree[2]. In 2013 Chen *et al* published work showing that BCR-ABL and JAK2 interact directly through each binding to AHI-1, which is found in high levels in CML CD34+ve cells. Interrupting either of these interactions led to a marked increase in the sensitivity of CML CD34+ve cells to imatinib therapy, suggesting that the direct interaction of these three proteins play a significant part in the survival of CML stem cells following imatinib therapy[105].

In this work we showed that there are alterations in gene expression of downstream JAK2 targets in K562 cells following treatment with a range of JAK2 inhibitors, however an alteration of cell cycle in these cells seemed to require the inhibition of additional kinases aside form JAK2, such as BCR-ABL itself or the Aurora kinases.

### 3.3.2 Apoptosis in CML

Alteration of apoptosis either by increasing the activity of anti-apoptotic proteins or inhibiting pro-apoptotic pathways is a recognised mechanism used by many cancers to promote their survival. In CML, BCR-ABL activity protects the cells from stresses which would normally induce apoptosis, as well as allowing the cells to survive for longer without cytokine stimulation[200]. This is due to BCR-ABL increases the expression of anti-apoptotic Bcl-2 family members while interfering with the inhibitory effects of pro-apoptotic proteins, which leads to prevention of the activation of caspases by stopping the release of cytochrome-c from the mitochondria[181]. This interference leads to a survival advantage for the CML cells and allows expansion of the clone. Our data confirmed abnormalities of several genes involved in the regulation of apoptosis with an increase in BCL2L1 in both CD34+ve cells and in PB MNCs. There was also a decrease in the anti-apoptotic MCL-1 in CML CD34+ve cells which has previously been shown to be induced by BCR-ABL and inhibited by TKI therapy. Finally the decrease of TNFSF10 has previously been shown to be reduced in CML as a result of a BCR-ABL mediated increase of preferentially expressed antigen of melanoma (PRAME) which in turn inhibits the expression of TNFSF10 via EZH2[201].

The alterations in apoptotic genes led us to evaluate the functional effect of JAK2 inhibitors on apoptosis in K562 cells. The use of TG101209 in imatinib resistant K562 cells has previously been shown to induce apoptosis at a similar dose range as used here. The role JAK2 has to play in prevention of apoptosis in K562 cells was confirmed by significant increases in apoptosis with the two other JAK2 inhibitors.

### 3.3.3 Inflammation and cytokine driven interferon response in CML

Patients with CML often present with symptoms suggestive of an activated inflammatory response, with fevers and sweats as well as weight loss. Nievergall *et al* recently showed that multiple inflammatory cytokines, chemokines and growth factors are elevated in the serum of patients with CML at diagnosis and that these can be used to identify patients with a failure to achieve an early molecular response[202]. In particular high TGF-α and IL-6 levels were shown to correlate well with a failure to achieve an early molecular response confirming the important role inflammation plays in these patients. Plasma levels of IFN-α and IFN-γ were evaluated in these patients and were not found to be significantly elevated in CML patients at diagnosis, however when plasma was extracted from bone marrow samples CXCL10 was found to be significantly elevated[202]. CXCL10, previously known as IFN-γ-inducible protein 10 (IP-10), is directly affected by IFN-γ activation. In CML there is hyperactivity of JAK signalling which may result in an increase in IFN-γ signalling in the absence of a significantly increased level of IFN-γ in the circulation. This postulated elevation in IFN signalling would explain the increase in the level of PML gene expression in CML cells compared to normal.

### 3.3.4 The role on PML in cell cycle and apoptosis in CML

The promyelocytic leukaemia protein has been shown to be down regulated in a number of solid tumours mostly through epigenetic alterations leading to gene silencing. As a result PML is normally considered a tumour suppressor[164]. However in CML there is an increase in PML expression in the leukaemia stem cells[165] which is thought to aid in the survival of these cells following TKI therapy. Mouse models of CML with loss of PML showed that there was an increase in cell cycling and a loss of long-term repopulating ability suggesting that PML plays a critical role in maintaining the quiescent state of the most primitive disease cells[165]. In this study we demonstrate that PML interacts with JAK2, which has also been linked to the maintenance of primitive CML cells, which suggests that these two proteins may be of critical importance as targets for the eradication of CML progenitors. Given that there are drugs already in clinical use which target JAK2 activity and PML stability, in the form of ruxolitinib and arsenic trioxide respectively, investigating this dual targeting approach would be an interesting area for further study.

# 4 Activity of JAK2 tyrosine kinase in JAK2 V617F myeloproliferative disease

## 4.1 Introduction

Polycythaemia vera is a clonal abnormality of haematopoiesis characterised by uncontrolled signalling in the JAK2/STAT pathway. This is almost always due to the presence of the JAK2 V617F mutation, which causes a conformational change in the JAK2 protein leading to constitutive activation[112,113,110,111]. The most obvious clinical manifestation of this is myeloid expansion with elevated peripheral red blood cell, granulocyte and platelet counts[203]. These patients also have a significantly elevated risk of thrombosis, which is likely driven by a combination of hyperviscosity, hyper-reactivity of platelets and chronic inflammation[203]. PV patients have a well-recognised inflammatory phenotype which leads to the majority of the chronic symptomatology and reduced quality of life[152]. These symptoms include lethargy, itch (particularly aquagenic itch), and sweats which can occasionally be drenching. The current therapy for PV focuses on controlling peripheral blood counts and reduction of thrombotic risk, but is not particularly effective at controlling inflammatory symptoms[133]. Recently, JAK2 inhibitors have been developed and investigated aiming to reduce signalling through this pathway and therefore abrogate the disease. The only JAK2 inhibitor currently in use is ruxolitinib. This was initially approved for use in symptomatic myelofibrosis following the results of the COMFORT trials[204]. A further study into the use of ruxolitinib in PV has shown encouraging results in terms of blood count and symptom control[133] leading to its approval for use in PV patients who are resistant to or intolerant of hydroxycarbamide.

The cause of the inflammation in PV patients has been studied for some time, but it is clear that the mechanisms underlying the problem are still not fully elucidated. There are several areas that have been identified as abnormal, including increased reactive oxygen species (ROS) generation by neutrophils from PV patients[149] and elevated circulating inflammatory cytokines, such as IL-6 and TNF-α[150]. These cytokines are thought to play a role in mediating the symptoms and in supporting the malignant clone. In addition to this, there is evidence to show that there is platelet dysfunction[205] and abnormal interactions of haematopoietic cells with endothelial cells[206]. We therefore decided to look at the alterations in PV and

whether these were corrected by treating cell lines containing the JAK2 V617F mutation with JAK2 inhibitors

Many epigenetic and transcriptional regulators are known to interact with the PML NBs, which acts as a hub for active protein complexes necessary for these critical roles[207]. Proteins that interact with the PML NB are SUMOylated and bind to SUMO-interacting motifs within the NB[158]. Evidence shows that JAK2 requires SUMOylation to enter the nucleus before going on to effect alterations in epigenetic and transcriptional regulation within the nucleus[78], and it would be possible that SUMOylation of JAK2 plays a dual role in both allowing nuclear localisation and interaction with the PML NB to mediate the nuclear JAK2 effects. In addition to this JAK2 is critical in mediating inflammatory cytokine signalling, such as IFN-γ, which is associated with increased size and number of PML NBs[208]. As a result the interaction of JAK2 and PML NBs may be an important regulator of the phenotype of JAK2 V617F mediated disease.

## 4.2 Results

### 4.2.1 Gene expression of PV PB MNC

Using the same gene expression array designed for analysis of JAK2-dependent genes and interferon-dependent genes as in the CML samples (chapter 3), RNA from the peripheral blood of patients with PV was analysed and compared to normal peripheral blood controls, with RNA extracted immediately after isolation of PB MNCs. The RNA was quantified and an equal amount of RNA from each sample was used to carry out gene expression analysis. This allowed a direct comparison of two alternative mechanisms by which over-activity of the JAK pathway occurs in MPN; CML samples where the JAK2 protein is normal but is over-stimulated, while in the PV samples the presence of the JAK2 V617F mutation leads to ligand independent activation of the JAK2 protein.

Our results demonstrate several marked changes in the gene expression pattern of PV PB MNCs compared to normal. Interestingly, there was much more heterogeneity seen in the PV samples than in the CML samples which appear to maintain a much more consistent pattern of abnormalities between samples. This may be as a result of the increasing JAK2 V617F allele burden seen in PV patients over time as these patients had samples collected at various time points following diagnosis, while the CML patient samples were all collected at diagnosis. Here there are clear abnormalities in several cell cycle genes as well as transcriptional regulators and interferon-dependent genes, but this difference is less consistent between patients.

**Figure 4.1 Gene expression heat map of PV PB MNC**

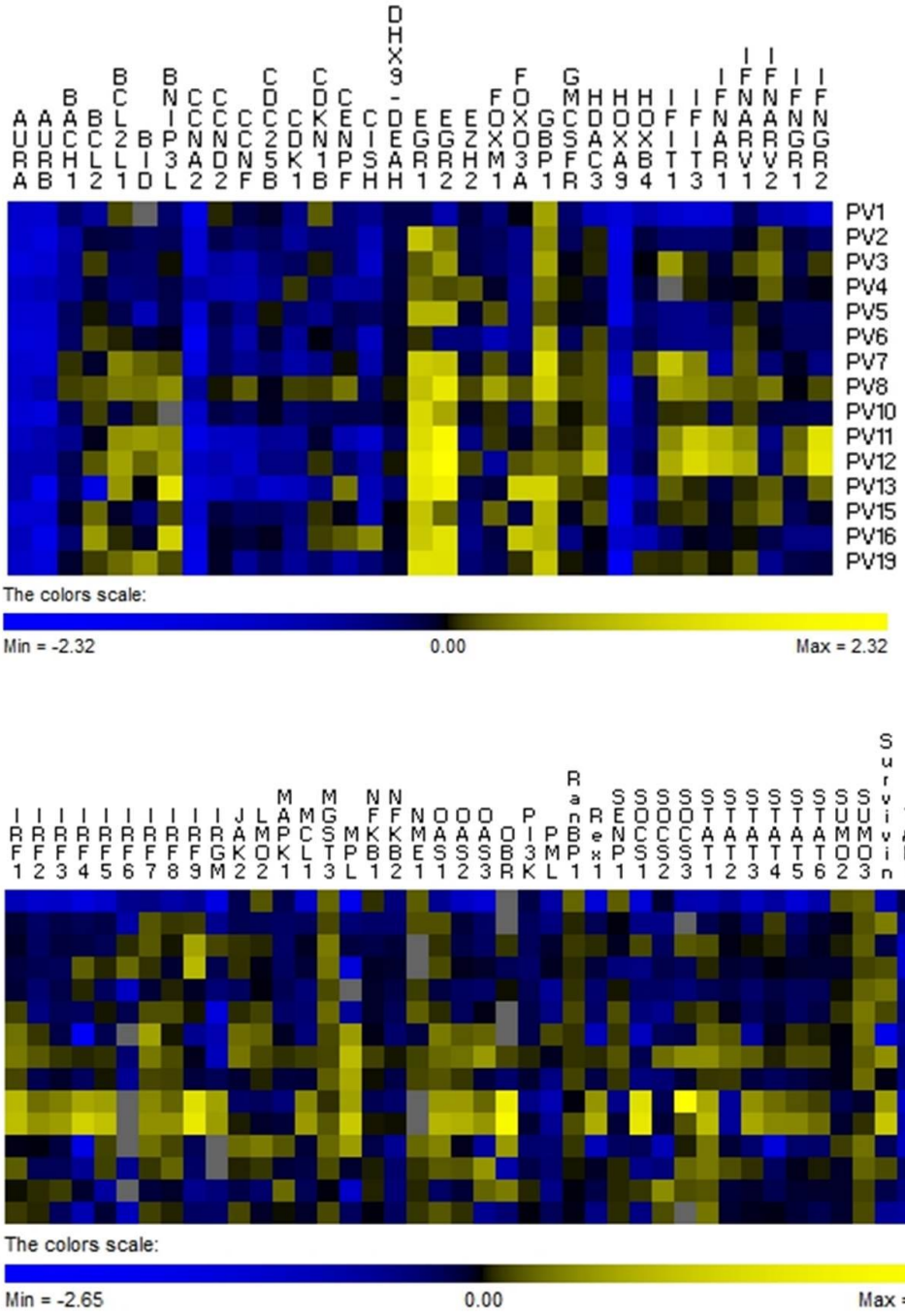


**Using the data from the microarrays, genes were selected and primers designed to look at JAK2-dependent genes and the interferon response (Table 2.2.4.8). Fluidigm quantitative real-time PCR was performed and the relative expression of the genes compared to normal controls was calculated using the $2^{-\Delta\Delta CT}$ method. A base 10 logarithmic transformation was then performed and this data was entered in to PermutMatrix to generate a heatmap representation of the gene expression.**

The heatmap (Figure 4.1) shows alteration in the gene expression profile of a number of important genes in a range of cellular processes. These include cell cycle, differentiation, IFN response and SUMOylation. The heatmap clearly shows a global deregulation of many of these genes with several being markedly altered consistently in all samples. These particularly cluster in genes associated with the cell cycle and cell division, and may reflect the fact that patient samples were not collected at diagnosis, but often when patients were already on therapy, most frequently with hydroxycarbamide.

Looking more closely at the cellular processes gives a better understanding of how the JAK2 V617F mutation affects different aspects of cellular function. However, it was important to try to identify alterations that could be accounted for by the use of hydroxycarbamide in the patients, which was not being used by the normal controls.

As discussed previously, apoptosis is the process of programmed cell death and is often affected by the presence of oncogenes which can increase anti-apoptotic genes, while also decreasing pro-apoptotic genes. Here we can see that the presence of the JAK2 V617F mutation leads to changes in some samples, but not in all. As a result, there is little in the way of significant changes in apoptosis in PV PB MNCs. This differs from CML where there are clear alterations in *BCL2L1* and *BNIP3L*. This may reflect the fact that the cells in the peripheral blood of CML patients have a higher proportion of immature granulocytes compared with normal donors and PV patients. In PV, the presence of immature cells in the peripheral blood is less pronounced and so the apoptosis of the terminally differentiated cells in PV more closely resembles that of normal donors. The use of MNCs for the assessment of gene expression meant that alterations in gene expression of any of the peripheral blood cells would be represented. However this also means that alterations are not specific to one lineage, and it would be of interest to carry out expression profiles on neutrophils, monocytes and lymphocytes to assess the effect the JAK2 V617F mutation had on each of these cell groups.

**Figure 4.2 Apoptosis in PV**

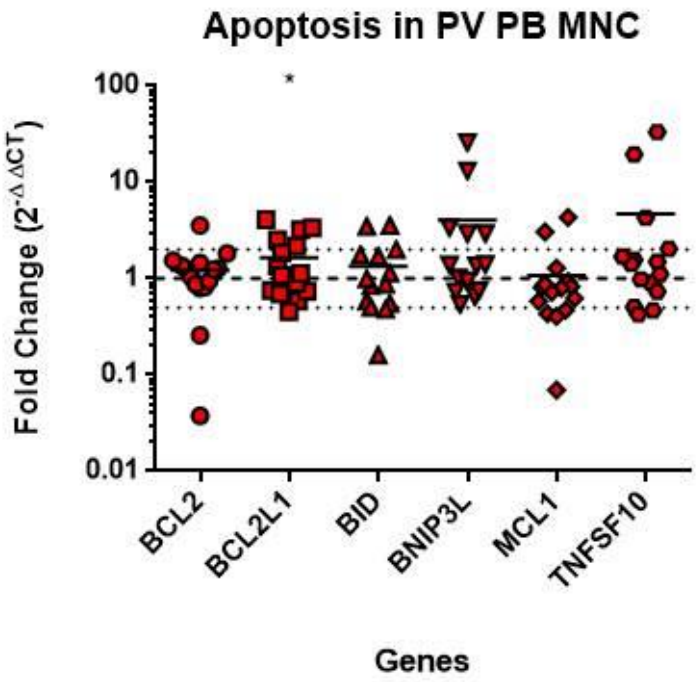


**Fluidigm® quantitative real-time PCR was carried out on RNA extracted from PV PB MNCs. The fold change compared to normal was calculated using the $2^{-\Delta\Delta CT}$ method. The data points were then graphed using GraphPad Prism 6 and a two tailed Students *t*-test was used to calculate significance (* $p \leq 0.05$). The two dotted lines indicate a 2- fold change from the control, indicated by the dashed line.**

Cytokine signalling plays a key role in many myeloid conditions, and PV is no exception. The major molecular abnormality, JAK2 V617F, directly affects the JAK2/STAT pathway through constitutive activation of JAK2 leading to ligand independent expansion of myeloid precursors in the bone marrow. This is reflected in the low levels of EPO seen in patients with PV, where there is uncontrolled erythroid lineage growth without the requirement for EPO to initiate signalling[209]. In the PV samples studied there was variability between samples. However some of the interesting alterations in gene expression were associated with cytokine signalling, with an increase in *STAT1*, a reduction in *CISH*, and variable *MPL* expression, depending on the patient.

The thrombopoietin receptor is transcribed by MPL and mutations of this gene are seen in a proportion of patients with ET and MF, but are not seen in PV. *MPL* expression has been shown to be abnormal in MPN. Interestingly the expression seems to be high in patients with a low JAK2 V617F allele burden and low in those with a high allele burden[210]. This would explainthe spread in *MPL* expressionseen in this study although the allele burden data is not available.

Cytokine-inducible SH2-containing protein is a negative regulator of cytokine signalling and is part of the SOCS family. Reduced expression of *CISH* has previously been reported in ET and in combination with *FOSB*, was found to discriminate between JAK2 V617F positive and negative status, with downregulation of CISH seen in patients negative for the JAK2 V617F mutation[211]. Interestingly, in the PV patients studied here, all were JAK2 V617F positive, with a significant decrease in the level of *CISH* expression. This reduced expression is unexpected as the increase in signalling through the JAK/STAT pathway should result in an increase in the expression of *CISH* in its negative regulatory capacity, and the paradoxical expression levels may be due to the STAT independent signalling engendered by constitutive JAK2 activation.

STAT1 is an important regulator of IFN signalling and is usually considered a tumour suppressor in solid tumours, where there is an imbalance between the activity of STAT1 and STAT3[212]. In MPN there is evidence to suggest a differential in the expression of STAT1 in normal CD34+ve cells associated with either an ET-like or PV-like phenotype, with increased expression tending towards an ET phenotype[213]. This study was carried out in erythroid precursors from ET and PV

patients and compared to JAK2 V617F negative erythroid precursors from the same patients[213]. The different results observed from our data may reflect the populations of cells studied, we investigated PB MNCs, with the cells in the peripheral blood exposed to the higher levels of circulating pro-inflammatory cytokines which occur in PV. This would lead to increased activation of cytokine receptors and an increase in transcription of target genes. Interestingly there is no significant alteration in the transcription of the other STAT proteins in the MNCs of PV patients.

**Figure 4.3 Cytokine signalling in PV**

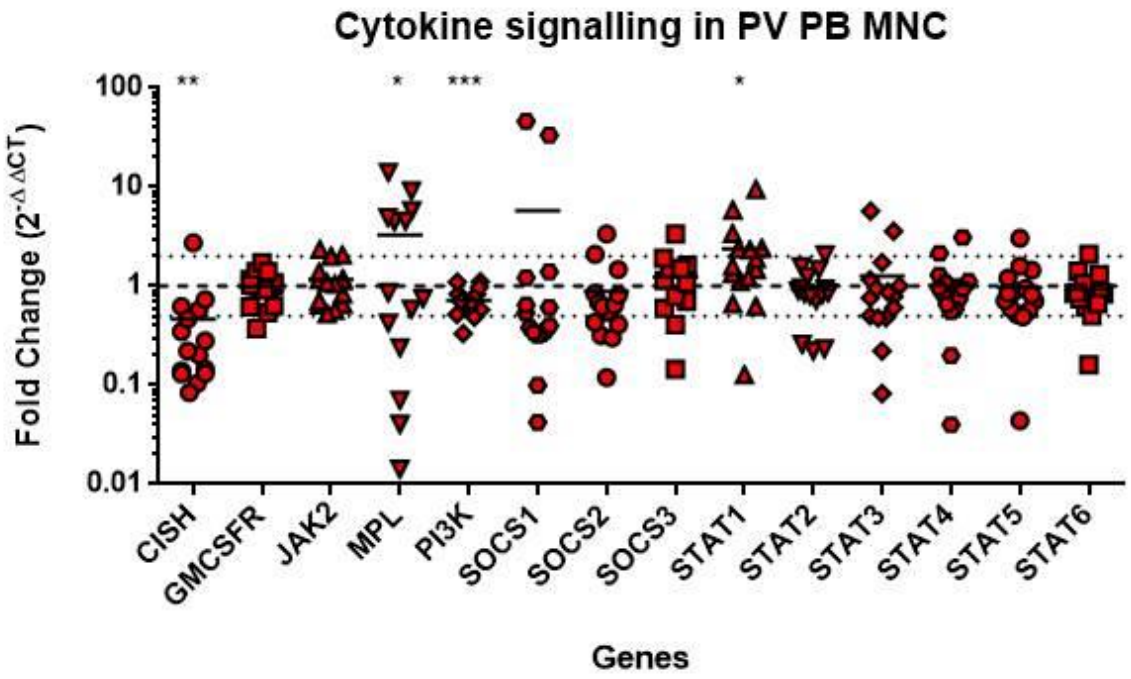


**Fluidigm® quantitative real-time PCR was carried out on RNA extracted from PV PB MNCs. The fold change compared to normal was calculated using the $2^{-\Delta\Delta CT}$ method. The data points were then graphed using GraphPad Prism 6 and a two tailed Students *t*-test was used to calculate significance (* p ≤ 0.05, ** p ≤ 0.01, *** p ≤ 0.001). The two dotted lines indicate a 2- fold change from the control, indicated by the dashed line.**

Unsurprisingly, there is alteration in the expression of numerous transcriptional regulators in PV, with many playing an important role in haematopoiesis. The transcription factor EGR1 plays an important role in maintenance of HSCs, but has been shown to be downregulated as cells start to differentiate and proliferate[214]. The increase in *EGR1* in PB MNCs suggests that there is either more immature cells present in the peripheral blood or that the cells in the peripheral blood are maintaining a more immature gene expression profile despite terminal differentiation. This increase in *EGR1* has been reported in neutrophils extracted from PV patients, although the reason for its elevation remains unclear[215].

An increase in *EGR2*, which is essential for the proliferation of inflammatory B- and T-cells[216], was also shown. This supports the suggestion that inflammation in PV is multifactorial and involves the interaction of the whole immune system. Most research to date has focused on the effect of the JAK2 V617F mutation on granulocytes, as these cells harbour the mutation. Of interest, evidence suggests that when there is induced differentiation of haematopoietic cells there is an increase in the level of *EGR2*[217]. In the context of PV, where there is an increase in the proliferation of maturing haematopoietic cells, it may be that the increase in *EGR2* observed is driven by this rather than a defect in T cell function, especially given the myeloid cell compartment is affected by the JAK2 V617F mutation.

Other important transcription factors in cell differentiation and proliferation include TAF1 which is part of a regulatory complex that controls histone acetyltransferase activity in haematopoietic tissues[218] and was decreased in PV samples, and TFDP1 which acts as a cofactor for E2F in the regulation of EZH2[219], which was increased. Interestingly *TFDP1*, *E2F* and *EZH2* tend to alter in the same way in samples with an increase in *TFDP1* and *E2F* leading to an increase in transcription of *EZH2*, so the lack of change in EZH2 suggests that, although there is an increase in *TFDP1*, E2F expression may be unaffected. This might be an interesting pathway to investigate further in more immature cells, as it is important in the production of proteins necessary for the transition into S phase[219,220]. As a result, the abnormality in terminally differentiated peripheral blood cells may not give an adequate assessment of the role of these genes in the more primitive stem cell population which sustains the disease.

**Figure 4.4 Transcriptional regulation in PV**

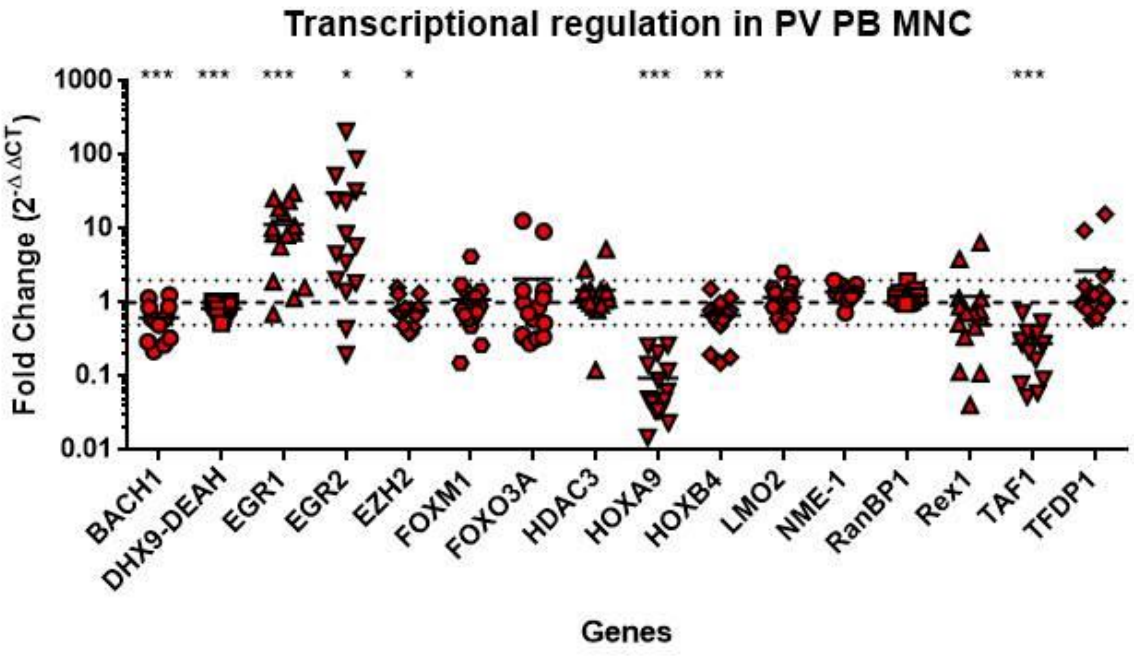


**Fluidigm® quantitative real time PCR was carried out on RNA extracted from PV PB MNCs. The fold change compared to normal was calculated using the $2^{-\Delta\Delta CT}$ method. The data points were then graphed using GraphPad Prism 6 and a two tailed Students *t*-test was used to calculate significance (* p ≤ 0.05, ** p ≤ 0.01, *** p ≤ 0.001). The two dotted lines indicate a 2- fold change from the control, indicated by the dashed line.**

The expression of cell cycle genes in PV patient samples was unexpectedly reduced in most cases. This is likely to represent the effect of hydroxycarbamide on these genes, which all patients were taking. Even though these are mature cells they still have the capacity to proliferate (T & B cells) and undergo terminal differentiation (monocytes), therefore these genes are still expressed in normal PB MNCs and were reduced in PV samples (Figure 4.5). Hydroxycarbamide controls peripheral counts in people with myeloproliferative neoplasms by decreasing the production of deoxyribonucleic acids through inhibiton of ribonuclease reductase. This leads to a reduction in the rate of DNA synthesis and cell division, predominantly in rapidly dividing cells, and therefore inhibiting cell division. This inhibition of cell division would be expected to reduce the Aurora kinases, which are involved in spindle formation and mitosis, and regulators of the various stages of cell cycle. It would be interesting to collect samples from patients at diagnosis, prior to initiation of therapy, to compare to these results.

**Figure 4.5 Cell cycle in PV**

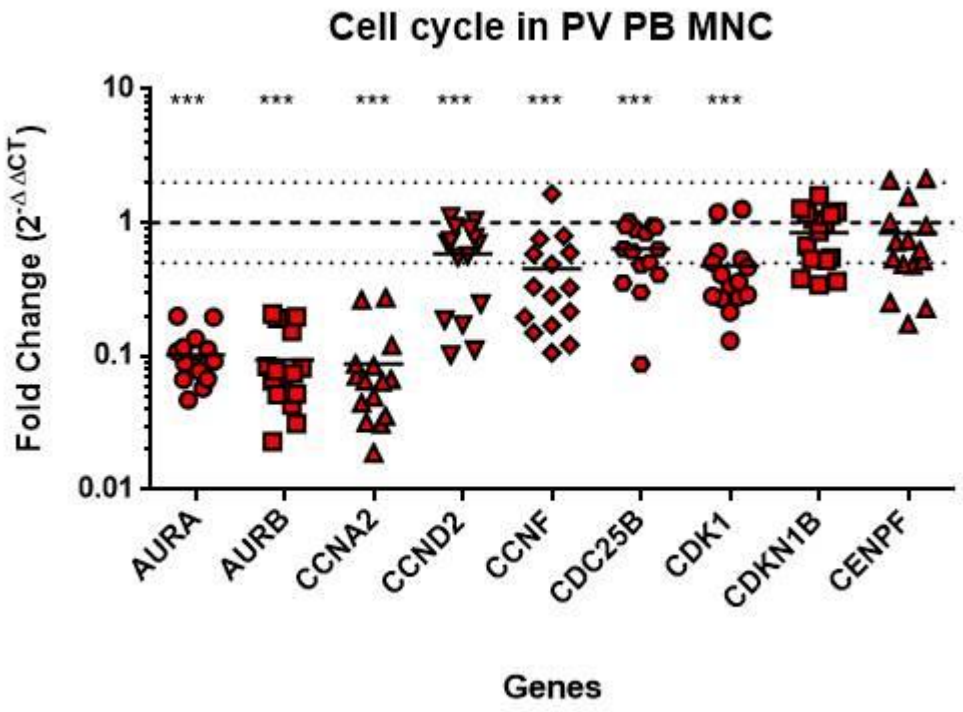


**Fluidigm® quantitative real-time PCR was carried out on RNA extracted from PV PB MNCs. The fold change compared to normal was calculated using the $2^{-\Delta\Delta CT}$ method. The data points were then graphed using GraphPad Prism 6 and a two tailed Students *t*-test was used to calculate significance (* p ≤ 0.05, ** p ≤ 0.01, *** p ≤ 0.001). The two dotted lines indicate a 2- fold change from the control, indicated by the dashed line.**

Inflammation in PV has been a focus of research over the recent past to try and elucidate the role it plays in the presentation and progression of disease, as well as its place in the development of complications such as thrombosis and secondary malignancies[152,221]. The cause of the inflammation appears to be multifactorial, with reported alterations in inflammatory cytokines, neutrophil production of ROS and alteration of the interaction of platelets with the vascular endothelium.

The expression of interferon-associated genes was variable between samples. Interestingly, consistent alterations include *IRF6*, *IRF7* and *PML* which showed significant changes and an average of at least 2-fold alteration from normal. The role of *IRF6* is not clearly elucidated, but is likely to be involved in Toll-like receptor signalling, while IRF7 is involved in the transcription of type I interferons and plays an essential role in the amplification of their signalling[222,223].

**Figure 4.6 Inflammation in PV**

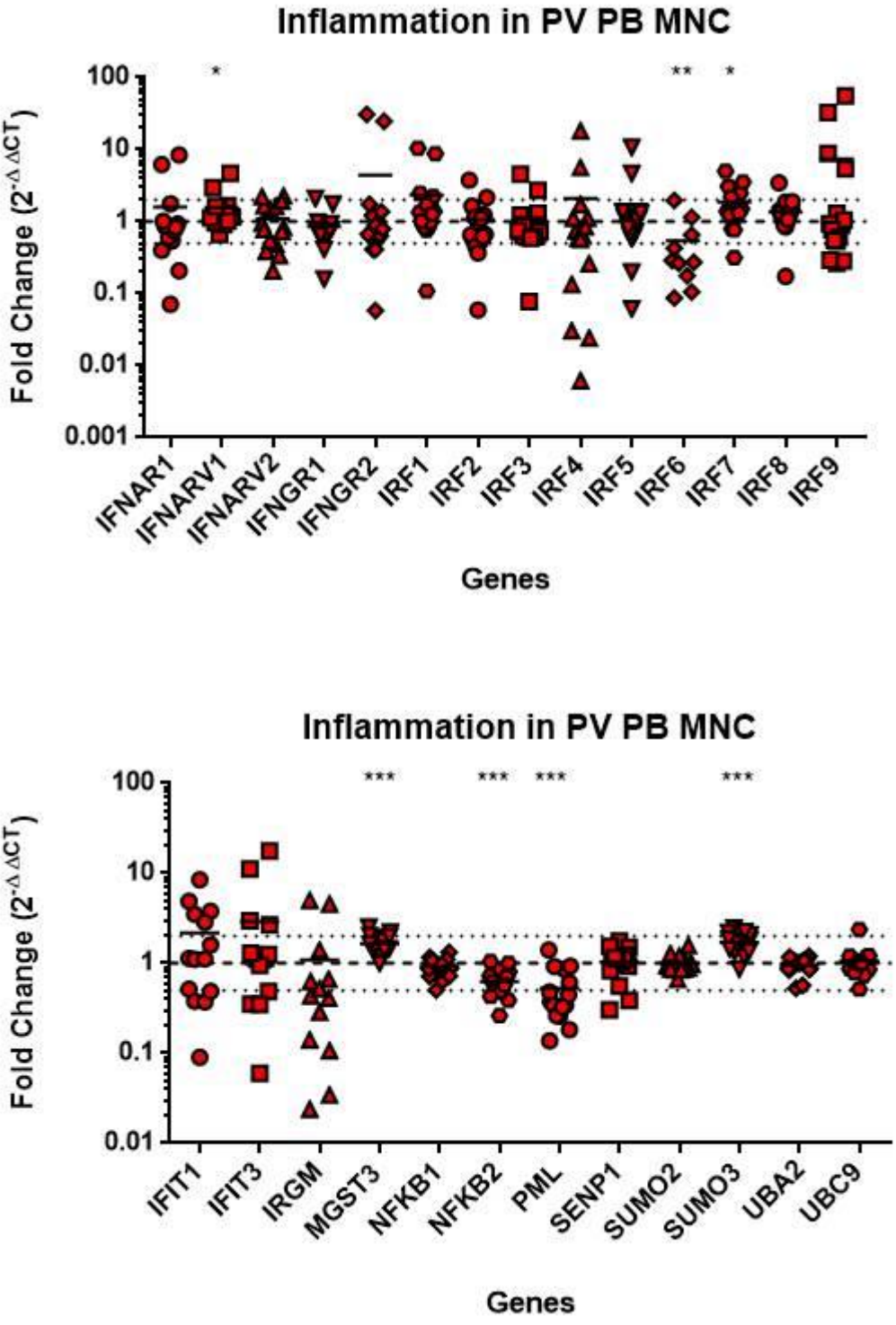


**Fluidigm® quantitative real-time PCR was carried out on RNA extracted from PV PB MNCs. The fold change compared to normal was calculated using the $2^{-\Delta\Delta CT}$ method. The data points were then graphed using GraphPad Prism 6 and a two tailed Students *t*-test was used to calculate significance (* p ≤ 0.05, ** p ≤ 0.01, *** p ≤ 0.001). The two dotted lines indicate a 2- fold change from the control, indicated by the dashed line.**

### 4.2.2 Dose finding of JAK2 inhibitors for UKE1 and SET2 cells

Following the interesting results seen in the gene expression of PV patients, we decided to look at the effect of JAK2 inhibition on the activity of two JAK2 V617F cell lines, UKE1 and SET2. Both cell lines were created from patients with JAK2 V617F positive ET who developed secondary AML, but, unusually, on transformation they retained the JAK2 V617F abnormality in the AML clone. As for K562 cells, the XTT metabolic assays were used to identify a range of doses for ruxolitinib, TG101209 and AT9283 (Figure 4.7), which were then carried forward into trypan blue exclusion testing. The trypan blue exclusion tests were then carried out at 24, 48 and 72 hours and the $IC_{50}$ dose calculated based on these results. In addition, XTT assays were carried out using ATO, which causes PML to undergo SUMOylation and subsequent degradation, to identify a dose affecting the cellular growth to be used in combination studies. Following identification of the $IC_{50}$, a lower and higher dose were identified that resulted in an alteration in cell counts at 72 hours, but had live cells present at 24 hours which could then be analysed for changes in gene and protein expression using Western blotting and immunofluorescence techniques.

**Figure 4.7 XTT assays of JAK2 inhibitors and arsenic trioxide in UKE1 cells**

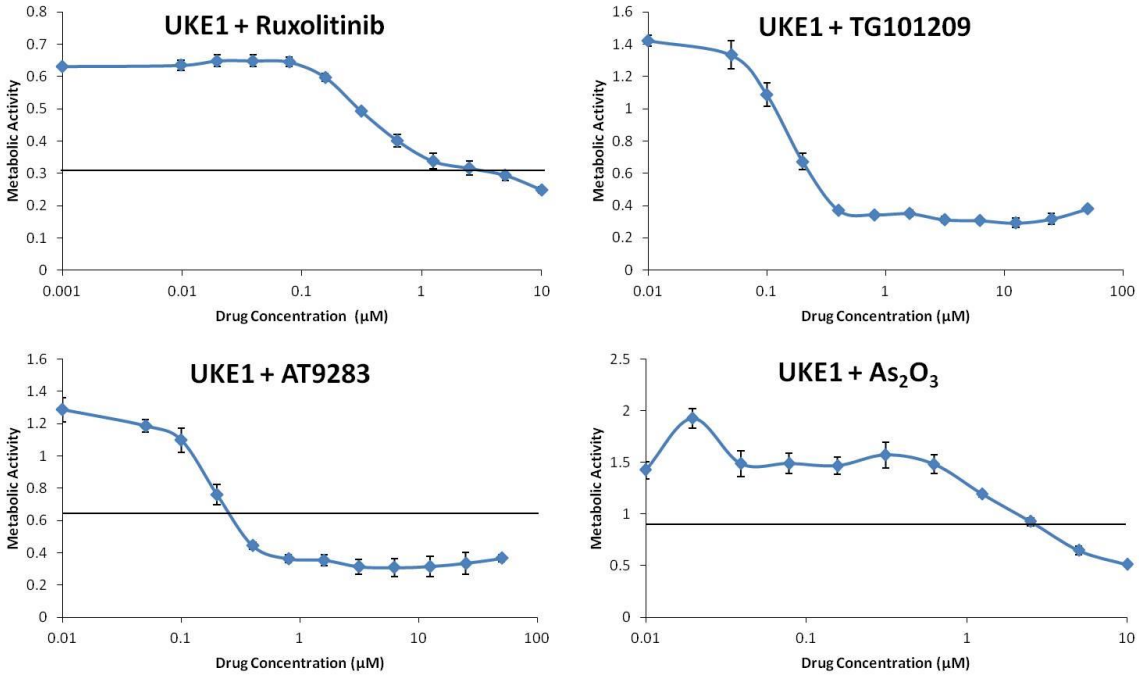


**XTT assays were carried out in 4 simultaneous wells with the mean plotted in the above graphs +/-standard deviation. The solid line indicates the dose of inhibitor necessary to reduce the metabolic activity by 50%. The no drug control is indicated by the first plot point at the Y axis.**

**Figure 4.8 XTT assays of JAK2 inhibitors and arsenic trioxide in SET2 cells**

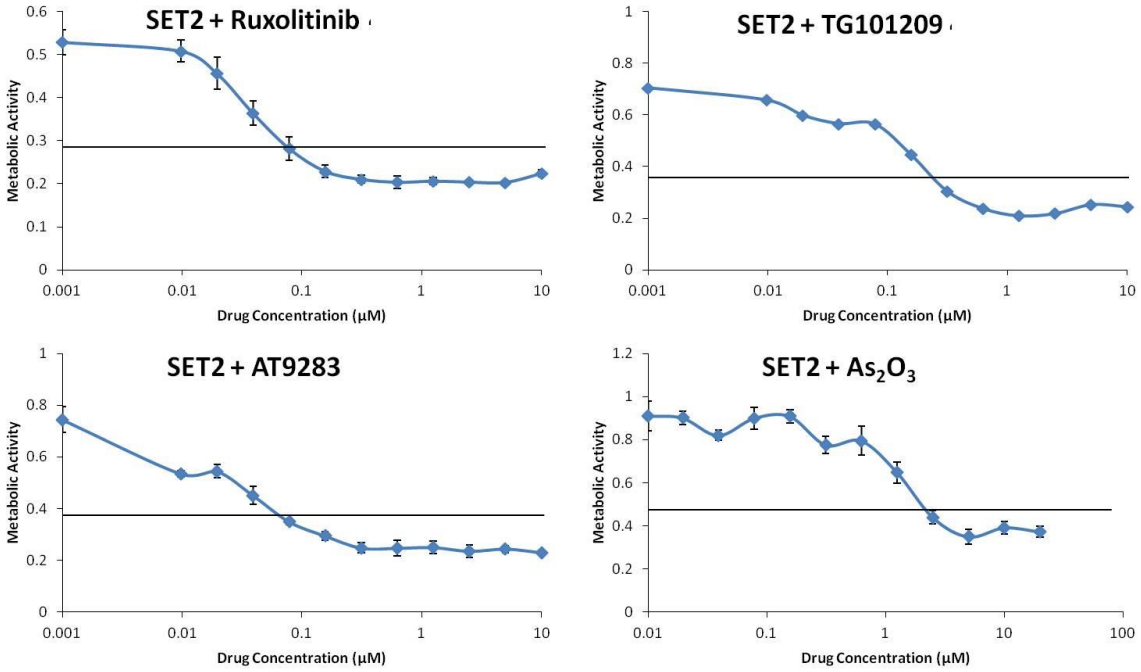


**XTT assays were carried out in 4 simultaneous wells with the mean plotted in the above graphs +/-standard deviation. The solid line indicates the dose of inhibitor necessary to reduce the metabolic activity by 50%. The no drug control is indicated by the first plot point by the Y axis.**

**Table 4.1 Doses chosen for further experiments with UKE1 and SET2 cells following trypan blue exclusion counting**

| Cell line | Ruxolitinib | TG101209 | AT9283 | Arsenic trioxide |
|---|---|---|---|---|
| UKE1 | 250nM<br>750nM<br>1000nM | 250nM<br>700nM<br>1000nM | 10nM<br>15nM<br>30nM | 2000nM |
| SET2 | 50nM<br>100nM<br>200nM | 100nM<br>250nM<br>500nM | 10nM<br>25nM<br>50nM | 2000nM |

### 4.2.3 Western blots

The activity of the JAK2 inhibitors in UKE1 and SET2 cells were assessed by Western blotting. Antibodies to downstream proteins were used to evaluate the relative levels present in a cohort of samples. UKE1 cells were treated with each JAK2 inhibitor at three doses before having protein extracted and run on polyacrylamide gels. Following transfer to a nitrocellulose membrane the samples were probed for STAT1 and STAT5 in both the phosphorylated and unphosphorylated state, with SHPTP2 being used to confirm equal loading. Interestingly, at 24 hours there was a marked increase in the levels of phospho-STAT1 and phospho-STAT5 following treatment with ruxolitinib compared to untreated cells. This seemed to be most pronounced in the lower doses of ruxolitinib, which may be due to the ability of the cells to overcome the inhibitory effect of the ruxolitinib more easily leading to a rebound overactivity of the pathway. There was also a reduction in the level of STAT1 in cells treated with ruxolitinib at the higher doses, with an associated reduction in the level of phospho-STAT1, while there is an increase in the level of phospho-STAT1 when cells are treated with ruxolitinib at 250nM without any alteration in the level of total STAT1 when compared to untreated cells. There is also an increase in the level of phospho-STAT5 in cells treated with TG101209, which appears consistent at all doses assessed, when compared to untreated cells. Treatment of cells with AT9283 appeared to lead to little alteration in phospo-STAT1 or phospho-STAT5 levels.

**Figure 4.9 Western blotting of UKE1 cells treated with JAK2 inhibitors at 24 hours**

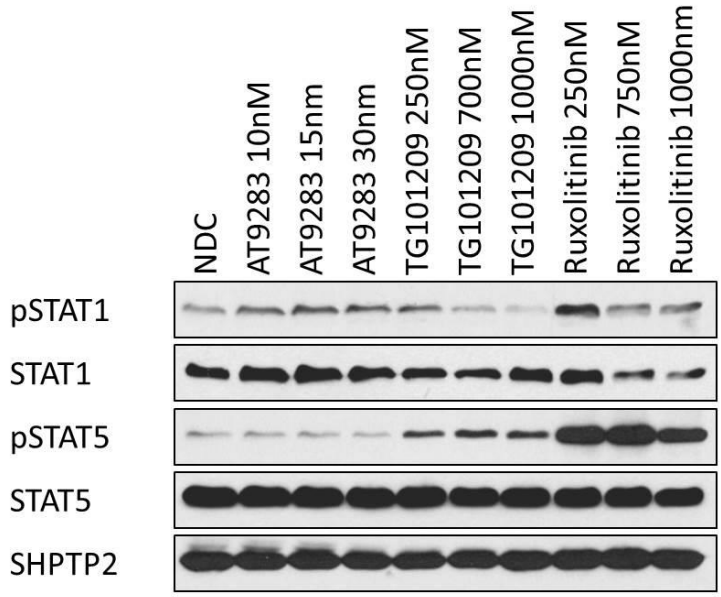


**Protein samples were obtained from UKE1 cells following 24 hours of culture in media alone or supplemented with increasing doses of ruxolitinib, TG101209 or AT9283. The lysates were then run according to the protocol described previously (2.4.4.2). The nitrocellulose membranes were then probed using antibodies to the proteins indicated above and detected using HRP-conjugated antibodies. Equal protein loading of the samples was ensured by probing for SHPTP2. Three independent experiments were carried out with this image being representative of these.**

Based on these appearances we looked at the effect of ruxolitinib on cells over a 24 hour period. This showed that the effect of ruxolitinib on STAT5 phosphorylation was relatively short lived with phospho-STAT5 only reducing from baseline for between 4 and 8 hours, returning to baseline signal by 8 hours of treatment and increasing to above the baseline signal for untreated cells by 24 hours.

**Figure 4.10 Western blotting of UKE1 cells treated with ruxolitinib over 24 hours**

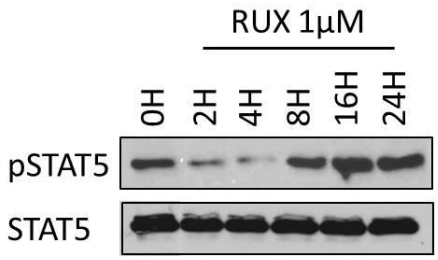


**Protein samples were obtained from UKE1 cells following 24 hours of culture in media alone or supplemented with increasing doses of ruxolitinib, TG101209 or AT9283. The lysates were then run according to the protocol described previously (2.4.4.2). The nitrocellulose membranes were then probed using antibodies to the proteins indicated above and detected using HRP-conjugated antibodies. Three independent experiments were carried out with this image being representative of these.**

A similar, but less pronounced effect is seen in SET2 cells treated with JAK2 inhibitors for 24 hours, with little alteration in STAT1 or STAT5 phosphorylation with AT9283 and an increase in STAT5 phosphorylation with ruxolitinib. The effect on phosphorylation of STAT1 was less clear as it proved difficult to get clear images despite short exposure times.

**Figure 4.11 Western blotting of SET2 cells treated with JAK2 inhibitors at 24 hours**

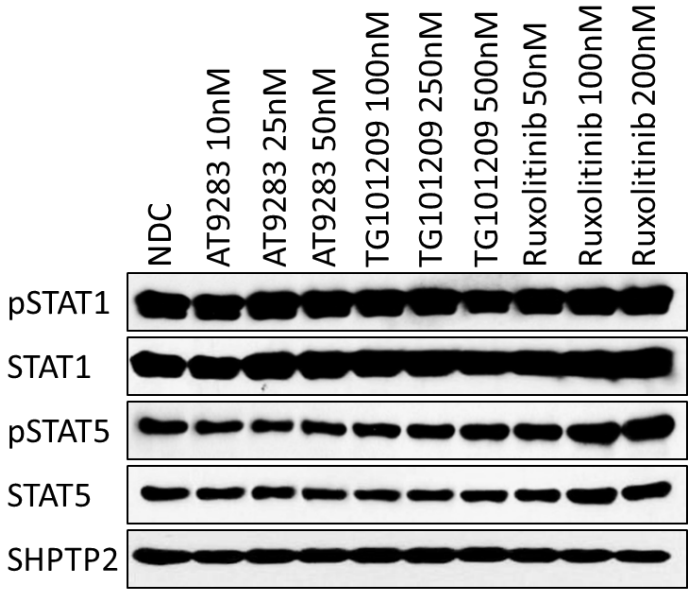


**Protein samples were obtained from SET2 cells following 24 hours of culture in media alone or supplemented with increasing doses of ruxolitinib, TG101209 or AT9283. The lysates were then run according to the protocol described previously (2.4.4.2). The nitrocellulose membranes were then probed using antibodies to the proteins indicated above and detected using HRP-conjugated antibodies. Equal protein loading of the samples was ensured by probing for SHPTP2. Three independent experiments were carried out with this image being representative of these.**

Again samples were taken over a 24 hour period after treatment with ruxolitinib, and showed an even shorter effect of JAK2 inhibition in SET2 cells compared to UKE1 cells with recovery of STAT5 phosphorylation to baseline by 4 hours and an increase at 24 hours.

**Figure 4.12 Western blotting of SET2 cells treated with ruxolitinib over 24 hours**

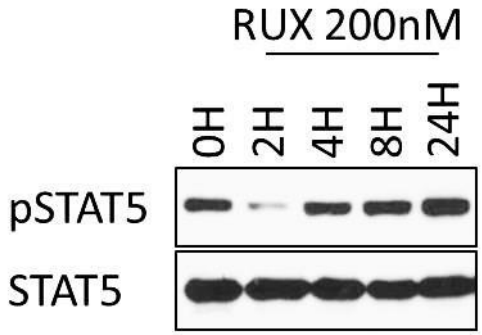


**Protein samples were obtained from SET2 cells following 24 hours of culture in media alone or supplemented with increasing doses of ruxolitinib, TG101209 or AT9283. The lysates were then run according to the protocol described previously (2.4.4.2). The nitrocellulose membranes were then probed using antibodies to the proteins indicated above and detected using HRP-conjugated antibodies. Three independent experiments were carried out with this image being representative of these.**

### 4.2.4 Gene expression of UKE1 cells treated with JAK2 inhibitors

UKE1 cells were treated for 24 hours with concentration of each inhibitor indicated above (Figure 4.7). RNA was then processed to prepare for Fluidigm® real-time PCR as described previously (Section 2.4.3). With UKE1 cells, 86 genes were analysed for each of the 3 JAK2 inhibitors. The heat map demonstrates that treatment with JAK2 inhibitors results in an alteration of the gene expression in UKE1 cells. Genes which failed to be expressed by Fluidigm, either in the treatment groups or in the control cells were removed. This leaves 81 genes which were mapped for alterations in the expression following treatment with the previously used JAK2 inhibitors. The heatmaps show that the gene expression of several key pathways are altered following treatment with JAK2 inhibitors. Treatment with ruxolitinib and TG101209 results in a similar pattern of alteration in UKE1 cells compared to treatment with AT9283.

**Figure 4.13 Gene expression heat map of UKE1 cells treated with JAK2 inhibitors**

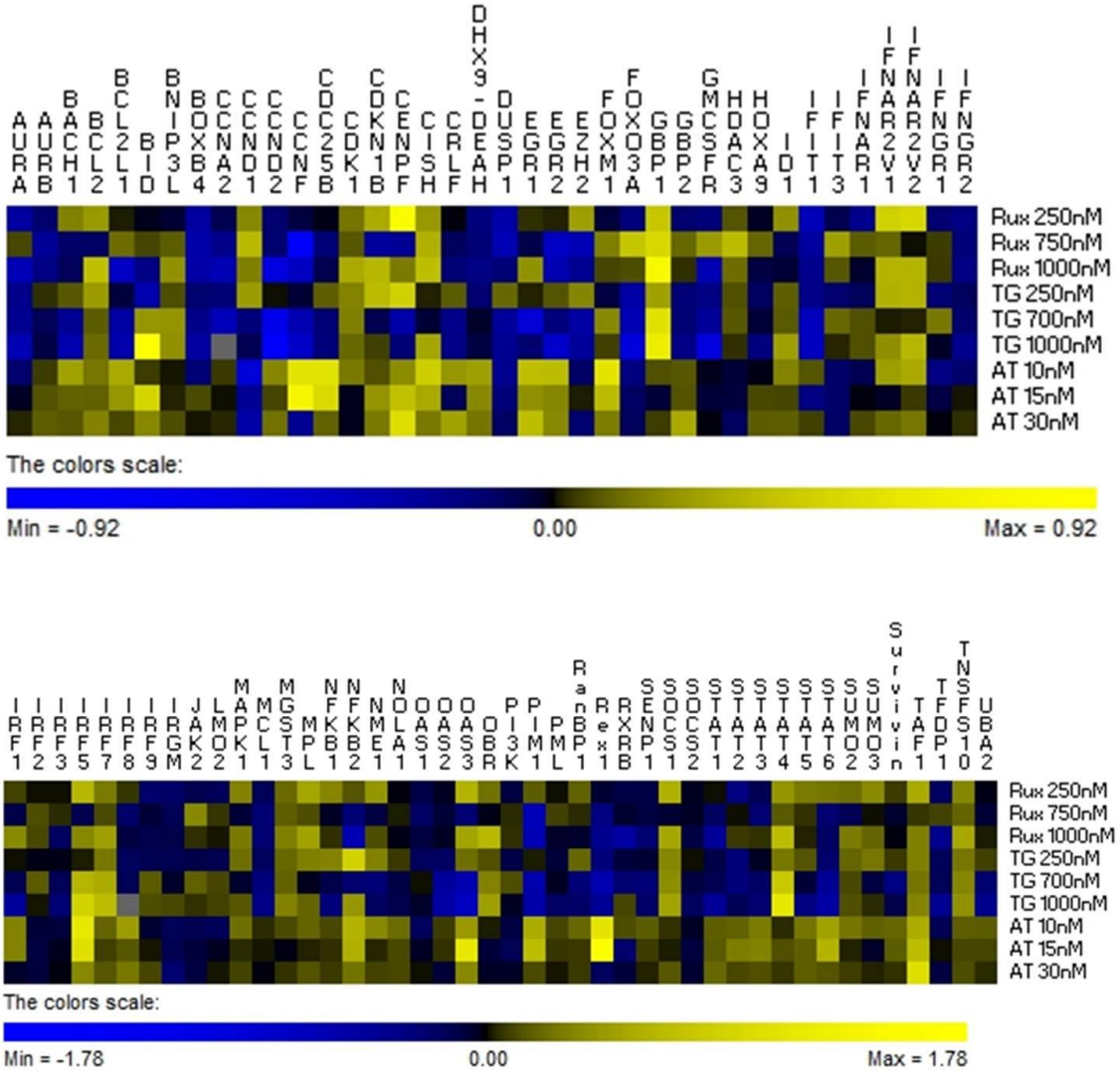


**Using the data from the microarrays, genes were selected and primers designed to look at JAK2 dependent genes and the interferon response (Table 2.2.4.8). Fluidigm quantitative real-time PCR was performed and the relative expression of the genes compared to no drug controls was calculated using the $2^{-\Delta\Delta CT}$ method. A base 10 logarithmic transformation was then performed and this data was entered in to PermutMatrix to generate a heatmap representation of the gene expression of UKE1 cells treated with JAK2 inhibitors.**

Examining the analysed data of UKE1 cells treated with each of the JAK2 inhibitors separately, the significant alterations in gene expression achieved by the highest dose of each inhibitor were graphed below (Figure 4.14). Treatment with ruxolitinib leads to alterations in the expression of genes over a range of cellular processes. The cell cycle genes *AURA* and *CCNA2* were reduced in patient samples and are also further decreased following treatment of cell lines with ruxolitinib and TG101209, which supports the hypothesis that these changes in the patient samples are mediated by hydroxycarbamide. Interestingly, the increase in *TFDP1* in patient samples is reversed following treatment of UKE1 cells with both ruxolitinib and TG101209 (Figures 4.14 and 4.15).

In cytokine signalling, TG101209 appears to have a broader effect on the gene expression than ruxolitinib, but both affect *STAT1* which is a key regulator of interferon signalling. In addition to this, the clear reduction in the STAT target gene *PIM1* is in keeping with a reduction in the activity of the STAT proteins following JAK2 inhibition. This sustained alteration of gene expression is not in keeping with the changes seen in Western blotting where the effect of JAK2 inhibitors on phosphorylation of the STAT proteins appears to be relatively short lived.

**Figure 4.14 Gene expression of UKE1 cells following treatment with ruxolitinib**

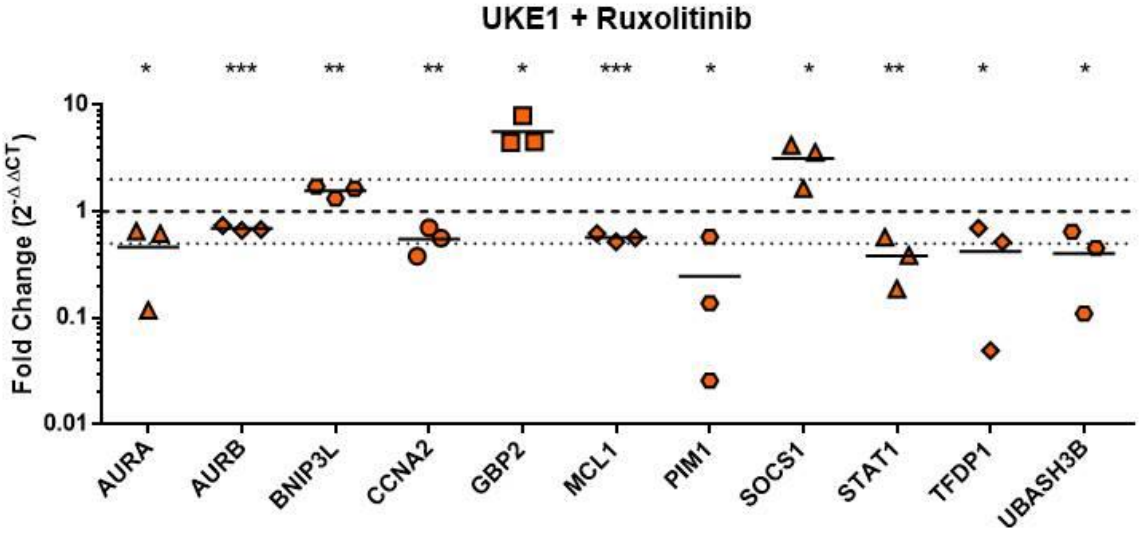


**Fluidigm® quantitative real time PCR was carried out on RNA extracted from UKE1 cells treated with ruxolitinib 1000nM for 24 hours. The fold change compared to untreated samples was calculated using the $2^{-\Delta\Delta CT}$ method. The data points were then graphed using GraphPad Prism 6 and a two tailed Students *t*-test was used to calculate significance (* $p \leq 0.05$, ** $p \leq 0.01$, *** $p \leq 0.001$). The two dotted lines indicate a 2- fold change from the control, indicated by the dashed line.**

**Figure 4.15 Gene expression of UKE1 cells following treatment with TG101209**

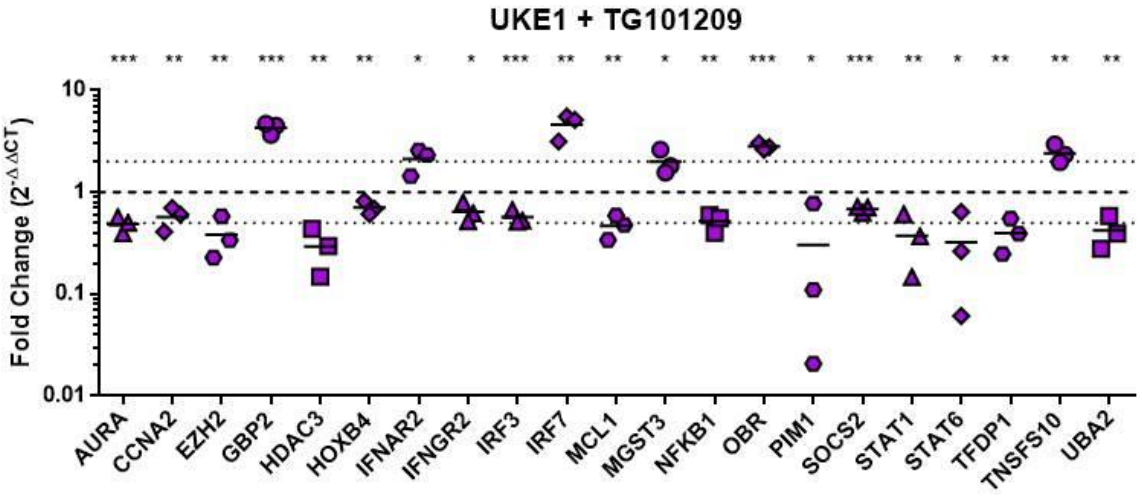


**Fluidigm® quantitative real time PCR was carried out on RNA extracted from UKE1 cells treated with TG101209 1000nM for 24 hours. The fold change compared to untreated samples was calculated using the 2-ΔΔCT method. The data points were then graphed using GraphPad Prism 6 and a two tailed Students *t*-test was used to calculate significance (* p ≤ 0.05, ** p ≤ 0.01, *** p ≤ 0.001). The two dotted lines indicate a 2- fold change from the control, indicated by the dashed line.**

In contrast to the wide ranging effects of AT9283 on K562 cells the effects on UKE1 cells is very limited. The reason for this is unclear as the doses used resulted in marked reduction in the viability of cells and would be expected to result in significant alterations in various critical pathways in cellular functioning (Figure 4.16). The expression of *IFNAR1* and *NOLA* were stastically significant following treatment with AT9283, but the alteration from baseline was minimal suggesting there was no real change compared to untreated cells.

**Figure 4.16 Gene expression of UKE1 cells following treatment with AT9283**

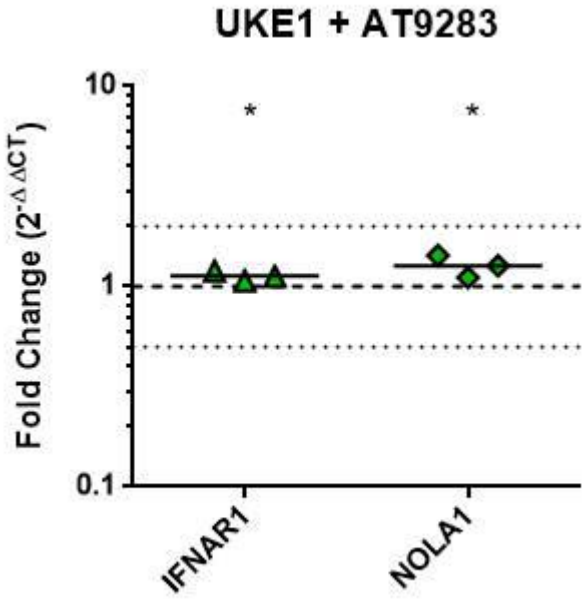


**Fluidigm® quantitative real time PCR was carried out on RNA extracted from UKE1 cells treated with AT9283 30nM for 24 hours. The fold change compared to untreated samples was calculated using the 2-ΔΔCT method. The data points were then graphed using GraphPad Prism 6 and a two tailed Students t-test was used to calculate significance (* p ≤ 0.05, ** p ≤ 0.01, *** p ≤ 0.001).**

### 4.2.5 Gene expression of SET2 cells treated with JAK2 inhibitors

Based on the experiments carried out with PV PB MNCs and UKE1 cells, a more limited gene expression panel was investigated with SET2 cells. A selection of 41 genes were assessed and the results shown in the heatmap below (Figure 4.17) The changes induced in SET2 cells following JAK2 inhibition again cover a range of genes representing many aspects of cellular functions including cell cycle, transcriptional regulation and apoptosis.

**Figure 4.17 Gene expression heat map of SET2 cells treated with JAK2 inhibitors**

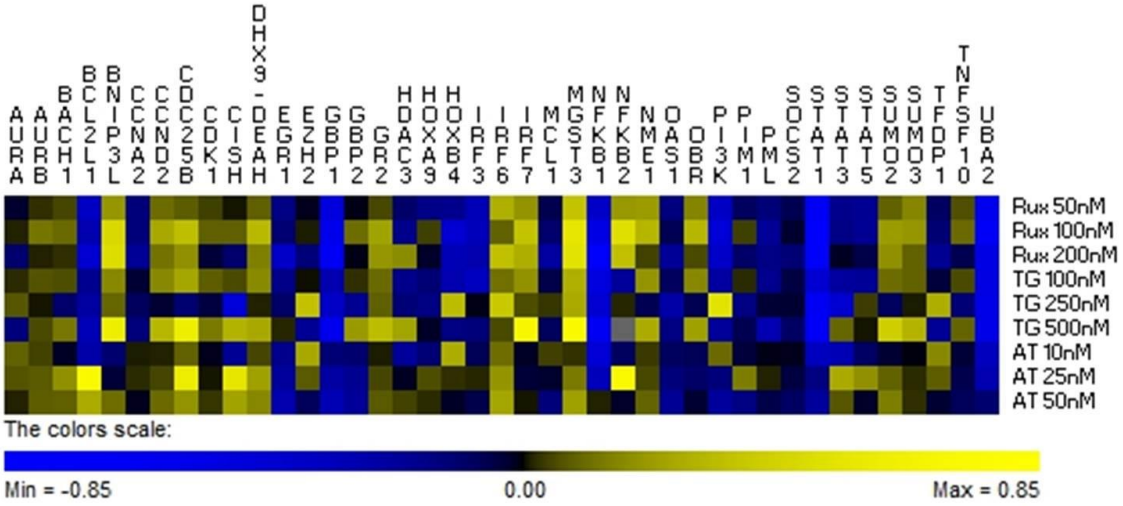


**Using the data from the microarrays, genes were selected and primers designed to look at JAK2-dependent genes and the interferon response (Table 2.2.4.8). Fluidigm quantitative real time PCR was performed and the relative expression of the genes compared to no drug controls was calculated using the $2^{-\Delta\Delta CT}$ method. A base 10 logarithmic transformation was then performed and this data was entered in to PermutMatrix to generate a heatmap representation of the gene expression of SET2 cells treated with JAK2 inhibitors.**

The gene expression alterations in SET2 cells treated with the highest dose of each inhibitor were then graphed. Treating SET2 cells with ruxolitinib or TG101209 led to reductions in the expression of *STAT1* when compared to untreated cells. This reverses the increase seen in PV PB MNCs and matches the reduction seen following treatment of UKE1 cells with the same inhibitors.

The reduction of *UBA2*, part of the E1 ligase complex in SUMOylation, following treatment with ruxolitinib or TG101209 has not been previously described. The SUMO system is known to play an important role in the regulation of JAK/STAT pathway, with several proteins undergoing post-translational SUMOylation[78,224]. Additionally SUMOylation plays an important role in many pathways and is a key component for bringing proteins in to PML nuclear bodies. Therefore the reduction of E1 ligase capability would have wide ranging and complex effects on the cell, and may play a role in the effect JAK2 inhibitors have on the interaction of JAK2 and PML within the nuclear bodies.

**Figure 4.18 Gene expression of SET2 cells following treatment with ruxolitinib**

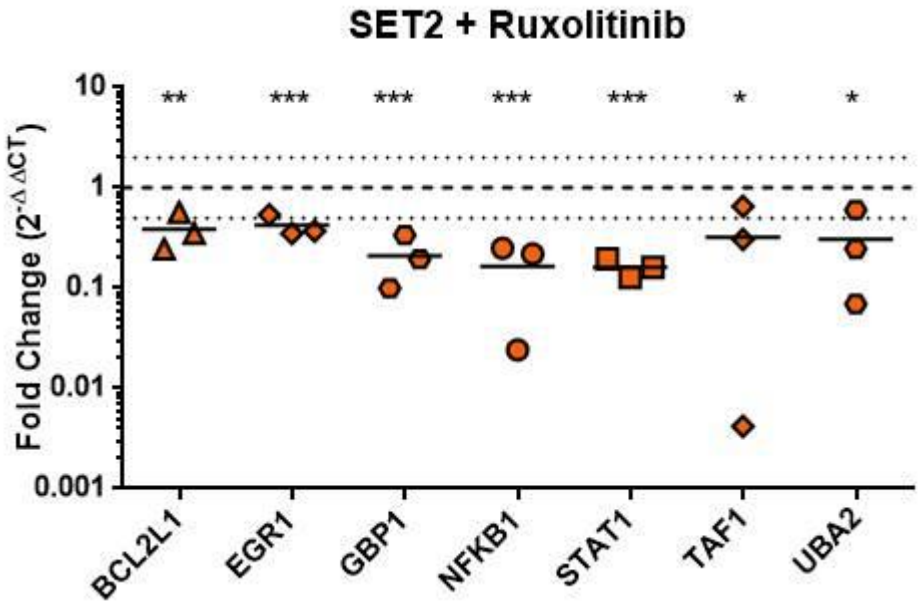


**Fluidigm® quantitative real-time PCR was carried out on RNA extracted from SET2 cells treated with ruxolitinib 200nM for 24 hours. The fold change compared to untreated samples was calculated using the $2^{-\Delta\Delta CT}$ method. The data points were then graphed using GraphPad Prism 6 and a two tailed Students *t*-test was used to calculate significance (* p ≤ 0.05, ** p ≤ 0.01, *** p ≤ 0.001). The two dotted lines indicate a 2- fold change from the control, indicated by the dashed line.**

**Figure 4.19 Gene expression of SET2 cells following treatment with TG101209**

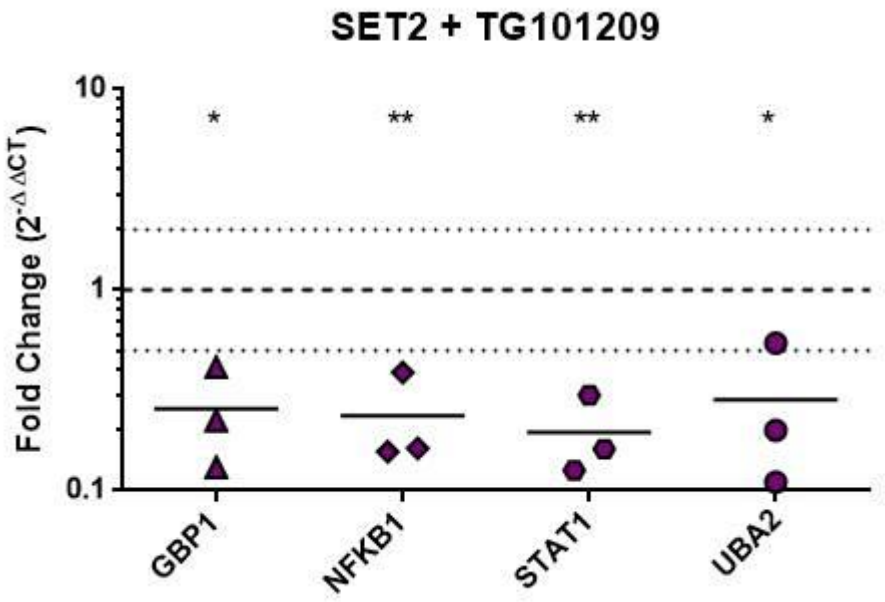


**Fluidigm® quantitative real time PCR was carried out on RNA extracted from SET2 cells treated with TG101209 500nM for 24 hours. The fold change compared to untreated samples was calculated using the $2^{-\Delta\Delta CT}$ method. The data points were then graphed using GraphPad Prism 6 and a two tailed Students *t*-test was used to calculate significance (* $p \leq 0.05$, ** $p \leq 0.01$, *** $p \leq 0.001$). The two dotted lines indicate a 2- fold change from the control, indicated by the dashed line.**

SET2 cells treated with AT9283 showed few significant alterations in gene expression, but did have a similar effect on *EGR1* to that seen in SET2 cells treated with ruxolitinib. The reduction in *EGR1* following JAK2 inhibition suggests that the increase seen in PB MNCs is a direct effect of the over-activity of JAK2 signalling.

**Figure 4.20 Gene expression of SET2 cells following treatment with AT9283**

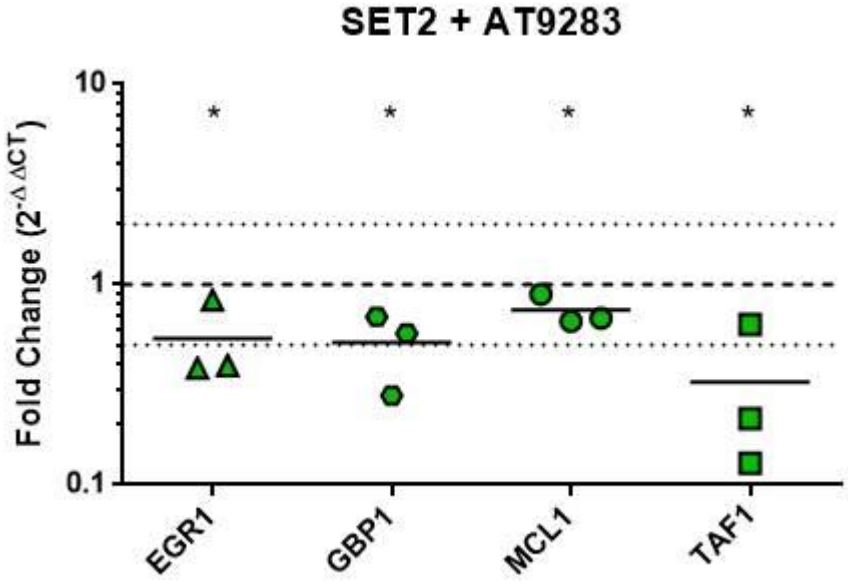


**Fluidigm® quantitative real-time PCR was carried out on RNA extracted from SET2 cells treated with AT9283 50nM for 24 hours. The fold change compared to untreated samples was calculated using the $2^{-\Delta\Delta CT}$ method. The data points were then graphed using GraphPad Prism 6 and a two tailed Students *t*-test was used to calculate significance (* $p \leq 0.05$, ** $p \leq 0.01$, *** $p \leq 0.001$). The two dotted lines indicate a 2- fold change from the control, indicated by the dashed line.**

### 4.2.6 Apoptosis is increased in UKE1 cells following treatment with JAK2 inhibitors

Again to assess the functional significance of the gene expression data, UKE1 cells were cultured in the presence of each of the JAK2 inhibitors for 24, 48 and 72 hours before being assessed for the degree of apoptosis induced. Table 4.2 shows the changes seen at 24 and 48 hours following treatment with the three inhibitors. Interestingly, in this cell line, there are significant alterations in the percentage of live cells within 24 hours with some clear evidence of induction of apoptosis. This is more marked by 48 hours and there is a further increase by 72 hours. Despite little effect on the expression of apoptotic genes in cells treated with AT9283, there is a clear and marked increase in apoptosis with this treatment, suggesting the alterations are either at a protein level, or the genes affected are not the ones looked at above. The reason for this may be that the genes that were altered by AT9283 were not investigated in this study. However, in the ruxolitinib and TG101209 treated cells the increase in apoptosis is in keeping with the reduction of the anti-apoptotic *MCL1* seen in both these treatment groups.

**Table 4.2 Apoptosis at 24 and 48 hours in UKE1 cells treated with JAK2 inhibitors**

| 24 hours | Live | +/- | Early | +/- | Late | +/- | Dead | +/- |
|---|---|---|---|---|---|---|---|---|
| NDC | 83.3% | 0.9 | 12.6% | 1.2 | 3.6% | 0.4 | 0.5% | 0.1 |
| Ruxolitinib 250nM | 83.7% | 0.5 | 11.7% | 1.3 | 3.9% | 0.8 | 0.7% | 0.3 |
| Ruxolitinib 750nM | 81.0% | 0.8 | 13.0% | 1.5 | 5.0% | 0.8 | 1.0% | 0.2 |
| Ruxolitinib 1000nM | 65.6% | 1.7 | 23.6% | 2.2 | 9.1% | 1.2 | 1.7% | 0.3 |
| TG101209 250nM | 80.3% | 3.1 | 13.3% | 2.4 | 5.6% | 1.7 | 0.8% | 0.1 |
| TG101209 700nM | 76.6% | 1.1 | 15.1% | 1.7 | 7.6% | 1.7 | 0.8% | 0.1 |
| TG101209 1000nM | 74.7% | 1.8 | 17.3% | 1.9 | 7.4% | 2.0 | 0.6% | 0.1 |
| AT9283 10nM | 81.1% | 2.1 | 12.4% | 2.3 | 5.4% | 1.1 | 1.1% | 0.4 |
| AT9283 15nM | 70.4% | 1.6 | 17.2% | 2.3 | 11.3% | 1.9 | 1.2% | 0.5 |
| AT9283 30nM | 64.0% | 1.0 | 20.8% | 3.7 | 13.9% | 2.4 | 1.3% | 0.4 |

| 48 hours | Live | +/- | Early | +/- | Late | +/- | Dead | +/- |
|---|---|---|---|---|---|---|---|---|
| NDC | 81.9% | 0.3 | 13.2% | 1.0 | 4.5% | 0.6 | 0.5% | 0.1 |
| Ruxolitinib 250nM | 76.9% | 3.6 | 13.8% | 2.6 | 7.5% | 1.2 | 1.8% | 0.9 |
| Ruxolitinib 750nM | 63.4% | 5.2 | 18.5% | 4.0 | 14.6% | 1.9 | 3.6% | 1.7 |
| Ruxolitinib 1000nM | 57.0% | 4.7 | 25.2% | 3.2 | 16.4% | 2.6 | 1.4% | 0.1 |
| TG101209 250nM | 78.4% | 3.1 | 12.4% | 2.5 | 7.3% | 0.8 | 1.9% | 1.0 |
| TG101209 700nM | 56.3% | 3.8 | 20.5% | 4.4 | 20.1% | 0.7 | 3.1% | 0.7 |
| TG101209 1000nM | 39.1% | 2.8 | 25.4% | 5.0 | 30.9% | 1.2 | 4.6% | 0.9 |
| AT9283 10nM | 82.1% | 1.3 | 12.6% | 1.6 | 4.4% | 0.5 | 0.9% | 0.1 |
| AT9283 15nM | 75.1% | 4.0 | 14.7% | 2.8 | 7.5% | 1.2 | 2.6% | 0.8 |
| AT9283 30nM | 44.5% | 4.3 | 31.8% | 3.0 | 20.3% | 2.3 | 3.3% | 1.0 |

**The tables show the percentage of events analysed by FACS for Annexin V and 7AAD in each of the four quadrants equating to the live cell population, those cells undergoing the early and late stages of apoptosis and dead cells (Figure 2.2). The SEM is in the column to the right of each condition (n=3). Statistical analysis was by two-way ANOVA with Tukeys post-test correction. Significant changes compared to NDC are highlighted in red ($p \leq 0.05$). NDC; no drug control.**

**Figure 4.21 Apoptosis in UKE1 cells treated with ruxolitinib**

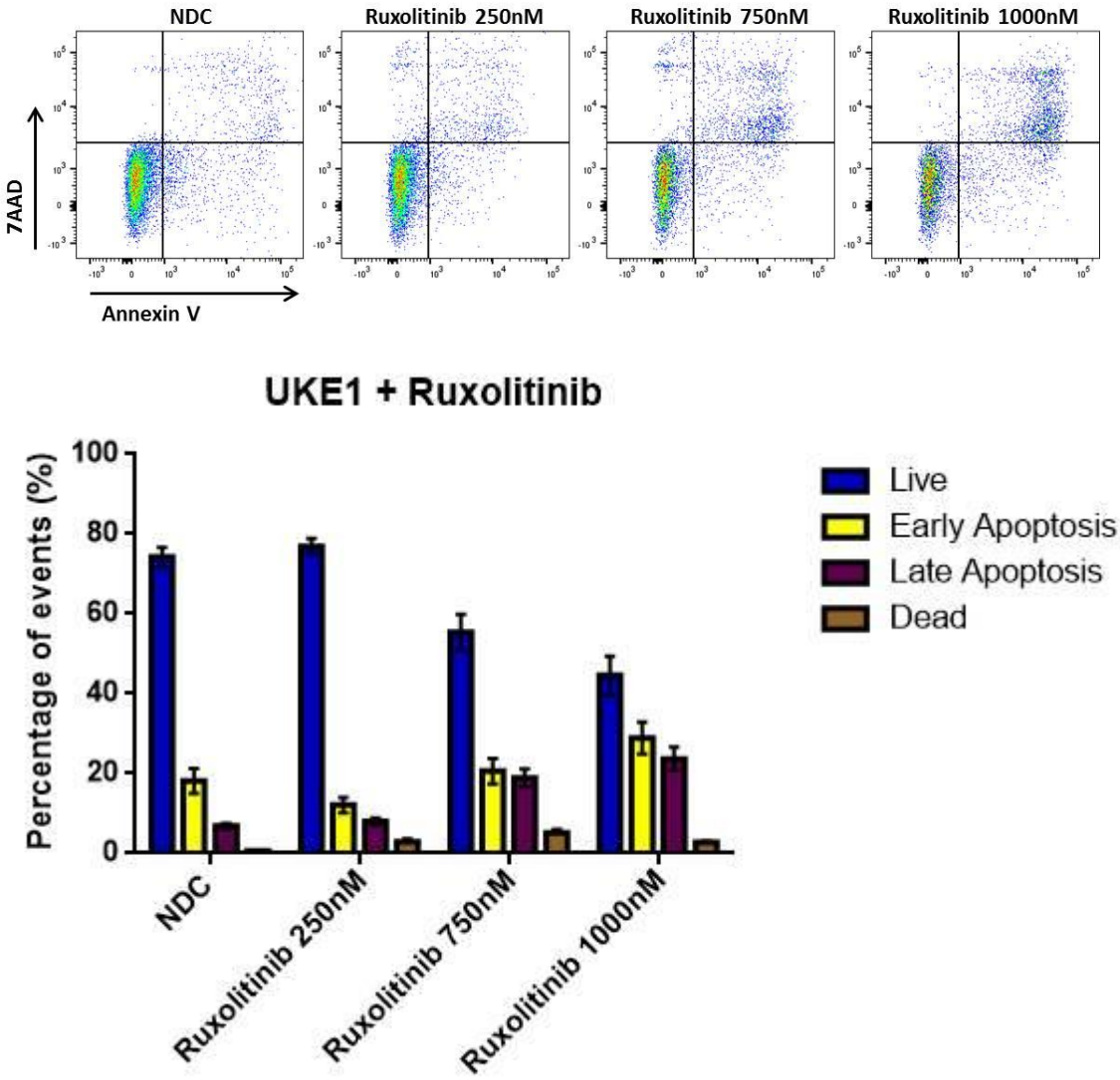


| Live | | | |
|---|---|---|---|
| Rux250 | NS | | |
| Rux750 | **** | **** | |
| Rux1000 | **** | **** | * |
| | NDC | Rux250 | Rux750 |

| Early | | | |
|---|---|---|---|
| Rux250 | NS | | |
| Rux750 | NS | NS | |
| Rux1000 | * | *** | NS |
| | NDC | Rux250 | Rux750 |

| Late | | | |
|---|---|---|---|
| Rux250 | NS | | |
| Rux750 | * | * | |
| Rux1000 | *** | *** | NS |
| | NDC | Rux250 | Rux750 |

| Dead | | | |
|---|---|---|---|
| Rux250 | NS | | |
| Rux750 | NS | NS | |
| Rux1000 | NS | NS | NS |
| | NDC | Rux250 | Rux750 |

**The dot plots show representative results from the apoptosis assay by FACS. The bar graphs show the changes in live cells, early and late apoptosis, and dead cells treated with ruxolitinib at 72 hours presented as the mean +/- SEM (n=3). Statistical significance was determined by two-way ANOVA with Tukey's post-test correction for multiple comparisons (* $p \leq 0.05$, ** $p \leq 0.01$, *** $p \leq 0.001$). The tables show the significance of each comparison for each stage of apoptosis.**

**Figure 4.22 Apoptosis in UKE1 cells treated with TG101209**

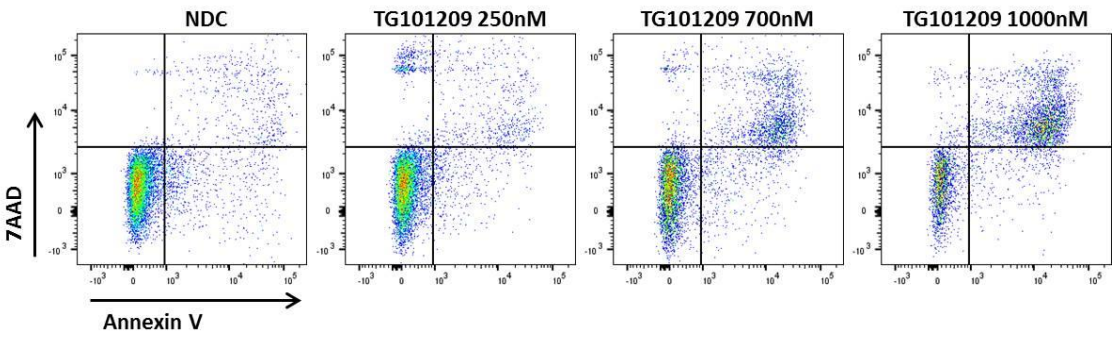


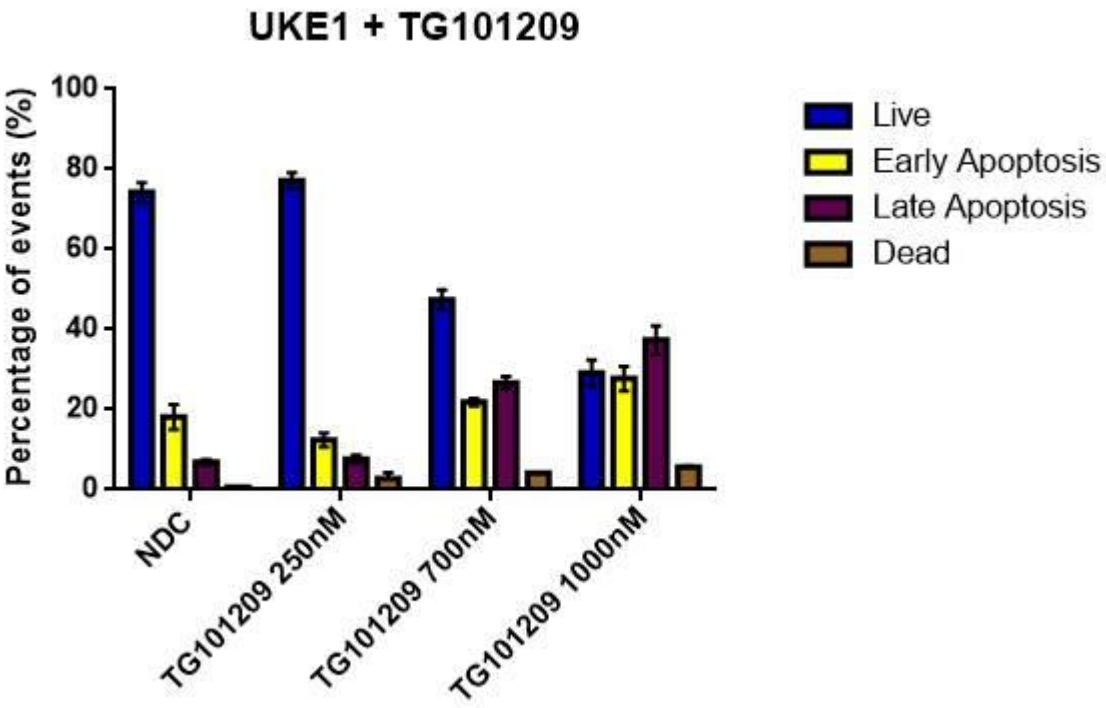


| Live | | | |
|---|---|---|---|
| TG250 | NS | | |
| TG700 | **** | **** | |
| TG1000 | **** | **** | **** |
| | NDC | TG250 | TG700 |

| Early | | | |
|---|---|---|---|
| TG250 | NS | | |
| TG700 | NS | * | |
| TG1000 | * | **** | NS |
| | NDC | TG250 | TG700 |

| Late | | | |
|---|---|---|---|
| TG250 | NS | | |
| TG700 | **** | **** | |
| TG1000 | **** | **** | ** |
| | NDC | TG250 | TG700 |

| Dead | | | |
|---|---|---|---|
| TG250 | NS | | |
| TG700 | NS | NS | |
| TG1000 | NS | NS | NS |
| | NDC | TG250 | TG700 |

**The dot plots show representative results from the apoptosis assay by FACS. The bar graphs show the changes in live cells, early and late apoptosis, and dead cells treated with ruxolitinib at 72 hours presented as the mean +/- SEM (n=3). Statistical significance was determined by two-way ANOVA with Tukey's post-test correction for multiple comparisons (* $p \leq 0.05$, ** $p \leq 0.01$, *** $p \leq 0.001$). The tables show the significance of each comparison for each stage of apoptosis.**

**Figure 4.23 Apoptosis in UKE1 cells treated with AT9283**

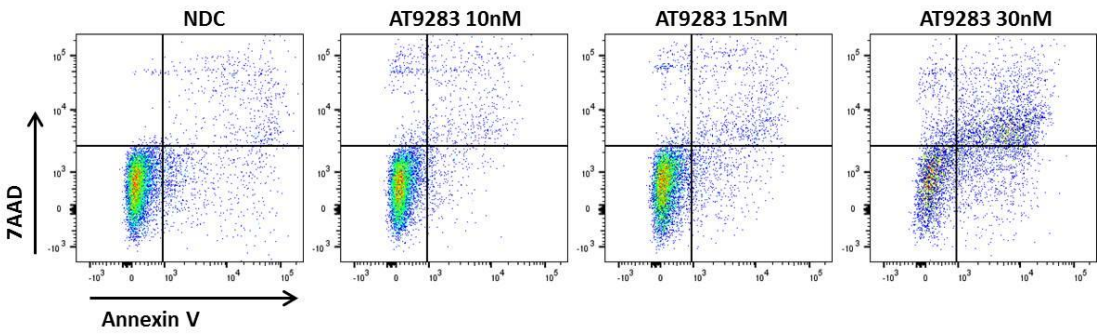


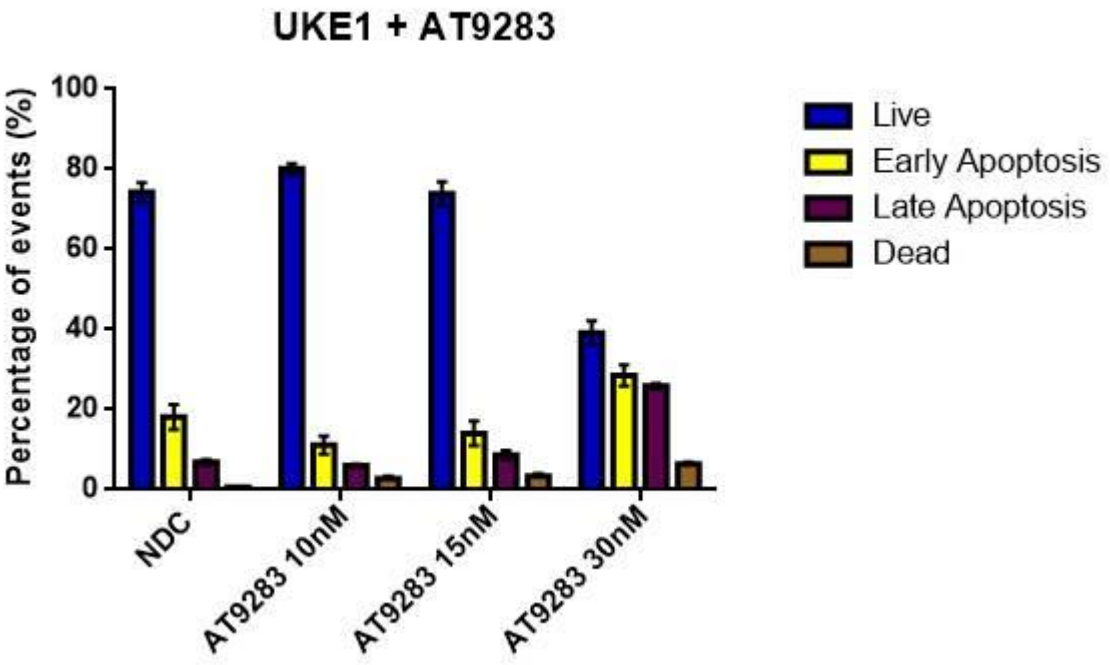


| Live | | | |
|---|---|---|---|
| AT10 | NS | | |
| AT15 | NS | NS | |
| AT30 | **** | **** | **** |
| | NDC | AT10 | AT15 |

| Early | | | |
|---|---|---|---|
| AT10 | NS | | |
| AT15 | NS | NS | |
| AT30 | ** | **** | ***** |
| | NDC | AT10 | AT15 |

| Late | | | |
|---|---|---|---|
| AT10 | NS | | |
| AT15 | NS | NS | |
| AT30 | **** | **** | **** |
| | NDC | AT10 | AT15 |

| Dead | | | |
|---|---|---|---|
| AT10 | NS | | |
| AT15 | NS | NS | |
| AT30 | NS | NS | NS |
| | NDC | AT10 | AT15 |

**The dot plots show representative results from the apoptosis assay by FACS. The bar graphs show the changes in live cells, early and late apoptosis, and dead cells treated with ruxolitinib at 72 hours presented as the mean +/- SEM (n=3). Statistical significance was determined by two-way ANOVA with Tukey's post-test correction for multiple comparisons (* $p \leq 0.05$, ** $p \leq 0.01$, *** $p \leq 0.001$). The tables show the significance of each comparison for each stage of apoptosis.**

### 4.2.7 Apoptosis is increased in SET2 cells following treatment with JAK2 inhibitors

The effect of the three JAK2 inhibitors was then investigated in the SET2 cell line. The gene expression changes were more limited in this setting, but treatment with ruxolitinib did result in a significant decrease in the expression of the anti-apoptotic *BCL2L1*, indicating the effect of JAK2 inhibition in apoptosis programmes in these cells. As with in the UKE1 cells, there are clear decreases in the live cell populations with all three inhibitors within 24 hours, which became more pronounced with further time spent in culture with the inhibitors. The higher concentrations of each inhibitor did have a more pronounced effect with a significant reduction in live cells in the highest concentration compared to the lowest with all three inhibitors. The marked effect that JAK2 inhibition has on apoptosis in these cells is not mirrored in the gene expression changes seen in SET2 cells treated with each of the JAK2 inhibitors, with only TG101209 causing a significant decrease in the anti-apoptotic *BCL2L1*.

**Table 4.3 Apoptosis at 24 and 48 hours in SET2 cells treated with JAK2 inhibitors**

| 24 hours | Live | +/- | Early | +/- | Late | +/- | Dead | +/- |
|---|---|---|---|---|---|---|---|---|
| NDC | 77.3% | 1.1 | 9.4% | 0.3 | 12.5% | 1.6 | 0.7% | 0.1 |
| Ruxolitinib 50nM | 78.2% | 1.7 | 8.5% | 0.4 | 12.4% | 1.4 | 1.0% | 0.2 |
| Ruxolitinib 100nM | 74.2% | 1.5 | 10.4% | 0.4 | 14.5% | 1.4 | 0.9% | 0.4 |
| Ruxolitinib 200nM | 73.1% | 1.8 | 9.9% | 1.1 | 15.6% | 1.3 | 1.4% | 0.1 |
| TG101209 100nM | 75.6% | 2.4 | 11.2% | 1.3 | 12.5% | 1.8 | 0.6% | 0.8 |
| TG101209 250nM | 69.0% | 1.9 | 13.6% | 1.1 | 16.5% | 2.2 | 0.9% | 0.2 |
| TG101209 500nM | 60.2% | 2.6 | 15.7% | 1.6 | 22.3% | 2.8 | 1.9% | 0.8 |
| AT9283 10nM | 74.2% | 1.9 | 12.7% | 1.1 | 12.6% | 1.9 | 0.5% | 1.7 |
| AT9283 25nM | 70.7% | 1.5 | 12.6% | 2.7 | 15.5% | 2.2 | 1.1% | 1.3 |
| AT9283 50nM | 68.0% | 2.7 | 14.6% | 1.0 | 16.7% | 4.5 | 0.7% | 2.6 |

| 48 hours | Live | +/- | Early | +/- | Late | +/- | Dead | +/- |
|---|---|---|---|---|---|---|---|---|
| NDC | 83.2% | 0.8 | 4.3% | 1.3 | 9.9% | 0.7 | 2.6% | 0.5 |
| Ruxolitinib 50nM | 73.1% | 1.8 | 7.1% | 1.8 | 17.2% | 2.6 | 2.6% | 0.9 |
| Ruxolitinib 100nM | 71.9% | 0.9 | 4.0% | 3.7 | 18.6% | 2.0 | 5.5% | 1.2 |
| Ruxolitinib 200nM | 62.0% | 0.9 | 5.2% | 3.7 | 24.5% | 3.9 | 8.3% | 1.0 |
| TG101209 100nM | 81.1% | 0.8 | 2.5% | 1.0 | 11.3% | 2.4 | 5.1% | 1.9 |
| TG101209 250nM | 71.7% | 3.9 | 3.9% | 4.7 | 17.5% | 0.8 | 6.8% | 1.4 |
| TG101209 500nM | 49.7% | 1.9 | 4.8% | 4.9 | 30.7% | 3.1 | 14.9% | 0.5 |
| AT9283 10nM | 80.6% | 5.2 | 2.2% | 4.0 | 10.5% | 2.5 | 6.7% | 1.6 |
| AT9283 25nM | 68.5% | 4.1 | 4.2% | 3.9 | 19.1% | 2.3 | 8.2% | 1.8 |
| AT9283 50nM | 61.7% | 5.0 | 6.5% | 3.6 | 23.2% | 3.4 | 8.5% | 1.3 |

**The tables show the percentage of events analysed by FACS for Annexin V and 7AAD in each of the four quadrants on the equating to the live cell population, those cells undergoing the early and late stages of apoptosis and dead cells. The SEM is in the column to the right of each condition (n=3). Statistical analysis was by two-way ANOVA with Tukeys post-test correction. Significant changes compared to NDC are highlighted in red ($p \leq 0.05$).**

**Figure 4.24 Apoptosis in SET2 cells treated with ruxolitinib**

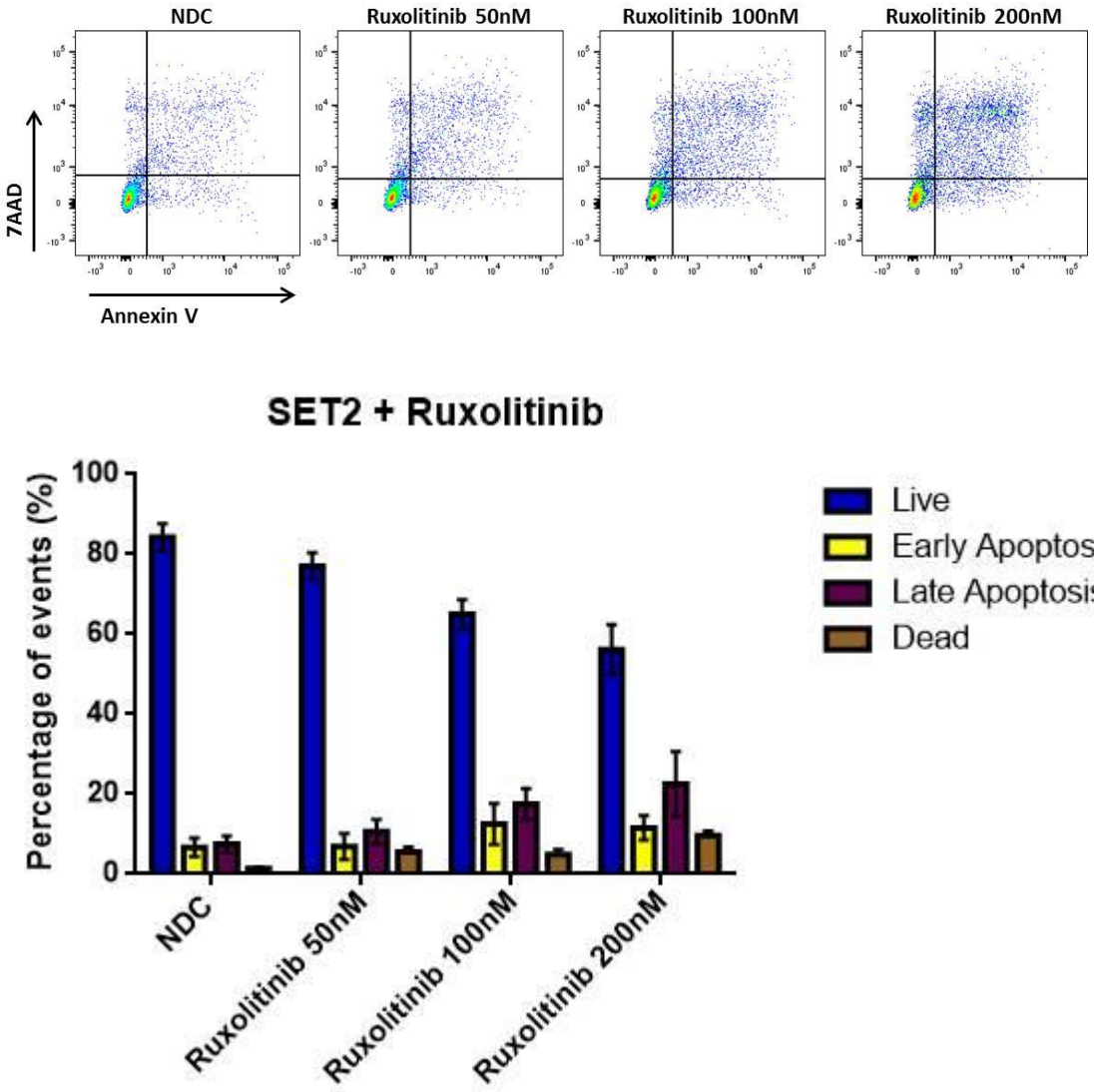


| Live | | | |
|---|---|---|---|
| Rux50 | NS | | |
| Rux100 | ** | NS | |
| Rux200 | **** | ** | NS |
| | NDC | Rux50 | Rux100 |

| Early | | | |
|---|---|---|---|
| Rux50 | NS | | |
| Rux100 | NS | NS | |
| Rux200 | NS | NS | NS |
| | NDC | Rux50 | Rux100 |

| Late | | | |
|---|---|---|---|
| Rux50 | NS | | |
| Rux100 | NS | NS | |
| Rux200 | * | NS | NS |
| | NDC | Rux50 | Rux100 |

| Dead | | | |
|---|---|---|---|
| Rux50 | NS | | |
| Rux100 | NS | NS | |
| Rux200 | NS | NS | NS |
| | NDC | Rux50 | Rux100 |

**The dot plots show representative results from the apoptosis assay by FACS. The bar graphs show the changes in live cells, early and late apoptosis, and dead cells treated with ruxolitinib at 72 hours presented as the mean +/- SEM (n=3). Statistical significance was determined by two-way ANOVA with Tukey's post-test correction for multiple comparisons (* $p \leq 0.05$, ** $p \leq 0.01$, *** $p \leq 0.001$). The tables show the significance of each comparison for each stage of apoptosis.**

**Figure 4.25 Apoptosis in SET2 cells treated with TG101209**

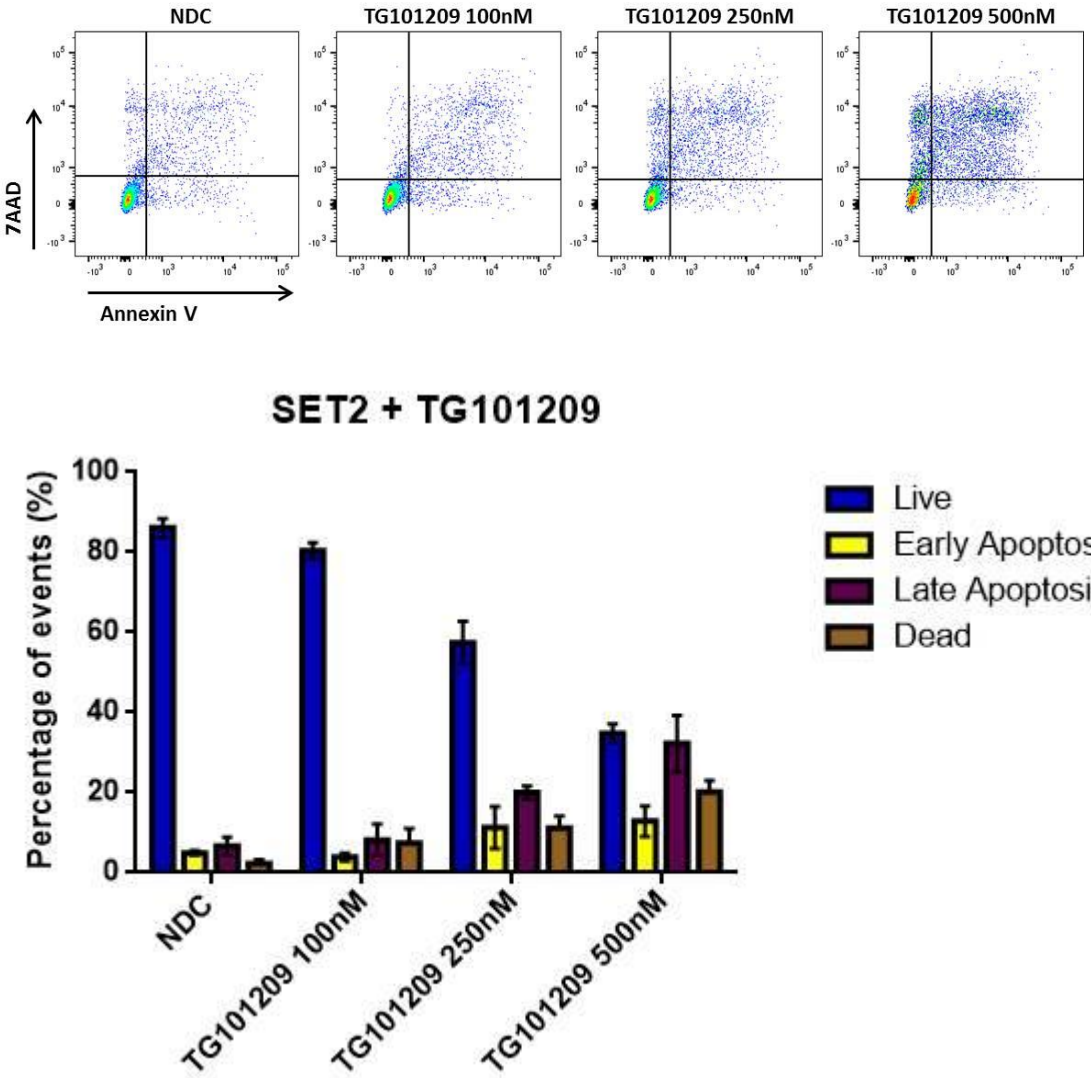


| Live | | | |
|---|---|---|---|
| TG100 | NS | | |
| TG250 | **** | *** | |
| TG500 | **** | **** | *** |
| | NDC | TG100 | TG250 |

| Early | | | |
|---|---|---|---|
| TG100 | NS | | |
| TG250 | NS | NS | |
| TG500 | NS | NS | NS |
| | NDC | TG100 | TG250 |

| Late | | | |
|---|---|---|---|
| TG100 | NS | | |
| TG250 | * | NS | |
| TG500 | **** | *** | NS |
| | NDC | TG100 | TG250 |

| Dead | | | |
|---|---|---|---|
| TG100 | NS | | |
| TG250 | NS | NS | |
| TG500 | ** | NS | NS |
| | NDC | TG100 | TG250 |

**The dot plots show representative results from the apoptosis assay by FACS. The bar graphs show the changes in live cells, early and late apoptosis, and dead cells treated with ruxolitinib at 72 hours presented as the mean +/- SEM (n=3). Statistical significance was determined by two-way ANOVA with Tukey's post-test correction for multiple comparisons (* $p \leq 0.05$, ** $p \leq 0.01$, *** $p \leq 0.001$). The tables show the significance of each comparison for each stage of apoptosis.**

**Figure 4.26 Apoptosis in SET2 cells treated with AT9283**

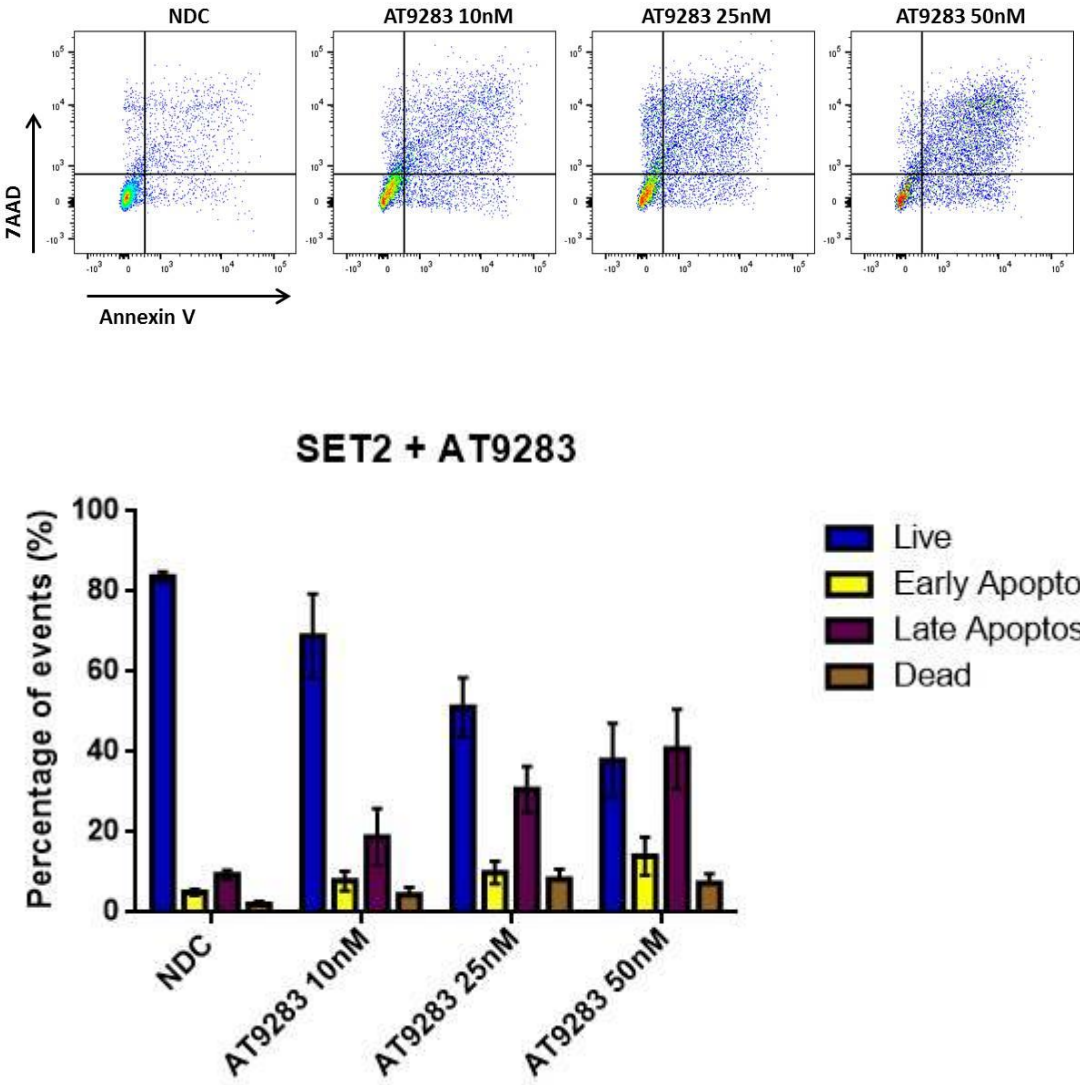


| Live | | | |
|---|---|---|---|
| AT10 | NS | | |
| AT25 | ** | NS | |
| AT50 | **** | ** | NS |
| | NDC | AT10 | AT25 |

| Early | | | |
|---|---|---|---|
| AT10 | NS | | |
| AT25 | NS | NS | |
| AT50 | NS | NS | NS |
| | NDC | AT10 | AT25 |

| Late | | | |
|---|---|---|---|
| AT10 | NS | | |
| AT25 | * | NS | |
| AT50 | ** | * | NS |
| | NDC | AT10 | AT25 |

| Dead | | | |
|---|---|---|---|
| AT10 | NS | | |
| AT25 | NS | NS | |
| AT50 | NS | NS | NS |
| | NDC | AT10 | AT25 |

**The dot plots show representative results from the apoptosis assay by FACS. The bar graphs show the changes in live cells, early and late apoptosis, and dead cells treated with ruxolitinib at 72 hours presented as the mean +/- SEM (n=3). Statistical significance was determined by two-way ANOVA with Tukey's post-test correction for multiple comparisons (* $p \leq 0.05$, ** $p \leq 0.01$, *** $p \leq 0.001$). The tables show the significance of each comparison for each stage of apoptosis.**

### 4.2.8 Cell cycle is altered in UKE1 cells following treatment with JAK2 inhibitors

In JAK2 V617F mutated myeloproliferative neoplasms the cell cycle is deregulated with an increase in cell cycle in the malignant clone, giving it a survival advantage over normal cells. Interestingly, this advantage appears to emerge as the cells proliferate and mature rather than at the stem cell level. When the JAK2 V617F mutated UKE1 cells are treated with the JAK2 inhibitor ruxolitinib there was no significant change in any stage of the cell cycle when compared to untreated cells. However both TG101209 and AT9283 produced a significant alteration in cell cycle with the highest dose used compared to other treatment arms. Of interest is the fact that AT9283 did not disrupt the cell cycle analysis to the point where no useful data was obtained as seen in K562 cells (Figure 3.20). This would suggest the Aurora kinase effect is less marked with the doses used in this cell line, than in K562 cells, where a higher dose of AT9203 was used. However the alteration seen led to an increase in S-G2-M which may still reflect a degree of Aurora kinase activity and an accumulation of multinucleate cells.

**Figure 4.27 Cell cycle analysis of UKE1 cells following treatment with ruxolitinib**

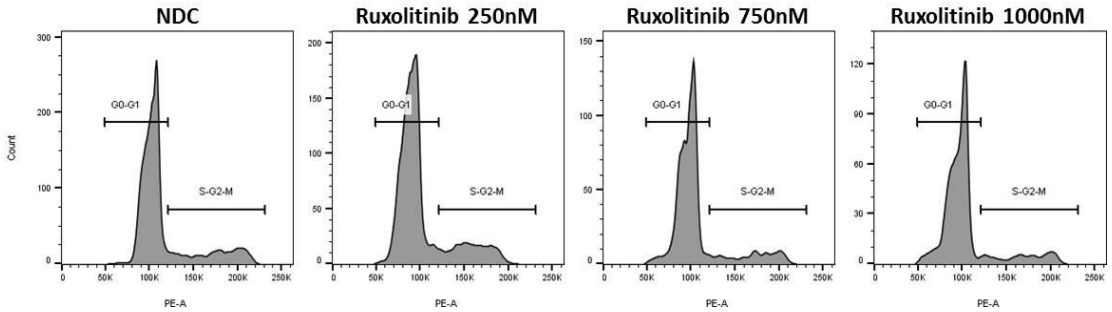


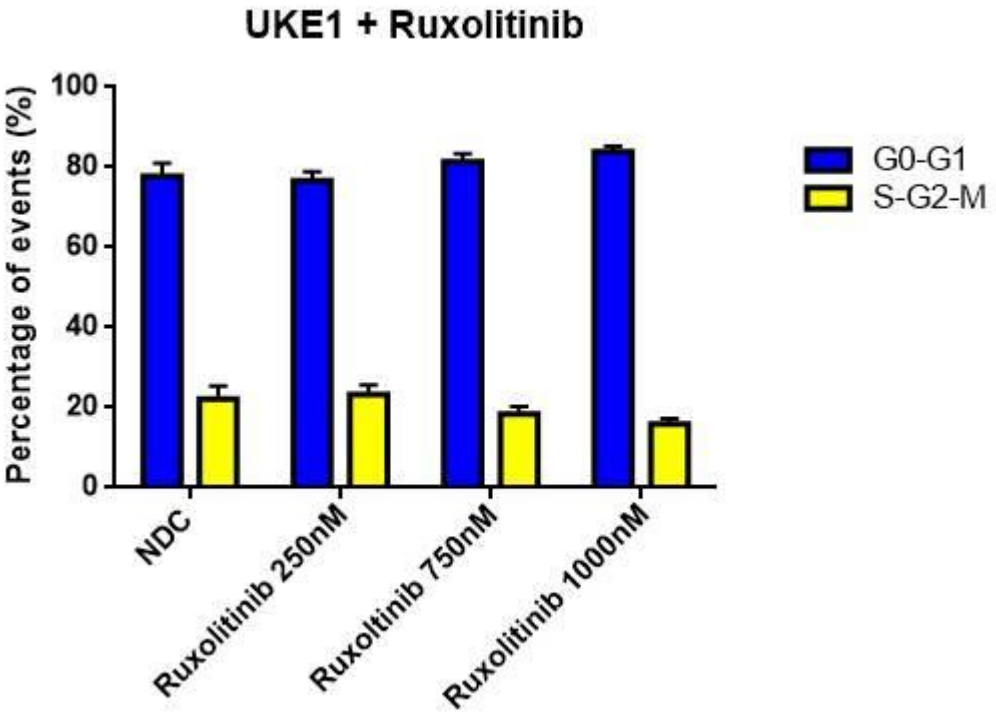


| G0-G1 | | | |
|---|---|---|---|
| Rux250 | NS | | |
| Rux750 | NS | NS | |
| Rux1000 | NS | NS | NS |
| | NDC | Rux250 | Rux750 |

| S-G2-M | | | |
|---|---|---|---|
| Rux250 | NS | | |
| Rux750 | NS | NS | |
| Rux1000 | NS | NS | NS |
| | NDC | NS | Rux750 |

**The histogram plots show representative results from FACS and show the gating strategy used. The bar graphs show the changes in cell cycle following treatment with ruxolitinib for 72 hours, highlighting those actively undergoing cell cycle (S-G2-M) and those that are quiescent (G0-G1). They are presented as the mean +/- SEM (n=3). Statistical significance was determined by two-way ANOVA with Tukey's post-test correction for multiple comparisons (* $p \leq 0.05$, ** $p \leq 0.01$, *** $p \leq 0.001$, **** $p \leq 0.0001$)..**

**Figure 4.28 Cell cycle analysis of UKE1 cells following treatment with TG101209**

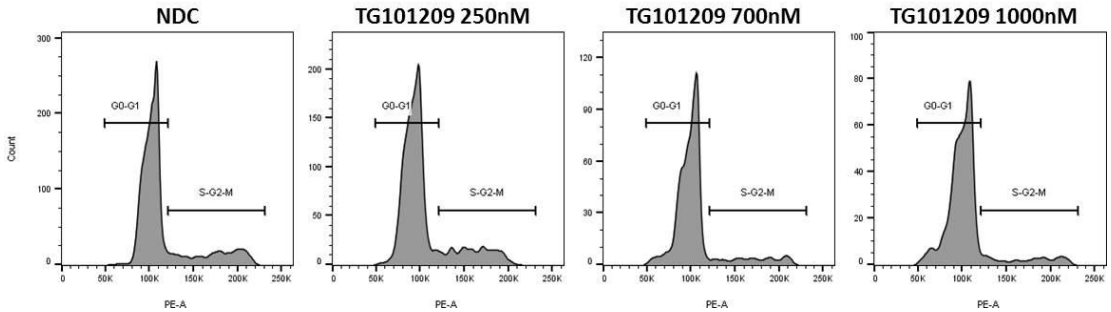


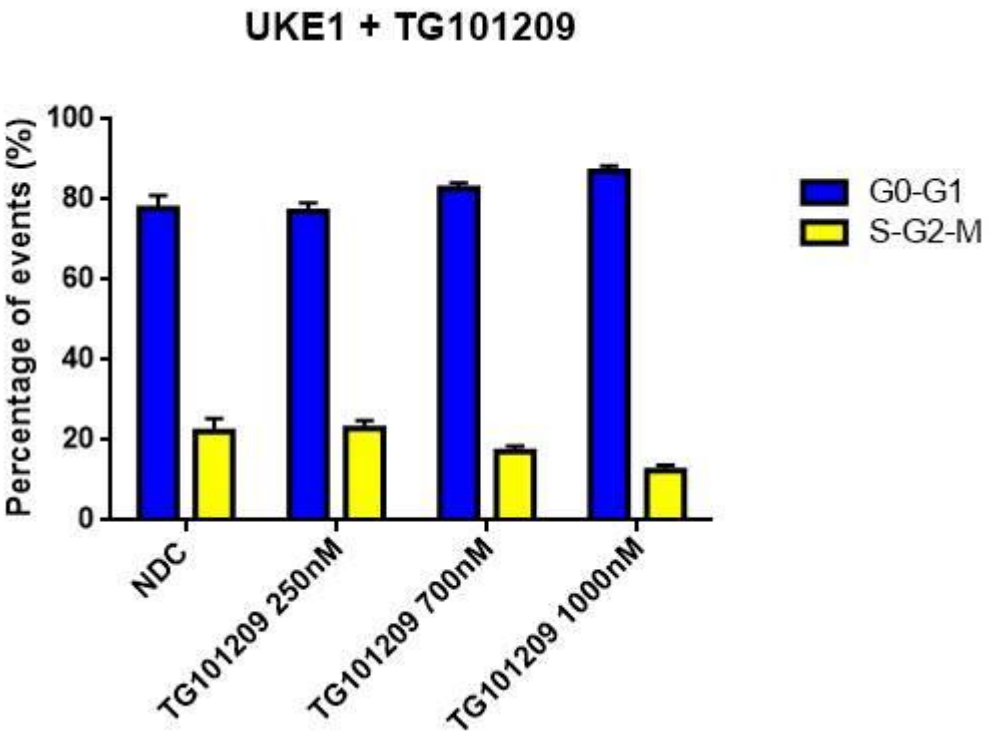


| G0-G1 | | | |
|---|---|---|---|
| TG250 | NS | | |
| TG700 | NS | NS | |
| TG1000 | * | * | NS |
| | NDC | TG250 | TG700 |

| S-G2-M | | | |
|---|---|---|---|
| TG250 | NS | | |
| TG700 | NS | NS | |
| TG1000 | * | * | NS |
| | NDC | TG250 | TG700 |

**The histogram plots show representative results from FACS and show the gating strategy used. The bar graphs show the changes in cell cycle following treatment with ruxolitinib for 72 hours, highlighting those actively undergoing cell cycle (S-G2-M) and those that are quiescent (G0-G1). They are presented as the mean +/- SEM (n=3). Statistical significance was determined by two-way ANOVA with Tukey's post-test correction for multiple comparisons (* p ≤ 0.05, ** p ≤ 0.01, *** p ≤ 0.001, **** p ≤ 0.0001)..**

**Figure 4.29 Cell cycle analysis of UKE1 cells following treatment with AT9283**

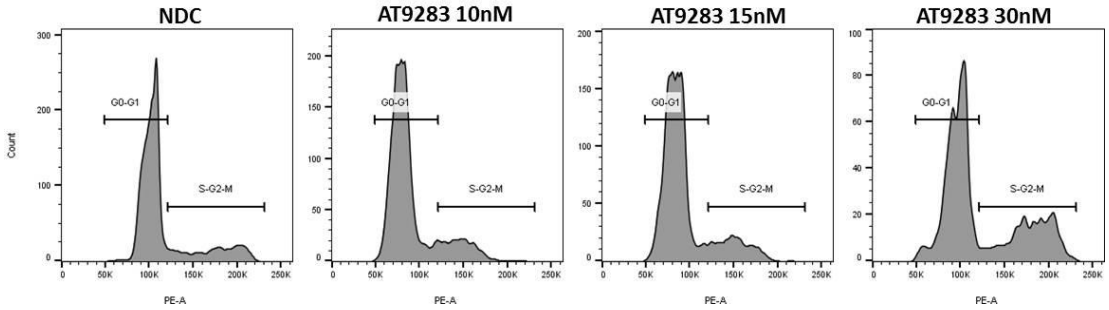


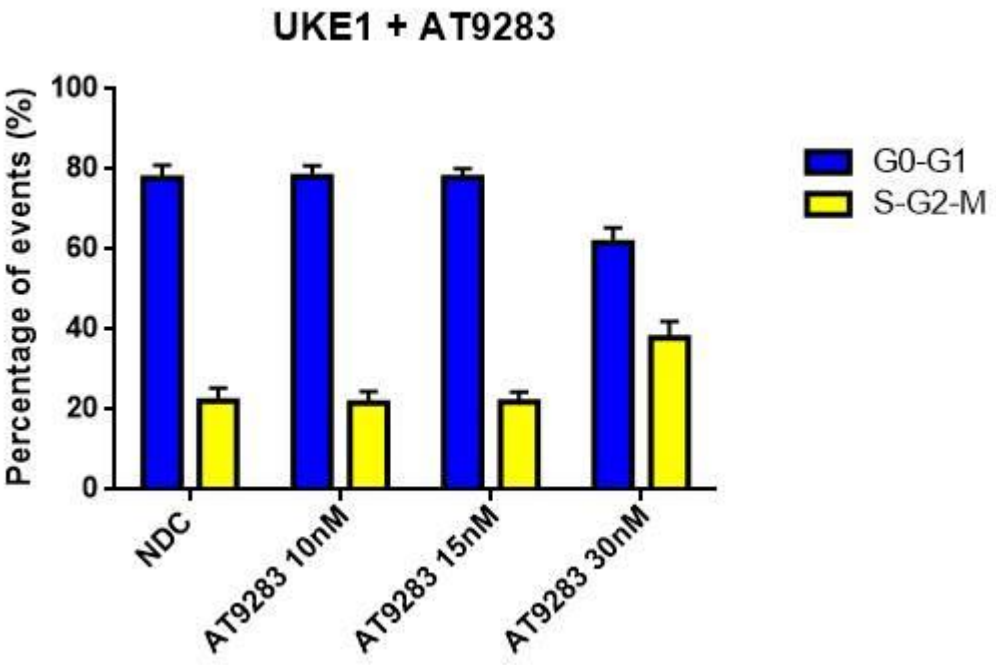


| G0-G1 | | | |
|---|---|---|---|
| AT10 | NS | | |
| AT15 | NS | NS | |
| AT30 | * | ** | * |
| | NDC | AT10 | AT15 |

| S-G2-M | | | |
|---|---|---|---|
| AT10 | NS | | |
| AT15 | NS | NS | |
| AT30 | * | * | * |
| | NDC | AT10 | AT15 |

**The histogram plots show representative results from FACS and show the gating strategy used. The bar graphs show the changes in cell cycle following treatment with ruxolitinib for 72 hours, highlighting those actively undergoing cell cycle (S-G2-M) and those that are quiescent (G0-G1). They are presented as the mean +/- SEM (n=3). Statistical significance was determined by two-way ANOVA with Tukey's post-test correction for multiple comparisons and defined as * p≤0.05 ** p≤0.01.**

### 4.2.9 Cell cycle is altered in SET2 cells following treatment with JAK2 inhibitors

SET2 cells treated with each of the JAK2 inhibitors showed a clear G0-G1 arrest when treated with ruxolitinib or TG101209 at all doses compared to untreated cells. This pattern is more in keeping with published data where treatment of the JAK2 V617F containing erythroleukaemia cell line HEL with TG101209 induced a G0-G1 arrest, which was mimicked to a lesser degree in K562 cells used as a comparator in that paper[193]. This second finding was not replicated in K562 cells treated with TG101209 in our study (Figure 3.19). The expression data for these cells did not show any specific changes in cell cycle genes at 24 hours, but this would not preclude a cumulative effect over a 72 hour period leading to the changes seen in cell cycle here. Interestingly, the SET2 cells treated with AT9283 had a similar appearance to that seen in K562 cells making it difficult to draw any meaningful conclusions in this cell type. The reason for this is not entirely clear, as the doses used in SET2 cells are similar to those used in UKE1 cells, but may represent a greater sensitivity in SET2 cells to the Aurora kinase activity of AT9283 compared to UKE1 cells.

**Figure 4.30 Cell cycle analysis of SET2 cells following treatment with ruxolitinib**

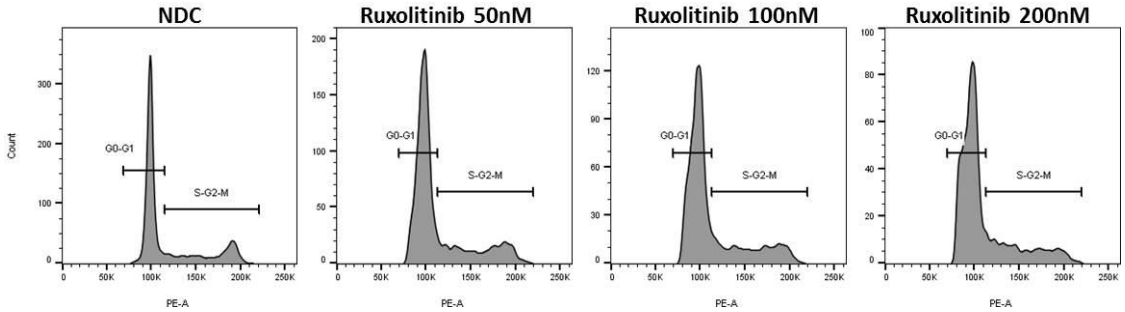


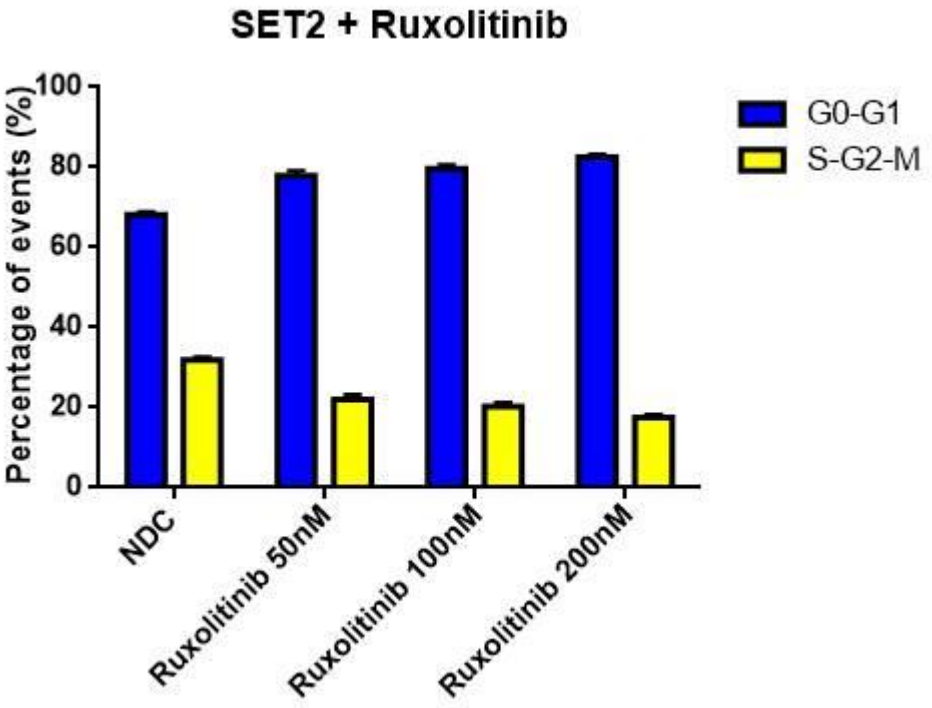


| G0-G1 | | | |
|---|---|---|---|
| Rux50 | **** | | |
| Rux100 | **** | NS | |
| Rux200 | **** | * | NS |
| | NDC | Rux50 | Rux100 |

| S-G2-M | | | |
|---|---|---|---|
| Rux50 | **** | | |
| Rux100 | **** | NS | |
| Rux200 | **** | * | NS |
| | NDC | Rux50 | Rux100 |

**The histogram plots show representative results from FACS and show the gating strategy used. The bar graphs show the changes in cell cycle following treatment with ruxolitinib for 72 hours, highlighting those actively undergoing cell cycle (S-G2-M) and those that are quiescent (G0-G1). They are presented as the mean +/- SEM (n=3). Statistical significance was determined by two-way ANOVA with Tukey's post-test correction for multiple comparisons (* p≤0.05, ** p≤0.01, *** p≤0.001, **** p≤0.0001).**

**Figure 4.31 Cell cycle analysis of SET2 cells following treatment with TG101209**

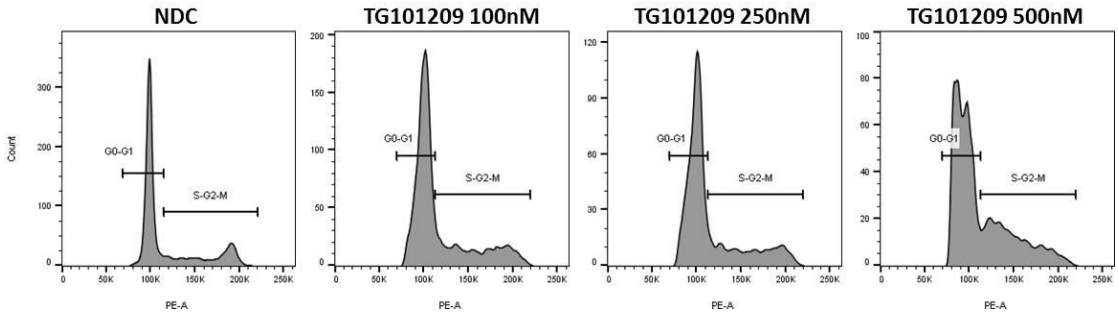


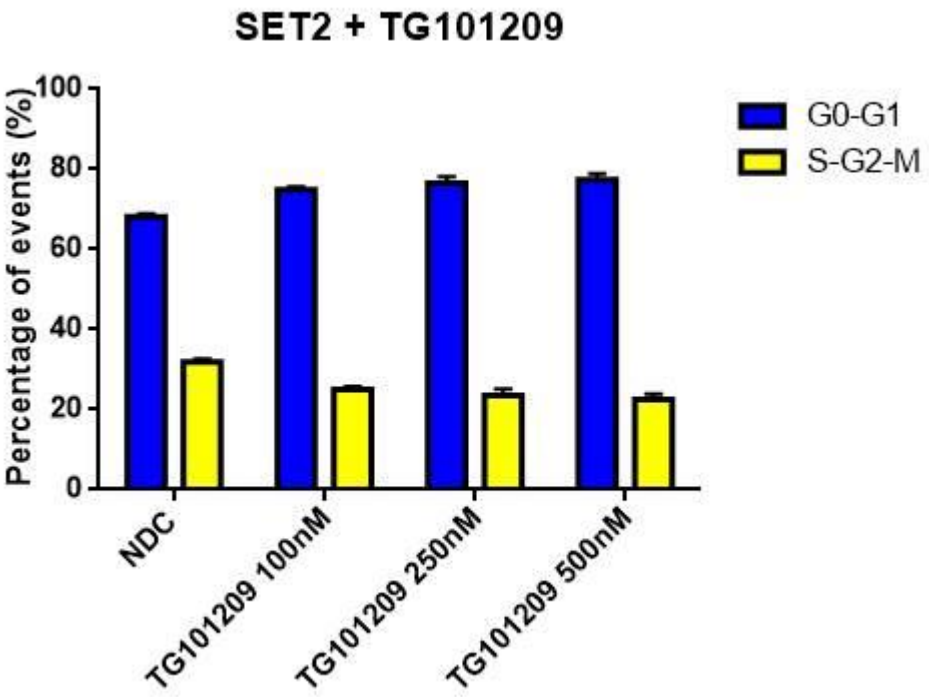


| G0-G1 | | | |
|---|---|---|---|
| TG100 | ** | | |
| TG250 | *** | NS | |
| TG500 | *** | NS | NS |
| | NDC | TG100 | TG250 |

| S-G2-M | | | |
|---|---|---|---|
| TG100 | ** | | |
| TG250 | *** | NS | |
| TG500 | *** | NS | NS |
| | NDC | TG100 | TG250 |

**The histogram plots show representative results from FACS and show the gating strategy used. The bar graphs show the changes in cell cycle following treatment with ruxolitinib for 72 hours, highlighting those actively undergoing cell cycle (S-G2-M) and those that are quiescent (G0-G1). They are presented as the mean +/- SEM (n=3). Statistical significance was determined by two-way ANOVA with Tukey's post-test correction for multiple comparisons (* p≤0.05, ** p≤0.01, *** p≤0.001, **** p≤0.0001).**

**Figure 4.32 Cell cycle analysis of SET2 cells following treatment with AT9283**

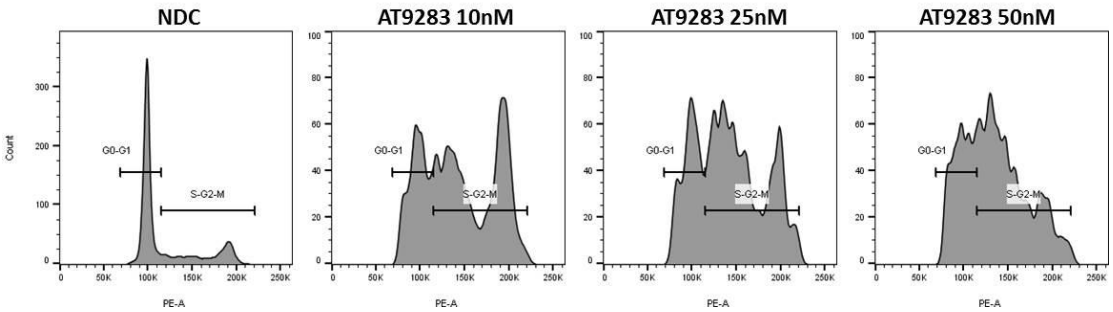


**The histogram plots show representative results from the PI staining and FACS analysis. When the normal gating strategy was applied it was difficult to extract any meaningful data from cells treated with AT9283.**

### 4.2.10 Immunofluorescence of UKE1 cells following treatment with JAK2 inhibitors or IFN-γ

Previous studies have shown that in CD34+ve cells the JAK2 V617F mutation accumulates preferentially in the nucleus compared to wild type JAK2[225]. This is supported by further data showing that JAK2 needs to be active and phosphorylated before SUMO proteins can attach and give the protein the ability to enter the nucleus[78], and that the JAK2 V617F mutant can be SUMOylated and enter the nucleus. This combination of constitutive activation of JAK2 and the SUMOylation of phosphorylated JAK2 leads to the preferential entry of the JAK2 V617F mutant into the nucleus of CD34+ve cells. Interestingly, this increase of JAK2 V617F in the nucleus was not seen in lineage-committed fractions of bone marrow cells[225].

UKE1 cells were cultured for 24 hours with ruxolitinib, TG101209 or IFNγ, used as a positive control of JAK2 activation in inflammation, before being processed for immunofluorescence or Duolink® immunofluorescent co-localisation assay. The immunofluorescence shows the presence of PML within the nuclear bodies, and SUMO 2/3 predominantly in the cytoplasm, but also existing within the nucleus in discrete structures. JAK2 follows a similar pattern in UKE1 cells, with predominantly cytoplasmic localisation, but also discrete punctate localisation within the nucleus (Figure 4.33).

**Figure 4.33 Immunofluorescence of UKE1 cells following treatment with JAK2 inhibitors or IFN-γ**

**a) UKE1 cells probed for JAK2 and PML**

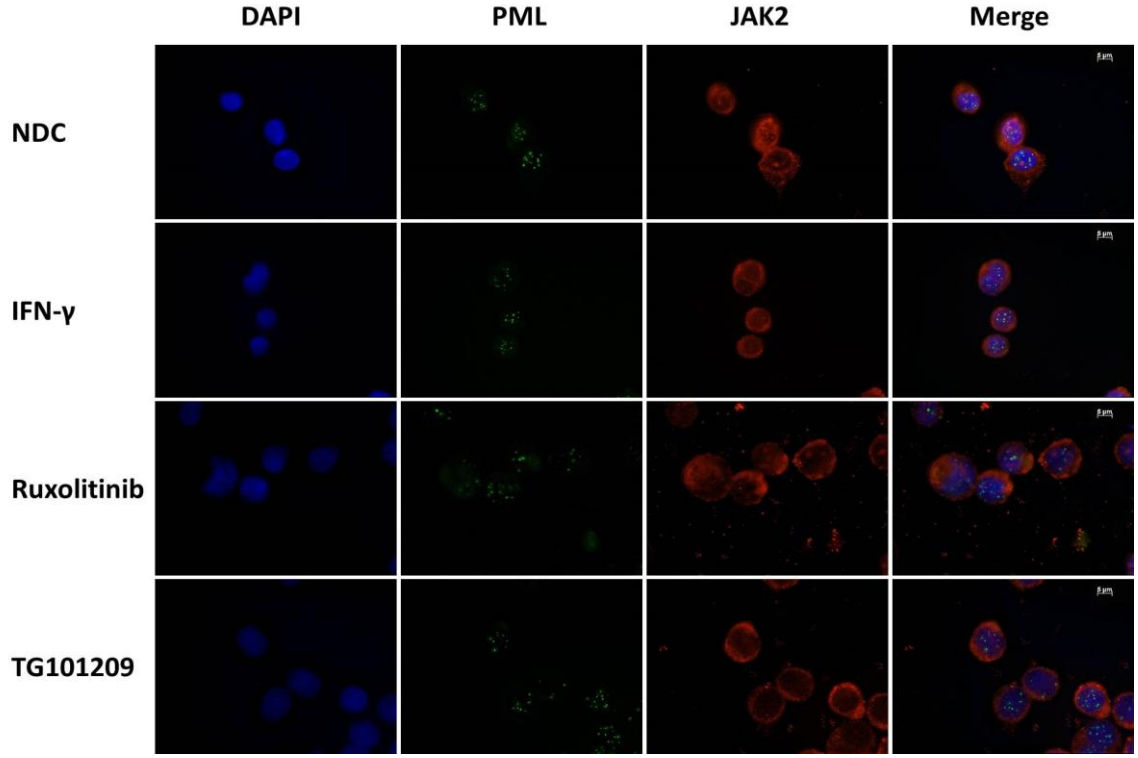


**b) UKE1 cells probed for JAK2 and SUMO 2/3**

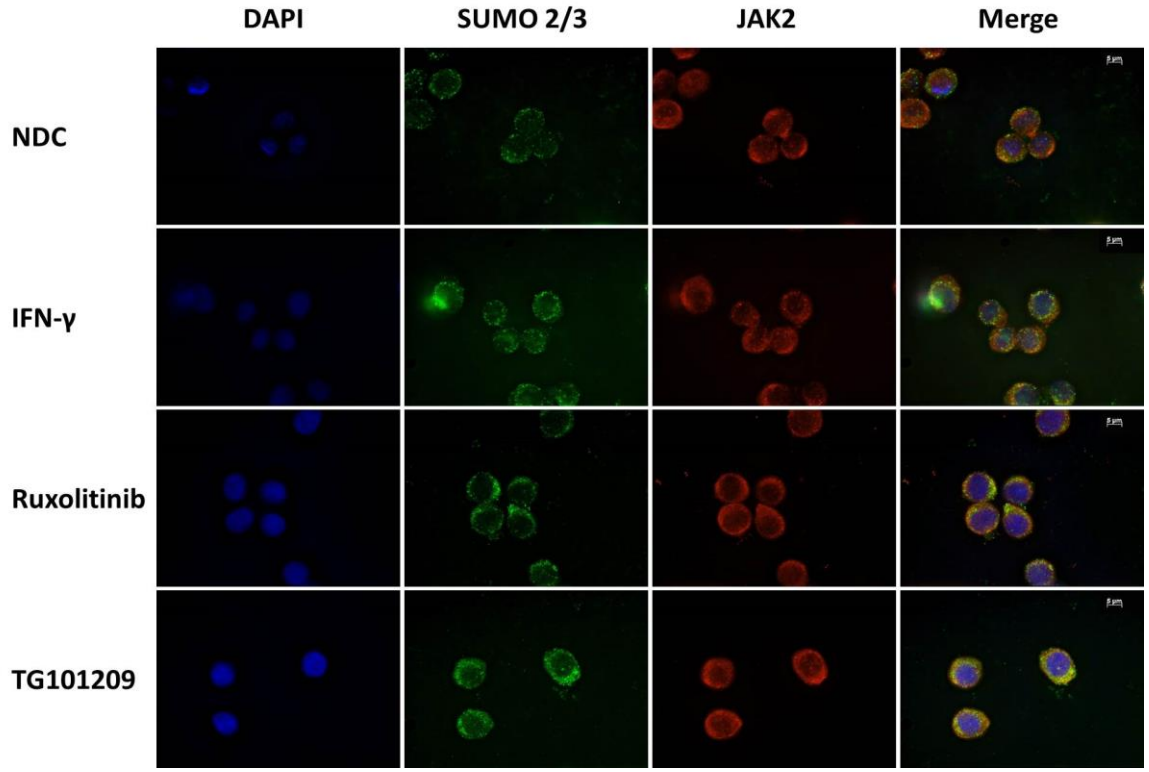


**UKE1 cells were treated for 24 hours then prepared for immunofluorescence as described previously. 3 separate experiments were carried out and representative images are shown above with cells being assessed for JAK2 and PML in a) and for JAK2 and SUMO in b).**

Based on the immunofluorescence appearances, Duolink® colocalisation assay was carried out to assess the effect of JAK2 inhibition in UKE1 cells. Unfortunately the assay failed in SET2 cells on two separate experiments so results are not available for that cell line. As expected, treatment of UKE1 cells with IFNγ led to a marked increase in the localisation of JAK2 with both PML and SUMO2/3. Interestingly there is an unexpected increase in the localisation of JAK2 and PML following treatment with ruxolitinib, while TG101209 leads to a reduction in the localisation of JAK2 and SUMO2/3 (Figure 4.34b). The increase seen in the localisation following treatment with ruxolitinib is not what would be expected following inhibition of JAK2, but was consistent across each experiment.

**Figure 4.34 Duolink co-localisation assay in UKE1 cells treated with JAK2 inhibitors**

**a) Duolink co-localisation images**

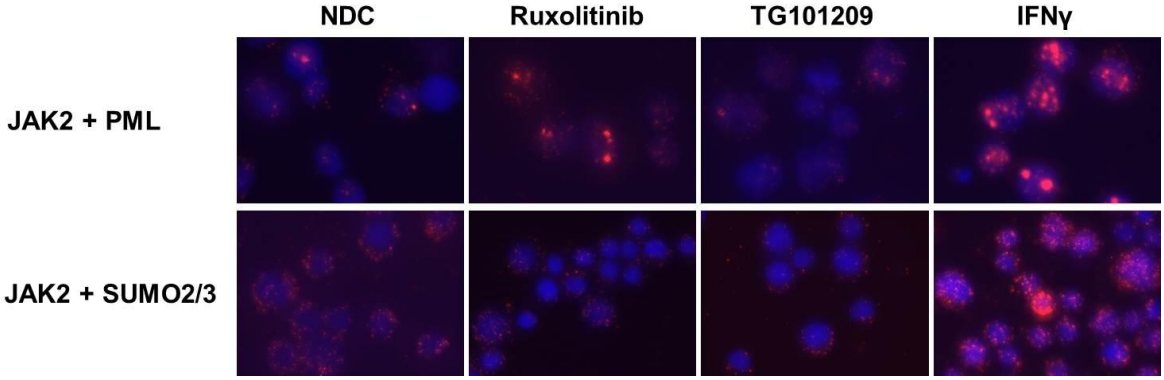


**b) Corrected total cell fluorescence**

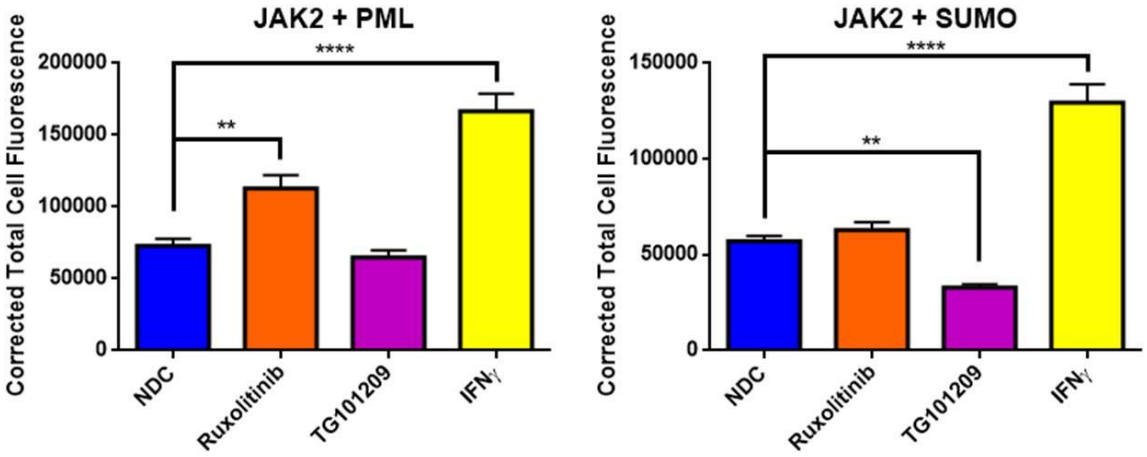


**UKE1 cells were treated for 24 hours then prepared for Duolink immunofluorescent co-localisation assay as described previously. 80 cells were counted for each treatment in 3 separate experiments with the corrected total cell fluorescence calculated. The images (3a) are representative of the experiments while the graphs (3b) show the average of the corrected total cell fluorescence for all 3 experiments +/- SEM. AT9283 was not included due to a lack of adherence of sufficient cells for analysis. Statistical significance was determined by one way ANOVA with Dunnett's correction for multiple comparisons (* p≤0.05, ** p≤0.01, *** p≤0.001, **** p≤0.0001).**

### 4.2.11 Effect of Arsenic trioxide and ruxolitinib on protein expression in JAK2 V617F containing cell lines

After showing the alteration in the interaction of JAK2 and PML following treatment with JAK2 inhibitors, we decided to treat UKE1 and SET2 cells with ruxolitinib in combination with arsenic trioxide. Arsenic trioxide is used in the treatment of acute promyelocytic leukaemia as it causes degradation of the aberrant PML-RARα protein through SUMO and ubiquitin mediated processes[226]. It has been shown that arsenic trioxide does the same to normal PML[227] and therefore provides a useful tool for researching the functional importance of interference with both the JAK2 pathway and PML function. To assess the effect of ruxolitinib and arsenic trioxide on JAK2 signalling, SET2 cells were treated with each compound alone and in combination over a 24 hour time course with samples taken at 0, 1, 4, 8 and 24 hours. The samples were then probed for phosphorylated and total STAT1 and STAT5. This showed the reduction and subsequent increase of phosphorylation of the two proteins with ruxolitinib seen previously and a mild reduction in phosphorylation of STAT5 with arsenic trioxide compared to untreated cells. This effect of arsenic trioxide leads to an attenuation of the ruxolitinib induced increase in phospho-STAT5 signal when both compounds are used together.

**Figure 4.35 Western blotting of SET2 cells treated with ruxolitinib and arsenic trioxide alone and in combination over 24 hours**

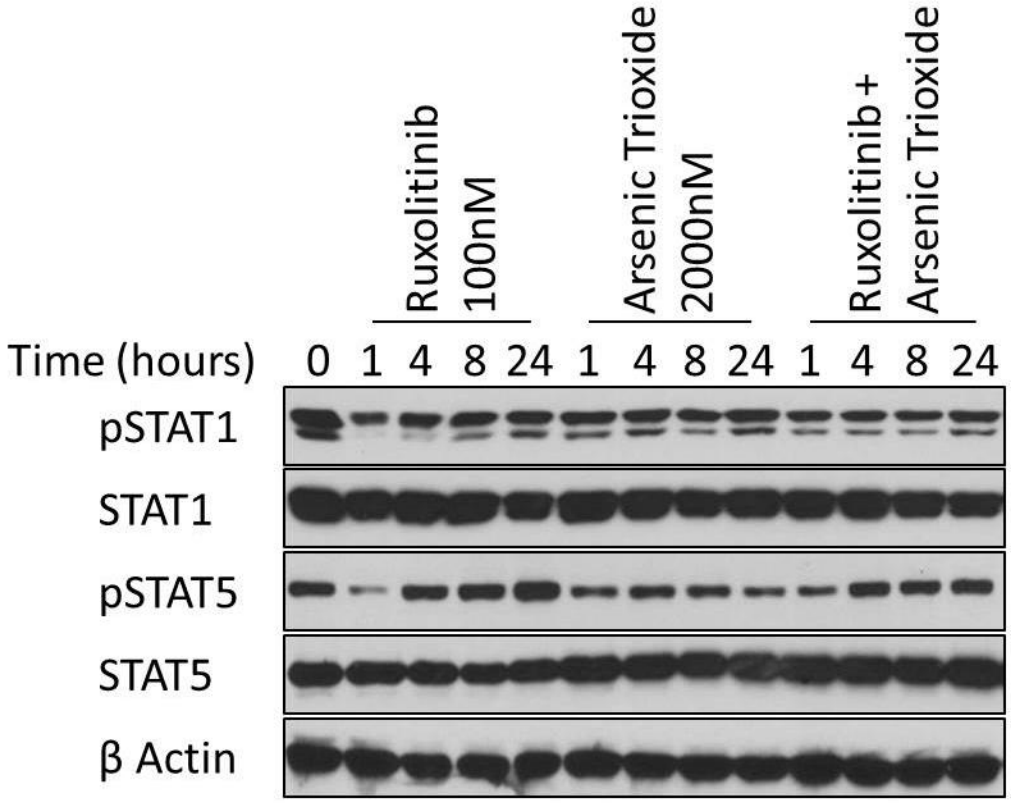


**Protein samples were obtained from SET2 cells following 24 hours of culture in media alone or supplemented with ruxolitinib and arsenic trioxide alone and in combination. The lysates were then run according to the protocol described previously (2.4.4.2). The nitrocellulose membranes were then probed using antibodies to the proteins indicated above and detected using HRP-conjugated antibodies. Equal protein loading of the samples was ensured by probing for β actin. Two independent experiments were carried out with this image being representative of these.**

### 4.2.12 Ruxolitinib in combination with arsenic trioxide increases apoptosis in both UKE1 and SET2 cells

After seeing the effect of ruxolitinib and arsenic trioxide on JAK2 signalling in SET2 cells, we went on to see if this had an effect on apoptosis and cell cycle. UKE1 cells were treated with the $IC_{50}$ dose of ruxolitinib (750nM) in combination with a clinically achievable dose of arsenic trioxide (2μM)[228]. After 24 hours, there was a significant reduction in live cells treated with ruxolitinib and the combination of ruxolitinib and arsenic trioxide compared to untreated cells (Table 4.4). This alteration was more marked in the combination treatment than either compound alone and also increased with longer treatment, where at 72 hours there was a significant reduction in live cells in the combination arm compared to all other treatment groups (Figure 4.36). There was also a significant increase in late apoptotic cells compared to untreated cells.

**Table 4.4 Apoptosis at 24 and 48 hours in UKE1 cells treated with ruxolitinib and arsenic trioxide**

| 24 hours | Live | +/- | Early | +/- | Late | +/- | Dead | +/- |
|---|---|---|---|---|---|---|---|---|
| NDC | 84.3% | 2.4 | 9.7% | 1.3 | 4.8% | 1.0 | 1.2% | 0.7 |
| Ruxolitinib 750nM | **74.8%** | 4.1 | 13.8% | 1.3 | 9.4% | 2.3 | 2.0% | 0.9 |
| Arsenic Trioxide 2μM | 81.4% | 3.6 | 11.3% | 1.7 | 5.9% | 1.6 | 1.4% | 0.3 |
| Ruxolitinib + Arsenic | **69.0%** | 4.2 | 17.3% | 1.2 | 10.1% | 2.1 | 3.6% | 1.6 |

| 48 hours | Live | +/- | Early | +/- | Late | +/- | Dead | +/- |
|---|---|---|---|---|---|---|---|---|
| NDC | 79.5% | 2.3 | 12.3% | 1.6 | 7.0% | 0.9 | 1.2% | 0.7 |
| Ruxolitinib 750nM | 69.6% | 2.3 | 13.5% | 1.6 | 10.7% | 1.3 | 6.2% | 3.2 |
| Arsenic Trioxide 2μM | 76.9% | 3.3 | 9.6% | 2.0 | 7.3% | 0.9 | 6.2% | 3.9 |
| Ruxolitinib + Arsenic | **55.4%** | 3.9 | 20.1% | 4.4 | 16.2% | 1.5 | 8.3% | 7.1 |

**The tables show the percentage of events analysed by FACS for Annexin V and 7AAD in each of the four quadrants which are the live cell population, those cells undergoing the early and late stages of apoptosis and dead cells. The SEM is in the column to the right of each condition (n=3). Statistical analysis was by two-way ANOVA with Tukeys post-test correction. Significant changes compared to NDC are highlighted in red ($p \leq 0.05$).**

**Figure 4.36 Apoptosis in UKE1 cells treated with ruxolitinib and arsenic trioxide**

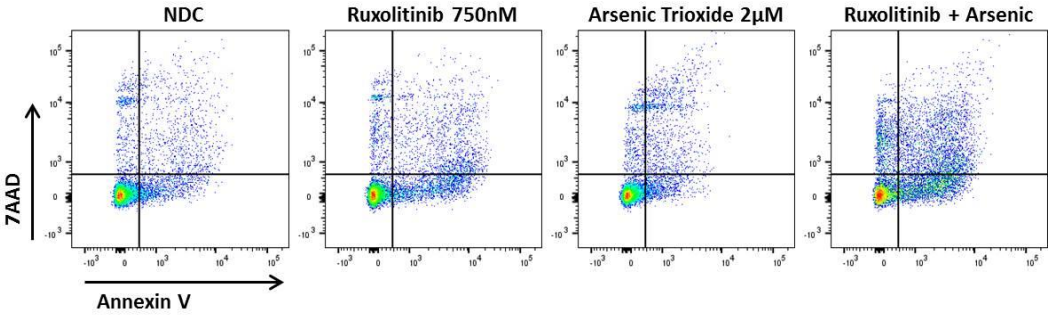


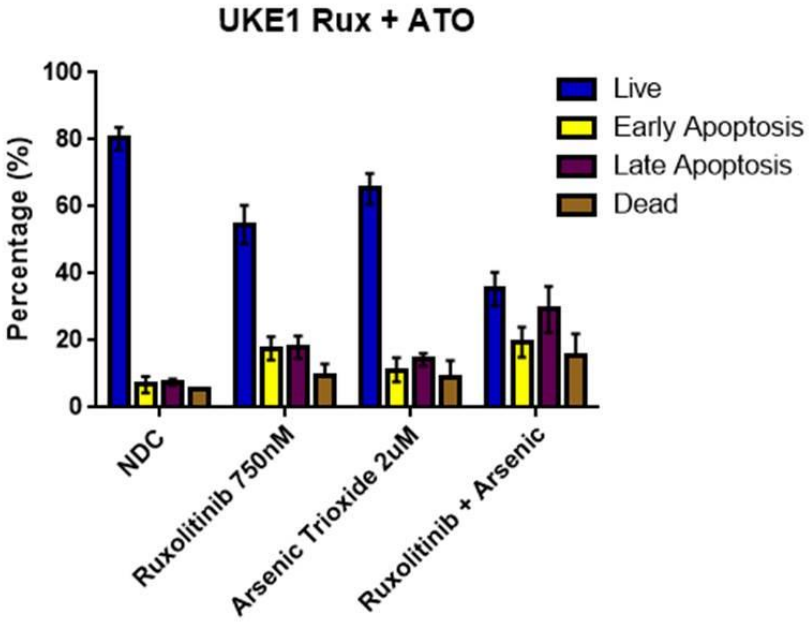


| Live | | | |
|---|---|---|---|
| Rux750 | *** | | |
| ATO | NS | NS | |
| R+A | **** | * | *** |
| | NDC | Rux750 | ATO |

| Early | | | |
|---|---|---|---|
| Rux750 | NS | | |
| ATO | NS | NS | |
| R+A | NS | NS | NS |
| | NDC | Rux750 | ATO |

| Late | | | |
|---|---|---|---|
| Rux750 | NS | | |
| ATO | NS | NS | |
| R+A | ** | NS | NS |
| | NDC | Rux750 | ATO |

| Dead | | | |
|---|---|---|---|
| Rux750 | NS | | |
| ATO | NS | NS | |
| R+A | NS | NS | NS |
| | NDC | Rux750 | ATO |

**The dot plots show representative results from the apoptosis assay by FACS. The bar graphs show the changes in live cells, early and late apoptosis, and dead cells treated with ruxolitinib and arsenic trioxide alone or in combination at 72 hours presented as the mean +/- SEM (n=3). Statistical significance was determined by two-way ANOVA with Tukey's post-test correction for multiple comparisons (* $p \leq 0.05$, ** $p \leq 0.01$, *** $p \leq 0.001$). The tables show the significance of each comparison for each stage of apoptosis.**

Subsequently SET2 cells were also treated with ruxolitinib at the previously identified $IC_{50}$ dose (100nM) in combination with arsenic trioxide (2μM). This led to a significant reduction in live cells with the combination treatment at 24 hours. At 48 hours (Table 4.5), all treatment groups had a significant reduction in live cells and increase in late apoptotic cells compared to the untreated group. At 72 hours, the cells treated with both compounds led to a significant decrease in live cells and increase in late apoptosis compared to all treatment groups. Each treatment group also had a significant reduction in live cells compared to untreated cells (Figure 4.37).

**Table 4.5 Apoptosis at 24 and 48 hours in SET2 cells treated with ruxolitinib and arsenic trioxide**

| 24 hours | Live | +/- | Early | +/- | Late | +/- | Dead | +/- |
|---|---|---|---|---|---|---|---|---|
| **NDC** | 77.2% | 1.4 | 12.1% | 3.0 | 10.1% | 2.5 | 0.6% | 0.2 |
| **Ruxolitinib 100nM** | 75.1% | 2.1 | 12.1% | 0.9 | 11.6% | 2.8 | 1.2% | 0.5 |
| **Arsenic Trioxide 2μM** | 73.3% | 3.6 | 12.9% | 0.2 | 12.3% | 3.2 | 1.5% | 0.3 |
| **Ruxolitinib + Arsenic** | **57.3%** | 2.7 | 25.4% | 1.6 | 15.8% | 3.7 | 1.6% | 0.5 |

| 48 hours | Live | +/- | Early | +/- | Late | +/- | Dead | +/- |
|---|---|---|---|---|---|---|---|---|
| **NDC** | 79.6% | 1.4 | 9.7% | 1.7 | 9.6% | 0.7 | 1.0% | 0.2 |
| **Ruxolitinib 100nM** | **64.3%** | 2.4 | 13.7% | 2.0 | **19.8%** | 0.8 | 2.3% | 0.5 |
| **Arsenic Trioxide 2μM** | **65.1%** | 0.9 | 14.0% | 0.8 | **18.5%** | 1.2 | 2.5% | 0.3 |
| **Ruxolitinib + Arsenic** | **35.6%** | 2.4 | **22.8%** | 2.5 | **37.2%** | 0.7 | 4.4% | 0.8 |

**The tables show the percentage of events analysed by FACS for Annexin V and 7AAD in each of the four quadrants which are the live cell population, those cells undergoing the early and late stages of apoptosis and dead cells. The SEM is in the column to the right of each condition (n=3). Statistical analysis was by two-way ANOVA with Tukeys post-test correction. Significant changes compared to NDC are highlighted in red ($p \leq 0.05$).**

**Figure 4.37 Apoptosis in SET2 cells treated with ruxolitinib and arsenic trioxide**

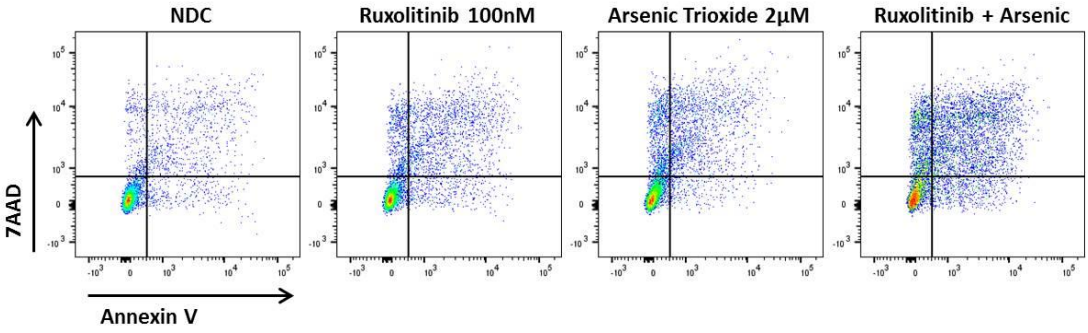


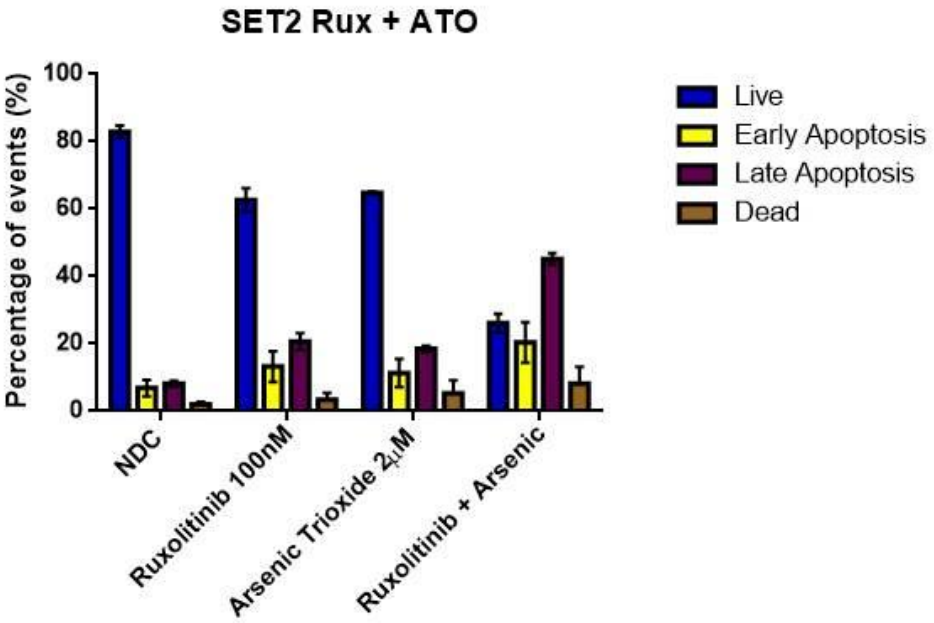


| Live | | | |
|---|---|---|---|
| Rux | *** | | |
| ATO | ** | NS | |
| R+A | **** | **** | **** |
| | NDC | Rux | ATO |

| Early | | | |
|---|---|---|---|
| Rux | NS | | |
| ATO | NS | NS | |
| R+A | * | NS | NS |
| | NDC | Rux | ATO |

| Late | | | |
|---|---|---|---|
| Rux | * | | |
| ATO | NS | NS | |
| R+A | **** | **** | **** |
| | NDC | Rux | ATO |

| Dead | | | |
|---|---|---|---|
| Rux | NS | | |
| ATO | NS | NS | |
| R+A | NS | NS | NS |
| | NDC | Rux | ATO |

**The dot plots show representative results from the apoptosis assay by FACS. The bar graphs show the changes in live cells, early and late apoptosis, and dead cells treated with ruxolitinib and arsenic trioxide alone or in combination at 72 hours presented as the mean +/- SEM (n=3). Statistical significance was determined by two-way ANOVA with Tukey's post-test correction for multiple comparisons (* $p \leq 0.05$, ** $p \leq 0.01$, *** $p \leq 0.001$). The tables show the significance of each comparison for each stage of apoptosis.**

This shows that the combination of JAK2 inhibition and disruption of PML leads to a significant increase in apoptosis and reduced cell survival compared to either compound used alone. This interaction has not been previously investigated and the combination of two compounds currently in clinical use raises the possibility of investigating this further as a therapeutic modality in JAK2 V617F positive disease.

### 4.2.13 The effect on cell cycle of ruxolitinib and arsenic trioxide in combination

UKE1 and SET2 cells were treated with ruxolitinib and arsenic trioxide alone and in combination for 72 hours before being prepared for assessment of cell cycle as previously described. In UKE1 cells, there was no significant alteration in cell cycle in each of the treatment groups (Figure 4.38). Interestingly, in SET2 cells treated with ruxolitinib there was a G0-G1 arrest while the arsenic trioxide treated cells had an S-G2-M arrest. When both compounds were used together the two treatments appeared to cancel each other out and resulted in no significant alteration in cell cycle in the combination treated cells compared to untreated cells, but a significant alteration when compared to the cells treated with each compound alone (Figure 4.39).

**Figure 4.38 Apoptosis in UKE1 cells treated with ruxolitinib and arsenic trioxide**

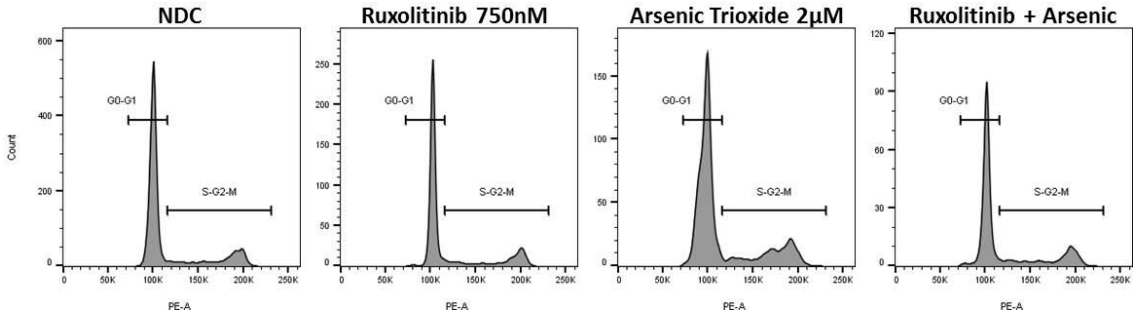


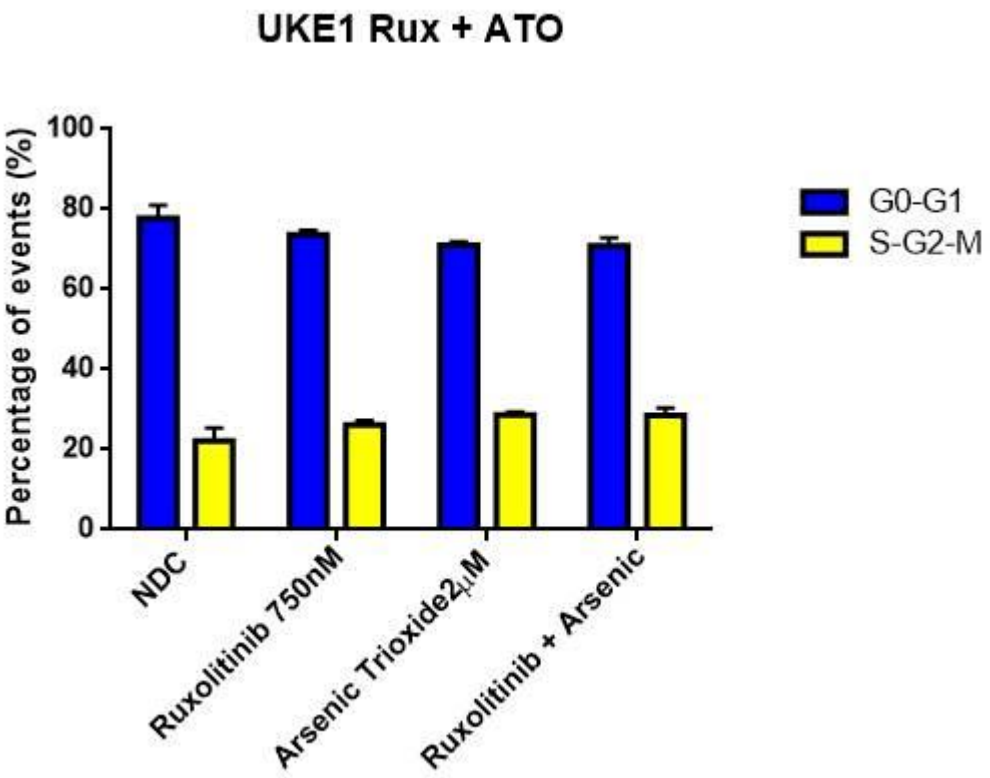


| G0-G1 | | | |
|---|---|---|---|
| Rux750 | NS | | |
| ATO | NS | NS | |
| R+A | NS | NS | NS |
| | NDC | Rux750 | ATO |

| S-G2-M | | | |
|---|---|---|---|
| Rux750 | NS | | |
| ATO | NS | NS | |
| R+A | NS | NS | NS |
| | NDC | Rux750 | ATO |

**The histogram plots show representative results from FACS and show the gating strategy used. The bar graphs show the changes in cell cycle following treatment with ruxolitinib for 72 hours, highlighting those actively undergoing cell cycle (S-G2-M) and those that are quiescent (G0-G1). They are presented as the mean +/- SEM (n=3). Statistical significance was determined by two-way ANOVA with Tukey's post-test correction for multiple comparisons (* p ≤ 0.05, ** p ≤ 0.01, *** p ≤ 0.001, **** p ≤ 0.0001)..**

**Figure 4.39 Apoptosis in SET2 cells treated with ruxolitinib and arsenic trioxide**

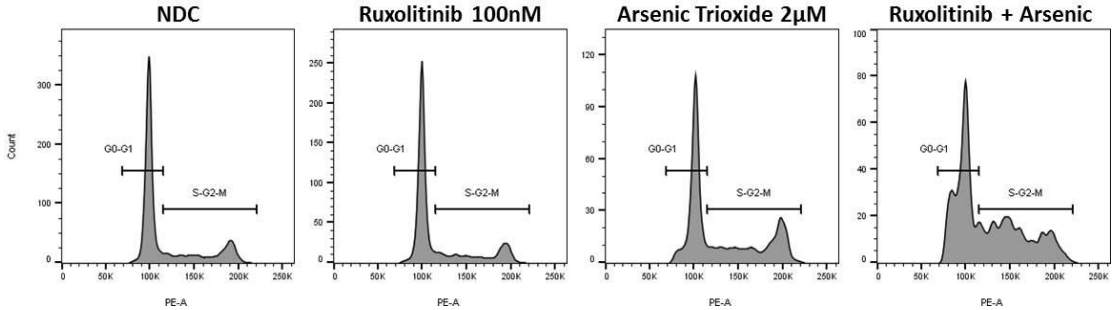


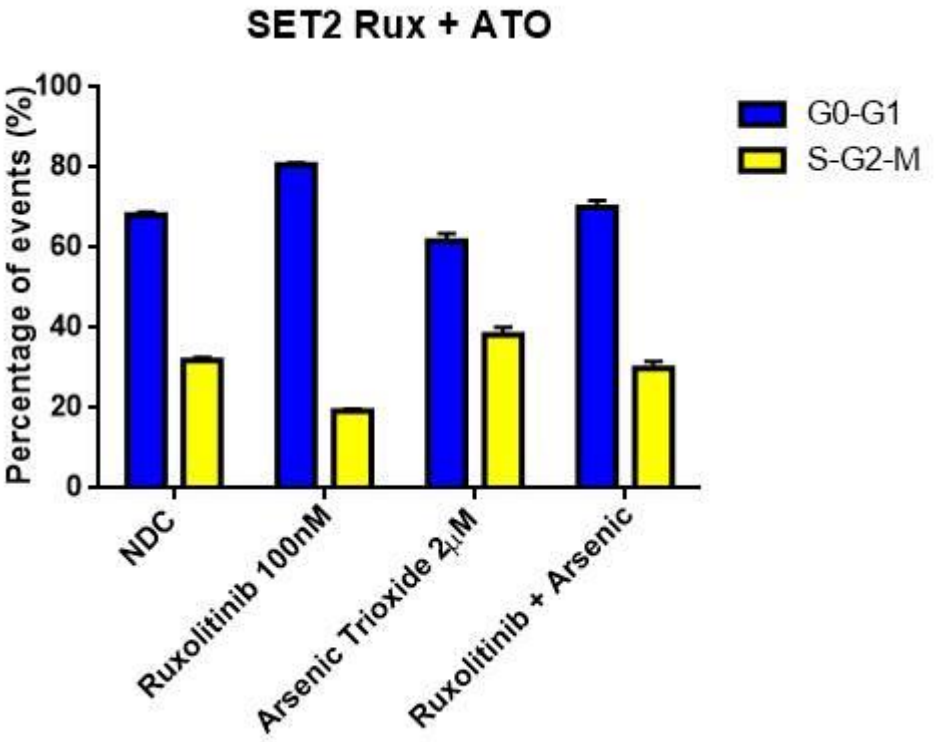


| G0-G1 | | | |
|---|---|---|---|
| Rux | **** | | |
| ATO | * | **** | |
| R+A | NS | *** | ** |
| | NDC | Rux | ATO |

| S-G2-M | | | |
|---|---|---|---|
| Rux | **** | | |
| ATO | * | **** | |
| R+A | NS | *** | ** |
| | NDC | Rux | ATO |

**The histogram plots show representative results from FACS and show the gating strategy used. The bar graphs show the changes in cell cycle following treatment with ruxolitinib for 72 hours, highlighting those actively undergoing cell cycle (S-G2-M) and those that are quiescent (G0-G1). They are presented as the mean +/- SEM (n=3). Statistical significance was determined by two-way ANOVA with Tukey's post-test correction for multiple comparisons (* $p \leq 0.05$, ** $p \leq 0.01$, *** $p \leq 0.001$, **** $p \leq 0.0001$).**

### 4.2.14 Apoptosis in PV and normal PB MNCs following treatment with ruxolitinib and arsenic trioxide

Based on the findings in cell lines we looked at the effect of ruxolitinib and arsenic trioxide treatment in PV and normal MNCs. Given that these cells are terminally differentiated, cell cycle was not assessed. At 72 hours treatment, there was marked variation between both normal and PV samples, but there was a non-significant reduction in live cells in all the PV treatment groups compared to normal. However the only significant alteration within one group was the reduction in live cells in the PV samples treated with ruxolitinib compared to those treated with ruxolitinib and arsenic trioxide together (Figure 4.40).

**Figure 4.40 Apoptosis in PV PB MNCs treated with ruxolitinib and arsenic trioxide**

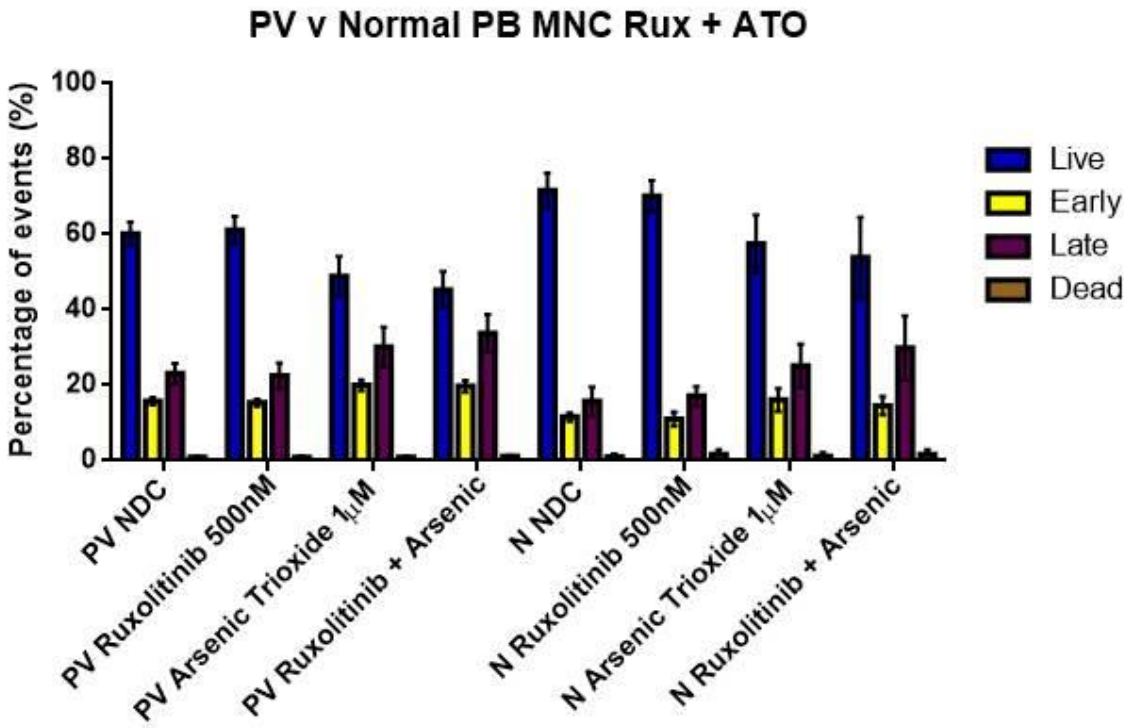

| Live | | | | | | | |
|---|---|---|---|---|---|---|---|
| N Rux | NS | | | | | | |
| N ATO | NS | NS | | | | | |
| N R+A | NS | NS | NS | | | | |
| PV NDC | NS | NS | NS | NS | | | |
| PV Rux | NS | NS | NS | NS | NS | | |
| PV ATO | ** | ** | NS | NS | NS | NS | |
| PV R+A | *** | *** | NS | NS | NS | * | NS |
| | N NDC | N Rux | N ATO | N R+A | PV NDC | PV Rux | PV ATO |

| Early | | | | | | | |
|---|---|---|---|---|---|---|---|
| N Rux | NS | | | | | | |
| N ATO | NS | NS | | | | | |
| N R+A | NS | NS | NS | | | | |
| PV NDC | NS | NS | NS | NS | | | |
| PV Rux | NS | NS | NS | NS | NS | | |
| PV ATO | NS | NS | NS | NS | NS | NS | |
| PV R+A | NS | NS | NS | NS | NS | NS | NS |
| | N NDC | N Rux | N ATO | N R+A | PV NDC | PV Rux | PV ATO |

| Late | | | | | | | |
|---|---|---|---|---|---|---|---|
| N Rux | NS | | | | | | |
| N ATO | NS | NS | | | | | |
| N R+A | NS | NS | NS | | | | |
| PV NDC | NS | NS | NS | NS | | | |
| PV Rux | NS | NS | NS | NS | NS | | |
| PV ATO | NS | NS | NS | NS | NS | NS | |
| PV R+A | * | NS | NS | NS | NS | NS | NS |
| | N NDC | N Rux | N ATO | N R+A | PV NDC | PV Rux | PV ATO |

| Dead | | | | | | | |
|---|---|---|---|---|---|---|---|
| N Rux | NS | | | | | | |
| N ATO | NS | NS | | | | | |
| N R+A | NS | NS | NS | | | | |
| PV NDC | NS | NS | NS | NS | | | |
| PV Rux | NS | NS | NS | NS | NS | | |
| PV ATO | NS | NS | NS | NS | NS | NS | |
| PV R+A | NS | NS | NS | NS | NS | NS | NS |
| | N NDC | N Rux | N ATO | N R+A | PV NDC | PV Rux | PV ATO |

**The bar graphs show the changes in live cells, early and late apoptosis, and dead cells treated with ruxolitinib and arsenic trioxide alone or in combination at 72 hours presented as the mean +/- SEM (n=3). Statistical significance was determined by two-way ANOVA with Tukey's post-test correction for multiple comparisons (* $p \leq 0.05$, ** $p \leq 0.01$, *** $p \leq 0.001$). The tables show the significance of each comparison for each stage of apoptosis following 72 hours of treatment.**

## 4.3 Discussion

### 4.3.1 Proliferation and cell cycle in PV

In JAK2 V617F positive disease there is a proliferation advantage in maturing cells leading to expansion of the clone[151]. This advantage drives the clinical phenotype of elevated peripheral counts, with the JAK2 V617F being found in the myeloid cells. In normal circumstances the activation of JAK2 leads to a controlled signalling cascade that transiently increases the proliferation of cells via the Akt/PI3K and Ras/MEK/ERK pathways as well as the actions of STATs[178]. However with the constitutive action conferred by the V617F mutation, there is ligand independent activity of these pathways which is not controlled by the inhibitory actions of negative regulators[178]. Of interest is the finding that similar pathways are altered by the JAK2 V617F mutation and BCR-ABL, but the clinical pictures are different in MPN compared to CML. This may be due to the fact that BCR-ABL is an abnormal protein which does not have appropriate negative regulation, while JAK2 V617F is an alteration of a normal protein which is still subject, to some degree, to normal homeostatic measures to control cytokine signalling.

### 4.3.2 Apoptosis in PV

In MPN patients, JAK2 inhibitors are able to improve symptoms, but in the majority of patients there is some improvement in disease burden, but there is not complete eradication of disease[133], suggesting that in patients there is no real effect on apoptosis of the diseased cells. The reason for this is not entirely clear, but is may relate to the limitations of dose escalation as a result of JAK2 inhibitors affecting both normal and mutant JAK2 proteins, although there is more of an effect on the mutated protein[194]. As a result of this, there has been an interest in combining JAK2 inhibitors with other pharmacological agents targeting different pathways to induce apoptosis of abnormal cells in MPN. Our data shows it is clear that combining JAK2 inhibition with disruption of PML leads to a significant increase in apoptosis of JAK2 V617F containing cell lines, although this does not translate to a significant alteration in PB MNCs of patients with PV when compared to normal. However there did appear to be a trend towards an increase in apoptosis in terminally differentiated cells here and it would be interesting to see how this combination affected more primitive cells containing the JAK2 V617F mutation.

### 4.3.3 Inflammation and cytokine driven interferon response in PV

Inflammation in PV has been an area of interest in recent years with increasing evidence of abnormal cytokine production leading to chronic inflammation[150,4]. A key driver of chronic inflammation, TNF-α, is elevated in PV, ET and MF, and the serum level has been shown to correlate with the JAK2 V617F allele burden[151]. Interestingly colony formation in the presence of TNF-α is reduced in normal controls, but JAK2 V617F positive cells are resistant to the suppressive effects of TNF-α. In addition to this knocking out TNF-α in a JAK2 V617F positive murine model led to attenuation of the MPN disease phenotype suggesting that the MPN progenitors gain a survival advantage by the presence of chronic inflammation[151].

Inflammation has also been linked to thrombotic complications in MPN, which is a major cause of morbidity and mortality in this patient group[229155,230]. A retrospective analysis of serum markers of inflammation, high sensitivity CRP (hs CRP) and pentraxin 3, showed a strong correlation between patients with the highest hs CRP and cardiovascular events, a PV phenotype and JAK2 V617F allele burden greater than 50%[230]. Pentraxin 3 was less able to differentiate between these feature in PV and ET patients, but lower levels were associated with an increased rate of thrombosis. Chronic inflammatory conditions are known to cause alterations in endothelial cell function and increase the risk of atherosclerotic disease in non-haematological conditions such as rheumatoid arthritis[153], and in recent years it has become increasingly clear that cardiovascular disease is an inflammatory condition in itself[231] with much of the protective effects of statins coming from an anti-inflammatory effect on the endothelium[232]. This would indicate that other conditions associated with chronic inflammation will be associated with an increase in the risk of thrombotic disease.In this study there is gene expression data indicating a significant alteration of many important regulators of inflammation. Consistent changes were seen in the expression of *IRF6*, *IRF7* and *PML*, but many varied across the patient samples assessed. The genes with wide variation between patients may correlate with risk of thrombosis and disease progression, but would need to be assessed in a much larger patient cohort.

### 4.3.4 The role of PML in cell cycle and apoptosis in PV

Promyelocytic leukaemia protein is a key component in PML NBs within the nucleus, in addition to Sp100 and SUMO proteins[207]. The NBs are found at transcriptionally active sites in the genome[233] and appear to act as a hub for signalling proteins entering the nucleus to interact with each other[158]. The proteins that localise to the PML NBs are SUMOylated and attach to SUMO-interacting-motifs (SIMs) within the nuclear body[234]. Several apoptotic pathways rely on the function of PML NBs to potentiate their signals including p53 dependent apoptosis[162] and FAS ligand signalling[235]. In addition to this, it links IFN-α signalling with the tumour-necrosis factor superfamily, member 10 (TNFSF10) pathway[236], resulting in a multi-faceted control of apoptosis. PML knockout mice have been shown to develop normally, but are resistant to the apoptotic effects of TNF-α and have an increased incidence of development of carcinomas and lymphomas following exposure to tumour-promoting agents[237].

In addition to the role PML plays in apoptosis, there is also a clear role for PML in cell cycle regulation. The expression of PML alters through the cell cycle with entry into the cell cycle disrupting the normal NB structure[238]. This is in keeping with the evidence that PML is important in activating p53-mediated cell senescence and permanent exit from the cell cycle[239]. This is achieved by recruiting E2F transcription factors into the PML NB and blocking their proliferative role. This action was dependent on also recruiting retinoblastoma proteins to the NBs[239].

In this study there was a reduction in the expression of PML at the messenger RNA level, however there appeared to be an increase in the interaction of JAK2 with PML in JAK2 V617F mutation positive PV monocytes compared to normal. There is also an alteration in the JAK2 and PML interaction with manipulation of JAK2 in JAK2 V617F positive cell lines, with an increase in association following treatment with IFN-γ, which was mirrored by an increase in the association of JAK2 and SUMO 2/3, and following treatment with ruxolitinib, which was not seen in cells assessed for JAK2 and SUMO 2/3 interaction. Interestingly, there was a reduction in the association of JAK2 and SUMO 2/3 following treatment with TG101209. It would be interesting to further assess this in patient samples and investigate if this has a positive of negative effect on apoptosis and cell signalling.

# 5 Delineating the potential mechanisms underlying chronic inflammation in polycythaemia vera

## 5.1 Introduction

In response to trauma or infection the body has an effective response designed to remove and repair damaged or infected tissue. A major component of this is inflammation which in normal circumstances will trigger and effect the required response needed and contain it within the affected area[240]. However many conditions are associated with an abnormal inflammatory response either locally or systemically including cancer[241], rheumatological disease[153] and atherosclerotic disease[231]. The MPNs have previously been shown to be associated with elevated levels of inflammatory cytokines and inflammatory markers, which is worst in advanced disease[150]. This leads to a significant symptomatic burden which is poorly managed in clinic at present. The introduction of JAK2 inhibitors to clinical practice has changed this for some patients, with significant improvements in symptom scores for patients with PV and MF on ruxolitinib[132,133].

The role of inflammatory cytokines in maintaining MPN is a topic of interest with evidence that PV HSCs behave differently in response to inflammatory signalling. When exposed to TNF-α, which is increased in MPN, normal HSCs will not proliferate, while PV HSCs are resistant to TNF-$\alpha$ inhibitory effect[151]. Additionally PV cells in the BM alter the behaviour of the normal BM stoma cells to produce cytokines to further enhance their survival[151]. This alteration leads to chronic inflammation in the BM, which in turn can drive an increase in fibrous tissue deposition and transformation to MF[242]. This increase in inflammation is also thought to contribute to the increased risk of leukaemic transformation, with cells tending to be JAK2 V617F mutation negative on transformation[136], suggesting that it arises from cells independent of the MPN clone, that have been exposed to the chronic inflammatory milieu of the BM.

The molecular aspects of the deregulation of inflammation in MPN are of interest as it represents a complex interaction of different pathways and processes, which have been altered to support the abnormal clone. The recent discovery that JAK2 enters the nucleus to directly affect epigenetic regulators of myeloid cell growth[80]

opens a new area to investigate the alterations JAK2 V617F makes to cells. With respect to the inflammatory response in PV it is known there is an increase in the level of IFN-γ in patients with PV and ET[150]. IFN-γ has a well-recognised effect on mobilising HSCs out of quiescence and promoting myelopoiesis[243]. In addition IFN-γ can affect the activity of PML NBs where multiple signals for cell growth, apoptosis and DNA repair converge. The normal mechanism for the increase in PML expression following exposure to IFN-γ is through JAK1/JAK2/STAT1 signalling leading to an increase in the activity of interferon response elements which act on the expression of PML[158,163].

This study looked at the role mature myeloid cells, in particular monocytes, play in the inflammatory phenotype seen in PV. Serum samples were processed from normal aged matched donors and PV patients and analysed to determine whether PV patients showed any alterations in serum cytokines associated with inflammation. In addition, the monocyte subsets were measured in normal age matched donors and PV patients to ascertain whether these were altered in PV. Following separation, monocytes were differentiated towards M1 and M2 macrophage phenotypes and cultured in the presence of 20% serum taken either from normal controls or PV patients to see what effect the serum had on these mature cells and if it differs depending on cell source. We also assessed these differentiated macrophages for their level of PML and JAK2

## 5.2 Results

### 5.2.1 Alteration of monocyte subsets in the peripheral blood of JAK2 V617F positive PV patients

Monocytes are a group of cells in the peripheral blood which are identified morphologically as large cells with abundant grey-blue cytoplasm, fine cytoplasmic granulation and large irregularly contoured nuclei. Functionally there are 3 distinct groups of monocytes; classical monocytes, which make up 85-90% of monocytes, non-classical monocytes which make up 5% of monocytes, and intermediate monocytes which comprise the remaining 5%[34,244]. Classical monocytes are typically phagocytic and produce some inflammatory cytokines including G-CSF, CCL2, CCL5 and IL-6[245]. Non-classical monocytes are anti-inflammatory with constitutive production of IL1-RA, while the intermediate monocytes are pro-inflammatory producing TNFα in response to stimulation[245]. Interest in the

intermediate monocytes has increased recently due to the finding that higher levels of these in the peripheral blood is associated with an increased risk of cardiovascular disease[37]. Peripheral blood monocytes can be placed in subsets based on the surface expression of CD14 and CD16[34]. Samples taken from patients with PV and normal controls were analysed for expression of CD14 and CD16, with classical monocytes being $CD14^{Hi}$, $CD16^{Low}$, intermediate monocytes $CD14^{Hi}$, $CD16^{Hi}$ and non-classical monocytes $CD14^{Low}$, $CD16^{Hi}$.

**Figure 5.1 Monocyte subsets in PV**

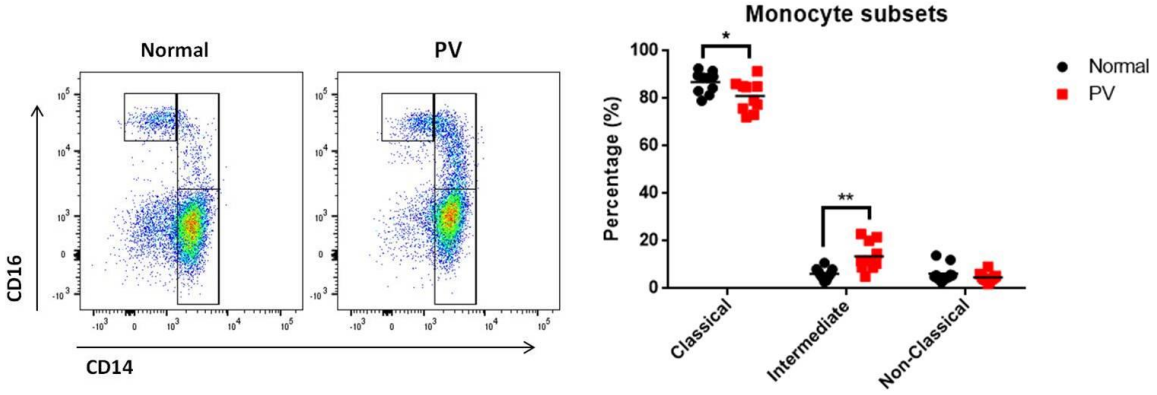


**Mononuclear cells were obtained from peripheral blood of PV patients (n=10) and normal controls (n=8) following Ficol gradient separation. $1x10^6$ cells were incubated with fluorescent labelled CD14 and CD16 antibodies before analysing monocytes. Gates were placed based on relative expression of these proteins to identify classical, non-classical and intermediate monocytes. Each result has the mean indicated by a line. Results were compared using the Students *t*-test (* p≤0.05, ** p≤0.01).**

The majority of monocytes are of the classical subset with about 10% comprising non-classical and intermediate monocytes. Ten normal samples and 11 PV samples were assessed using flow cytometry and showed that PV samples had an increase in the pro-inflammatory intermediate subset with a reduction in classical monocytes. Non-classical monocytes were not significantly different between the two groups. Interestingly, higher than normal intermediate monocyte numbers have recently been identified as a positive predictor of cardiovascular events, where they play a significant role in vascular inflammation through secretion of TNFα and IL-1β[37]. Intermediate monocytes also express CCR2 and CCR5, which are critical for monocyte homing and trans-endothelial migration into atherosclerotic plaques[244]. Platelet activation and blood coagulation are also

initiated at the site of injury by monocyte/macrophage secreted exosomes and microvesicles which contain tissue factor and P-selectin glycoprotein ligand-1 on their surface[246]. It is therefore not unreasonable to postulate that the increased risk of cardiovascular complications observed in PV patients could, in part, be linked to these elevated intermediate monocyte levels.

### 5.2.2 Co-localisation of JAK2 with PML and SUMO 2/3 is increased by the presence of the JAK2 V617F mutation in peripheral blood monocytes

Based on the alteration of JAK2 co-localising with PML and SUMO 2/3 in cell lines following JAK2 manipulation, we looked at the effect of the JAK2 V617F mutation in peripheral blood monocytes using the Duolink® immunofluorescent co-localisation assay. Peripheral blood monocytes were suspended in Promocell monocyte adhesion media before incubating them on microscope slides. The non-adherent cells were washed off and the remaining attached monocytes were processed as before. By using ImageJ analysis of corrected total cell fluorescence we showed there was an increase in the degree of localisation of JAK2 with both PML and SUMO 2/3 in monocytes derived from PV patients compared to normal controls (Figure 5.2).

**Figure 5.2 Duolink co-localisation assay in normal and PV monocytes**

**a) Duolink co-localisation images**

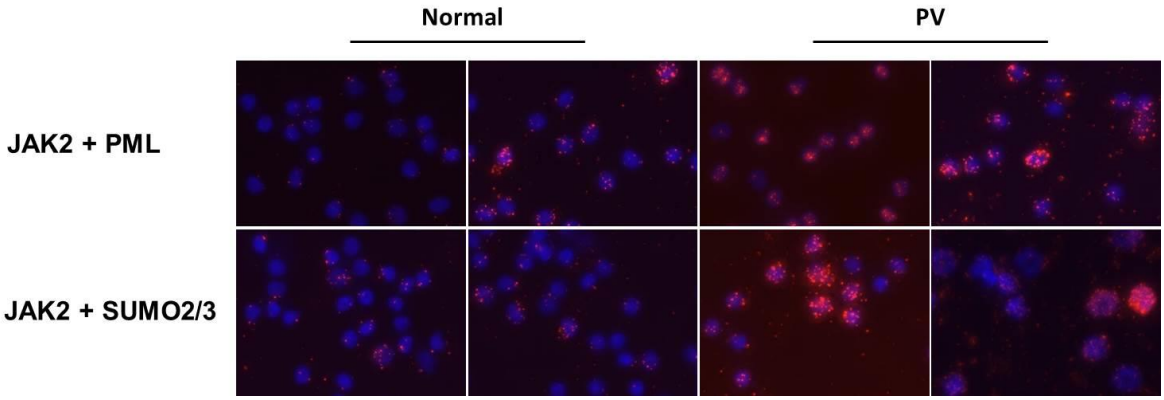


**a) Corrected total cell fluorescence graphs**

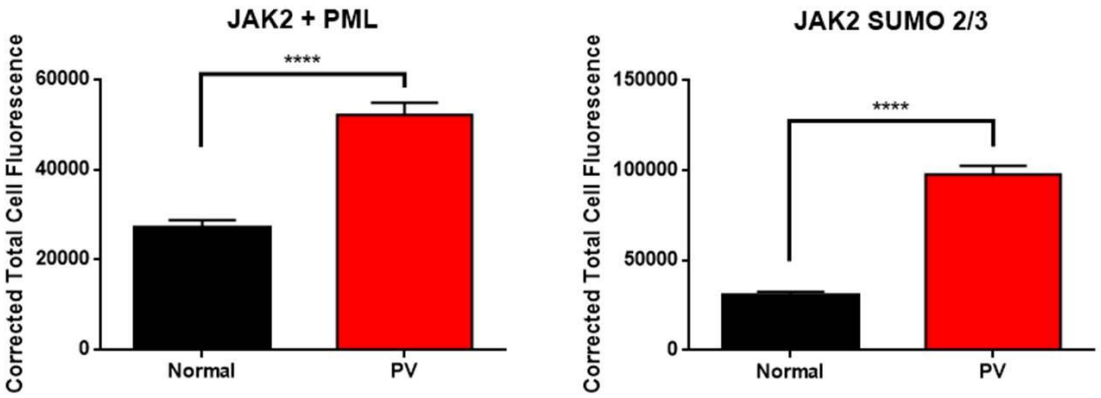


**Peripheral blood mononuclear cells were incubated in monocyte attachment media on microscope slides. After the non-adherent cells were washed off those remaining were prepared for Duolink immunofluorescent co-localisation assay as described previously. At least 90 cells were counted for each sample with 4 normal samples and 5 PV samples being assessed. The corrected total cell fluorescence was calculated and statistical significance was assessed using Students *t*-test and annotated as * p≤0.05, ** p≤0.01, *** p≤0.001, **** p≤0.0001. The images (3a) are representative of the experiments while the graphs (3b) show the average of the corrected total cell fluorescence for all samples +/- SEM.**

### 5.2.3 Alteration of serum cytokine profiles in PV

Some studies have previously been carried out looking at cytokine profiles in MPN. A study by Pourcelot *et al* looked at plasma cytokines in ET and PV, comparing levels between disease phenotypes and between JAK2 V617F positive and negative states, with comparisons also being made to previously reported normal ranges rather than to normal samples tested at the same time. This study looked at 13 cytokines and growth factors and found that both PV and ET had elevated concentrations of all cytokines when compared to normal physiological ranges. Additionally there was an increased concentration of 8 factors including IL-4, IL-8, IFN-γ and VEGF in ET compared to PV[150].

Serum was collected from 10 PV patients and 8 normal controls to assess the concentration of 29 inflammation-associated cytokines and chemokines using a multiplex array and analysed using Luminex technology. Many of those tested were pro-inflammatory cytokines or associated with proliferation and maintenance of cells of the immune system, but some were anti-inflammatory (IL-1 RA, IL-10) or immunomodulatory (IL-7, IL-2). Of the 29 cytokines and chemokines tested, 19 were significantly increased in PV samples compared to normal, 5 were not significantly changed and 5 had too many results below the limit of detection for significance to be assessed. Those that were significantly altered included predominantly the pro-inflammatory cytokines and growth factors (IFNγ, G-CSF Figure 5.3 and Figure 5.4), but 3 of the 4 anti-inflammatory (IL-1 RA, IL-4, IL-10 and 1 of the 2 immunomodulatory cytokines (IL-7) (Figure 5.5) were also increased in PV compared to normal. This shows that there is a complex and wide ranging alteration of inflammatory and immune responses in these patients potentially impacting on a wide range of cellular processes and interactions.

IFN-γ and TNF-α are both well recognised pro-inflammatory cytokines which play an important role in both the local and systemic response to microbial pathogens, and are significantly elevated in PV patients compared to normal (Figure 5.3). IFN-γ tends to cause a more global anti-viral response through up-regulation of inflammatory macrophages systemically, leading to increased levels of both IFN-γ and TNF-α. TNF–α drives pyrexia and, when extremely high levels are present, can cause shock and death[247]. HSCs from PV patients have been shown to be resistant to the apoptotic effects of TNF-α through a combination of reduced proliferation and inducing quiescence in normal HSCs, giving a survival advantage to the abnormal clone[151].

**Figure 5.3 Pro-inflammatory cytokines in PV**

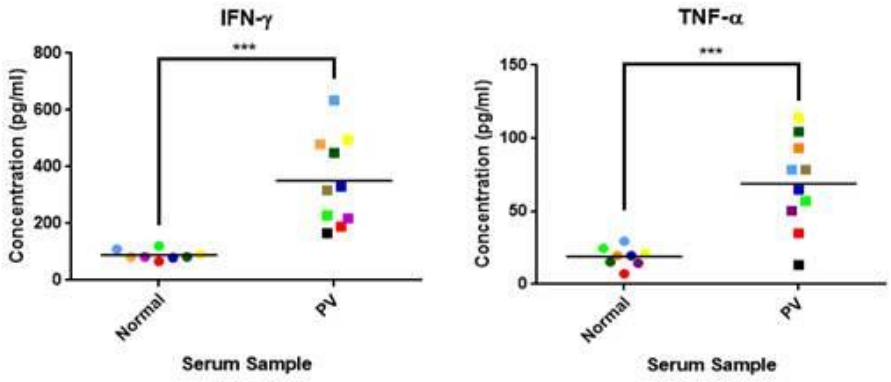


**Serum cytokines were measured by Luminex technology on samples taken from 8 normal and 10 PV patients. Each result has the mean indicated by a line. Statistical significance was determined using unpaired *t*-test with Welch's correction for unequal standard deviation (* p≤0.05, ** p≤0.01, *** p≤0.001, **** p≤0.0001).**

The role of G-CSF in haematopoiesis as a regulator of granulocyte differentiation is well described. The G-CSF receptor exists on myeloid precursors, and stimulation leads to proliferation of these cells and differentiation to mature neutrophils. In PV, the JAK2 V617F mutation results in activation of the G-CSF receptor, rendering the need for activation unnecessary, however there is still an increase in the circulating levels of this cytokine which will augment the increase in signalling (Figure 5.4). VEGF has previously been shown to be elevated in PV, which is confirmed by our data (Figure 5.4), and is thought to contribute to angiogenesis[248].

**Figure 5.4 Growth factors in PV**

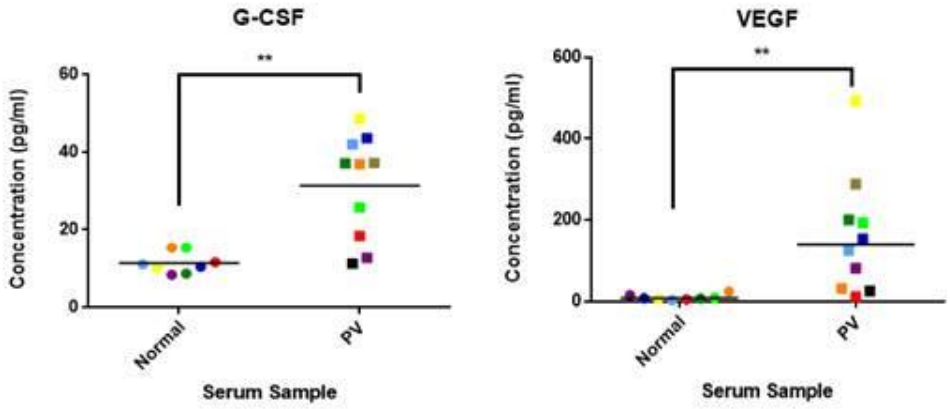


**Serum cytokines were measured by Luminex technology on samples taken from 8 normal and 10 PV patients. Each result has the mean indicated by a line. Statistical significance was determined using unpaired *t*-test with Welch's correction for unequal standard deviation (* p≤0.05, ** p≤0.01, *** p≤0.001, **** p≤0.0001).**

The pro-inflammatory chemokines are important in attracting and activating different cells of the immune system to areas of inflammation. CCL3 and CCL4 are important attractant and activating signals for macrophages, monocytes and NK cells, with CCL3 being produced by monocytes and CCL4 by CD8 positive T cells. CXCL10 is produced by monocytes and endothelial cells in response to stimulation by IFN-γ and is therefore directly related to the increased levels of IFN-γ seen in PV (Figure 5.4).

**Figure 5.5 Chemokines in PV**

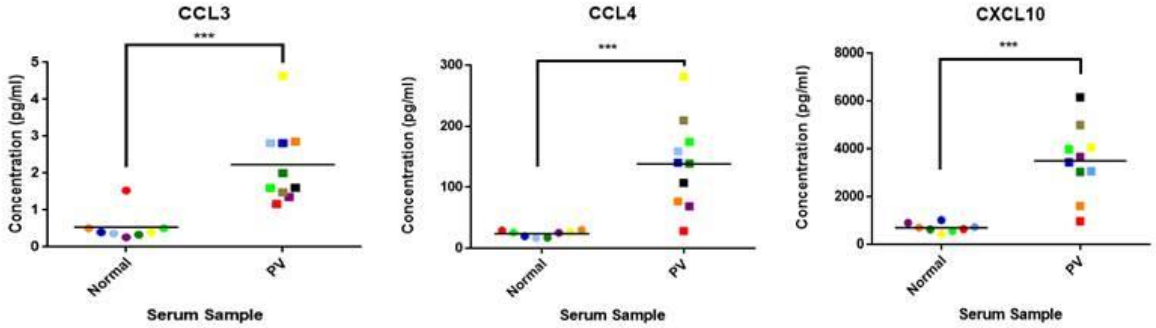


**Serum cytokines were measured by Luminex technology on samples taken from 8 normal and 10 PV patients. Each result has the mean indicated by a line. Statistical significance was determined using unpaired *t*-test with Welch's correction for unequal standard deviation (* p≤0.05, ** p≤0.01, *** p≤0.001, **** p≤0.0001).**

IL-6 has been shown to be significantly increased in PV in many studies however in this case the difference was found to be non-significant, but the number of samples in which a detectable level was present in the normal controls is small making comparison difficult. Of interest is that there are more detectable levels in the PV samples than in the normal samples which would suggest that the known increase is present and would become apparent either using more sensitive testing or by increasing the number of samples tested.

**Table 5.1 Serum cytokines from normal and PV patients**

| Cytokine | Normal median (pg/ml) | St dev | PV median (pg/ml) | St dev | p value |
|---|---|---|---|---|---|
| **Pro-inflammatory cytokines** | | | | | |
| **IL1-β** | **0.9** | 0.4 | **5.1** | 3.6 | **0.0072** |
| **IL-5** | **28.2** | 4.5 | **127.2** | 33.3 | **<0.0001** |
| IL-6 | 0.6 | 0.3 | 3.5 | 4.9 | 0.0648 |
| **IL-8** | **1.9** | 0.7 | **11.7** | 9.2 | **<0.0001** |
| **IL-9** | **26.1** | 6.7 | **74.7** | 29.1 | **0.0004** |
| **IL12 (p70)** | **4.4** | 2.9 | **74.9** | 85.9 | **0.0049** |
| **IL-17** | **32.2** | 9.5 | **99.6** | 53.7 | **0.0028** |
| **CCL11** | **80.7** | 51.9 | **310.8** | 155.1 | **0.0021** |
| **G-CSF** | **10.7** | 2.7 | **37.0** | 13.4 | **0.001** |
| **IFNγ** | **82.6** | 17.6 | **323.9** | 157.1 | **0.0005** |
| **CXCL10** | **672.4** | 187.0 | **3550.3** | 1501.1 | **0.0002** |
| PDGF-BB | 3697.2 | 1898.1 | 7276.0 | 8520.9 | 0.0587 |
| CCL2 | 0.6 | 0.2 | 1.6 | 7.9 | 0.3241 |
| **CCL3** | **0.4** | 0.4 | **1.8** | 1.1 | **0.0006** |
| **CCL4** | **25.8** | 5.3 | **139.4** | 73.6 | **0.0008** |
| **CCL5** | **3771.0** | 1331.8 | **13047.1** | 4377.6 | **0.0002** |
| **TNF-α** | **19.6** | 6.8 | **71.6** | 31.3 | **0.0006** |
| **VEGF** | **7.1** | 6.8 | **139.1** | 146.5 | **0.0099** |
| **Anti-inflammatory cytokines** | | | | | |
| **IL-1RA** | **16.6** | 9.4 | **52.1** | 73.1 | **0.0049** |
| **IL-4** | **7.2** | 2.0 | **24.4** | 10.1 | **0.0005** |
| **IL-10** | **1.0** | 1.0 | **11.8** | 9.8 | **0.0061** |
| **IL-13** | **0.8** | 7.4 | **12.6** | 7.6 | **0.0631** |
| **Immunomodulatory cytokines** | | | | | |
| IL-2 | 1.12 | 0.6 | 3.34 | 4.3 | 0.965 |
| **IL-7** | **15.29** | 26.8 | **170.7** | 131.5 | **0.0046** |

**Luminex technology was used to analyse 29 cytokines in the serum of 8 normal and 10 PV samples. Of these 29, 5 cytokines (IL-15, FGF-basic, GM-CSF, CXCL1, IFN-α) failed to produce usable results. Significance was determined using an unpaired *t*-test with Welch's correction for unequal standard deviation, and defined as p ≤0.05. Significant results are highlighted in bold.**

Several of the pro-inflammatory cytokines signal through JAK2 alone (IL-6, G-CSF) or in combination with another JAK protein (IFN-γ, IL-5), meaning the presence of the JAK2 mutation will either render the pathway either constitutively active or more reactive/sustained than normal[48]. Given that many of these cytokines are increased above basal levels in PV, this will potentiate these signalling pathways even further leading to a cycle of chronic inflammation. The

anti-inflammatory cytokines may be increased as a homeostatic measure to try and control this abnormal cytokine profile.

### 5.2.4 Assessment of efficacy of macrophage differentiation

Macrophages are involved in a wide range of actions within the body. The main role they play is in pathogen removal and inflammation, where different types of macrophages play differing roles. In addition to this, they play a critical role in red cell development, by providing the environment needed for red cells to obtain iron for haemoglobin and to remove the nucleus, a step required for the final stages of erythropoiesis. In mouse models of PV, where there has been pharmacological ablation of BM macrophages, the PV phenotype does not develop[249]. It also leads to a less severe phenotype in β-thalassaemia models and leads to impaired red cell recovery following induced anaemia, suggesting that macrophages play a key role in stress erythropoiesis[249].

The classical inflammatory macrophages develop at the site of inflammation to help remove infecting organisms, damaged cells and play a key role in tissue remodelling. Given that these mature cells develop from circulating monocytes, we looked at the effect the alteration in monocyte subsets had on PV monocytes to differentiate towards M1 and M2 macrophage subsets. Using the Promocell® macrophage differentiation protocol (Section 2.3.1.8) monocytes from peripheral blood samples were cultured in the presence of cytokines to drive differentiation to M1 or M2 primed macrophages. To assess the efficacy, of this primed macrophages were assessed for the presence of M1 (CD80 and CD86) and M2 (CD163 and CD206) surface markers (Figure 5.6). This shows that both M1 and M2 macrophages expressed markers consistent with effective differentiation in both the normal and PV samples.

**Figure 5.6 Assessment of the efficacy of macrophage differentiation by FACS**

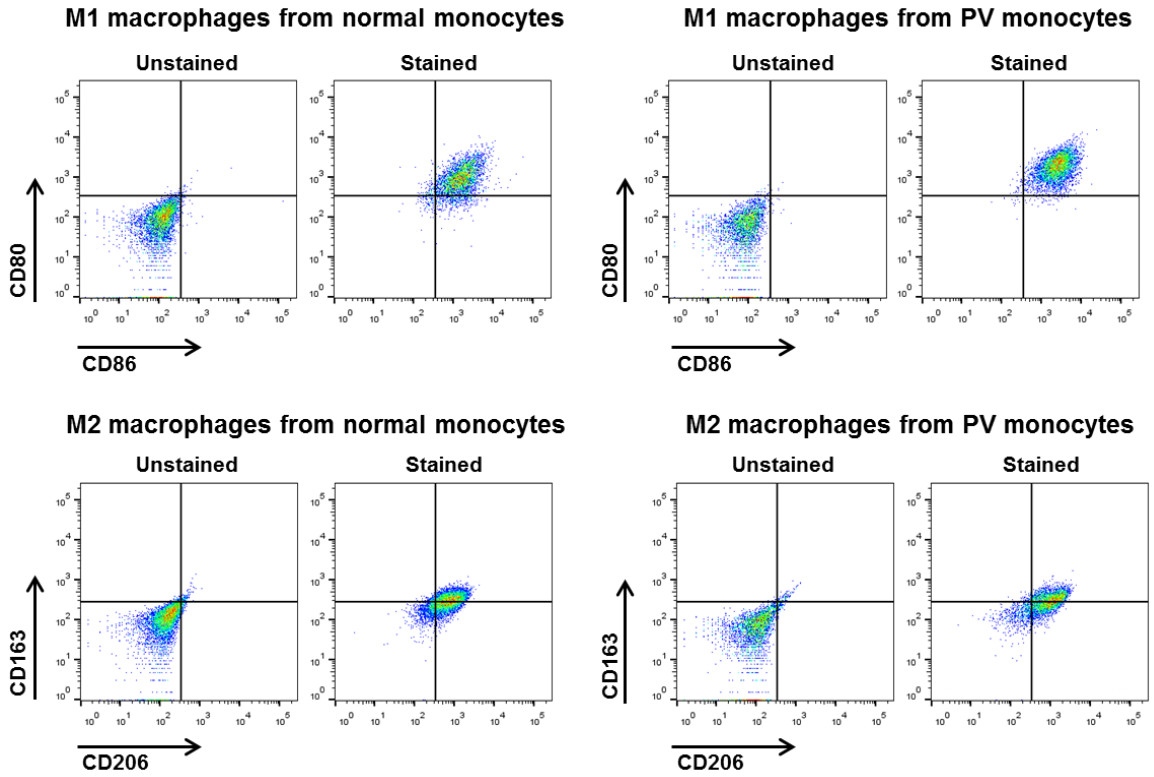


**Following differentiation, macrophages were removed from culture plates using the Promocell® macrophage detachment solution. Cells were incubated with fluorescent labelled CD80, CD86, CD163 and CD206 antibodies. CD80 and CD86 were used to assess the M1 macrophages, while CD163 and CD206 were used to assess M2 macrophages by flow cytometry using FACSCanto, with representative dot plots shown.**

### 5.2.5 Co-localisation of JAK2 and PML in the nucleus of macrophages

As above, monocytes were isolated using monocyte attachment media differentiated into M1 or M2 macrophages in chambered slides. Five normal samples and 6 PV samples were prepared in this way. Following completion of the culture as described previously (Section 2.4.1.8) cells were fixed using paraformaldehyde and prepared as described (Section 2.3.5.1).

These images show the appearance of M1 and M2 macrophages under different culture conditions. M1 macrophages tend to be circular with a central nucleus often described as a “fried egg” appearance, while M2 macrophages tended to be more elongated. When cultured in normal serum with no stimulation the normal M1 macrophages had some variability in the appearance, with some elongated forms present among the classical M1 phenotype, while the PV M1 macrophages all had the classical fried egg appearance regardless of their culture conditions (Figure 5.7). The M2 macrophages generated from normal monocytes showed a classical elongated appearance when cultured in normal serum both with no stimulation and stimulation with IL-4, while in the presence of PV serum, regardless of the stimulation, there tended to be a more M1 phenotype. The M2 macrophages generated from PV monocytes had an M2 phenotype in normal serum with IL-4 stimulation, but all other culture conditions resulted in an M1 phenotype (Figure 5.7).

The immunofluorescent images show clear localisation of JAK2 to the cytoplasm and nuclear co-localisation with PML. The number of PML NBs does not appear to change when comparing macrophages derived from PV or normal monocytes, or when comparing those cultured with PV or normal serum. The M1 macrophages which have been stimulated with IFN-γ appear to have larger NBs than those which have not been stimulated, and this appears to be the same for both normal and PV samples. The difference in the M2 macrophages does not appear to be as marked, and this may be due to the known effect of IFN-γ stimulation on PML NBs (Figure 5.8).

**Figure 5.7 M1 macrophages**

**a) M1 macrophages from normal monocytes**

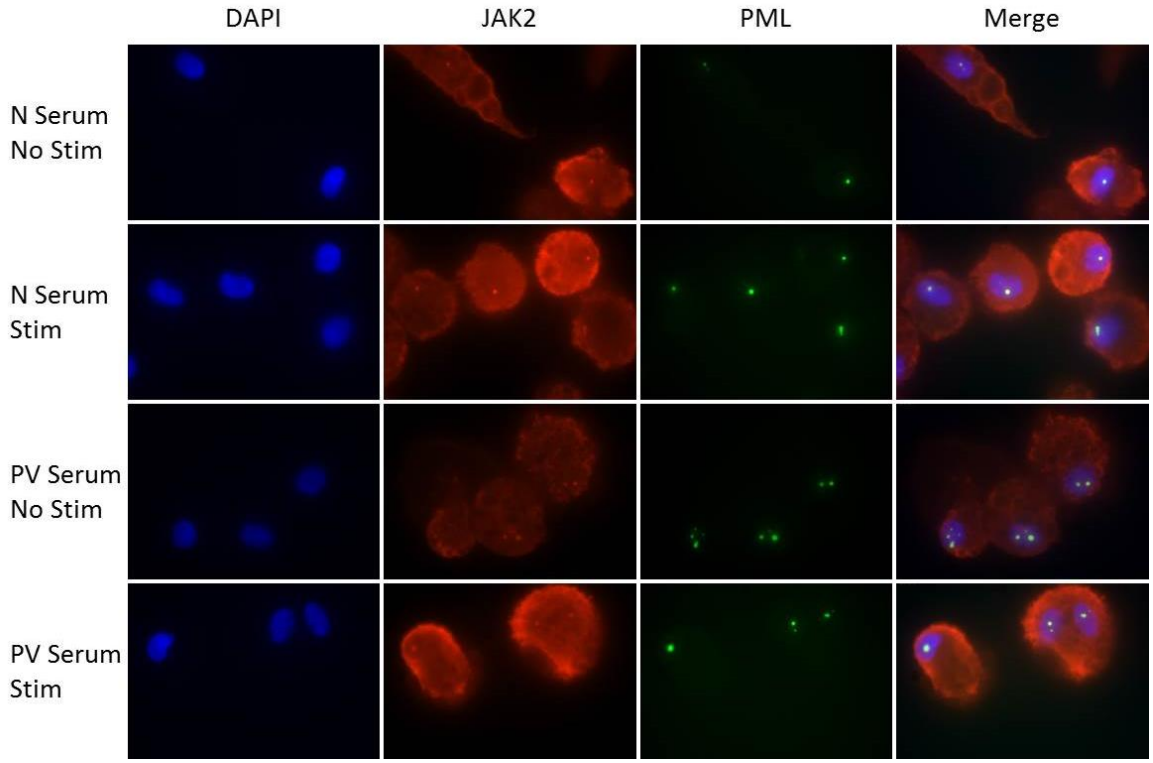


**b) M1 macrophages from PV monocytes**

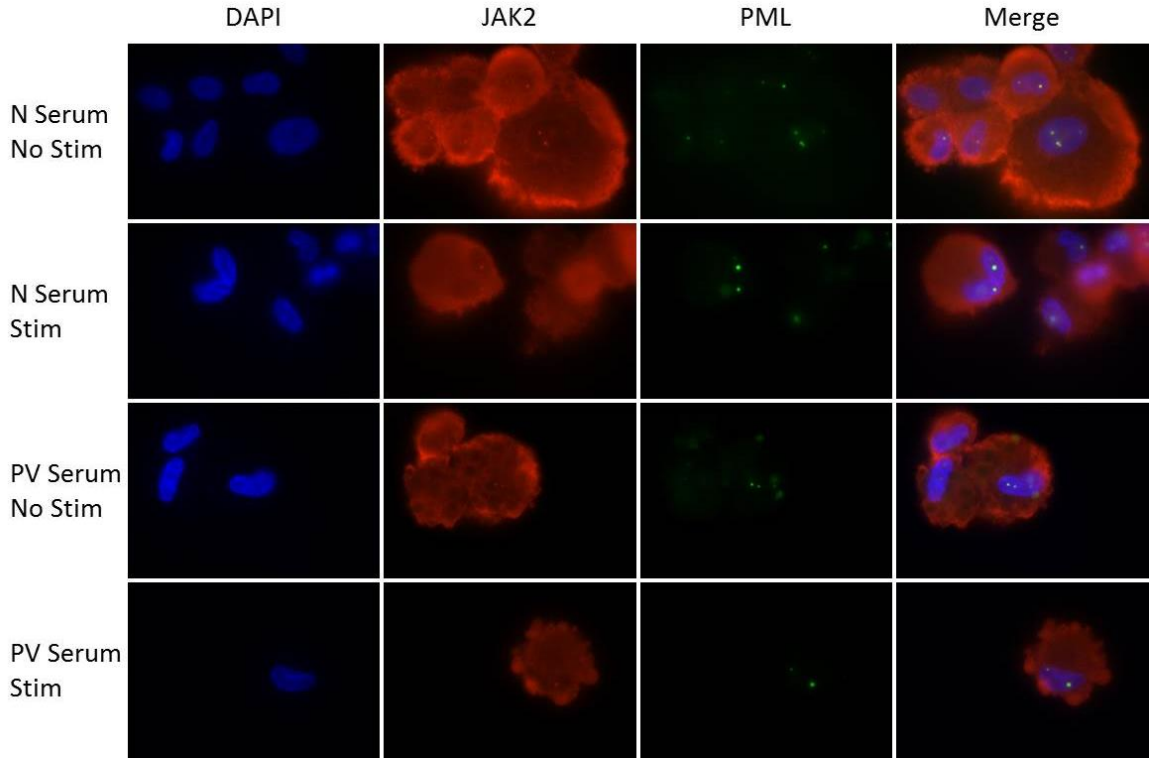


**Representative immunofluorescent images of M1 macrophages generated from normal (a) and PV (b) monocytes. Monocytes were cultured in the presence of macrophage generation media + 20% normal or PV serum with or without stimulation with LPS and IFN-γ. Experiments were carried out on 5 normal and 6 PV samples.**

**Figure 5.8 M2 macrophages**

**a) M2 macrophages from normal monocytes**

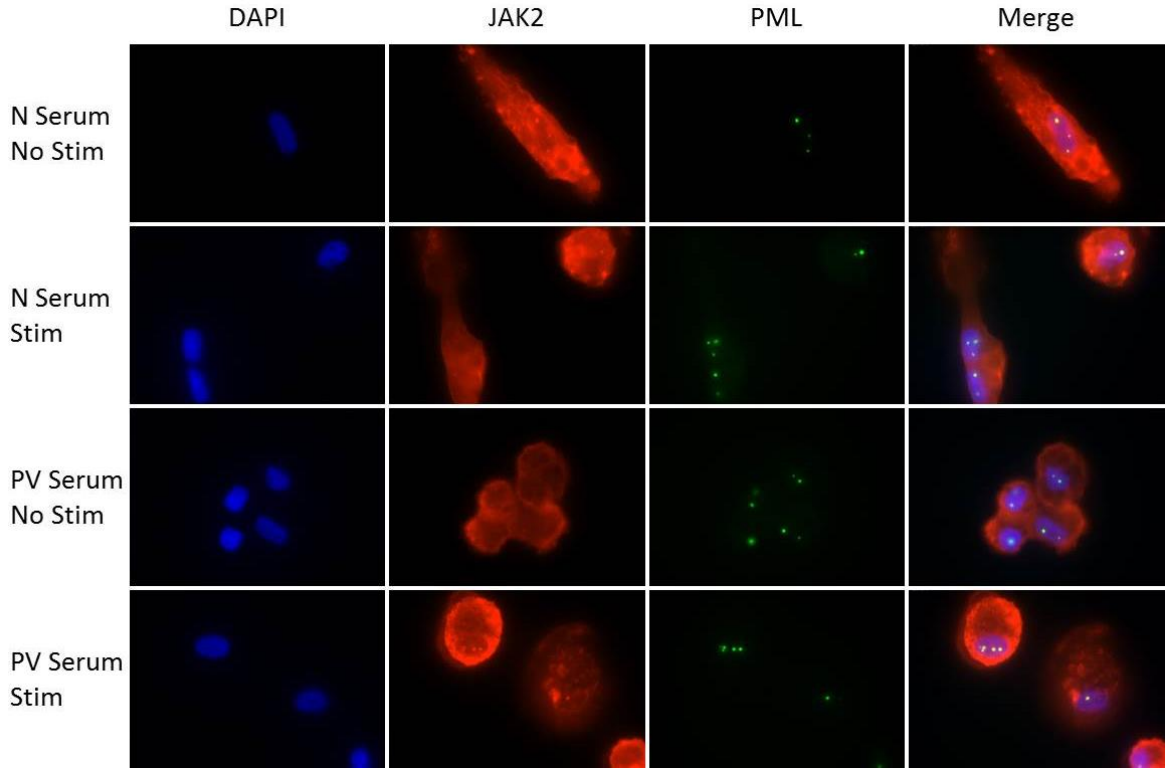


**b) M2 macrophages from PV monocytes**

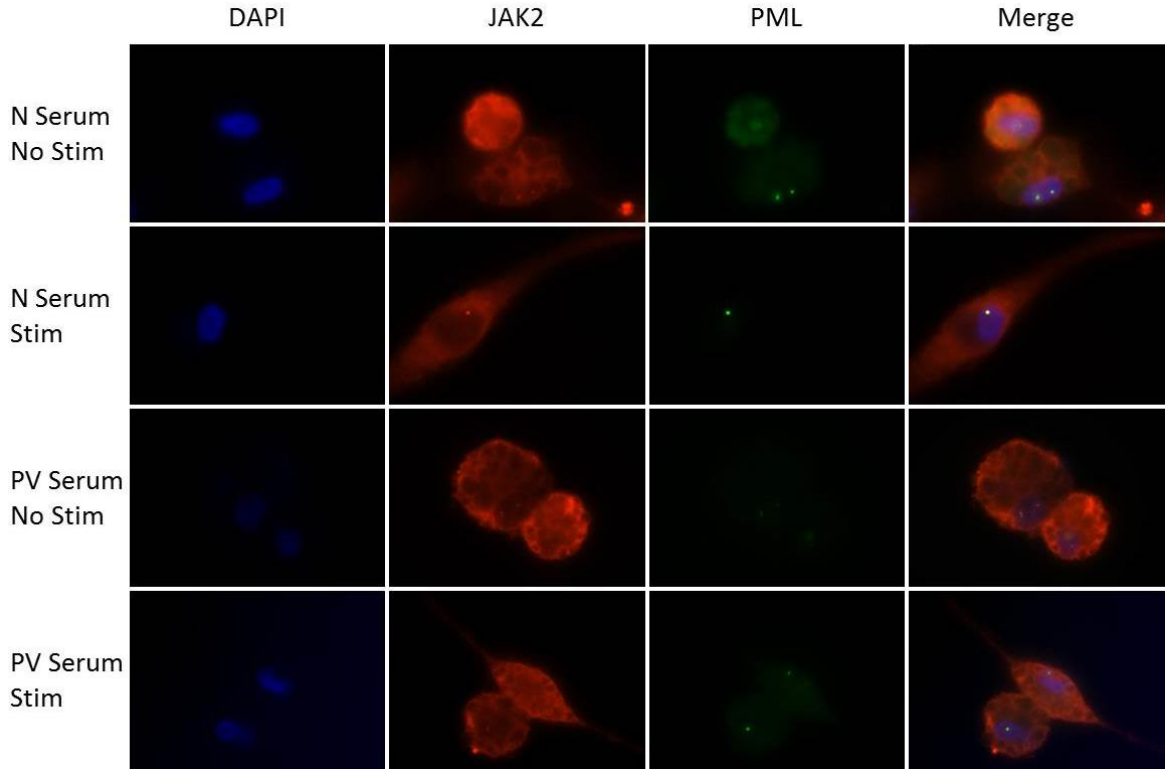


**Representative immunofluorescent images of M2 macrophages generated from normal (a) and PV (b) monocytes. Monocytes were cultured in the presence of macrophage generation media + 20% normal or PV serum with or without stimulation with IL-4. Experiments were carried out on 5 normal and 6 PV samples.**

### 5.2.6 Effects of the JAK2 V617F mutation on macrophage cytokine production

Macrophages are cells that reside in tissues and develop from peripheral blood monocytes[39]. Under pressures from specific cytokines these macrophages can develop into either M1 macrophages or M2 macrophages[250]. M1 macrophages develop in response to exposure to LPS produced from bacterial membranes or in response to stimulation from IFN-γ and GM-CSF[251]. M2 macrophages have a more immunomodulatory role and develop in response to signalling from $Th_2$ T lymphocytes through IL-4 or IL-13[252]. As a result M1 macrophages are involved in killing of intracellular pathogens, tumour destruction and tissue damage while M2 macrophages are involved in clearance of parasites, tissue remodelling and immune regulation[39]. The role macrophages play in the inflammation seen in PV has not previously been investigated, and given the important role the cells play in the immune system we have created a model to investigate this further by generating M1 and M2 macrophages from peripheral blood monocytes as described above (Section 2.4.1.8). For this we investigated 5 normal samples and 6 PV samples in total. Per experiment monocytes were isolated from one normal sample and one/two PV samples, differentiated into macrophages and then stimulated as outlined using either normal or PV serum (Figure 5.9).

**Figure 5.9 Experimental conditions compared to base media**

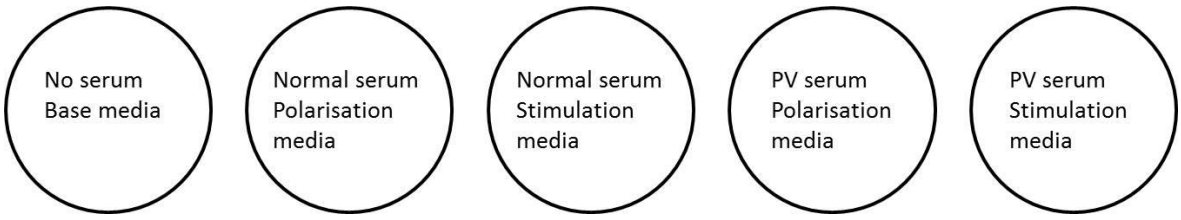


**Culture conditions for generation of macrophages from peripheral blood monocytes. M1 polarisation media was the Promocell® macrophage differentiation base media supplemented with GM-CSF 5ng/ml, with stimulation media using the same base media supplemented with LPS 100ng/ml and IFNγ 20ng/ml. M2 polarisation media was the Promocell® macrophage differentiation base media supplemented with M-CSF 50ng/ml, with stimulation media using the same base media supplemented with M-CSF 10ng/ml and IL-4 20ng/ml.**

The effect the presence of the JAK2 mutation has on macrophage function has not previously been investigated. This is of interest as it is likely that a significant proportion of macrophages will develop with the JAK2 V617F mutation present, and this could potentially alter the responses of these macrophages to stimulation. In turn this may lead to a change in the cytokines subsequently produced by these cells.

#### 5.2.6.1 M1 Macrophages

M1 macrophages produce a range of pro-inflammatory cytokines including IL-1β, IL-6, IL-8, IFN-γ and TNF-α in response to stimulation[253]. We tested these cytokines, and others, to see if there was any alteration in the levels produced when macrophages were exposed to serum collected from PV patients or normal controls, if they differed between macrophages derived from PV monocytes or normal monocytes, or if they behaved differently when stimulated with LPS and IFN-γ.

The effect on cytokine production of culturing monocyte-derived M1 macrophages in the different culture conditions was assessed as previously described (Section 2.3.1.8). As expected there was an alteration in the concentration of IFN-γ in the stimulated conditions, with an increase of more than ten-fold above the unstimulated cells. The level of IFN-γ in the unstimulated culture conditions was higher than would be expected as a result of the serum being added (Figure 5.10), which supports the data showing successful differentiation into M1 macrophages (Figure 5.6). Unexpectedly the levels of CXCL10, usually produced as a direct result of IFN-γ stimulation, were higher in the base media conditions of both sample groups than in the unstimulated conditions, and the normal samples had slightly higher, concentrations than the PV samples cultured the same way.

**Figure 5.10 Interferon-γ and CXCL10 production from M1 macrophages**

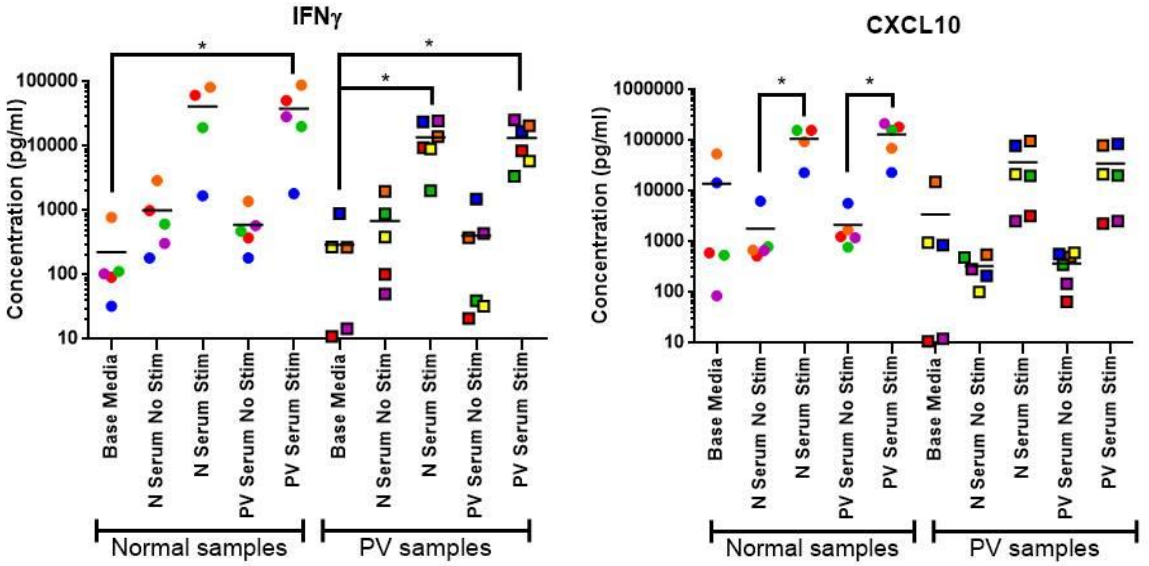


**Cytokines produced by M1 macrophages generated from patient monocytes were measured by Luminex technology using media following culture in the previously described culture conditions. 5 normal and 5 PV samples were used. Each result has the mean indicated by a line. Samples with undetectable levels are shown as 0pg/ml and statistical significance was determined using Students *t*-test (* p≤0.05, ** p≤0.01).**

M1 macrophages release a range of cytokines and growth factors. CCL11 is a chemokine which attracts myeloid cells, particularly eosinophils, to the site of inflammation[254]. Following culture, M1 macrophages increased their production of CCL11 compared to base media. The differences are more than would be expected just from adding serum and were more marked in the normal samples compared to the PV samples (Figure 5.11). Similarly PDGF-BB was increased in all culture conditions compared to base media, but with a less marked increase in samples cultured with PV serum compared to normal serum and with fewer significant alterations in PV samples compared to normal samples (Figure 5.11).

**Figure 5.11 Inflammatory cytokines produced by M1 macrophages**

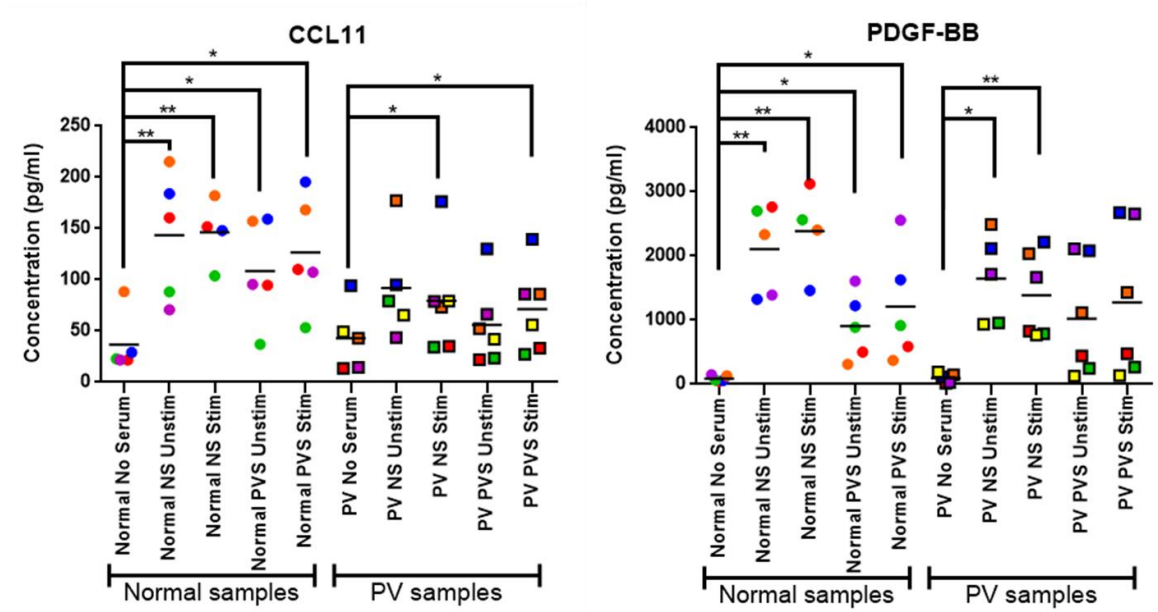


**Cytokines produced by M1 macrophages generated from patient monocytes were measured by Luminex technology using media following culture in the previously described culture conditions. Each result has the mean indicated by a line. 5 normal and 5 PV samples were used. Samples with undetectable levels are shown as 0pg/ml and statistical significance was determined using Students *t*-test (* p≤0.05, ** p≤0.01).**

When comparing normal M1 macrophage cytokine production with PV M1 macrophage production there is a surprising trend. Looking at the cells cultured in their own serum with no stimulation, there appears to be a blunting of production of CCL11, PDGF-BB and IL-7, with an increased production of CCL5 (Figure 5.12). Interestingly, following stimulation there is only a significant alteration in CCL11, with PV samples having lower levels than normal samples as seen in the unstimulated samples. The presence of the JAK2 V617F mutation and chronic activation of JAK2 dependent signalling pathways could lead to compensatory mechanisms within the cell. This chronic activation of signalling would lead to reduced responsiveness within the cells and alter the cytokine production. The differences seen may also relate to other cytokines being produced within the culture. The cells were cultured for 24 hours in the different treatment arms, which would be enough time for cytokines produced to have an autocrine effect on the behaviour of the cells in culture.

**Figure 5.12 M1 macrophage cytokines**

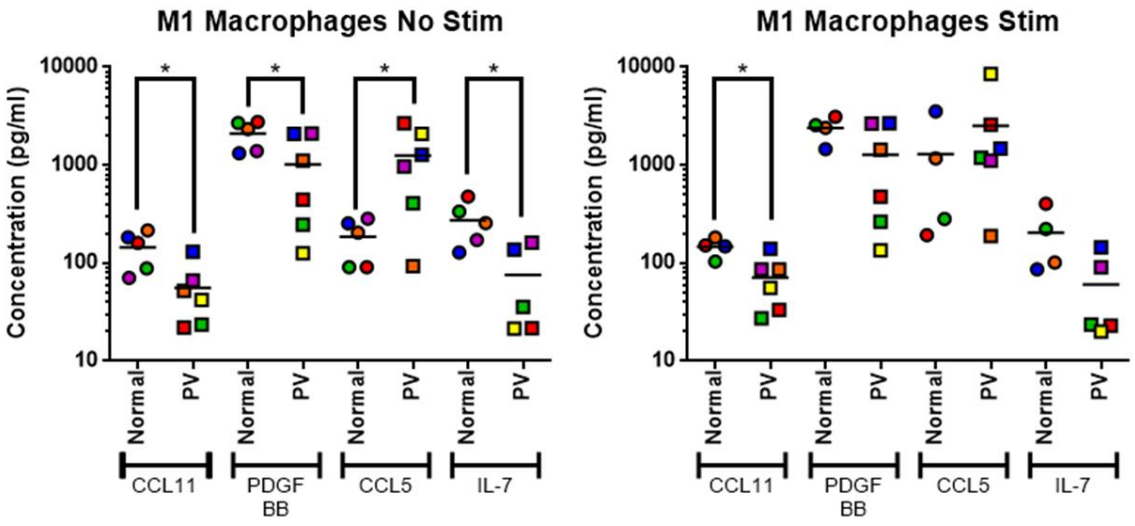


**Cytokines produced by M1 macrophages generated from patient monocytes were measured by Luminex technology using media following culture in the previously described culture conditions. Each result has the mean indicated by a line. 5 normal and 5 PV samples were used. Samples with undetectable levels are shown as 0pg/ml and statistical significance was determined using Students *t*-test (* p≤0.05, ** p≤0.01).**

The complete list of cytokines produced by M1 macrophages in this model is summarised in Appendix 1.

### 5.2.6.2 M2 macrophages

M2 macrophages are viewed as having a more immunomodulatory role with the ability to help with tissue repair following inflammation, producing IL-1RA, IL-4, IL-10, VEGF and FGF basic[252]. Alterations in these cytokines were seen following culture, although the only significant alteration was in normal M2 macrophages cultured in PV serum following stimulation with IL-4. It was not possible to assess the effect of stimulation on IL-4 production as this was masked by the presence of IL-4 in the culture, but when samples stimulated with serum alone were assessed there was a slight, but non-significant, increase in the amount of IL-4 produced, suggesting the serum produced a direct stimulatory effect (Figure 5.13).

**Figure 5.13 Immunomodulatory cytokines in M2 macrophages**

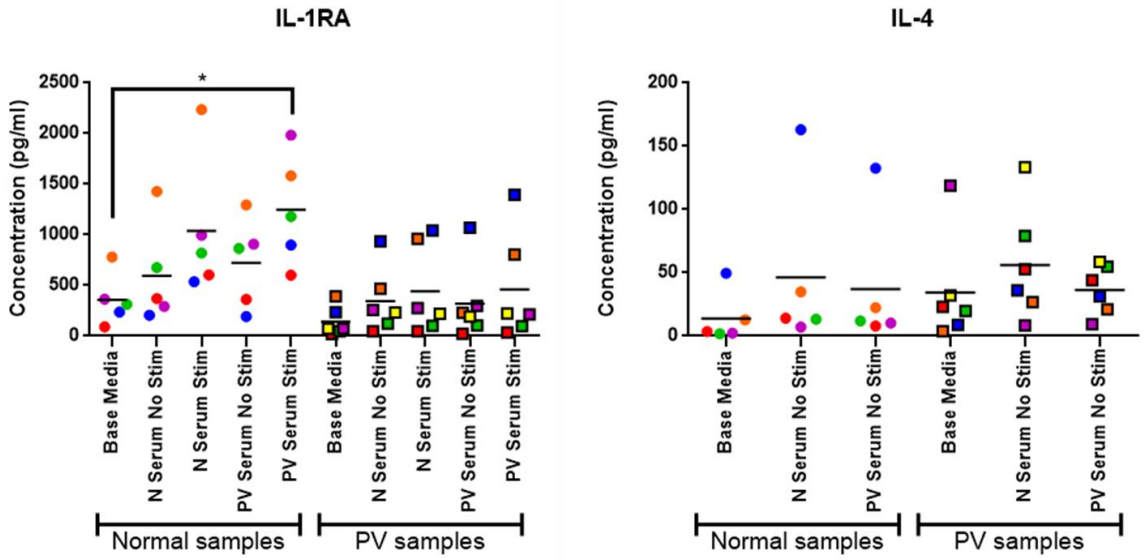


**Cytokines produced by M2 macrophages generated from patient monocytes were measured by Luminex technology using media following culture in the previously described culture conditions. 5 normal and 5 PV samples were used. Each result has the mean indicated by a line. Samples with undetectable levels are shown as 0pg/ml and statistical significance was determined using Students *t*-test (* p≤0.05, ** p≤0.01).**

Several cytokines were altered in unexpected ways in these samples including an increase in TNF-α and PDGF-BB following culture in serum as M2 macrophages would not be expected to produce these. The TNF-α results show significant increases in both normal and PV samples compared to base media, which appears to increase further in the normal samples following stimulation with IL-4 (Figure 5.13). While the high levels of PDGF-BB present following serum stimulated may be partially explained by the high levels present in the PV serum, the similar results elicited by the normal serum which have much lower levels (Table 5.1), suggest it was a direct effect of serum stimulating the M2 cells to produce PDGF-BB.

**Figure 5.14 Inflammatory cytokines in M2 macrophages**

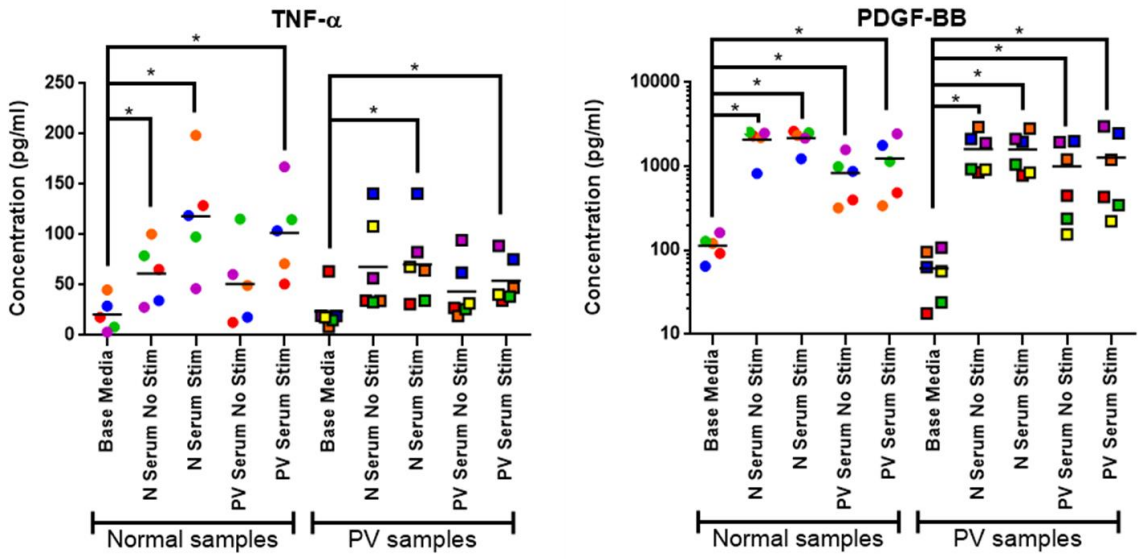


**Cytokines produced by M2 macrophages generated from patient monocytes were measured by Luminex technology using media following culture in the previously described culture conditions. 5 normal and 5 PV samples were used. Each result has the mean indicated by a line. Samples with undetectable levels are shown as 0pg/ml and statistical significance was determined using Students *t*-test (* p≤0.05, ** p≤0.01).**

CXCL1 is a chemo-attractant chemokine that is produced by M1 macrophages to attract neutrophils to a site of inflammation[255]. In macrophages primed to develop into M2 macrophages following culture in M-CSF only CXCL1 was detected, which then reduced following the introduction of serum and stimulation with IL-4. This may be an indication that the macrophages underwent further differentiation/maturation following the introduction of stimulation and serum to the culture. IL-7 is an immunomodulatory cytokine that acts predominantly on lymphocytes to mediate proliferation of all lymphoid lineages[256]. There is also more recent evidence that elevated levels of IL-7 are seen in mice with advanced atherosclerosis and the levels dropped following cholesterol lowering interventions. In this model, it was seen that IL-7 induced recruitment of monocytes which then differentiated to macrophages in the vascular endothelium[257]. We see an increase in IL-7 levels produced by normal samples cultured in serum, which was more marked following stimulation with IL-4. Interestingly, this was not seen in the PV cells. However the level of IL-7 in the serum is already increased in PV patients compared to normal (Figure 5.15).

**Figure 5.15 Cytokines and chemokines in M2 macrophages**

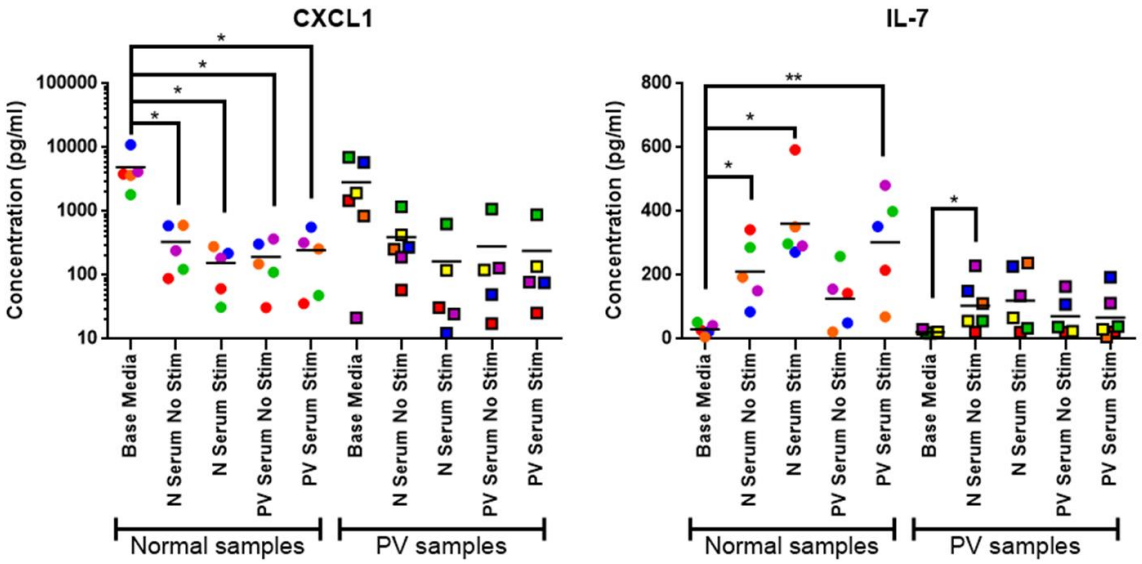


**Cytokines produced by M2 macrophages generated from patient monocytes were measured by Luminex technology using media following culture in the previously described culture conditions. 5 normal and 5 PV samples were used. Each result has the mean indicated by a line. Samples with undetectable levels are shown as 0pg/ml and statistical significance was determined using Students *t*-test (* p≤0.05, ** p≤0.01).**

The complete list of cytokines produced by M2 macrophages in this model is summarised in Appendix 2. Overall our results suggest that M1 and M2 derived macrophages from PV patients and normal donors express similar levels of chemokines/cytokines, but PV patient-derived macrophages are less responsive to stimulation compared to their normal counterpart. This may be due to the V617F JAK2 mutation causing up-regulation of negative regulators of signalling, leading to a damping down of the pro-stimulatory effects mediated by LPS, IFN-γ and IL-4.

### 5.2.7 Effect of the JAK2 V617F mutation on neutrophil cytokine production

Given the alterations in chemokine and cytokine profiles observed in PV patient-derived macrophages, next we investigated whether mature neutrophils from PV patients also displayed altered responses. We compared cells separated from PV patients to normal individuals. Neutrophils were cultured for 24 hours in the presence or absence of PV or normal serum, with or without stimulation by LPS. The media was then collected for cytokine analysis and tested using multiplex bead technology for 29 cytokines and chemokines as previously described, with each sample being tested in duplicate and compared to standards to determine the final concentration. Statistical significance was assessed using Students two-tailed *t*-test and determined as $p \leq 0.05$.

The addition of serum led to an alteration of cytokine production by neutrophils. Vascular endothelial growth factor (VEGF) reduces in the presence of serum, with other growth factors GM-CSF and FGF-basic both being present in neutrophils cultured in the absence of serum but being undetectable in those cultured in the presence of serum (Figure 5.16). G-CSF behaved in exactly the opposite way being almost or completely undetectable in samples cultured in base media and increased when serum was added. This is not accounted for by the G-CSF in the serum samples added as the levels seen in serum (Table 5.1) was less than would be seen in these culture conditions suggesting the neutrophils were producing G-CSF directly.

**Figure 5.16 Growth factors in normal and PV neutrophil culture**

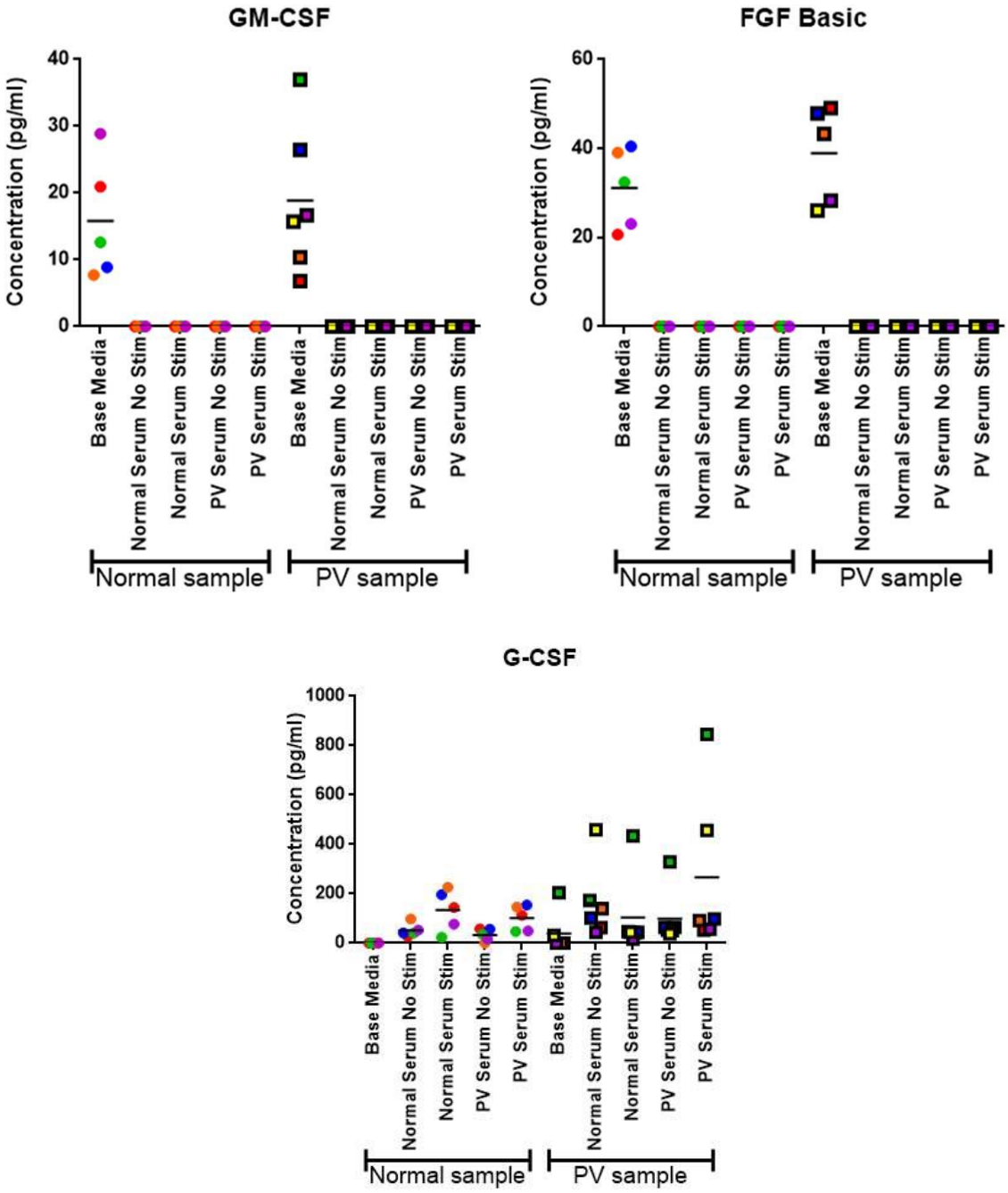


**Neutrophil cytokines were measured by Luminex technology using media following 24 hours of culture in the previously described culture conditions. 5 normal and 5 PV samples were used. Each result has the mean indicated by a line. Samples with undetectable levels are shown as 0pg/ml and statistical significance was determined using Students *t*-test (* p≤0.05, ** p≤0.01).**

Pro-inflammatory cytokines, such as CCL11 and PDGF-BB, also increased in both normal and PV neutrophil cultures under the different culture conditions with concentrations much higher than those measured in the serum alone (Figure 5.17). Although not significant, the PV neutrophils secreted higher levels of CCL11 than normal neutrophils following stimulation. IL-9 also increased following stimulation with either normal or PV serum, but only when LPS was added to stimulate the neutrophils, again PV neutrophils showed a bias towards higher levels.

**Figure 5.17 Pro-inflammatory cytokines in normal and PV neutrophils**

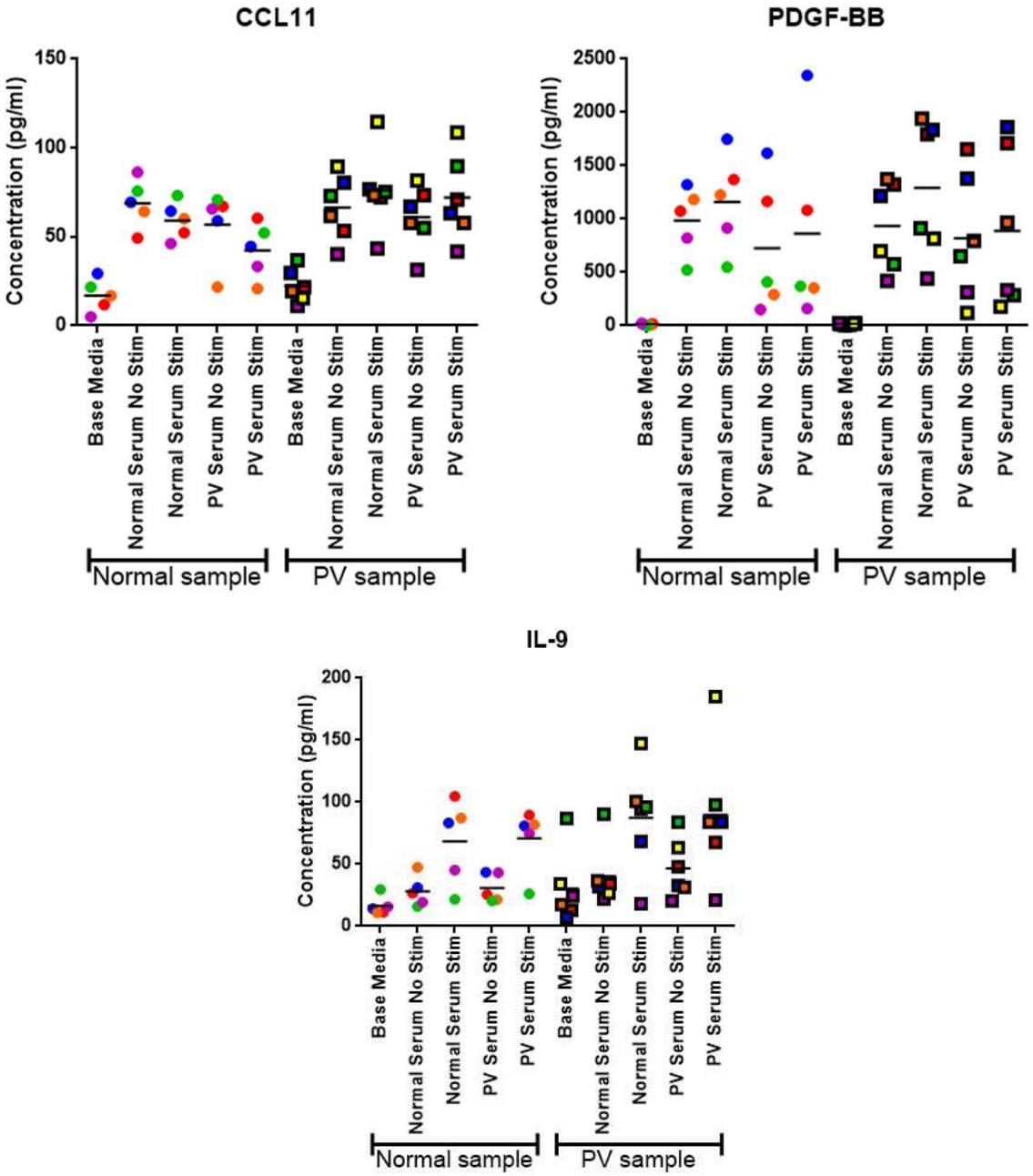


**Neutrophil cytokines were measured by Luminex technology using media following 24 hours of culture in the previously described culture conditions. 5 normal and 5 PV samples were used. Each result has the mean indicated by a line. Samples with undetectable levels are shown as 0pg/ml and statistical significance was determined using Students *t*-test (* p≤0.05, ** p≤0.01).**

Some cytokines, such as CCL5 and CXCL10, were increased from baseline at a level which would be explained by the dilution of the serum when added to culture alone, suggesting there is no real increase when compared to neutrophils cultured in media alone (Figure 5.18). Alteration in the levels of these would also be unexpected as neither are produced by neutrophils normally. The cytokine results for all samples are presented in Appendix 3.

**Figure 5.18 Unchanged cytokines in normal and PV neutrophils**

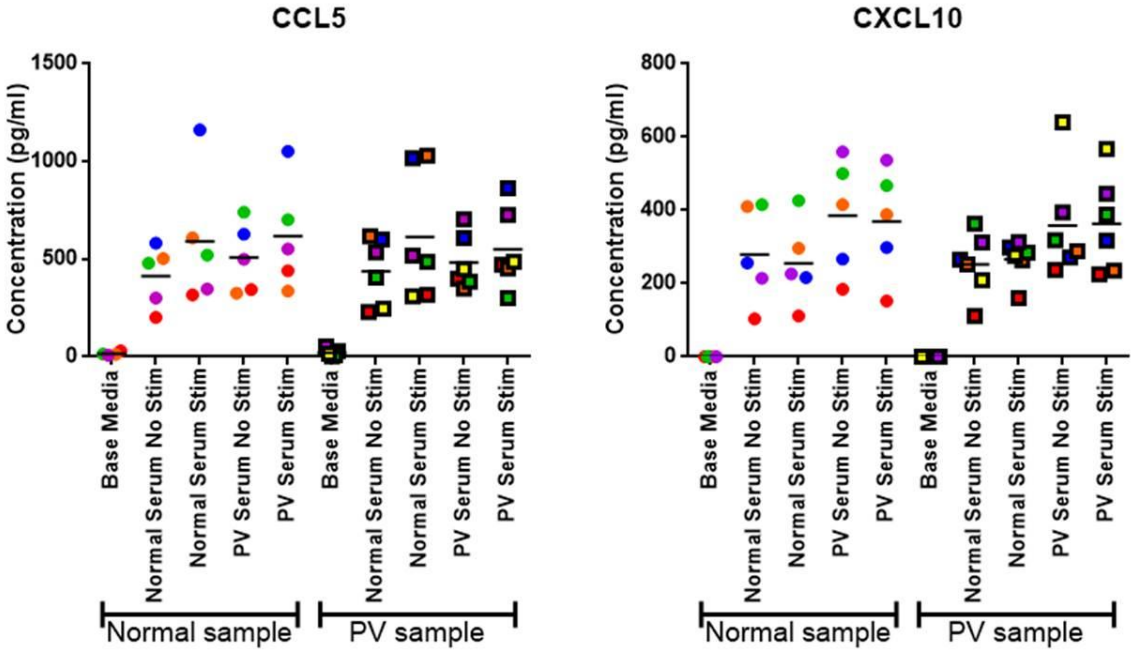


**Neutrophil cytokines were measured by Luminex technology using media following 24 hours of culture in the previously described culture conditions. 5 normal and 5 PV samples were used. Each result has the mean indicated by a line. Samples with undetectable levels are shown as 0pg/ml and statistical significance was determined using paired Students *t*-test (* p≤0.05, ** p≤0.01).**

## 5.3 Discussion

Inflammation is one of the major features of myeloproliferative disease, with evidence that this confers a survival benefit to the abnormal clone[151], as well as driving many of the symptoms and contributing to the complications of the conditions[230]. Recently, there has been increasing evidence that MPN cells have abnormal functions in addition to being present in increased numbers[149,205,4]. Previous studies have identified several clear abnormalities of MPN cell function with basal neutrophil reactive oxygen species production increased in MPN patients with the JAK2 V617F mutation when compared to normal neutrophils and to JAK2 V617F negative MPN[149]. There is also evidence to show that abnormal cytokine levels are associated with alterations in the peripheral blood counts such as an increase in IL-1β, IL-2 and IL-7 in patients with leucocytosis[258]. There is no data directly correlating JAK2 V617F allele burden to cytokine expression profiles. However there is data showing different cytokine profiles associated with ET, PV and myelofibrosis which would suggest that allele burden has an effect on cytokine production[150,258].

The JAK2 inhibitor ruxolitinib is known to have a relatively specific effect on JAK2. However in the initial studies assessing this compound it is clear that it has an equally important effect on JAK1[194]. The combination of JAK1 and JAK2 is an important one as these two JAKs are often associated with inflammatory cytokine receptors together (IL-5 and IFN-γ) or separately (IL-15 and IFN-α). This dual inhibitory effect of ruxolitinib is likely to be part of the reason it is so effective in reducing clinically significant inflammatory symptoms in patients[133,204] where there is significantly abnormal cytokine activity. However given that the predominant abnormality here is the JAK2 V617F mutation causing chronic activation of signalling it is likely that most of the effect seen is due to inhibition of JAK2. This is supported by the fact that both fedratinib and pacritinib achieved improvements in both symptoms and spleen size despite having no JAK1 activity[259,260].

In this study we have shown neutrophil cytokine responses are also abnormal, although many of the abnormalities are not significant, there are clear trends towards an increased production of inflammatory cytokines by PV neutrophils compared to normal. We have also shown that monocytes from PV patients have an abnormal distribution with an increase in the pro-inflammatory intermediate

monocytes at the expense of classical monocytes. This has implications not only in the serum cytokine levels but in aspects of arterial thrombosis, where monocyte infiltration of vascular endothelium and differentiation into tissue macrophages is an important initiating step in atherosclerosis[37]. It appears that IL-7, which is elevated in PV, is a key regulator of the expression of adhesion molecules on the vascular endothelium which act to increase monocyte adhesion[257]. This is an important step in the initiation of atherosclerosis with accumulation of macrophages in the vascular endothelium. Given that we have shown that macrophages derived from peripheral blood monocytes behave abnormally this could explain the alterations in endothelial function and partly explain the increase in arterial vascular events seen in these patients.

Macrophages are known to be important for red cell maturation, particularly provision of iron for haemoglobin production and in aiding the expulsion of the nucleus in maturing red cells[249]. Despite this key role in erythropoiesis, the role of macrophages in the support of erythropoiesis in PV has not been investigated. Here we show that PV macrophages have an abnormal response, both as M1 and M2 macrophages, in response to culturing in serum and to stimulation. These cells exist throughout the body and have a wide range of roles, from tissue specific roles such as macrophages seen in the bone marrow, liver and lungs[261], to responding to infection or inflammation through egress and differentiation of blood monocytes into the affected tissues[253]. Tissue resident macrophages tend to be self-maintaining in the steady state with support from monocyte derived macrophages in the context of acute inflammation[262]. As a result tissue resident macrophages are less likely to harbour the JAK2 V617F mutation at the time of diagnosis. However given the chronic inflammation seen there may be an increased trafficking of monocytes from the blood into the tissues. It would be interesting to evaluate if these is an accumulation of tissue resident macrophages harbouring the JAK2 V617F mutation occurred with time, and whether this was associated with increased inflammatory symptoms.

# 6 Summary of findings

## 6.1 JAK2 dependent gene expression

Signalling through JAK2 and STAT5 is a key pathway in haematopoiesis especially myelopoiesis, with multiple cytokine receptors relying on this signalling pathway to activate intracellular effects[138]. It is also a frequently overactive in haematological malignancy, both myeloid and lymphoid[263], either as a result of a mutation activating the pathway[111,114,142,264] , or due to overactivity of the normal pathway mediated through other oncogenic mutations[265]. In this study we looked at two models of overactivity; the JAK2 V617F mutation causing constitutive activation of the pathway, and overactive wild-type JAK2 through activation of the pathway by the novel oncoprotein BCR-ABL. The JAK2 V617F mutation leads to ligand independence of receptors associated with JAK2 on both intracellular arms[266,267], while those where JAK2 associates with another JAK protein this is thought to be via a prolongation of the response following activation of the receptor by ligand[47,268]. The data presented here shows that there is extensive gene expression abnormalities seen in both CML and PV with similar genes being altered in each condition. These included important genes involved in cell cycle progression (*CCND2, CCNF*), cytokine signalling (*STAT1*, *PI3K*), apoptosis (*BCL2L1, MCL1*) transcriptional regulation (*TAF1*, *EGR2*) and inflammation (*IRF6, PML, SUMO3*). Many of the changes have been seen before, but it was interesting to see that although similar genes were altered, often they were not changed in the same way between CML and PV; decreased expression of *EGR2* in CML and increased expression in PV, increased expression of *PML* in CML with decreased expression in PV, and increased expression of *TAF1* in CML while this was decreased in PV. There were also some new changes identified such as alterations in *SUMO* expression. The importance of SUMO in CML has not previously been explored, but given the increasingly diverse cellular processes altered by SUMOylation[269] this could be an interesting area to look in to further.

## 6.2 JAK2 interactions in the nucleus

The role of JAK2 in the nucleus is a recent finding that has changed the way we think about JAK2 signalling[78,79]. While the classical model of JAK-STAT signalling has a wide role to play in many aspects of cellular function, the direct role JAK2 plays in the epigenetic regulation of target gene expression opens an entire new

area of research. While it has been shown that following phosphorylation JAK2 acquires the ability to enter the nucleus through post-translational modification with SUMO proteins, the regulation of JAK2 signalling and how it mediates its actions within the nucleus is less clear. Here we show that following entry into the nucleus JAK2 associates with the PML NB and this interaction can be modified following treatment with a known PML inducer, IFN-γ, or JAK2 inhibition. In addition to this there is a clear increase in the degree of association between JAK2 and PML in PV peripheral blood monocytes compared to normal indicating that this interaction results from activation of the JAK2 protein. PML NBs have long been known to act as a hub where proteins are brought into association with targets to effect changes[237,270]. In addition to this PML NBs associate with transcriptionally active sites, where effector proteins can interact with histones[271]. Finally PML NBs have been shown to be involved in the degradation of proteins[272–274] through facilitating ubiquitination and proteosomal degradation. Exactly which of these actions is achieved by the interaction of JAK2 and PML is not yet clear however the increase in apoptosis seen following treatment of cells with ruxolitinib and arsenic trioxide would suggest that the interaction enhances the effects of JAK2s activity within the nucleus. The normal role of PML has typically been associated with enhancing apoptosis[270,275] and control of cellular proliferation through downregulation of PI3K signalling at the level of Akt[276] and reduction of c-Myc and c-Myc target genes[277], so it may be that the interaction in PV may result in JAK2 exerting an inhibitory effect on normal PML functions thereby promoting cellular proliferation and differentiation.

## 6.3 JAK2 in inflammation

The cardiovascular risk associated with PV improves dramatically following aggressive normalisation of haematocrit and platelet count[278], but does not return to the expected risk associated with age matched controls[279]. There is evidence to show that an abnormal intermediate monocyte subset is associated with an increase in the risk of acute cardiovascular events[37]. Over the last decade it has become clear that arterial thrombotic events are increased in conditions with chronic inflammation[153], with elevated intermediate monocyte subsets increasing the risk of cardiovascular events in rheumatoid arthritis[280]. In addition to this, patients with an elevated intermediate monocyte subset at the time of myocardial infarction had a higher risk of death and poor myocardial recovery[281]. The PV

patients in this study were mostly on effective treatment at the time of sampling, but still had elevated intermediate monocytes and reduced classical monocytes. It is unclear if this alteration in monocyte subsets is due to the underlying PV or occurs as a result of treatment with hydroxycarbamide, but the abnormality may in part explain why patients do not have a complete correction of their cardiovascular risk following correction of the peripheral blood counts. In addition to this there is an ongoing low level of inflammation which has been shown in several studies[150,230,282]. In this study the serum cytokine levels remain abnormal despite ongoing therapy indicating that the ongoing inflammation is independent of the correction of counts. This ongoing inflammation will continue to support the malignant clone as the diseased stem cells are resistant to the apoptotic effects of inflammatory cytokines such as TNF-α[151].

## 6.4 Conclusions

In this study we have shown patients with CML and PV have significant alterations to many cellular processes that support the survival of the abnormal clone and that JAK2 is a central regulator of many of these changes. We have also confirmed recent evidence that JAK2 enters the nucleus and furthered the understanding of its role by demonstrating an interaction with PML NBs which can be modulated by inhibition of JAK2 or stimulation with IFN-γ. This interaction is not limited to cell lines only, but is demonstrated in both normal and PV patient monocytes and macrophages. The presence of the JAK2 V617F mutation in patient monocytes leads to an increase in the localisation of JAK2 and PML indicating that activation of JAK2 is required for these proteins to come together. To further highlight that this is a functionally relevant interaction, treating JAK2 V617F containing cell lines with the JAK2 inhibitor ruxolitinib and arsenic trioxide, which degrades PML, in combination led to a significant increase in apoptosis when compared to either compound alone. Currently we don't know exactly what the nature of this interaction is, but this would be an interesting area to investigate further.

We have also shown that in PV, cells of the innate immune system behave differently from normal samples. Based on findings in other conditions, the increase of inflammatory intermediate monocytes seen in PV would in part explain the ongoing cardiovascular risk seen in these patients and it will be interesting to

see if, in time, the use of JAK2 inhibitors will lead to a normalisation of monocyte subsets and a reduction in cardiovascular risk.

# 7 Future Work

The work presented in this thesis shows that the role JAK2 plays in cellular signalling networks is complex and that the presence of JAK2 V617F activating mutation has profound effects on cellular function. However the full story has not been elucidated here and there are several interesting findings that could be investigated further either as individual projects or in collaboration with other research teams.

The interaction of JAK2 and PML identified here is a novel interaction which is likely to be of importance to the functioning of haematopoietic cells. Both JAK2 and PML play key roles in many cellular functions including cell cycle, apoptosis, cellular growth and the inflammatory response. Here we show that combining pharmacological inhibition of JAK2 and PML using ruxolitinib and arsenic trioxide leads to an increase in apoptosis in cell lines harbouring the JAK2 V617F mutation. It would be of interest to see if this combination is synergistic or merely additive. This would need formal synergy experiments to be carried out wither using flow cytometry or trypan blue exclusion counts as a method of assessing cell viability. In addition to this the co-localisation of JAK2 and PML raises many avenues for further evaluation. The functional consequences of this interaction were not elucidated here making it difficult to ascertain for certain the reason for the interaction. It may be that JAK2 enters the PML NBs to be marked for degradation following completion of its activity within the nucleus, or it may be that entering the PML NB brings JAK2 into proximity with histones and proteins to allow JAK2 to directly alter their activity and increase transcription of target genes. Finally the interaction may allow JAK2 to directly alter the functioning of PML itself which is associated with cellular senescence and potentiation of apoptotic signals.

Another interesting finding in this thesis is the increase in intermediate monocytes seen in PV compared to normal. These monocytes display a more inflammatory phenotype and have been shown to play an important role in the development of cardiovascular disease in patients without the JAK2 V617F mutation. Patients with PV are known to have a persistent increase in the risk of cardiovascular disease despite normalisation of peripheral counts. The underlying cause of this has been previously attributed to a chronic inflammatory response as part of the disease and an alteration of platelet responsiveness driven by the presence of the JAK2 V617F

mutation. However the finding that intermediate monocytes are increased in patients with PV raises the possibility that the underlying mechanisms of cardiovascular disease are more complex than previously thought. It would be of significant interest to investigate the interaction of PV monocytes with vascular endothelium and whether this plays a role in the development of cardiovascular disease. This would probably best be achieved through collaboration between a cardiovascular research team who would be able to provide models of cardiovascular disease and a haematology research team who would provide patient samples.

The final area of particular interest raised in this work is the abnormal function of macrophages derived from PV patient monocytes. The macrophages generated in this project showed abnormal function with blunting of some cytokine responses and heightening of others. However there was marked heterogeneity in the concentration of cytokines released with these samples and it would be interesting to obtain further samples and try to obtain more meaningful results in the first instance. It would also be of interest to look at the effect of the JAK2 V617F mutation on other functional aspects of the macrophages such as tissue remodelling and response to pathogens. The other area of macrophage biology which could be investigated is whether the JAK2 V617F mutation enters the tissue resident macrophage pool. The currently available evidence suggests that tissue resident macrophages maintain themselves with monocyte derived macrophages only developing in response to inflammatory stimuli[262]. However bone marrow macrophages, that are essential for the development of red cells, would be of particular interest to investigate further as they may be more susceptible to the introduction of the JAK2 V617F mutation into the pool, which would be likely to lead to alterations in their function. Given the role that macrophages play in tissue remodelling the presence of the JAK2 mutation within these cells may have a role to play in disease progression to myelofibrosis.

# 8 Appendix

## Appendix 1a. Cytokine levels of M1 macrophages generated from normal monocytes

| Cytokine | Normal Samples (pg/ml) | | | | | | | | | |
|---|---|---|---|---|---|---|---|---|---|---|
| | Base Media | St dev | N Serum Unstim | St dev | N Serum Stim | St dev | PV Serum Unstim | St dev | PV Serum Stim | St dev |
| **Pro-inflammatory** | | | | | | | | | | |
| **IL-1β** | 284 | 203 | 168 | 47 | 444 | 234 | 161 | 45 | 230 | 56 |
| **IL-5** | 26 | 7 | 62 | 15 | 69 | 18 | 47 | 13 | 48 | 12 |
| **IL-6** | 766 | 426 | 453 | 243 | 5469 | 1948 | 317 | 144 | 2872 | 882 |
| **IL-8** | 22829 | 12401 | 25418 | 16842 | 73427 | 56598 | 21549 | 8965 | 45046 | 25841 |
| **IL-9** | 93 | 36 | 180 | 66 | 210 | 79 | 164 | 61 | 178 | 71 |
| **IL-12(p70)** | 11 | 5 | 30 | 21 | 30 | 21 | 13 | 8 | 17 | 14 |
| **IL-15** | 44 | 40 | 106 | 97 | 195 | 175 | 103 | 100 | 173 | 162 |
| **IL-17** | 85 | 35 | 104 | 19 | 133 | 28 | 85 | 12 | 102 | 22 |
| **CCL11** | 37 | 13 | 144 | 28 | 146 | 16 | 109 | 23 | 127 | 25 |
| **FGF basic** | 31 | 13 | 33 | 19 | 47 | 20 | NA | NA | 45 | 31 |
| **G-CSF** | 54 | 33 | 140 | 67 | 313 | 204 | 95 | 38 | 258 | 155 |
| **GM-CSF** | 4932 | 1528 | 1874 | 885 | NA | NA | 1427 | 728 | 681 | 326 |
| **IFN-γ** | 224 | 140 | 1003 | 498 | 41267 | 18561 | 602 | 208 | 38056 | 14898 |
| **CXCL10** | 14066 | 10465 | 1804 | 1135 | 108961 | 32402 | 2143 | 910 | 131124 | 36265 |
| **CCL2** | 313 | 159 | 918 | 470 | 1473 | 515 | 704 | 495 | 1242 | 435 |
| **CCL3** | 6648 | 4056 | 4594 | 2188 | 10373 | 4291 | 48264 | 44650 | 23373 | 12142 |
| **PDGF-bb** | 90 | 21 | 2103 | 313 | 2389 | 346 | 907 | 236 | 1213 | 398 |
| **CCL4** | 7459 | 4397 | 1855 | 512 | 4930 | 3405 | 2582 | 1129 | 4653 | 2663 |
| **CCL5** | 3677 | 3037 | 185 | 41 | 1295 | 778 | 289 | 118 | 1089 | 426 |
| **TNF-α** | 32 | 14 | 110 | 27 | 4056 | 2437 | 77 | 22 | 3577 | 1901 |
| **VEGF** | 30 | 13 | 39 | 26 | 64 | 33 | 30 | 22 | 60 | 39 |
| **CXCL1** | 1925 | 1308 | 225 | 86 | 2127 | 934 | 135 | 43 | 1702 | 703 |
| **IFN-α** | 7.0 | 3.7 | 81.9 | 40.0 | 195.0 | 103.1 | 44.8 | 16.0 | 210.9 | 142.9 |
| **Anti-inflammatory** | | | | | | | | | | |
| **IL-1RA** | 379 | 130 | 773 | 245 | 770 | 270 | 713 | 175 | 977 | 309 |
| **IL-4** | 24 | 10 | 90 | 63 | 81 | 55 | 79 | 60 | 72 | 52 |
| **IL-10** | 13 | 8 | 35 | 23 | 31 | 20 | 31 | 24 | 29 | 22 |
| **IL-13** | 146 | 140 | 24 | 11 | 57 | 44 | 15 | 10 | 15 | 11 |
| **Immunomodulatory** | | | | | | | | | | |
| **IL-2** | 45 | 29 | 62 | 38 | 76 | 42 | 50 | 38 | 65 | 45 |
| **IL-7** | 73 | 34 | 274 | 62 | 203 | 73 | 158 | 42 | 106 | 25 |

**Media taken from the culture of M1 macrophages generated from normal monocytes, was analysed using BioRad Bio-Plex cytokine assays. The table shows the median result of 5 normal samples with standard deviation for each culture condition in pg/ml.**

## Appendix 1b. Cytokine levels of M1 macrophages generated from PV monocytes

| Cytokine | PV Samples (pg/ml) | | | | | | | | | |
|---|---|---|---|---|---|---|---|---|---|---|
| | Base Media | St dev | N Serum Unstim | St dev | N Serum Stim | St dev | PV Serum Unstim | St dev | PV Serum Stim | St dev |
| **Pro-inflammatory** | | | | | | | | | | |
| **IL-1β** | 183 | 54 | 529 | 235 | 604 | 209 | 461 | 176 | 627 | 204 |
| **IL-5** | 25 | 7 | 54 | 15 | 49 | 17 | 46 | 15 | 50 | 16 |
| **IL-6** | 918 | 496 | 568 | 258 | 1667 | 773 | 508 | 305 | 1764 | 695 |
| **IL-8** | 21934 | 12980 | 136836 | 115015 | 9165 | 1154 | 14538 | 7512 | 17942 | 7013 |
| **IL-9** | 99 | 28 | 169 | 39 | 167 | 24 | 134 | 27 | 164 | 20 |
| **IL-12(p70)** | 18 | 4 | NA | NA | 22 | 6 | 16 | 5 | 14 | 5 |
| **IL-15** | 44 | 25 | 89 | 53 | 129 | 59 | 58 | 28 | 90 | 39 |
| **IL-17** | 83 | 31 | 107 | 22 | 107 | 18 | 83 | 19 | 107 | 15 |
| **CCL11** | 43 | 15 | 92 | 23 | 79 | 21 | 56 | 16 | 71 | 17 |
| **FGF basic** | 40 | 8 | 44 | 17 | 41 | 11 | NA | NA | 34 | 9 |
| **G-CSF** | 65 | 27 | 136 | 54 | 132 | 47 | 89 | 37 | 134 | 45 |
| **GM-CSF** | 5788 | 2507 | 2260 | 856 | 341 | 217 | 1542 | 772 | 386 | 257 |
| **IFN-γ** | 291 | 161 | 682 | 360 | 13797 | 3625 | 401 | 233 | 13440 | 3619 |
| **CXCL10** | 3449 | 2993 | 329 | 85 | 37190 | 16579 | 375 | 93 | 35365 | 15388 |
| **CCL2** | 396 | 282 | 672 | 410 | 1353 | 394 | 563 | 404 | 1519 | 352 |
| **CCL3** | 4471 | 2634 | 9852 | 3161 | 11194 | 3034 | 7998 | 2815 | 10066 | 2535 |
| **PDGF-bb** | 98 | 34 | 1645 | 310 | 1384 | 274 | 1021 | 368 | 1274 | 478 |
| **CCL4** | 5755 | 2003 | 5461 | 2493 | 8148 | 2677 | 6279 | 3151 | 7942 | 2984 |
| **CCL5** | 901 | 308 | 1050 | 293 | 2660 | 1298 | 1247 | 401 | 2519 | 1248 |
| **TNF-α** | 45 | 13 | 121 | 32 | 1128 | 384 | 101 | 63 | 1166 | 745 |
| **VEGF** | 33 | 5 | 25 | 12 | 44 | 16 | 24 | 6 | 34 | 8 |
| **CXCL1** | 1745 | 1009 | 326 | 139 | 1328 | 524 | 217 | 132 | 1340 | 592 |
| **IFN-α** | 15.2 | 0.1 | 70.7 | 24.9 | 130.9 | 42.4 | 35.0 | 20.3 | 85.9 | 31.2 |
| **Anti-inflammatory** | | | | | | | | | | |
| **IL-1RA** | 361 | 161 | 451 | 126 | 364 | 138 | 372 | 168 | 429 | 171 |
| **IL-4** | 30 | 11 | 82 | 33 | 56 | 15 | 48 | 12 | 47 | 10 |
| **IL-10** | 11 | 4 | 21 | 7 | 21 | 7 | 15 | 4 | 15 | 5 |
| **IL-13** | 10 | 3 | 25 | 7 | 21 | 2 | 16 | 4 | 14 | 4 |
| **Immunomodulatory** | | | | | | | | | | |
| **IL-2** | 29 | 7 | 55 | 17 | 42 | 13 | 31 | 6 | 40 | 7 |
| **IL-7** | 27 | 9 | 120 | 32 | 63 | 16 | 76 | 28 | 61 | 23 |

**Media taken from the culture of M1 macrophages generated from PV monocytes, was analysed using BioRad Bio-Plex cytokine assays. The table shows the median result of 6 PV samples with standard deviation for each culture condition in pg/ml.**

## Appendix 2a. Cytokine levels of M2 macrophages generated from normal monocytes

| Cytokine | Normal Samples (pg/ml) | | | | | | | | | |
|---|---|---|---|---|---|---|---|---|---|---|
| | Base Media | St dev | N Serum Unstim | St dev | N Serum Stim | St dev | PV Serum Unstim | St dev | PV Serum Stim | St dev |
| **Pro-inflammatory** | | | | | | | | | | |
| **IL-1β** | 224 | 160 | 42 | 27 | 189 | 86 | 101 | 54 | 246 | 108 |
| **IL-5** | 15 | 5 | 41 | 10 | 96 | 36 | 28 | 5 | 106 | 67 |
| **IL-6** | 1608 | 1025 | 377 | 256 | 375 | 194 | 250 | 112 | 566 | 314 |
| **IL-8** | 17163 | 4208 | 4465 | 1664 | 14460 | 6720 | 22559 | 13105 | 12939 | 5162 |
| **IL-9** | 77 | 32 | 110 | 39 | 293 | 152 | 113 | 34 | 353 | 225 |
| **IL-12(p70)** | 13 | 7 | 18 | 11 | 47 | 35 | 9 | 6 | 47 | 32 |
| **IL-15** | 60 | 52 | 81 | 71 | 167 | 155 | 132 | 97 | 273 | 266 |
| **IL-17** | 70 | 27 | 59 | 8 | 129 | 31 | 57 | 11 | 132 | 45 |
| **CCL11** | 31 | 10 | 97 | 19 | 202 | 53 | 78 | 17 | 230 | 105 |
| **FGF basic** | 22 | 13 | 34 | 14 | 52 | 31 | NA | NA | 100 | 82 |
| **G-CSF** | 46 | 26 | 95 | 48 | 208 | 96 | 71 | 29 | 209 | 102 |
| **GM-CSF** | 315 | 307 | NA | NA | 95 | 75 | NA | NA | 111 | 101 |
| **IFN-γ** | 151 | 93 | 666 | 338 | 1316 | 653 | 455 | 155 | 1075 | 246 |
| **CXCL10** | 658 | 360 | 543 | 84 | 516 | 74 | 1911 | 817 | 1216 | 269 |
| **CCL2** | 1208 | 582 | 1335 | 474 | 895 | 493 | 964 | 595 | 1057 | 566 |
| **CCL3** | 3822 | 2641 | 174 | 155 | 3094 | 2610 | 1067 | 907 | 15936 | 8106 |
| **PDGF-bb** | 114 | 17 | 2079 | 320 | 2177 | 248 | 834 | 228 | 1240 | 395 |
| **CCL4** | 5780 | 4219 | 863 | 316 | 2996 | 1575 | 954 | 309 | 3063 | 1800 |
| **CCL5** | 2916 | 2628 | 69 | 11 | 253 | 116 | 72 | 19 | 260 | 135 |
| **TNF-α** | 21 | 8 | 61 | 14 | 118 | 25 | 51 | 18 | 102 | 20 |
| **VEGF** | 34 | 14 | 22 | 15 | 71 | 48 | 21 | 11 | 112 | 93 |
| **CXCL1** | 4933 | 1603 | 331 | 113 | 156 | 47 | 194 | 63 | 246 | 98 |
| **IFN-α** | 7 | 4 | 82 | 40 | 195 | 103 | 45 | 16 | 211 | 143 |
| **Anti-inflammatory** | | | | | | | | | | |
| **IL-1RA** | 357 | 116 | 595 | 223 | 1038 | 311 | 725 | 199 | 1249 | 245 |
| **IL-4** | 14 | 9 | 46 | 30 | 16162 | 550 | 37 | 24 | 15794 | 1736 |
| **IL-10** | 17 | 11 | 28 | 18 | 66 | 46 | 35 | 28 | 92 | 77 |
| **IL-13** | 6 | 4 | 14 | 7 | 40 | 21 | 12 | 6 | 53 | 41 |
| **Immunomodulatory** | | | | | | | | | | |
| **IL-2** | 18 | 10 | 28 | 19 | 108 | 72 | 27 | 20 | 194 | 172 |
| **IL-7** | 30 | 8 | 212 | 46 | 361 | 59 | 126 | 42 | 304 | 73 |

**Media taken from the culture of M2 macrophages generated from normal monocytes, was analysed using BioRad Bio-Plex cytokine assays. The table shows the median result of 5 normal samples with standard deviation for each culture condition in pg/ml.**

## Appendix 2b. Cytokine levels of M2 macrophages generated from PV monocytes

| Cytokine | PV Samples (pg/ml) | | | | | | | | | |
|---|---|---|---|---|---|---|---|---|---|---|
| | Base Media | St dev | N Serum Unstim | St dev | N Serum Stim | St dev | PV Serum Unstim | St dev | PV Serum Stim | St dev |
| **Pro-inflammatory** | | | | | | | | | | |
| **IL-1β** | 200 | 109 | 438 | 162 | 490 | 165 | 374 | 153 | 506 | 180 |
| **IL-5** | 11 | 1 | 40 | 12 | 53 | 18 | 40 | 13 | 55 | 16 |
| **IL-6** | 808 | 330 | 471 | 176 | 425 | 213 | 397 | 208 | 552 | 260 |
| **IL-8** | 10932 | 945 | 19313 | 10159 | 6959 | 1837 | 10562 | 3245 | 10312 | 4685 |
| **IL-9** | 80 | 20 | 158 | 35 | 181 | 34 | 130 | 28 | 170 | 31 |
| **IL-12(p70)** | 23 | 6 | 23 | 8 | 34 | 4 | 17 | 5 | 16 | 6 |
| **IL-15** | 65 | 29 | 105 | 49 | 102 | 46 | 57 | 26 | 69 | 29 |
| **IL-17** | 58 | 16 | 92 | 19 | 107 | 20 | 83 | 22 | 102 | 17 |
| **CCL11** | 18 | 4 | 76 | 22 | 101 | 30 | 52 | 16 | 78 | 22 |
| **FGF basic** | 33 | 8 | 46 | 15 | 44 | 16 | 35 | 4 | 38 | 8 |
| **G-CSF** | 40 | 15 | 112 | 49 | 162 | 70 | 78 | 35 | 125 | 54 |
| **GM-CSF** | 116 | 50 | 60 | 9 | 174 | 69 | 43 | 6 | 191 | 68 |
| **IFN-γ** | 29 | 10 | 529 | 331 | 821 | 457 | 346 | 227 | 562 | 307 |
| **CXCL10** | 85 | 32 | 262 | 71 | 277 | 86 | 360 | 91 | 417 | 130 |
| **CCL2** | 903 | 280 | 1226 | 396 | 514 | 235 | 640 | 296 | 585 | 224 |
| **CCL3** | 1966 | 1223 | 6964 | 2658 | 20707 | 11023 | 5282 | 2315 | 8926 | 2578 |
| **PDGF-bb** | 61 | 15 | 1608 | 349 | 1591 | 337 | 998 | 343 | 1275 | 485 |
| **CCL4** | 6262 | 2934 | 4866 | 1767 | 6128 | 2026 | 5497 | 2712 | 6314 | 2452 |
| **CCL5** | 833 | 448 | 703 | 147 | 873 | 214 | 965 | 329 | 1348 | 372 |
| **TNF-α** | 24 | 8 | 68 | 19 | 70 | 16 | 43 | 12 | 54 | 9 |
| **VEGF** | 41 | 11 | 33 | 12 | 31 | 10 | 25 | 6 | 23 | 8 |
| **CXCL1** | 2868 | 1180 | 398 | 164 | 164 | 109 | 282 | 186 | 242 | 149 |
| **IFN-α** | 15 | 0 | 71 | 25 | 131 | 42 | 35 | 20 | 86 | 31 |
| **Anti-inflammatory** | | | | | | | | | | |
| **IL-1RA** | 140 | 59 | 344 | 132 | 441 | 181 | 320 | 155 | 462 | 217 |
| **IL-4** | 34 | 17 | 56 | 18 | 14626 | 2407 | 36 | 8 | 13928 | 2306 |
| **IL-10** | 14 | 4 | 26 | 7 | 29 | 6 | 16 | 5 | 17 | 5 |
| **IL-13** | 12 | 3 | 21 | 5 | 39 | 10 | 21 | 7 | 23 | 6 |
| **Immunomodulatory** | | | | | | | | | | |
| **IL-2** | 24 | 5 | 48 | 14 | 62 | 14 | 28 | 6 | 45 | 11 |
| **IL-7** | 22 | 2 | 104 | 31 | 120 | 39 | 71 | 26 | 67 | 29 |

**Media taken from the culture of M2 macrophages generated from PV monocytes, was analysed using BioRad Bio-Plex cytokine assays. The table shows the median result of 6 PV samples with standard deviation for each culture condition in pg/ml.**

## Appendix 3a. Cytokine levels of normal neutrophils

| Cytokine | Normal Samples (pg/ml) | | | | | | | | | |
|---|---|---|---|---|---|---|---|---|---|---|
| | Base Media | St dev | N Serum Unstim | St dev | N Serum Stim | St dev | PV Serum Unstim | St dev | PV Serum Stim | St dev |
| **Pro-inflammatory** | | | | | | | | | | |
| **IL-1β** | NA | NA | 4 | 1 | 41 | 13 | 4 | 1 | 33 | 11 |
| **IL-5** | NA | NA | 94 | 17 | 99 | 18 | 109 | 11 | 99 | 22 |
| **IL-6** | NA | NA | NA | NA | 329 | 122 | 52 | 25 | 308 | 96 |
| **IL-8** | 982 | 389 | 368 | 119 | 3632 | 1449 | 310 | 77 | 2640 | 921 |
| **IL-9** | 16 | 3 | 28 | 6 | 68 | 15 | 31 | 5 | 71 | 11 |
| **IL-12(p70)** | 24 | 7 | NA | NA | 5 | 2 | 4 | 1 | 10 | 4 |
| **IL-15** | 2 | 0 | 3 | 1 | 4 | 2 | 2 | 1 | 2 | 1 |
| **IL-17** | 15 | 2 | NA | 4 | 50 | 9 | NA | NA | 37 | 11 |
| **CCL11** | 17 | 4 | 69 | 6 | 59 | 5 | 57 | 9 | 42 | 7 |
| **FGF basic** | 31 | 4 | NA | NA | NA | | NA | NA | NA | |
| **G-CSF** | NA | NA | 52 | 12 | 134 | 37 | 33 | 11 | 102 | 23 |
| **GM-CSF** | 16 | 4 | NA | NA | NA | | NA | NA | NA | |
| **IFN-γ** | NA | NA | 223 | 64 | 327 | 90 | 251 | 68 | 361 | 71 |
| **CXCL10** | NA | NA | 280 | 60 | 255 | 52 | 385 | 70 | 369 | 67 |
| **PDGF-BB** | 13 | 3 | 985 | 142 | 1162 | 204 | 727 | 284 | 863 | 403 |
| **CCL2** | NA | NA | 28 | 19 | 34 | 22 | 70 | 45 | 51 | 37 |
| **CCL3** | 8 | 7 | 1 | 0 | 77 | 27 | 2 | 1 | 50 | 25 |
| **CCL4** | 165 | 113 | 95 | 40 | 718 | 177 | 146 | 59 | 638 | 153 |
| **CCL5** | 16 | 4 | 413 | 70 | 591 | 153 | 508 | 80 | 617 | 124 |
| **TNF-α** | 7 | 2 | 26 | 3 | 37 | 9 | 13 | 3 | 24 | 5 |
| **VEGF** | 146 | 22 | 11 | 4 | 41 | 6 | 29 | 8 | 61 | 17 |
| **Anti-inflammatory** | | | | | | | | | | |
| **IL-1RA** | 18 | 3 | 109 | 26 | 166 | 40 | 153 | 80 | 229 | 93 |
| **IL-4** | 3 | 1 | 17 | 2 | 19 | 3 | 15 | 4 | 15 | 4 |
| **IL-10** | 4 | 1 | 2 | 1 | 4 | 1 | 2 | 1 | 5 | 2 |

**Media taken from the culture of normal neutrophils, was analysed using BioRad Bio-Plex cytokine assays. The table shows the median result of 5 normal samples with standard deviation for each culture condition in pg/ml.**

## Appendix 3b. Cytokine levels of PV neutrophils

| Cytokine | PV Samples (pg/ml) | | | | | | | | | |
|---|---|---|---|---|---|---|---|---|---|---|
| | Base Media | St dev | N Serum Unstim | St dev | N Serum Stim | St dev | PV Serum Unstim | St dev | PV Serum Stim | St dev |
| **Pro-inflammatory** | | | | | | | | | | |
| **IL-1β** | NA | NA | 5 | 1 | 82 | 45 | 6 | 1 | 121 | 73 |
| **IL-5** | NA | NA | 96 | 18 | 102 | 18 | 117 | 14 | 121 | 13 |
| **IL-6** | NA | NA | 59 | 36 | 1139 | 921 | 63 | 22 | 1781 | 1305 |
| **IL-8** | 2161 | 1368 | 271 | 118 | 4820 | 2673 | 305 | 166 | 5680 | 4324 |
| **IL-9** | 30 | 13 | 31 | 3 | 96 | 22 | 36 | 7 | 101 | 28 |
| **IL-12(p70)** | 29 | 5 | NA | NA | 7 | 3 | 5 | 3 | 10 | 3 |
| **IL-15** | NA | NA | 6 | 1 | 6 | 1 | 2 | 1 | 2 | 1 |
| **IL-17** | 26 | 9 | NA | NA | 71 | 13 | 16 | 1 | 67 | 18 |
| **CCL11** | 22 | 4 | 64 | 8 | 79 | 11 | 54 | 12 | 72 | 11 |
| **FGF basic** | 39 | 5 | NA | NA | NA | NA | NA | NA | NA | NA |
| **G-CSF** | NA | NA | 55 | 18 | 180 | 71 | 54 | 5 | 257 | 135 |
| **GM-CSF** | 19 | 5 | NA | NA | NA | NA | NA | NA | NA | NA |
| **IFN-γ** | NA | NA | 251 | 41 | 564 | 139 | 250 | 61 | 579 | 206 |
| **CXCL10** | NA | NA | 245 | 34 | 264 | 24 | 367 | 66 | 365 | 59 |
| **PDGF-BB** | 15 | 3 | 978 | 172 | 1310 | 282 | 753 | 286 | 892 | 333 |
| **CCL2** | 3 | 1 | 123 | 100 | 93 | 87 | 71 | 43 | 69 | 41 |
| **CCL3** | 106 | 84 | 4 | 3 | 424 | 355 | 5 | 3 | 1263 | 1119 |
| **CCL4** | 654 | 456 | 105 | 22 | 979 | 271 | 163 | 52 | 909 | 315 |
| **CCL5** | 22 | 9 | 444 | 77 | 621 | 146 | 458 | 76 | 560 | 86 |
| **TNF-α** | 22 | 10 | 25 | 4 | 54 | 19 | 18 | 3 | 63 | 28 |
| **VEGF** | 179 | 38 | 12 | 7 | 37 | 11 | 26 | 10 | 51 | 15 |
| **Anti-inflammatory** | | | | | | | | | | |
| **IL-1RA** | 66 | 41 | 106 | 19 | 231 | 43 | 174 | 95 | 314 | 91 |
| **IL-4** | 4 | 1 | 17 | 2 | 21 | 2 | 15 | 3 | 20 | 2 |
| **IL-10** | 6 | 1 | 2 | 1 | 6 | 1 | 2 | 1 | 5 | 1 |

**Media taken from the culture of PV neutrophils, was analysed using BioRad Bio-Plex cytokine assays. The table shows the median result of 6 PV samples with standard deviation for each culture condition in pg/ml.**

# 9 References


1. Rhodes, S., Copland, M., Hopcroft, L., Sayeski, P. & Wheadon, H. Identification of JAK2 dependent transcriptional regulators in CML. *Exp. Hematol.* **41,** S47 (2017).

2. Gallipoli, P. *et al.* JAK2/STAT5 inhibition by nilotinib with ruxolitinib contributes to the elimination of CML CD34+ cells in vitro and in vivo. *Blood* **124,** 1492–1501 (2014).

3. Abstracts. *Br. J. Haematol.* **169,** 1–104 (2015).

4. Rhodes, S. C., Gavriilidou, R., Drummond, M. W., Copland, M. & Wheadon, H. Characterizing the Inflammasome in Polycythemia Vera. *Blood* **126,** 2827 (2015).

5. Bryder, D., Rossi, D. J. & Weissman, I. L. Hematopoietic stem cells: the paradigmatic tissue-specific stem cell. *Am. J. Pathol.* **169,** 338–46 (2006).

6. Becker, A. J., McCulloch, E. A. & Till, J. E. Cytological Demonstration of the Clonal Nature of Spleen Colonies Derived from Transplanted Mouse Marrow Cells. *Nature* **197,** 452–454 (1963).

7. Siminovitch, L., McCulloch, E. a & Till, J. E. The distribution of colony-forming cells among spleen colonies. *J. Cell. Physiol.* **62,** 327–336 (1963).

8. Morrison, S. J. & Kimble, J. Asymmetric and symmetric stem-cell divisions in development and cancer. *Nature* **441,** 1068–1074 (2006).

9. Akashi, K., Traver, D., Miyamoto, T. & Weissman, I. L. A clonogenic common myeloid progenitor that gives rise to all myeloid lineages. *Nature* **404,** 193–197 (2000).

10. Kondo, M., Weissman, I. L. & Akashi, K. Identification of clonogenic common lymphoid progenitors in mouse bone marrow. *Cell* **91,** 661–672 (1997).

11. Kawamoto, H., Wada, H. & Katsura, Y. A revised scheme for developmental pathways of hematopoietic cells: the myeloid-based model. *Int. Immunol.* **22,** 65–70 (2010).

12. Notta, F. *et al.* Distinct routes of lineage development reshape the human blood hierarchy across ontogeny. *Science* **351,** aab2116 (2016).

13. Coskun, S. & Hirschi, K. K. Establishment and regulation of the HSC niche:

Roles of osteoblastic and vascular compartments. *Birth Defects Res. C. Embryo Today* **90,** 229–42 (2010).

14. Adolfsson, J. *et al.* Identification of $Flt3^+$ Lympho-Myeloid Stem Cells Lacking Erythro-Megakaryocytic Potential. *Cell* **121,** 295–306 (2016).

15. Furze, R. C. & Rankin, S. M. Neutrophil mobilization and clearance in the bone marrow. *Immunology* **125,** 281–288 (2008).

16. Barreda, D. R., Hanington, P. C. & Belosevic, M. Regulation of myeloid development and function by colony stimulating factors. *Developmental and Comparative Immunology* **28,** 509–554 (2004).

17. Parganas, E. *et al.* Jak2 Is Essential for Signaling through a Variety of Cytokine Receptors. *Cell* **93,** 385–395 (2016).

18. Hohaus, S. *et al.* PU.1 (Spi-1) and C/EBP alpha regulate expression of the granulocyte-macrophage colony-stimulating factor receptor alpha gene. *Mol. Cell. Biol.* **15,** 5830–5845 (1995).

19. Anderson, K. L. *et al.* PU.1 and the Granulocyte- and Macrophage Colony-Stimulating Factor Receptors Play Distinct Roles in Late-Stage Myeloid Cell Differentiation. *Blood* **94,** 2310 LP-2318 (1999).

20. Hattangadi, S. M., Wong, P., Zhang, L., Flygare, J. & Lodish, H. F. From stem cell to red cell: regulation of erythropoiesis at multiple levels by multiple proteins, RNAs, and chromatin modifications. *Blood* **118,** 6258 LP-6268 (2011).

21. Miyake, T., Kung, C. K. & Goldwasser, E. Purification of human erythropoietin. *J. Biol. Chem.* **252,** 5558–64 (1977).

22. Lin, F. K. *et al.* Cloning and expression of the human erythropoietin gene. *Proc. Natl. Acad. Sci. U. S. A.* **82,** 7580–7584 (1985).

23. Jacobs, K. *et al.* Isolation and characterization of genomic and cDNA clones of human erythropoietin. *Nature* **313,** 806–810 (1985).

24. Eschbach, J. W., Egrie, J. C., Downing, M. R., Browne, J. K. & Adamson, J. W. Correction of the anemia of end-stage renal disease with recombinant human erythropoietin. Results of a combined phase I and II clinical trial. *N. Engl. J. Med.* **316,** 73–78 (1987).

25. Wallach, I. *et al.* Erythropoietin-Receptor Gene Regulation in Neuronal Cells.

*Pediatr Res* **65,** 619–624 (2009).

26. Zafiriou, M. P. *et al.* Erythropoietin responsive cardiomyogenic cells contribute to heart repair post myocardial infarction. *Stem Cells* **32,** 2480–2491 (2014).

27. Tablin, F., Castro, M. & Leven, R. M. Blood platelet formation in vitro. The role of the cytoskeleton in megakaryocyte fragmentation. *J. Cell Sci.* **97 ( Pt 1),** 59–70 (1990).

28. Shivdasani, R. A. Molecular and transcriptional regulation of megakaryocyte differentiation. *Stem Cells* **19,** 397–407 (2001).

29. Malara, A. *et al.* The secret life of a megakaryocyte: emerging roles in bone marrow homeostasis control. *Cell. Mol. Life Sci.* **72,** 1517–1536 (2015).

30. Kuter, D. J., Beeler, D. L. & Rosenberg, R. D. The purification of megapoietin: a physiological regulator of megakaryocyte growth and platelet production. *Proc. Natl. Acad. Sci. U. S. A.* **91,** 11104–11108 (1994).

31. Grozovsky, R. *et al.* The Ashwell-Morell receptor regulates hepatic thrombopoietin production via JAK2-STAT3 signaling. *Nat Med* **21,** 47–54 (2015).

32. Yang, J., Zhang, L., Yu, C., Yang, X.-F. & Wang, H. Monocyte and macrophage differentiation: circulation inflammatory monocyte as biomarker for inflammatory diseases. *Biomark. Res.* **2,** 1 (2014).

33. Swirski, F. K. *et al.* Identification of Splenic Reservoir Monocytes and Their Deployment to Inflammatory Sites. *Science* **325,** 612–616 (2009).

34. Tolouei Semnani, R. *et al.* Human Monocyte Subsets at Homeostasis and Their Perturbation in Numbers and Function in Filarial Infection. *Infect. Immun.* **82,** 4438–4446 (2014).

35. Ziegler-Heitbrock, L. *et al.* Nomenclature of monocytes and dendritic cells in blood. *Blood* **116,** (2010).

36. Nicholson, L. B., Raveney, B. J. E. & Munder, M. Monocyte dependent regulation of autoimmune inflammation. *Curr. Mol. Med.* **9,** 23–29 (2009).

37. Ghattas, A., Griffiths, H. R., Devitt, A., Lip, G. Y. H. & Shantsila, E. Monocytes in coronary artery disease and atherosclerosis: where are we now? *J. Am. Coll. Cardiol.* **62,** 1541–51 (2013).

38. Richards, D. M., Hettinger, J. & Feuerer, M. Monocytes and Macrophages in Cancer: Development and Functions. *Cancer Microenviron.* **6,** 179–191 (2013).

39. Geissmann, F. *et al.* Development of monocytes, macrophages, and dendritic cells. *Science* **327,** 656–661 (2010).

40. Spellberg, B. & Edwards, J. E. Type 1/Type 2 Immunity in Infectious Diseases. *Clin. Infect. Dis.* **32,** 76–102 (2001).

41. Bingle, L., Brown, N. J. & Lewis, C. E. The role of tumour-associated macrophages in tumour progression: Implications for new anticancer therapies. *Journal of Pathology* **196,** 254–265 (2002).

42. Cook, J. & Hagemann, T. Tumour-associated macrophages and cancer. *Curr. Opin. Pharmacol.* **13,** 595–601 (2013).

43. Murray, P. J. The JAK-STAT Signaling Pathway: Input and Output Integration. *J. Immunol.* **178,** 2623–2629 (2007).

44. Usui, A. *et al.* Blood concentrations of G-CSF and myelopoiesis in patients undergoing aortocoronary bypass surgery. *Ann. Hematol.* **74,** 169–173 (1997).

45. Borojevic, R. *et al.* Stroma-mediated granulocyte-macrophage colony-stimulating factor (GM-CSF) control of myelopoiesis: spatial organisation of intercellular interactions. *Cell Tissue Res.* **313,** 55–62 (2003).

46. Lu, X. *et al.* Expression of a homodimeric type I cytokine receptor is required for JAK2V617F-mediated transformation. *Proc. Natl. Acad. Sci. U. S. A.* **102,** 18962–18967 (2005).

47. Koppikar, P. *et al.* Heterodimeric JAK-STAT activation as a mechanism of persistence to JAK2 inhibitor therapy. *Nature* **489,** 155–9 (2012).

48. Pradhan, A., Lambert, Q. T., Griner, L. N. & Reuther, G. W. Activation of JAK2-V617F by Components of Heterodimeric Cytokine Receptors. *J. Biol. Chem.* **285,** 16651–16663 (2010).

49. Yamada, O., Ozaki, K., Akiyama, M. & Kawauchi, K. JAK–STAT and JAK–PI3K–mTORC1 Pathways Regulate Telomerase Transcriptionally and Posttranslationally in ATL Cells. *Mol. Cancer Ther.* **11,** 1112 LP-1121 (2012).

50. Porta, C., Paglino, C. & Mosca, A. Targeting PI3K/Akt/mTOR Signaling in Cancer. *Front. Oncol.* **4,** 64 (2014).

51. Fransecky, L., Mochmann, L. H. & Baldus, C. D. Outlook on PI3K/AKT/mTOR inhibition in acute leukemia. *Mol. Cell. Ther.* **3,** 2 (2015).

52. Steelman, L. S. *et al.* JAK/STAT, Raf/MEK/ERK, PI3K/Akt and BCR-ABL in cell cycle progression and leukemogenesis. *Leukemia* **18,** 189–218 (2004).

53. Bogani, C. *et al.* mTOR inhibitors alone and in combination with JAK2 inhibitors effectively inhibit cells of myeloproliferative neoplasms. *PLoS One* **8,** e54826 (2013).

54. Baselga, J. Targeting the phosphoinositide-3 (PI3) kinase pathway in breast cancer. *Oncologist* **16 Suppl 1,** 12–19 (2011).

55. Zhang, J., Roberts, T. M. & Shivdasani, R. A. Targeting PI3K signaling as a therapeutic approach for colorectal cancer. *Gastroenterology* **141,** 50–61 (2011).

56. Bitting, R. L. & Armstrong, A. J. Targeting the PI3K/Akt/mTOR pathway in castration-resistant prostate cancer. *Endocr. Relat. Cancer* **20,** R83-99 (2013).

57. LoRusso, P. M. Inhibition of the PI3K/AKT/mTOR Pathway in Solid Tumors. *J. Clin. Oncol.* **34,** 3803–3815 (2016).

58. Roberts, P. J. & Der, C. J. Targeting the Raf-MEK-ERK mitogen-activated protein kinase cascade for the treatment of cancer. *Oncogene* **26,** 3291–3310

59. Chang, F. *et al.* Signal transduction mediated by the Ras//Raf//MEK//ERK pathway from cytokine receptors to transcription factors: potential targeting for therapeutic intervention. *Leukemia* **17,** 1263–1293

60. Karin, M. & Gallagher, E. From JNK to pay dirt: jun kinases, their biochemistry, physiology and clinical importance. *IUBMB Life* **57,** 283–295 (2005).

61. Kyriakis, J. M. & Avruch, J. Mammalian mitogen-activated protein kinase signal transduction pathways activated by stress and inflammation. *Physiol. Rev.* **81,** 807–869 (2001).

62. Riely, G. J., Marks, J. & Pao, W. KRAS mutations in non-small cell lung

cancer. *Proc. Am. Thorac. Soc.* **6,** 201–205 (2009).

63. Al-Shamsi, H. O., Alhazzani, W. & Wolff, R. A. Extended RAS testing in metastatic colorectal cancer—Refining the predictive molecular biomarkers. *J. Gastrointest. Oncol.* **6,** 314–321 (2015).

64. Ascierto, P. A. *et al.* The role of BRAF V600 mutation in melanoma. *J. Transl. Med.* **10,** 85 (2012).

65. Bottero, V., Withoff, S. & Verma, I. M. NF-[kappa]B and the regulation of hematopoiesis. *Cell Death Differ* **13,** 785–797 (2006).

66. Oeckinghaus, A., Hayden, M. S. & Ghosh, S. Crosstalk in NF-[kappa]B signaling pathways. *Nat Immunol* **12,** 695–708 (2011).

67. Pahl, H. L. Activators and target genes of Rel/NF-kappaB transcription factors. *Oncogene* **18,** 6853–6866 (1999).

68. Lee, J. J. *et al.* Toll-Like Receptor 4-Linked Janus Kinase 2 Signaling Contributes to Internalization of Brucella abortus by Macrophages. *Infect. Immun.* **81,** 2448–2458 (2013).

69. Hoesel, B. & Schmid, J. A. The complexity of NF-κB signaling in inflammation and cancer. *Mol. Cancer* **12,** 86 (2013).

70. Lawrence, T. The Nuclear Factor NF-κB Pathway in Inflammation. *Cold Spring Harb. Perspect. Biol.* **1,** a001651 (2009).

71. Velazquez, L., Fellous, M., Stark, G. R. & Pellegrini, S. A protein tyrosine kinase in the interferon alpha/beta signaling pathway. *Cell* **70,** 313–322 (1992).

72. Müller, M. *et al.* The protein tyrosine kinase JAK1 complements defects in interferon-alpha/beta and -gamma signal transduction. *Nature* **366,** 814–820 (1993).

73. Darnell, J. E., Kerr, I. M. & Stark, G. R. Jak-STAT pathways and transcriptional activation in response to IFNs and other extracellular signaling proteins. *Sci.* **264,** 1415–1421 (1994).

74. Schindler, C., Shuai, K., Prezioso, V. & Darnell, J. J. Interferon-dependent tyrosine phosphorylation of a latent cytoplasmic transcription factor. *Science (80-. ).* **257,** 809–813 (1992).

75. Yamaoka, K. *et al.* The Janus kinases (Jaks). *Genome Biol.* **5,** 253 (2004).

76. Feng, J. *et al.* Activation of Jak2 catalytic activity requires phosphorylation of Y1007 in the kinase activation loop. *Mol. Cell. Biol.* **17,** 2497–2501 (1997).

77. Neubauer, H. *et al.* Jak2 deficiency defines an essential developmental checkpoint in definitive hematopoiesis. *Cell* **93,** 397–409 (1998).

78. Sedek, M. & Strous, G. J. SUMOylation is a regulator of the translocation of Jak2 between nucleus and cytosol. *Biochem. J.* **453,** 231–239 (2013).

79. Dawson, M. A. *et al.* JAK2 phosphorylates histone H3Y41 and excludes HP1alpha from chromatin. *Nature* **461,** 819–822 (2009).

80. Dawson, M. A. *et al.* Three Distinct Patterns of Histone H3Y41 Phosphorylation Mark Active Genes. *Cell Rep.* **2,** 470–477 (2015).

81. Kalderon, D., Roberts, B. L., Richardson, W. D. & Smith, A. E. A short amino acid sequence able to specify nuclear location. *Cell* **39,** 499–509 (1984).

82. Robbins, J., Dilworth, S. M., Laskey, R. A. & Dingwall, C. Two interdependent basic domains in nucleoplasmin nuclear targeting sequence: identification of a class of bipartite nuclear targeting sequence. *Cell* **64,** 615–623 (1991).

83. Dang, C. V & Lee, W. M. Identification of the human c-myc protein nuclear translocation signal. *Mol. Cell. Biol.* **8,** 4048–4054 (1988).

84. Burgess, R. J. & Zhang, Z. Histones, histone chaperones and nucleosome assembly. *Protein Cell* **1,** 607–612 (2010).

85. Liu, F. *et al.* JAK2V617F-mediated phosphorylation of PRMT5 downregulates its methyltransferase activity and promotes myeloproliferation. *Cancer Cell* **19,** 283–294 (2011).

86. Vardiman, J. W. *et al.* The 2008 revision of the World Health Organization (WHO) classification of myeloid neoplasms and acute leukemia: rationale and important changes. *Blood* **114,** 937 LP-951 (2009).

87. Bennett, J. H. Case of Hypertrophy of the Spleen and Liver in which Death Took Place from Suppuration of the Blood. *Edinburgh Med. Surg. J.* 413–423 (1845).

88. Nowell, P. C. & Hungerford, D. A. Chromosome studies on normal and leukemic human leukocytes. *J Natl Cancer Inst* **25,** 85–109 (1960).

89. Rowley, J. D. A New Consistent Chromosomal Abnormality in Chronic

Myelogenous Leukaemia identified by Quinacrine Fluorescence and Giemsa Staining. *Nature* **243,** 290–293 (1973).

90. de Klein, A. *et al.* A cellular oncogene is translocated to the Philadelphia chromosome in chronic myelocytic leukaemia. *Nature* **300,** 765–767 (1982).

91. Jones, D. *et al.* BCR-ABL fusion transcript types and levels and their interaction with secondary genetic changes in determining the phenotype of Philadelphia chromosome–positive leukemias. *Blood* **112,** 5190 LP-5192 (2008).

92. Verstovsek, S. *et al.* Neutrophilic-chronic myeloid leukemia: low levels of p230 BCR/ABL mRNA and undetectable BCR/ABL protein may predict an indolent course. *Cancer* **94,** 2416–2425 (2002).

93. Savage, D. G., Szydlo, R. M. & Goldman, J. M. Clinical features at diagnosis in 430 patients with chronic myeloid leukaemia seen at a referral centre over a 16-year period. *Br. J. Haematol.* **96,** 111–116 (1997).

94. Sokal, J. E. *et al.* Prognostic discrimination in "good-risk" chronic granulocytic leukemia. *Blood* **63,** 789 LP-799 (1984).

95. Hasford, J. *et al.* A new prognostic score for survival of patients with chronic myeloid leukemia treated with interferon alfa. Writing Committee for the Collaborative CML Prognostic Factors Project Group. *J. Natl. Cancer Inst.* **90,** 850–858 (1998).

96. Hasford, J. *et al.* Predicting complete cytogenetic response and subsequent progression-free survival in 2060 patients with CML on imatinib treatment: the EUTOS score. *Blood* **118,** 686 LP-692 (2011).

97. Buchdunger, E. *et al.* Selective inhibition of the platelet-derived growth factor signal transduction pathway by a protein-tyrosine kinase inhibitor of the 2-phenylaminopyrimidine class. *Proc. Natl. Acad. Sci. U. S. A.* **92,** 2558–2562 (1995).

98. Heinrich, M. C. *et al.* Inhibition of c-kit receptor tyrosine kinase activity by STI 571, a selective tyrosine kinase inhibitor. *Blood* **96,** 925–932 (2000).

99. Deininger, M. & Druker, B. Specific targeted therapy of chronic myelogenous leukemia with imatinib. *Pharmacol. Rev.* **55,** 401–423 (2003).

100. Silver, R. T. *et al.* An Evidence-Based Analysis of the Effect of Busulfan,

Hydroxyurea, Interferon, and Allogeneic Bone Marrow Transplantation in Treating the Chronic Phase of Chronic Myeloid Leukemia: Developed for the American Society of Hematology. *Blood* **94,** 1517 LP-1536 (1999).

101. Druker, B. J. *et al.* Activity of a Specific Inhibitor of the BCR-ABL Tyrosine Kinase in the Blast Crisis of Chronic Myeloid Leukemia and Acute Lymphoblastic Leukemia with the Philadelphia Chromosome. *N. Engl. J. Med.* **344,** 1038–1042 (2001).

102. Druker, B. J. *et al.* Efficacy and safety of a specific inhibitor of the BCR-ABL tyrosine kinase in chronic myeloid leukemia. *N Engl J Med* **344,** 1031–1037 (2001).

103. Bower, H. *et al.* Life Expectancy of Patients With Chronic Myeloid Leukemia Approaches the Life Expectancy of the General Population. *J. Clin. Oncol.* **34,** 2851–2857 (2016).

104. Rousselot, P. *et al.* Imatinib mesylate discontinuation in patients with chronic myelogenous leukemia in complete molecular remission for more than 2 years. *Blood* **109,** 58 LP-60 (2006).

105. Chen, M. *et al.* Targeting primitive chronic myeloid leukemia cells by effective inhibition of a new AHI-1-BCR-ABL-JAK2 complex. *J Natl Cancer Inst* **105,** 405–423 (2013).

106. Heuck, G. Zwei Fälle von Leukämie mit eigenthümlichem Blut- resp. Knochenmarksbefund. *Arch. für Pathol. Anat. und Physiol. und für Klin. Med.* **78,** 475–496 (1879).

107. Vaquez, H. Sur une forme speciale de cyanose s'accompagnant d'hyperglobulie excessive et persistante. *C R Soc Biol* **44,** 384–388 (1892).

108. Epstein E, G. A. Hammorhagische thrombocythamie bei vasculerer schrumpfmilz. *Virch Arch (Pathol Anat)* 292–233 (1934).

109. Osler, S. W. Chronic cyanosis, with polycythaemia and enlarged spleen: a new clinical entity. *Amer. J. med. Sci.* **126,** 187–201 (1903).

110. Baxter, E. J. *et al.* Acquired mutation of the tyrosine kinase JAK2 in human myeloproliferative disorders. *Lancet* **365,** (2005).

111. Kralovics, R. *et al.* A Gain-of-Function Mutation of JAK2 in Myeloproliferative Disorders. *N. Engl. J. Med.* **352,** 1779–1790 (2005).

112. James, C. *et al.* A unique clonal JAK2 mutation leading to constitutive signalling causes polycythaemia vera. *Nature* **434,** 1144–1148 (2005).

113. Levine, R. L. *et al.* Activating mutation in the tyrosine kinase JAK2 in polycythemia vera, essential thrombocythemia, and myeloid metaplasia with myelofibrosis. *Cancer Cell* **7,** (2005).

114. Scott, L. M. *et al.* JAK2 exon 12 mutations in polycythemia vera or idiopathic erythrocytosis. *Haematologica* **356,** 1717–1718 (2007).

115. Pikman, Y. *et al.* MPLW515L is a novel somatic activating mutation in myelofibrosis with myeloid metaplasia. *PLoS Med.* **3,** 1140–1151 (2006).

116. Pardanani, A. D. *et al.* MPL515 mutations in myeloproliferative and other myeloid disorders: A study of 1182 patients. *Blood* **108,** 3472–3476 (2006).

117. Klampfl, T. *et al.* Somatic Mutations of Calreticulin in Myeloproliferative Neoplasms. *N. Engl. J. Med.* **369,** 2379–90 (2013).

118. Wada, I., Imai, S., Kai, M., Sakane, F. & Kanoh, H. Chaperone Function of Calreticulin When Expressed in the Endoplasmic Reticulum as the Membrane-anchored and Soluble Forms. *J. Biol. Chem.* **270,** 20298–20304 (1995).

119. Marty, C. *et al.* Calreticulin mutants in mice induce an MPL-dependent thrombocytosis with frequent progression to myelofibrosis. *Blood* **127,** 1317 LP-1324 (2016).

120. Rampal, R. *et al.* Integrated genomic analysis illustrates the central role of JAK-STAT pathway activation in myeloproliferative neoplasm pathogenesis. *Blood* **123,** (2014).

121. Reuther, G. W. Recurring mutations in myeloproliferative neoplasms alter epigenetic regulation of gene expression. *Am J Cancer Res* **1,** 752–762 (2011).

122. Zhang, S. J. & Abdel-Wahab, O. Disordered epigenetic regulation in the pathophysiology of myeloproliferative neoplasms. *Curr Hematol Malig Rep* **7,** 34–42 (2012).

123. Ortmann, C. A. *et al.* Effect of Mutation Order on Myeloproliferative Neoplasms. *N. Engl. J. Med.* **372,** 601–612 (2015).

124. Vannucchi, A. M. *et al.* Mutations and prognosis in primary myelofibrosis.

*Leukemia* **27,** 1861–1869 (2013).

125. Tefferi, A. & Barbui, T. Polycythemia vera and essential thrombocythemia: 2015 update on diagnosis, risk-stratification and management. *Am. J. Hematol.* **90,** 162–173 (2015).

126. Barbui, T. *et al.* Philadelphia-Negative Classical Myeloproliferative Neoplasms: Critical Concepts and Management Recommendations From European LeukemiaNet. *J. Clin. Oncol.* **29,** 761–770 (2011).

127. Landolfi, R. *et al.* Efficacy and safety of low-dose aspirin in polycythemia vera. *N. Engl. J. Med.* **350,** 114–124 (2004).

128. Passamonti, F. *et al.* A dynamic prognostic model to predict survival in post–polycythemia vera myelofibrosis. *Blood* **111,** 3383 LP-3387 (2008).

129. Cervantes, F., Passamonti, F. & Barosi, G. Life expectancy and prognostic factors in the classic BCR/ABL-negative myeloproliferative disorders. *Leukemia* **22,** 905–914 (2008).

130. McMullin, M. F. *et al.* Guidelines for the diagnosis, investigation and management of polycythaemia/erythrocytosis. *Br. J. Haematol.* **130,** 174–195 (2005).

131. Harrison, C. N. *et al.* Guideline for investigation and management of adults and children presenting with a thrombocytosis. *Br. J. Haematol.* **149,** 352–375 (2010).

132. Verstovsek, S. *et al.* Long-term outcomes of 107 patients with myelofibrosis receiving JAK1/JAK2 inhibitor ruxolitinib: survival advantage in comparison to matched historical controls. *Blood* **120,** 1202–1209 (2012).

133. Vannucchi, A. M. *et al.* Ruxolitinib versus Standard Therapy for the Treatment of Polycythemia Vera. *N. Engl. J. Med.* **372,** 426–435 (2015).

134. Pardanani, A. *et al.* Safety and Efficacy of Fedratinib in Patients With Primary or Secondary Myelofibrosis: A Randomized Clinical Trial. *JAMA Oncol.* **1,** 643–651 (2015).

135. Harrison, C. N. *et al.* Pacritinib (PAC) vs best available therapy (BAT) in myelofibrosis (MF): Outcomes in patients (pts) with baseline (BL) thrombocytopenia. in *J Clin Oncol* Abstract 7011 (2016).

136. Cerquozzi, S. & Tefferi, A. Blast transformation and fibrotic progression in

polycythemia vera and essential thrombocythemia: a literature review of incidence and risk factors. *Blood Cancer J.* **5,** e366 (2015).

137. Moliterno, A. R., Williams, D. M., Rogers, O., Isaacs, M. A. & Spivak, J. L. Phenotypic variability within the JAK2 V617F-positive MPD: Roles of progenitor cell and neutrophil allele burdens. *Exp. Hematol.* **36,** 1480–1486.e2 (2016).

138. Valentino, L. & Pierre, J. JAK/STAT signal transduction: regulators and implication in hematological malignancies. *Biochem Pharmacol* **71,** 713–721 (2006).

139. Balko, J. M. *et al.* Triple-negative breast cancers with amplification of JAK2 at the 9p24 locus demonstrate JAK2-specific dependence. *Sci. Transl. Med.* **8,** 334ra53 (2016).

140. Abubaker, K. *et al.* Inhibition of the JAK2/STAT3 pathway in ovarian cancer results in the loss of cancer stem cell-like characteristics and a reduced tumor burden. *BMC Cancer* **14,** 317 (2014).

141. Lee, H. J., Daver, N., Kantarjian, H. M., Verstovsek, S. & Ravandi, F. The role of JAK pathway dysregulation in the pathogenesis and treatment of acute myeloid leukemia. *Clin Cancer Res* **19,** 327–335 (2013).

142. Bercovich, D. *et al.* Mutations of JAK2 in acute lymphoblastic leukaemias associated with Down's syndrome. *Lancet* **372,** 1484–1492 (2008).

143. Wang, S. A. *et al.* Atypical chronic myeloid leukemia is clinically distinct from unclassifiable myelodysplastic/myeloproliferative neoplasms. *Blood* **123,** 2645 LP-2651 (2014).

144. Crans, H. N. & Sakamoto, K. M. Transcription factors and translocations in lymphoid and myeloid leukemia. *Leuk. Off. J. Leuk. Soc. Am. Leuk. Res. Fund, U.K* **15,** 313–331 (2001).

145. Sun, K.-X., Xia, H.-W. & Xia, R.-L. Anticancer effect of salidroside on colon cancer through inhibiting JAK2/STAT3 signaling pathway. *Int. J. Clin. Exp. Pathol.* **8,** 615–621 (2015).

146. Wang, S.-W. *et al.* AZD1480, a JAK inhibitor, inhibits cell growth and survival of colorectal cancer via modulating the JAK2/STAT3 signaling pathway. *Oncol. Rep.* **32,** 1991–1998 (2014).

147. Kumar, H., Kawai, T. & Akira, S. Pathogen recognition by the innate immune system. *Int. Rev. Immunol.* **30,** 16–34 (2011).

148. Boehm, T. Design principles of adaptive immune systems. *Nat Rev Immunol* **11,** 307–317 (2011).

149. Hurtado-Nedelec, M. *et al.* Increased reactive oxygen species production and p47phox phosphorylation in neutrophils from myeloproliferative disorders patients with JAK2 (V617F) mutation. *Haematologica* **98,** 1517–1524 (2013).

150. Pourcelot, E. *et al.* Cytokine profiles in polycythemia vera and essential thrombocythemia patients: Clinical implications. *Exp. Hematol.* **42,** 360–368 (2015).

151. Fleischman, A. G. *et al.* TNFα facilitates clonal expansion of JAK2V617F positive cells in myeloproliferative neoplasms. *Blood* **118,** 6392 LP-6398 (2011).

152. Hasselbalch, H. C. Perspectives on chronic inflammation in essential thrombocythemia, polycythemia vera, and myelofibrosis: is chronic inflammation a trigger and driver of clonal evolution and development of accelerated atherosclerosis and second cancer? *Blood* **119,** 3219–3225 (2012).

153. Han, C. *et al.* Cardiovascular disease and risk factors in patients with rheumatoid arthritis, psoriatic arthritis, and ankylosing spondylitis. *J. Rheumatol.* **33,** 2167–2172 (2006).

154. Hansson, G. K. Inflammation, Atherosclerosis, and Coronary Artery Disease. *N. Engl. J. Med.* **352,** 1685–1695 (2005).

155. Landolfi, R. & Di Gennaro, L. Pathophysiology of thrombosis in myeloproliferative neoplasms. *Haematologica* **96,** 183–186 (2011).

156. Tam, C. S. *et al.* The natural history and treatment outcome of blast phase BCR-ABL− myeloproliferative neoplasms. *Blood* **112,** 1628 LP-1637 (2008).

157. Grande, M. A. *et al.* PML-containing nuclear bodies: their spatial distribution in relation to other nuclear components. *J. Cell. Biochem.* **63,** 280–291 (1996).

158. Bernardi, R. & Pandolfi, P. P. Structure, dynamics and functions of

promyelocytic leukaemia nuclear bodies. *Nat Rev Mol Cell Biol* **8,** 1006–1016 (2007).

159. Salomoni, P., Dvorkina, M. & Michod, D. Role of the promyelocytic leukaemia protein in cell death regulation. *Cell Death Dis* **3,** e247 (2012).

160. Wu, W.-S. *et al.* Promyelocytic Leukemia Protein Sensitizes Tumor Necrosis Factor α-Induced Apoptosis by Inhibiting the NF-κB Survival Pathway. *J. Biol. Chem.* **278,** 12294–12304 (2003).

161. Salomoni, P. *et al.* The promyelocytic leukemia protein PML regulates c-Jun function in response to DNA damage. *Blood* **105,** 3686–3690 (2005).

162. Bernardi, R. *et al.* PML regulates p53 stability by sequestering Mdm2 to the nucleolus. *Nat Cell Biol* **6,** 665–672 (2004).

163. Heuser, M. *et al.* Induction of the pro-myelocytic leukaemia gene by type I and type II interferons. *Mediat. Inflamm* **7,** 319–325 (1998).

164. Gurrieri, C. *et al.* Loss of the Tumor Suppressor PML in Human Cancers of Multiple Histologic Origins. *J. Natl. Cancer Inst.* **96,** 269–279 (2004).

165. Ito, K. *et al.* PML targeting eradicates quiescent leukaemia-initiating cells. *Nature* **453,** 1072–1078 (2008).

166. Rowley, J. D., Golomb, H. M. & Dougherty, C. 15/17 translocation, a consistent chromosomal change in acute promyelocytic leukaemia. *Lancet (London, England)* **1,** 549–550 (1977).

167. Grignani, F. *et al.* The acute promyelocytic leukemia-specific PML-RAR alpha fusion protein inhibits differentiation and promotes survival of myeloid precursor cells. *Cell* **74,** 423–431 (1993).

168. Brown, N. J. M. *et al.* PML nuclear bodies in the pathogenesis of acute promyelocytic leukemia: active players or innocent bystanders? *Front. Biosci. (Landmark Ed.* **14,** 1684–1707 (2009).

169. Westervelt, P. *et al.* High-penetrance mouse model of acute promyelocytic leukemia with very low levels of PML-RARα expression. *Blood* **102,** 1857 LP-1865 (2003).

170. Livak, K. J. & Schmittgen, T. D. Analysis of relative gene expression data using real-time quantitative PCR and the 2(-Delta Delta C(T)) Method. *Methods* **25,** 402–8 (2001).

171. McCloy, R. A. *et al.* Partial inhibition of Cdk1 in G2 phase overrides the SAC and decouples mitotic events. *Cell Cycle* **13,** 1400–1412 (2014).

172. Faderl, S. *et al.* The Biology of Chronic Myeloid Leukemia. *N. Engl. J. Med.* **341,** 164–172 (1999).

173. Anand, M., Chodda, S. K., Parikh, P. M. & Nadkarni, J. S. Abnormal levels of proinflammatory cytokines in serum and monocyte cultures from patients with chronic myeloid leukemia in different stages, and their role in prognosis. *Hematol. Oncol.* **16,** 143–154 (1998).

174. Hiwase, D. K. *et al.* Blocking cytokine signaling along with intense Bcr-Abl kinase inhibition induces apoptosis in primary CML progenitors. *Leukemia* **24,** 771–778 (2010).

175. Jiang, X., Lopez, A., Holyoake, T., Eaves, A. & Eaves, C. Autocrine production and action of IL-3 and granulocyte colony-stimulating factor in chronic myeloid leukemia. *Proc. Natl. Acad. Sci.* **96,** 12804–12809 (1999).

176. Hantschel, O. *et al.* BCR-ABL uncouples canonical JAK2-STAT5 signaling in chronic myeloid leukemia. *Nat Chem Biol* **8,** 285–293 (2012).

177. Akada, H. *et al.* Critical role of Jak2 in the maintenance and function of adult hematopoietic stem cells. *Stem Cells* **32,** 1878–1889 (2014).

178. Ward, A. C., Touw, I. & Yoshimura, A. The Jak-Stat pathway in normal and perturbed hematopoiesis. *Blood* **95,** 19–29 (2000).

179. Wallace, T. A., VonDerLinden, D., He, K., Frank, S. J. & Sayeski, P. P. Microarray analyses identify JAK2 tyrosine kinase as a key mediator of ligand-independent gene expression. *Am J Physiol Cell Physiol* **287,** C981-91 (2004).

180. Elmore, S. Apoptosis: A Review of Programmed Cell Death. *Toxicol. Pathol.* **35,** 495–516 (2007).

181. Carter, B. Z. *et al.* Combined targeting of BCL-2 and BCR-ABL tyrosine kinase eradicates chronic myeloid leukemia stem cells. *Sci. Transl. Med.* **8,** 355ra117 LP-355ra117 (2016).

182. Aichberger, K. J. *et al.* Identification of mcl-1 as a BCR/ABL-dependent target in chronic myeloid leukemia (CML): evidence for cooperative antileukemic effects of imatinib and mcl-1 antisense oligonucleotides. *Blood*

**105,** 3303–3311 (2004).

183. Kok, C. H. *et al.* A 20 Gene Expression Signature That Predicts Early Molecular Response Failure in Chronic Phase CML Patients Treated with Frontline Imatinib. *Blood* **126,** 596 (2015).

184. Chinnadurai, G., Vijayalingam, S. & Gibson, S. B. BNIP3 subfamily BH3-only proteins: mitochondrial stress sensors in normal and pathological functions. *Oncogene* **27,** S114–S127

185. Nieborowska-Skorska, M., Hoser, G., Kossev, P., Wasik, M. A. & Skorski, T. Complementary functions of the antiapoptotic protein A1 and serine/threonine kinase pim-1 in the BCR/ABL-mediated leukemogenesis. *Blood* **99,** 4531–4539 (2002).

186. Klejman, A. *et al.* The Src family kinase Hck couples BCR/ABL to STAT5 activation in myeloid leukemia cells. *EMBO J.* **21,** 5766–5774 (2002).

187. Chen, X. *et al.* The forkhead transcription factor FOXM1 controls cell cycle-dependent gene expression through an atypical chromatin binding mechanism. *Mol. Cell. Biol.* **33,** 227–236 (2013).

188. Scotland, K. B., Chen, S., Sylvester, R. & Gudas, L. J. Analysis of Rex1 (Zfp42) function in embryonic stem cell differentiation. *Dev. Dyn.* **238,** 1863–1877 (2008).

189. Lee, M. Y., Lu, A. & Gudas, L. J. Transcriptional regulation of Rex1 (zfp42) in normal prostate epithelial cells and prostate cancer cells. *J. Cell. Physiol.* **224,** 17–27 (2010).

190. Watanabe, T. *et al.* The transcription factor IRF8 counteracts BCR-ABL to rescue dendritic cell development in chronic myelogenous leukemia. *Cancer Res.* **73,** 6642–53 (2013).

191. Schmidt, M. *et al.* Expression of interferon regulatory factor 4 in chronic myeloid leukemia: correlation with response to interferon alfa therapy. *J. Clin. Oncol.* **18,** 3331–3338 (2000).

192. Richardson, R. J. *et al.* Irf6 is a key determinant of the keratinocyte proliferation-differentiation switch. *Nat. Genet.* **38,** 1329–1334 (2006).

193. Pardanani, A. *et al.* TG101209, a small molecule JAK2-selective kinase inhibitor potently inhibits myeloproliferative disorder-associated JAK2V617F

and MPLW515L/K mutations. *Leukemia* **21,** 1658–1668 (2007).

194. Quintas-Cardama, A. *et al.* Preclinical characterization of the selective JAK1/2 inhibitor INCB018424: therapeutic implications for the treatment of myeloproliferative neoplasms. *Blood* **115,** 3109–3117 (2010).

195. Howard, S. *et al.* Fragment-based discovery of the pyrazol-4-yl urea (AT9283), a multitargeted kinase inhibitor with potent aurora kinase activity. *J. Med. Chem.* **52,** 379–388 (2009).

196. Kim, K. I. *et al.* Molecular characterization and prognostic significance of FLT3 in CML progression. *Leuk. Res.* **34,** 995–1001 (2010).

197. Tallini, G. & Asa, S. L. RET oncogene activation in papillary thyroid carcinoma. *Adv. Anat. Pathol.* **8,** 345–354 (2001).

198. Tanaka, R. *et al.* Activity of the multitargeted kinase inhibitor, AT9283, in imatinib-resistant BCR-ABL-positive leukemic cells. *Blood* **116,** 2089–2095 (2010).

199. Traer, E. *et al.* Blockade of JAK2-mediated extrinsic survival signals restores sensitivity of CML cells to ABL inhibitors. *Leukemia* **26,** 1140–1143 (2012).

200. Bedi, A., Zehnbauer, B. A., Barber, J. P., Sharkis, S. J. & Jones, R. J. Inhibition of apoptosis by BCR-ABL in chronic myeloid leukemia. *Blood* **83,** 2038–44 (1994).

201. De Carvalho, D. D. *et al.* BCR-ABL-mediated upregulation of PRAME is responsible for knocking down TRAIL in CML patients. *Oncogene* **30,** 223–233 (2011).

202. Nievergall, E. *et al.* TGF-[alpha] and IL-6 plasma levels selectively identify CML patients who fail to achieve an early molecular response or progress in the first year of therapy. *Leukemia* (2016). at <http://dx.doi.org/10.1038/leu.2016.34>

203. Tefferi, A. & Vainchenker, W. Myeloproliferative Neoplasms: Molecular Pathophysiology, Essential Clinical Understanding, and Treatment Strategies. *J. Clin. Oncol.* **29,** 573–582 (2011).

204. Harrison, C. *et al.* JAK inhibition with ruxolitinib versus best available therapy for myelofibrosis. *N Engl J Med* **366,** 787–798 (2012).

205. Patrono, C., Rocca, B. & De Stefano, V. Platelet activation and inhibition in

polycythemia vera and essential thrombocythemia. *Blood* **121,** 1701 LP-1711 (2013).

206. Neunteufl, T., Heher, S., Stefenelli, T., Pabinger, I. & Gisslinger, H. Endothelial dysfunction in patients with polycythaemia vera. *Br. J. Haematol.* **115,** 354–359 (2001).

207. Zhong, S., Salomoni, P. & Pandolfi, P. P. The transcriptional role of PML and the nuclear body. *Nat Cell Biol* **2,** E85–E90 (2000).

208. Gialitakis, M., Arampatzi, P., Makatounakis, T. & Papamatheakis, J. Gamma interferon-dependent transcriptional memory via relocalization of a gene locus to PML nuclear bodies. *Mol Cell Biol* **30,** 2046–2056 (2010).

209. Mossuz, P. *et al.* Diagnostic value of serum erythropoietin level in patients with absolute erythrocytosis. *Haematologica* **89,** 1194–1198 (2004).

210. Moliterno, A. R., Williams, D. M., Rogers, O. & Spivak, J. L. Molecular mimicry in the chronic myeloproliferative disorders: reciprocity between quantitative JAK2 V617F and Mpl expression. *Blood* **108,** 3913 LP-3915 (2006).

211. Puigdecanet, E. *et al.* Gene expression profiling distinguishes JAK2V617F-negative from JAK2V617F-positive patients in essential thrombocythemia. *Leukemia* **22,** 1368–1376 (2008).

212. Avalle, L., Pensa, S., Regis, G., Novelli, F. & Poli, V. STAT1 and STAT3 in tumorigenesis: A matter of balance. *JAK-STAT* **1,** 65–72 (2012).

213. Chen, E. *et al.* Distinct clinical phenotypes associated with JAK2V617F reflect differential STAT1 signaling. *Cancer Cell* **18,** 524–535 (2010).

214. Min, I. M. *et al.* The transcription factor EGR1 controls both the proliferation and localization of hematopoietic stem cells. *Cell Stem Cell* **2,** 380–391 (2008).

215. Slezak, S. *et al.* Gene and microRNA analysis of neutrophils from patients with polycythemia vera and essential thrombocytosis: down-regulation of micro RNA-1 and -133a. *J. Transl. Med.* **7,** 1–17 (2009).

216. Li, S. *et al.* The Transcription Factors Egr2 and Egr3 Are Essential for the Control of Inflammation and Antigen-Induced Proliferation of B and T Cells. *Immunity* **37,** 685–696 (2016).

217. Bland, J. B., Peralta, J. R. & Tse, W. T. Elevated EGR2 Expression Provides a Potential Link Between Cell Cycle Arrest and Induced Differentiation in Myeloid Progenitor Cells. *Blood* **124,** 2733 LP-2733 (2014).

218. Wassarman, D. A. & Sauer, F. TAF(II)250: a transcription toolbox. *J. Cell Sci.* **114,** 2895–2902 (2001).

219. Bracken, A. P., Ciro, M., Cocito, A. & Helin, K. E2F target genes: unraveling the biology. *Trends Biochem. Sci.* **29,** 409–417 (2016).

220. Nagel, S. *et al.* Polycomb repressor complex 2 regulates HOXA9 and HOXA10, activating ID2 in NK/T-cell lines. *Mol. Cancer* **9,** 151 (2010).

221. Fleischman, A. G. Inflammation as a Driver of Clonal Evolution in Myeloproliferative Neoplasm. *Mediators Inflamm.* **2015,** 606819 (2015).

222. Honda, K. & Taniguchi, T. IRFs: master regulators of signalling by Toll-like receptors and cytosolic pattern-recognition receptors. *Nat Rev Immunol* **6,** 644–658 (2006).

223. Honda, K. *et al.* IRF-7 is the master regulator of type-I interferon-dependent immune responses. *Nature* **434,** 772–777 (2005).

224. Rogers, R. S., Horvath, C. M. & Matunis, M. J. SUMO Modification of STAT1 and Its Role in PIAS-mediated Inhibition of Gene Activation. *J. Biol. Chem.* **278,** 30091–30097 (2003).

225. Rinaldi, C. R. *et al.* Preferential nuclear accumulation of JAK2V617F in CD34+ but not in granulocytic, megakaryocytic, or erythroid cells of patients with Philadelphia-negative myeloproliferative neoplasia. *Blood* **116,** 6023–6026 (2010).

226. Lallemand-Breitenbach, V. *et al.* Arsenic degrades PML or PML-RAR[alpha] through a SUMO-triggered RNF4/ubiquitin-mediated pathway. *Nat Cell Biol* **10,** 547–555 (2008).

227. Hands, K. J., Cuchet-Lourenco, D., Everett, R. D. & Hay, R. T. PML isoforms in response to arsenic: high-resolution analysis of PML body structure and degradation. *J. Cell Sci.* **127,** 365–375 (2014).

228. Shen, Z.-X. *et al.* Use of Arsenic Trioxide (As2O3 ) in the Treatment of Acute Promyelocytic Leukemia (APL): II. Clinical Efficacy and Pharmacokinetics in Relapsed Patient. *Blood* **89,** 3354 LP-3360 (1997).

229. Passamonti, F. *et al.* Prognostic factors for thrombosis, myelofibrosis, and leukemia in essential thrombocythemia: a study of 605 patients. *Haematologica* **93,** 1645–1651 (2008).

230. Barbui, T. *et al.* Inflammation and thrombosis in essential thrombocythemia and polycythemia vera: different role of C-reactive protein and pentraxin 3. *Haematologica* **96,** 315–318 (2011).

231. Duewell, P. *et al.* NLRP3 inflammasomes are required for atherogenesis and activated by cholesterol crystals. *Nature* **464,** 1357–1361 (2010).

232. Ridker, P. M. *et al.* Rosuvastatin to prevent vascular events in men and women with elevated C-reactive protein. *N. Engl. J. Med.* **359,** 2195–2207 (2008).

233. Wang, J. *et al.* Promyelocytic leukemia nuclear bodies associate with transcriptionally active genomic regions. *J Cell Biol* **164,** 515–526 (2004).

234. Wilkinson, K. A. & Henley, J. M. Mechanisms, regulation and consequences of protein SUMOylation. *Biochem J* **428,** 133–145 (2010).

235. Zhang, X., Tang, N., Hadden, T. J. & Rishi, A. K. Akt, FoxO and regulation of apoptosis. *Biochim. Biophys. Acta* **1813,** 1978–86 (2011).

236. Crowder, C., Dahle, O., Davis, R. E., Gabrielsen, O. S. & Rudikoff, S. PML mediates IFN-alpha-induced apoptosis in myeloma by regulating TRAIL induction. *Blood* **105,** 1280–1287 (2005).

237. Gang Wang, Z. *et al.* Role of PML in Cell Growth and the Retinoic Acid Pathway. *Science (80-. ).* **279,** 1547 LP-1551 (1998).

238. Reineke, E. L. & Kao, H. Y. Targeting promyelocytic leukemia protein: a means to regulating PML nuclear bodies. *Int J Biol Sci* **5,** 366–376 (2009).

239. Vernier, M. *et al.* Regulation of E2Fs and senescence by PML nuclear bodies. *Genes Dev.* **25,** 41–50 (2011).

240. Medzhitov, R. Origin and physiological roles of inflammation. *Nature* **454,** 428–435 (2008).

241. Grivennikov, S. I., Greten, F. R. & Karin, M. Immunity, Inflammation, and Cancer. *Cell* **140,** 883–899 (2016).

242. Baran-Marszak, F. *et al.* Expression level and differential JAK2-V617F-binding of the adaptor protein Lnk regulates JAK2-mediated signals in

myeloproliferative neoplasms. *Blood* **116,** 5961–5971 (2010).

243. de Bruin, A. M., Voermans, C. & Nolte, M. A. Impact of interferon-gamma on hematopoiesis. *Blood* **124,** 2479–2486 (2014).

244. Stansfield, B. K. & Ingram, D. A. Clinical significance of monocyte heterogeneity. *Clin. Transl. Med.* **4,** 5 (2015).

245. Wong, K. L. *et al.* The three human monocyte subsets: implications for health and disease. *Immunol. Res.* **53,** 41–57 (2012).

246. del Conde, I. *et al.* Effect of P-Selectin on Phosphatidylserine Exposure and Surface-Dependent Thrombin Generation on Monocytes. *Arterioscler. Thromb. Vasc. Biol.* **25,** 1065 LP-1070 (2005).

247. Schulte, W., Bernhagen, J. & Bucala, R. Cytokines in sepsis: Potent immunoregulators and potential therapeutic targets - An updated view. *Mediators Inflamm.* **2013,** (2013).

248. Theodoridou, S. *et al.* Elevated levels of serum vascular endothelial growth factor in patients with polycythaemia vera. *Acta Haematol.* **110,** 16–19 (2003).

249. Ramos, P. *et al.* Macrophages support pathological erythropoiesis in polycythemia vera and [beta]-thalassemia. *Nat Med* **19,** 437–445 (2013).

250. Stöger, J. L. *et al.* Distribution of macrophage polarization markers in human atherosclerosis. *Atherosclerosis* **225,** 461–8 (2012).

251. Eun, S. Y. *et al.* LPS potentiates nucleotide-induced inflammatory gene expression in macrophages via the upregulation of P2Y2 receptor. *Int. Immunopharmacol.* **18,** 270–276 (2014).

252. Roszer, T. Understanding the Mysterious M2 Macrophage through Activation Markers and Effector Mechanisms. *Mediators Inflamm.* 16 (2015). doi:10.1155/2015/816460

253. Martinez, F. O. & Gordon, S. The M1 and M2 paradigm of macrophage activation: time for reassessment. *F1000Prime Rep.* **6,** 13 (2014).

254. Rosenberg, H. F., Dyer, K. D. & Foster, P. S. Eosinophils: changing perspectives in health and disease. *Nat Rev Immunol* **13,** 9–22 (2013).

255. Engstrom, A., Erlandsson, A., Delbro, D. & Wijkander, J. Conditioned media from macrophages of M1, but not M2 phenotype, inhibit the proliferation of

the colon cancer cell lines HT-29 and CACO-2. *Int. J. Oncol.* **44,** 385–392 (2014).

256. Kang, J. & Coles, M. IL-7: the global builder of the innate lymphoid network and beyond, one niche at a time. *Semin. Immunol.* **24,** 190–197 (2012).

257. Li, R. *et al.* Interleukin-7 induces recruitment of monocytes/macrophages to endothelium. *Eur. Heart J.* **33,** 3114–3123 (2012).

258. Vaidya, R. *et al.* Plasma cytokines in polycythemia vera: phenotypic correlates, prognostic relevance, and comparison with myelofibrosis. *Am. J. Hematol.* **87,** 1003–1005 (2012).

259. Harrison, C. N. *et al.* Results Of a Randomized, Double-Blind, Placebo-Controlled Phase III Study (JAKARTA) Of The JAK2-Selective Inhibitor Fedratinib (SAR302503) In Patients With Myelofibrosis (MF). *Blood* **122,** 393 LP-393 (2013).

260. Mascarenhas, J. *et al.* Results of the Persist-2 Phase 3 Study of Pacritinib (PAC) Versus Best Available Therapy (BAT), Including Ruxolitinib (RUX), in Patients (pts) with Myelofibrosis (MF) and Platelet Counts <100,000/μl. *Blood* **128,** LBA-5 LP-LBA-5 (2016).

261. Davies, L. C., Jenkins, S. J., Allen, J. E. & Taylor, P. R. Tissue-resident macrophages. *Nat Immunol* **14,** 986–995 (2013).

262. Hashimoto, D. *et al.* Tissue resident macrophages self-maintain locally throughout adult life with minimal contribution from circulating monocytes. *Immunity* **38,** 10.1016/j.immuni.2013.04.004 (2013).

263. Chen, E., Staudt, L. M. & Green, A. R. Janus kinase deregulation in leukemia and lymphoma. *Immunity* **36,** 529–41 (2012).

264. Rosenwald, A. *et al.* Molecular diagnosis of primary mediastinal B cell lymphoma identifies a clinically favorable subgroup of diffuse large B cell lymphoma related to Hodgkin lymphoma. *J. Exp. Med.* **198,** 851–62 (2003).

265. Samanta, A. K. *et al.* Destabilization of Bcr-Abl/Jak2 Network by a Jak2/Abl Kinase Inhibitor ON044580 Overcomes Drug Resistance in Blast Crisis Chronic Myelogenous Leukemia (CML). *Genes Cancer* **1,** 346–359 (2010).

266. Dupont, S. *et al.* The JAK2 V617F mutation triggers erythropoietin hypersensitivity and terminal erythroid amplification in primary cells from

patients with polycythemia vera. *Blood* **110,** 1013 LP-1021 (2007).

267. Passamonti, F. *et al.* Relation between JAK2(V617F) mutation status, granulocyte activation, and constitutive mobilization of CD34+ cells into peripheral blood in myeloproliferative disorders. *Blood* **107,** 3676 LP-3682 (2006).

268. Reuther, G. W. JAK2 activation in myeloproliferative neoplasms: A potential role for heterodimeric receptors. *Cell Cycle* **7,** 714–719 (2008).

269. Flotho, A. & Melchior, F. Sumoylation: A Regulatory Protein Modification in Health and Disease. *Annu. Rev. Biochem.* **82,** 357–385 (2013).

270. Bernardi, R. & Pandolfi, P. P. Role of PML and the PML-nuclear body in the control of programmed cell death. *Oncogene* **22,** 9048–9057 (2003).

271. Salomoni, P. The PML-Interacting Protein DAXX: Histone Loading Gets into the Picture. *Front. Oncol.* **3,** 152 (2013).

272. St-Germain, J. R., Chen, J. & Li, Q. Involvement of PML nuclear bodies in CBP degradation through the ubiquitin-proteasome pathway. *Epigenetics* **3,** 342–349 (2008).

273. Qin, Q. *et al.* A novel GTPase, CRAG, mediates promyelocytic leukemia protein-associated nuclear body formation and degradation of expanded polyglutamine protein. *J. Cell Biol.* **172,** 497–504 (2006).

274. Kitagawa, D. *et al.* Release of RASSF1C from the nucleus by Daxx degradation links DNA damage and SAPK/JNK activation. *EMBO J.* **25,** 3286–3297 (2006).

275. Bernardi, R., Papa, A. & Pandolfi, P. P. Regulation of apoptosis by PML and the PML-NBs. *Oncogene* **27,** 6299–6312

276. Trotman, L. C. *et al.* Identification of a tumour suppressor network opposing nuclear Akt function. *Nature* **441,** 523–527 (2006).

277. Cairo, S. *et al.* PML interacts with Myc, and Myc target gene expression is altered in PML-null fibroblasts. *Oncogene* **24,** 2195–2203 (2005).

278. Marchioli, R. *et al.* Cardiovascular Events and Intensity of Treatment in Polycythemia Vera. *N. Engl. J. Med.* **368,** 22–33 (2012).

279. Tefferi, A. *et al.* Survival and prognosis among 1545 patients with contemporary polycythemia vera: an international study. *Leukemia* **27,**

1874–81 (2013).

280. Klimek, E. *et al.* Blood Monocyte Subsets and Selected Cardiovascular Risk Markers in Rheumatoid Arthritis of Short Duration in relation to Disease Activity. *Biomed Res. Int.* **2014,** 736853 (2014).

281. van der Laan, A. M. *et al.* A proinflammatory monocyte response is associated with myocardial injury and impaired functional outcome in patients with ST-segment elevation myocardial infarction: monocytes and myocardial infarction. *Am. Heart J.* **163,** 57–65.e2 (2012).

282. Hasselbalch, H. C. Chronic inflammation as a promotor of mutagenesis in essential thrombocythemia, polycythemia vera and myelofibrosis. A human inflammation model for cancer development? *Leuk Res* **37,** 214–220 (2013).